Universidade dos Açores
Departamento de Oceanografia e Pescas

Temporal variations of the Mid-Atlantic hydrothermal vent communities from the Lucky Strike vent field

By

Daphne Cuvelier

Dissertação apresentada à Universidade dos Açores para obtenção do Grau de Doutor no Ramo de Ciências do Mar e Especialidade em Ecologia Marinha

Horta, 2011

Temporal variations of the Mid-Atlantic hydrothermal vent communities from the Lucky Strike vent field

By

Daphne Cuvelier

Under the supervision of:

Dr. Ricardo Serrão Santos & Dr. Ana Colaço
Departamento de Oceanografia e Pescas
Universidade dos Açores

Dr. Daniel Desbruyères & Dr. Jozée Sarrazin
Département Études des Ecosystèmes Profonds
Institut Français de Recherche pour l'Exploitation de la Mer (Ifremer), Centre de Brest

Dr. Paul A. Tyler & Dr. Jon T. Copley
National Oceanography Centre, Southampton

Dr. Adrian G. Glover
Zoology Department
Natural History Museum, London

This research was funded by MarBEF Network of Excellence 'Marine Biodiversity and Ecosystem Functioning' which was part of the Sustainable Development, Global Change and Ecosystems Programme of the European Community's Sixth Framework Programme (contract no. GOCE-CT-2003-505446) and by FCT (Fundação de Ciência e Tecnologia, grant SFRH/BD/47301/2008).

ACKNOWLEDGMENTS

Here we go, 4.5 years of PhD, 7 supervisors, 3 countries (4 counting my home) and many friends, family and colleagues …. To start off I would like to thank my supervisors from all over Europe. I know you are all very busy people but I would like to thank you all together for your energy and dedication. It has not always been easy, far from it, but I learned a lot, starting with a new language (Portuguese) and freshen up another one (français), working in different labs, with different people, on research vessels and in all kinds of conditions!

I would like to acknowledge Dr. Ricardo Serrão Santos & Dr. Ana Colaço for hosting this PhD at the Department of Oceanography and Fisheries in Faial, in the Azores, and accepting me as a PhD-student, giving me the opportunity to learn to know the beauty of these islands. Even though Faial may be "uma ilha sem sabor tropical", it is a great place to live if you love the sea.
I would like to thank Dr. Ricardo for giving me the freedom to travel around so much, and supporting me to participate in different symposia. Even when being abroad so often, you always tried to spend some of your time reading my manuscripts and answering my practical questions and to meet up whenever you were around!
Ana, thanks for being committed to my PhD and for being available to talk about my work, for complying with the deadlines I proposed (sometimes on short notice) and for translating my abstract in Portuguese.
Muito obrigada a ambos!!

I owe much gratitude to Dr. Daniel Desbruyères and Dr. Jozée Sarrazin from Ifremer. Thanks for your support and granting me access to all your facilities, imagery and having me over at Ifremer (Brest). I think your involvement in my PhD has given it a superior value!
Daniel, c'est un grand honneur pour moi d'être ta dernière étudiante de thèse et merci de m'avoir appuyé jusqu'à la fin de ma thèse, d'avoir été aussi disponible et d'avoir partagé ta connaissance avec moi!!!
Jozée, je ne sais pas ce que j'aurais dû faire sans toi, bien que la distance n'a parfois pas facilité les choses, tu étais toujours lá, et je crois que tu m'as poussé à élever mon travail (et moi-même) à un niveau supérieur ! ! Un grand merci!!!!!!! Et aussi pour m'avoir invité chez toi sur des dîners sympas avec toi et ta famille !

I also would like to thank Dr. Paul Tyler and Dr. Jon Copley from National Oceanography Centre (NOC) in Southampton. Paul and Jon, thanks for being so accessible and committed, even if it was over tiny little things. The time spent at NOCS was very useful and it was great working with you up close. Thanks for making time for me whenever you could!

Dr. Adrian Glover thanks for inviting me over to the NHM, the guided tour behind the screens, his involvement and for being always optimistic!

Thanks to Dr. David Billet as Deepsets coordinator, for his interest and involvement whenever (and wherever) we met, and Dr. Andy Gooday as his successor.

Ackowledgments

Dr . Pierre-Marie Sarradin, merci P.M. pour ton intérêt et ton engagement vers mon sujet de thèse, pour les semaines passées en mer, et ton point de vue « chimiste ». Et merci pour m'ammener en mer et rester debout avec moi les nuits pour faire des manips !

Sandra Silva and Sandra Andrade, thanks for helping out with all the administration of being a scholarship student (bolseiro), travelling around and handing in receipts and for your help with all the hassle and paperwork that comes along with living abroad.

Un grand merci à tout le monde de l' Ifremer Brest, (Bénédicte Ritt, Marie-Claire Fabri, Anne Godfroy, Christian le Gall, Philippe Rodier, Philippe Noël, Karine Olu, Alexis Khripounoff, Joëlle Galéron, Lenaick Menot, Jean-Claude Caprais, Sophie Arnaud, Patrick Briand, Philippe Crassous, Annick Vangriesheim), pour m'avoir acceuilli si chaleureusement chaque fois je venais vous visiter. Pour partager vos bureaux avec moi, les apéros les vendredis ou chaque fois qu'il y avait quelque chose à fêter. Les missions en mer avec certains de vous etaient un vrai plaisir ! Béné, merci pour les conversations les soirs quand tout le monde etait déjà parti, il faut qu'on arrange quelque chose pour partir en mer ensemble!

I also owe many thanks to:

Nelia Mestre, Cedric Boulart and Alice Lefebvre for letting me stay at their place in Southampton the first couple of weeks, and together with Emily Dolan, for welcoming me with open arms and showing me around Southampton's bars and surroundings. It is a pleasure and great fun every time we meet, be it in the Azores, Belgium or in some far away location.

MiniDop and its inhabitants, probably the most vibrant and lively building from DOP! Também queria agradecer a malta de cá (Claudia, Maria João, Xana, Marco Aurélio, Hugo, Roberto, Filipe, Marco Dutra, Irma, Guedes, Ricardinho, Sandra) pela amizade, os jantares, os convivios, as saidas para o mar, os mergulhos e muito mais!!!! E a Inês para as conversas na fase final da tese.

My friends at home in Belgium (Dries, Laurence, Tine, Michael, Aline, Annelore, Frederik, Pie, Santi, Philippe, Geoff, Laurence, Jan, Inge, Griet, Riet, Dirk, Max, Griet, Klaas, Inne, Robin, Karin, Krieke, Isabel, and everyone I forgot!): thanks for being there for me every time I came over and organising great dinners, ladies nights, choosing nice restaurants, participating in and organising cool new year parties or just going out for drinks. It is a great feeling to come home, and be able to start chatting away in Flemish, and even more when it doesn't feel that I have been away for many months. Dank jullie wel!!! Tine, thanks for keeping me posted about how things were going back home, you made me smile many times when reading your emails! Isabel, thanks for being always ready to meet up and have a great night out! For several other friends, sorry to be out of touch…

My Family: grandparents (Oma, Opa, Moeke) and specially my parents, Mam & Pap, and my twin brother Nic(olas) for being there for me every part of the way, for coming to pick me up or drop me of at the airport at the craziest hours of day (or night) and for coming to visit me (together with Emilie). For taking care of so many (administrative and other) things

back in Belgium. And above all, for believing in me unconditionally and supporting every choice I make in life!

Fred for his love, kindness, humour, optimism, honesty and patience!!! For putting up with my PhD-related mood swings and stressed out 'I don't know what's. For making sure I had a life besides my PhD, and a great place to come home to!! It is not always easy to be far away from home, but with you around everything is alright. I guess words do not suffice….

Family, friends, colleagues and people I met along the way, thanks!!! It has been an unforgettable ride….

I also would like to acknowledge my funding agencies MarBEF Network of Excellence 'Marine Biodiversity and Ecosystem Functioning' which was part of the Sustainable Development, Global Change and Ecosystems Programme of the European Community's Sixth Framework Programme (contract no. GOCE-CT-2003-505446) and FCT (Fundação de Ciência e Tecnologia, grant SFRH/BD/47301/2008)

TABLE OF CONTENTS

Abstract (English)……i

Resumo (Português)……iii

Résumé (Français)……v

List of Figures……ix

List of Tables……xi

Chapter 1: Introduction and Thesis outline……**1**

1. Hydrothermal vents……3

1.1 Past and recent discoveries 3

1.2 Setting and characteristics 5

2. Hydrothermal vent fauna differences and specificities……8

2.1 Fauna 8

2.2 Adaptations to the vent environment 11

3. Temporal variation and succession at vents……16

3.1. Post-eruptive nascent vent studies 17

3.2. Temporal evolution studies under continuous venting 22

3.3 Nascent vs. continuous venting contrasts 26

4. The Atlantic as a study site……27

4.1 Atlantic 27

4.2 Lucky Strike 27

5. Aims and thesis outline……30

Chapter 2: Distribution and spatial variation of hydrothermal faunal assemblages at Eiffel Tower……**35**

1. Introduction……37

2. Material & Methods……38

2.1. Study site 38

2.2. Image acquisition 39

2.3. Video Analysis 40

2.4. Statistics 42

3. Results.....42

3.1. Eiffel Tower morphology and activity 42

3.2. Faunal composition of the Eiffel Tower edifice 43

3.3. Assemblages 45

3.4. Spatial distribution and size of the assemblages 46

3.5. Neighbouring patterns 50

4. Discussion.....51

4.1. Spatial and zonation patterns 52

4.2. Assemblages on the Eiffel Tower edifice 54

4.2.1. Mussel-based assemblages 54

4.2.2. Shrimp assemblage 56

4.3. Comparison between the edifice sides 56

4.4. Habitat and substrata 57

5. Conclusion.....58

Chapter 3: 14-years of community dynamics at the Eiffel Tower hydrothermal edifice.....63

1. Introduction.....65

2. Material & Methods.....67

2.1. Study site 67

2.2. Video analyses 68

2.3. Detailed community dynamics 72

2.4. Statistics 73

3. Results.....73

3.1. Temporal variations on the entire edifice 74

3.1.1. Variations in hydrothermal activity 74

3.1.2. Variations in faunal assemblages and substrata 74

3.2. Temporal variations on the different sides of the edifice 77

3.3. Community dynamics 80

4. Discussion.....84

4.1. Succession? 84

4.1.1. Eiffel Tower succession model 84

4.1.2. Comparison with other succession models 86

4.1.3. Comparison with the history of other sites and Mid-Oceanic Ridges 87

4.1.4. Rate of change 88
4.2. Role of physical disturbance 89
4.3. Temporal variations at Eiffel Tower 90
4.3.1. General tendencies over time 90
4.3.2. Faunal assemblages and substrata over time 90
4.3.3. Variations in hydrothermal activity 92
4.3.4. Others cues-biotic interactions 93
4.3.5. Decadal-scale stability? 93
5. Conclusion.....93

Chapter 4: Hydrothermal faunal assemblages and habitat characterisation at Eiffel Tower.....97
1. Introduction.....99
2. Material & Methods.....100
2.1. Study site 100
2.2. Assemblage sampling 101
2.3. Chemical sampling 102
2.4. Statistics 103
3. Results.....104
3.1. Faunal assemblage composition 104
3.2. Physical and chemical characterisation 106
3.3. Habitat characteristics 108
3.4. Fauna-Habitat relations 109
4. Discussion.....111
4.1. Physico-chemical characteristics of the assemblages 111
4.2. Faunal characteristics 113
4.3. Sample/assemblage similarity 115
4.4. Diversity 115
5. Conclusion.....115

Chapter 5: Temporal variations in faunal sampling and species composition at Lucky Strike.....119
1. Introduction.....121

2. Material & Methods.....121
2.1. Study site 121
2.2. Biocean database 122
2.3. Sampling bias 124
2.4. Statistics 124
3. Results.....125
3.1. The Lucky Strike vent field 125
3.1.1. Sampling sites 125
3.1.2. Sample or edifice similarity? 129
3.1.3. Species list and sampling effort 131
3.2. Species distribution over time 135
3.3. Beta diversity 138
3.4. Single vent edifices 138
3.4.1. Eiffel Tower 138
3.4.2. Bairro Alto 141
3.4.3. Sintra 144
3.4.4. Isabel 145
3.4.5. Y3 147
3.4.6. Elisabeth 147
3.4.7. Statue of Liberty 148
4. Discussion.....149
4.1. Limitations/Sampling Bias 149
4.2. Differences in faunal composition between edifices 150
5. Conclusion and future perspectives.....154
6. Appendix 1.....157

Chapter 6: Synthesis.....**169**

Bibliography.....**179**

Abstract – Resumo – Résumé

ABSTRACT

The first Mid-Atlantic hydrothermal vents were discovered in 1985 (Rona et al., 1986), almost 10 years after the first hydrothermal vent discovery at the Galápagos Rift (Lonsdale, 1979). Over three decades of research on these extreme deep-sea ecosystems has improved our knowledge on the mega-and macrofauna inhabiting these peculiar habitats substantially. Less is known about the community structure and the spatial and temporal distributions of the fauna in relation to abiotic and biotic factors. Ecological time-series studies of temporal variation are indispensable to comprehend the functioning of an ecosystem. However, such studies at hydrothermal vents are scarce and mostly restricted to well-known and more accessible sites in the East Pacific Ocean (EPR and NEP). Imagery analysis is an important tool to assess temporal variation at these often remote and extreme ecosystems both under conditions of continuous venting (Hessler et al., 1985, 1988; Fustec et al., 1987; Sarrazin et al., 1997; Desbruyères, 1998) and post-eruptive nascent vent development (Tunnicliffe et al., 1997; Shank et al., 1998a; Tsurumi & Tunnicliffe, 2001; Shank et al., 2003; Nees et al., 2008; Marcus et al., 2009). Until now, only one single long-term temporal dynamics study is available for the Mid-Atlantic Ridge (MAR), where decadal-scale changes were assessed at the TAG sulfide mound (Copley et al., 2007a).

The study presented here is the first high-resolution long-term variations study on the Mid-Atlantic Ridge, investigating both long-term (>10 years) variations in community structure as well as dynamics on shorter time-scales (1 to 4 years). In this dissertation, assemblage distribution patterns and zonation on the Eiffel Tower edifice (part of the Lucky Strike vent field, south of the Azores, situated at a mean depth of 1700m) is assessed by use of image analyses. The protocol wielded is described, which then was elaborated to allow comparisons between the years and to study 14 years of community dynamics. Trends in temporal variations are described. Overall decadal-scale constancy appears to persevere, however on smaller time and spatial scales, changes do occur. A succession model is proposed and a quantification of the rate of change at the slower-spreading MAR is evaluated and compared to that of faster-spreading ridges (NEP). While imagery analysis was used to unravel main temporal and spatial variation trends, discrete biological samples and physico-chemical measurements were analysed to better comprehend the discrepancies observed. Microhabitats were characterised by the extent of fluctuations in environmental variables, while temperature was identified as being a more limiting factor, separating the mussel-based assemblages from the shrimps. In addition, species lists from past and on-going sampling during the French cruises, stored in the

Biocean database (Fabri et al., 2006), were analysed to identify changes over time within the Lucky Strike vent field. Based on the data at hand, no significant differences in species composition between different edifices and years were revealed. This dissertation allowed us to gather new insights on the ecosystem functioning of Mid-Atlantic hydrothermal vents. Larger-scale applications and extrapolation of these results and models are proposed, for which the collection of new data is needed.

RESUMO

Os primeiros campos hidrotermais na Dorsal Médio Atlântica (MAR) foram descobertos apenas em 1985 (Rona et al., 1986), quase dez anos depois da primeiríssima fonte hidrotermal ter sido descoberta na dorsal das Galápagos (Lonsdale, 1979). O nosso conhecimento da mega e macrofauna que habitam estes ambientes peculiares progrediu imenso em mais de três décadas de estudos destes ecossistemas extremos. No entanto, pouco se sabe sobre a estrutura da comunidade, assim como da distribuição espacial e temporal da fauna em relação a factores bióticos e abióticos. São indispensáveis estudos ecológicos de séries temporais, de forma a compreender o funcionamento do ecossistema. Apesar disso, estes tipos de estudos em ecossistemas hidrotermais são raros, e estão limitados a campos já muito conhecidos ou de fácil acesso no Pacifico Oriental (EPR e NEP). Uma ferramenta importante para estudar variações temporais destes ecossistemas remotos e extremos, é a análise de imagens, quer em condições de emissão hidrotermal contínua (Hessler et al., 1985, 1988; Fustec et al., 1987; Sarrazin et al., 1997; Desbruyères, 1998) quer em condições de desenvolvimento de novas emissões após uma erupção vulcânica (Tunnicliffe et al., 1997; Shank et al., 1998a; Tsurumi & Tunnicliffe, 2001; Shank et al., 2003; Nees et al., 2008; Marcus et al., 2009). Até à data, apenas um estudo temporal de longo prazo foi realizado na Dorsal médio Atlântica, que descreve a dinâmica temporal à escala de uma década do campo hidrotermal TAG (Copley et al., 2007a).

O estudo aqui apresentado, é o primeiro efectuado sobre variações ecológicas de longa duração, em alta resolução na Dorsal Médio Atlântica. Este trabalho apresenta não só a variação da estrutura das comunidades durante 14 anos, mas também a dinâmica a uma escala mais curta de 1 a 4 anos. Nesta dissertação, a distribuição das assemblagens, a sua variação espacial, assim como a sua zonação sobre o edifício hidrotermal Torre Eiffel (estrutura do campo hidrotermal Lucky Strike, a sul dos Açores a uma profundidade de cerca de 1700 metros) são aqui descritos através da análise de imagens de vídeos. Um protocolo foi elaborado de forma a permitir comparações inter-anuais, sendo posteriormente utilizado para estudar a dinâmica das comunidades num período de 14 anos. As tendências das variações temporais foram descritas. Parece existir uma constância no espaço de uma década, apesar de ocorrerem variações a uma escala temporal e espaciais mais curtas. Um modelo de sucessão é proposto. A taxa de alteração é quantificada nesta dorsal caracterizada por ser lenta e comparada com uma dorsal rápida como a do Pacifico Oriental. Enquanto a análise de imagem foi utilizada para evidenciar tendências temporais e espaciais, uma amostragem biológica sistematizada, assim como a medição de variáveis físico-químicas, permitiram uma melhor compreensão e validação

das diferenças observadas. Os micro habitats foram caracterizados pela amplitude das flutuações das variáveis ambientais, enquanto que a temperatura foi identificada como o factor mais limitante, e que parece explicar a separação espacial das assemblagens à base de mexilhões e das assemblagens à base de camarões. Adicionalmente foi analisada a lista de espécies provenientes de amostragens passadas e presentes realizadas em missões francesas, armazenadas na base de dados Biocean (Fabri et al., 2006). A análise teve por objectivo estudar possíveis variações temporais da composição faunística no campo hidrotermal Lucky Strike. Baseado nestes dados, não foram observadas diferenças significativas na composição específica entre edifícios e entre anos neste campo hidrotermal. Este trabalho permitiu recolher novos dados sobre o funcionamento dos ecossistemas das fontes hidrotermais da Dorsal Médio Atlântica. A extrapolação destes resultados e modelos para uma escala espacial maior é também aqui proposta, em conjunto com a necessidade de recolher mais dados.

RÉSUMÉ

Les premières sources hydrothermales sur la dorsale médio-atlantique (MAR) ont été découvertes en 1985 (Rona et al., 1986), presque dix ans après celle des sources hydrothermales sur la ride des Galápagos (Lonsdale, 1977). Après plus de trois décennies de recherche scientifique sur ces écosystèmes extrêmes, notre connaissance de la méga- et macrofaune, qui vit dans ces habitats curieux, s'est beaucoup améliorée. Par contre, on en sait moins sur la structure des communautés et les distributions spatiales et temporelles de la faune en relation avec les facteurs biotique et abiotique. Les études écologiques prenant en compte la dimension temporelle sont indispensables afin de comprendre le fonctionnement des écosystèmes. Néanmoins, ces études sont rares pour les écosystèmes hydrothermaux et principalement limitées aux quelques sites les plus connus et les plus accessibles situés dans le Pacifique oriental (EPR et NEP). L'analyse des images est un outil important pour suivre les variations temporelles de ces environnements distants et extrêmes et ce, aussi bien dans des conditions d'émission hydrothermale continue (Hessler et al., 1985, 1988; Fustec et al., 1987; Sarrazin et al., 1997; Desbruyères, 1998) que dans le cas de nouvelles émissions, engendrées suite à une éruption (Tunnicliffe et al., 1997; Shank et al., 1998a; Tsurumi & Tunnicliffe, 2001; Shank et al., 2003; Nees et al., 2008; Marcus et al., 2009). Jusqu'à maintenant, une seule étude temporelle à long terme a été réalisée sur la dorsale médio-Atlantique; elle décrit la dynamique temporelle du site TAG, où des variations décennales ont été examinées (Copley et al., 2007a)

L'étude présentée ici est la première effectuée sur les variations écologiques à long terme à haute résolution sur la dorsale médio-Atlantique. Elle s'intéresse aux variations de la structure des communautés pendant 14 années aussi bien que la dynamique à plus court terme, sur 1-4 ans sur l'edifice Tour Eiffel, située dans le champ hydrothermal Lucky Strike, au sud des Açores, à une profondeur moyenne de 1700m.. Dans cette thèse, la distribution des assemblages, leur variation spatiale et leur zonation sur l'édifice Tour Eiffel ont été décrites en utilisant l'analyse d' images vidéos. Un protocole a été élaboré afin de permettre des comparaisons entre les années; il a été utilisée pour étudier la dynamique des communautés sur une période de 14 ans. Les tendances des variations temporelles ont été extraites. Il semble y avoir une constance décennale, bien que des changements se produisent sur des échelles de temps plus courtes et spatialement plus petites. Un modèle de succession a été proposé et le taux de changement a été évalué sur cette dorsale caractérisée par un faible taux d'écartement des plaques (MAR). Ces données ont été comparées avec celles obtenues sur une dorsale caractérisé par un taux d'écartement plus rapide (NEP). Alors que l'analyse des images a

permis de mettre en évidence les tendances temporelles et spatiales les plus importantes, un échantillonnage systématique de la faune et des caractéristiques physico-chimiques associées a permis de mieux comprendre les différences observées. Les habitats sont caractérisés par l'ampleur des fluctuations des variables environnementales, alors que la température est reconnue comme un facteur plus restrictif, qui semble expliquer la distribution spatiale distincte des assemblages de modioles et de crevettes. De surcroît, des listes d'espèces provenant d'échantillonnages passés et présents des campagnes françaises ont été extraites de la base de données Biocean (Fabri et al., 2006) et ont été analysés afin d'examiner d'éventuelles variations temporelles dans le champ hydrothermal Lucky Strike. A partir des données disponibles, aucune différence significative au niveau de la composition spécifique n'a pu être observée, ni entre les édifice, ni entre les années. Cette thèse a permis de recueillir de nouvelles données sur le fonctionnement des écosystèmes des sources hydrothermales de l'Atlantique. L'extrapolation des modèles proposés à de plus grandes échelles spatiales pourrait être possible, en autant que de nouvelles données soient recueillies.

LIST OF FIGURES

Chapter.Fig.

1.1 Global Map with known hydrothermal vent fields……4
1.2 Hydrothermal circulation at seafloor……6
1.3 Edifice formed by coalescence of various individual structures……7
1.4 Variation in faunal dominance at Mid-Oceanic Ridges……9
1.5 Link between chemosynthesis and photosynthesis……12
1.6 Main hydrothermal vent fields featuring temporal variation studies……18
1.7 Lucky Strike vent field and its main edifices……29
1.8 Hydrothermal activity features at Lucky Strike……29
1.9 Typical hydrothermal fauna inhabiting the Lucky Strike edifices……30
2.1 Localisation of Lucky Strike and the Eiffel Tower edifice……39
2.2 Faunal assemblages identification at Eiffel Tower hydrothermal edifice……44
2.3 Faunal assemblage distribution on the different sides of the Eiffel Tower……47
2.4 Ordination plot (RDA) and cluster analyses……49
2.5 Proximity to black smokers, flanges and diffusion zones……50
2.6 Zonation model……53
2.7 Idealized biological zonation of assemblages and substratum at Eiffel Tower……55
3.1 Major vent fields along the MAR and localisation of Lucky Strike and Eiffel Tower……67
3.2 Mosaic of Eiffel tower and assemblage identification……69
3.3 Variation in time of the South side of the Eiffel Tower……71
3.4 Grid-overlay and attribution of assemblages……72
3.5 Variation of hydrothermal activity throughout the years……74
3.6 Variation in percentage colonisation and link with hydrothermal activity, mussel coverage, microbial coverage……75
3.7 Percentage coverage of the different faunal assemblages and substrata over time……76
3.8 Non-metric Multi-Dimensional Scaling plots and Cluster analysis for all the sides over the years ……79
3.9 Frequencies of transfers (%) in grid-points of assemblages between the years analysed……82
3.10 Succession Model……83
3.11 The summit of the South side of the Eiffel Tower edifice over the years……92
4.1 Lucky Strike and Eiffel Tower localisation……101

4.2 Assemblage identification represented by sketches……102
4.3 Sample localities at Eiffel Tower……103
4.4 Temperature fluctuations over 10 minute time periods measured on the assemblages……...106
4.5 Boxplots of temperature and ΣS per assemblage……107
4.6 Total sulfide concentration versus temperature on the different assemblages……...109
4.7 Principle Components Analysis (PCA) based on species abundance data……110
4.8 Niche separation based on temperature measurements……110
5.1 Major known vent fields along the MAR……122
5.2 Map of the Lucky Strike vent field and image mosaics representing some
of the most well-defined edifices……123
5.3 Various markers at Lucky Strike……128
5.4 Cluster analyses of the sampled sites……130
5.5 Rank/proportion curve of species abundance……..130
5.6 Triangle plot representing beta-diversity……138
5.7 Eiffel Tower over time……139
5.8 Bairro Alto over time……...141
5.9 Sintra over time……144
5.10 Isabel over time……...146
5.11 Elisabeth over time……147
5.12 Statue of Liberty over time……148
5.Appendix Histograms of presence/absence frequencies of species……....157

LIST OF TABLES

Chapter.Fig.

1.1 Cruises and underwater vehicles that dove to the Lucky Strike vent field……...28

2.1 Composition of the faunal assemblages and substrata based on visual observations……41

2.2 Percentage colonisation of the Eiffel Tower edifice and number of activity features……..46

2.3 Dominant neighbouring patches……..51

3.1 Cruises incorporated in this study and side reconstructions possible.....……..68

3.2 Spearman rank correlations between assemblages and substrata over time……77

3.3 Percentage of colonisation and activity (sum of activity features) on each side of the edifice and periphery……..……78

3.4 Percentage of grid-points that stayed the same or changed between the consecutive years……..81

4.1 Species densities and taxonomic richness in the different faunal assemblages sampled……..105

4.2 Mean values of T°C, ΣS and CH_4 and their standard deviations……..107

5.1 Species presence/absence on the sites for which sample lists were present in Biocean……125

5.2 Sites visited during the cruises available for the Lucky Strike vent field……128

5.3 Species list of the Lucky Strike vent field alongside the species list as compiled by Desbruyères et al. (2006b)……..……..131

5.4 Species richness and number of samples for each site and year……...135

5.5 Kendall's coefficient of concordance at Eiffel Tower……..140

5.6 Kendall's coefficient of concordance at Bairro Alto……142

5.7 Kendall's coefficient of concordance at Sintra……144

5.8 Kendall's coefficient of concordance at Isabel……146

Chapter 1

Introduction

CHAPTER 1
Introduction

1. Hydrothermal vents

1.1. Past and recent discoveries

In 1976, the first hydrothermal vents were discovered. A plume was encountered at the Galápagos Spreading Centre and a towcam[1] was lowered which revealed a whole new ecosystem (Lonsdale, 1977). The existence of hydrothermal vents was already hypothesised as a logical outgrowth of plate tectonics and measurements of heat flow, however, the unusual fauna they harboured came as a big surprise (Tivey, 2007). In the subsequent years, hydrothermal vents were discovered all along the East Pacific Rise and searches expanded towards the North-East Pacific (Fig. 1.1). From the 80s onwards, hydrothermal vents were found in the Atlantic Ocean (TAG - Rona et al. 1986; and Snakepit – ODP leg 106 Scientific Part, 1986). In the same decade, hydrothermal vents were discovered in the western Pacific, starting with Manus Basin (Both et al., 1986).

About 65% the known vents are located along Mid-Oceanic ridges, with the remainder occurring in back-arc basins (22%) complemented with 12% along volcanic arcs, and 1% on intraplate volcanoes (Hannington et al., 2005). Generally, hydrothermal vents are associated with divergent plate boundaries, or spreading centres, and active convergent margins that generate island arcs, as these are two major areas of heat release leading to the formation of high temperature water activity (Tunnicliffe, 1991). However, there were also off-axis venting phenomena discovered, at the northern Gorda Ridge (Rona et al., 1990), in the Peru Basin (Marchig et al., 1999) and even more recently, in the Atlantic: a vent field called Lost City (Kelley et al., 2001).

The last ten years, greater attention has been drawn to the poles, as these could contain new species or mixes of various ocean basins. However, these latitudes do present some difficulties in carrying out marine research. At 71°N, on the Mohn ridge, the macrofauna has been described (Schander et al., 2010). More northwards, on the Gakkel Ridge, hydrothermal venting and associated fauna were localised (Edmonds et al., 2003), but identification of their fauna is awaited (Desbruyères et al., 2006b).

[1] Towed camera system that photographs the seafloor as it is towed above the ocean bottom behind an oceanographic research vessel

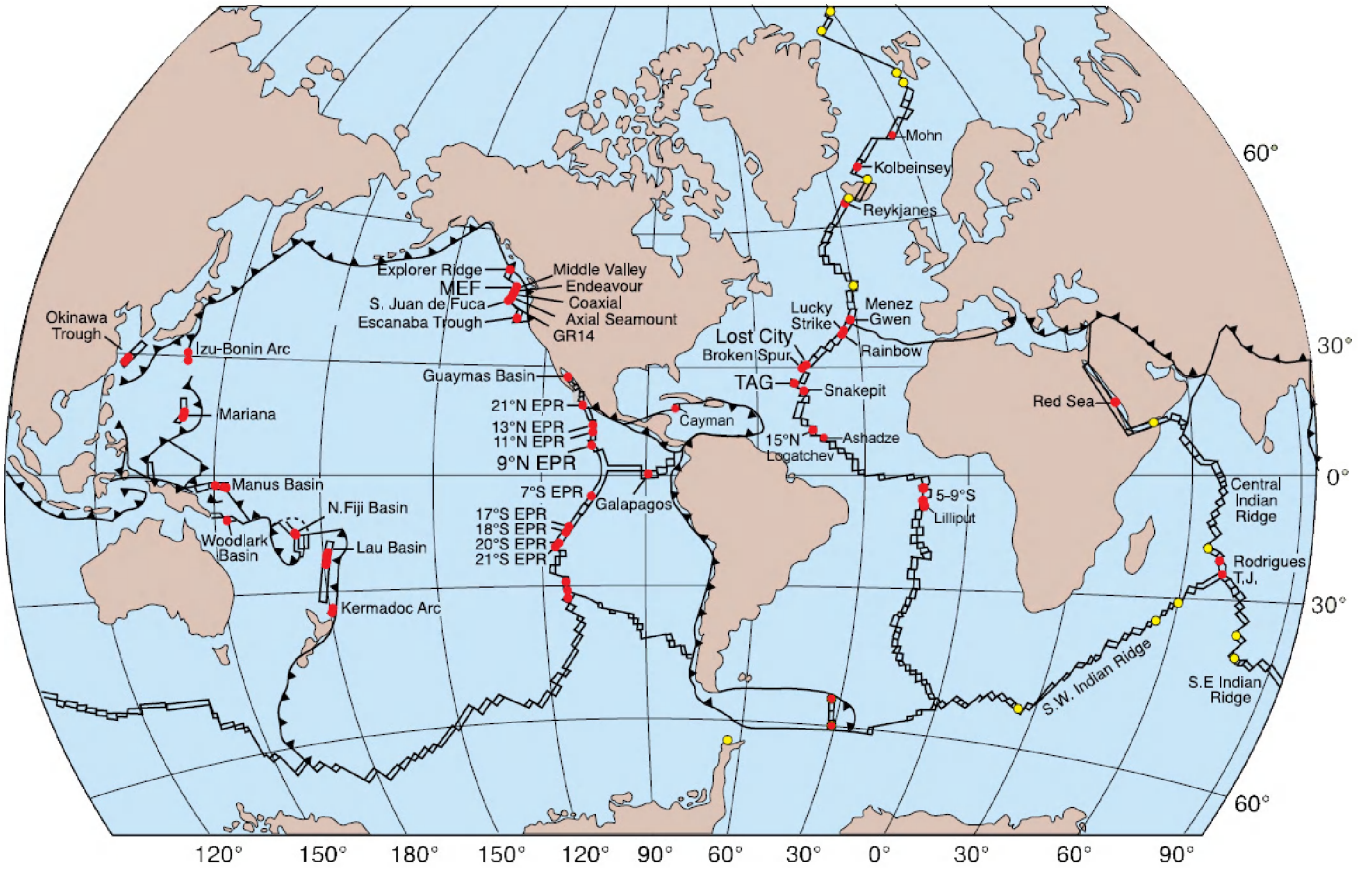

Fig. 1.1: Global map with known hydrothermal vents adjusted and updated from Tivey (2007). Red dots are the actual hydrothermal vent fields, while the yellow dots represent mid-water chemical anomalies. EPR=East Pacific Rise, MEF=Main Endeavour Field.

After over thirty years of research, less than 10% of the 60 000 km ridge crest has been investigated systematically for the presence or absence of hydrothermal activity (Baker & German, 2004; German et al., 2008b). Features used to identify or localise possible new hydrothermal vents are detection of plumes by temperature or chemical anomalies (Baker et al., 1995), coming across hydrothermally (e.g. Fe- or Mn-) enriched sediments and mineral deposits (Lalou, 1991; Juniper & Sarrazin, 1995), and for vents situated at shallower depths: water discoloration. Over the past decade, geophysical studies of the seafloor were combined with oceanographic investigations of the overlying water column, allowing prospecting for hydrothermal activity along previously unexplored sections of ridge crest (German et al., 2008a). The enrichment of hydrothermal fluids in several key chemical tracers (e.g., Mn, Fe, CH_4, H_2, He^3) relative to deep ocean waters offers an unambiguous method for detecting hydrothermal discharges in the water column even kilometres away from seafloor vent sites (Baker & German, 2004). However, the exact locality remains difficult to pinpoint, even when arriving on site and tow-yo-ing[2] with CTD's, the accuracy of localisation is restricted to a couple of hundred meters, which implies the use of Remotely Operated Vehicles (ROV) or manned submersibles to scan the area

[2] "tow" as it is towed behind the vessel and "yo" from yoyo as it is moved up and down in the water

to locate the actual origin of the plume (German et al., 2008a). Today, the continuously evolving technologies and methodologies for vent localisation get more and more refined. With the use of Autonomous Underwater Vehicles (AUV), the localisation of potentially interesting venting areas should be facilitated and diving time with ROV's and submersibles could be spent more efficiently (e.g. the discovery of hydrothermal vents in the South-Atlantic Ocean at 5°S (Devey et al. 2005, German et al. 2008b)). Recently a Hybrid Remotely Operated Vehicle (HROV) called Nereus (Woods Hole Oceanographic Institution) was developed and dove to 10 000 m depth in Mariana Trench. Nereus is unique in the sense that it can either be used as an autonomous diving robot (AUV) or as a tethered ROV allowing manipulations and sampling at great depths. This versatility could be used for hydrothermal vent discoveries and sampling in the near future.

1.2. Setting and characteristics

Mid-Oceanic Ridges (MOR) are under-water mountain ranges that are located on the boundaries between the tectonic plates that make up the Earth's crust. The heat deep within the mantle of the Earth drives the movement of the plates and the generation of new crust (Tunnicliffe, 1991). What differentiates the MOR's one from another is their spreading rate, going from ultra-slow to fast-spreading ridges. As the tectonic plates keep on moving, the MOR's keep on spreading and hydrothermal activity can emerge, shut down or re-activate. While such catastrophic perturbations occur on time scales of years to decades on fast-spreading ridges, they are far less common on slow-spreading ridges where a relative stability is observed (Lalou, 1991; Desbruyères et al., 2001). The rate in which the perturbations succeed each other has a reflection on the lifespan of the known vent fields on the different ridges. Along the slow-spreading Mid-Atlantic Ridge (MAR), the age of vent fields has been estimated between 140 000 years old (TAG sulfide mound, Lalou et al., 1993) and 45 000 years old (Lucky Strike, Humphris et al., 2002). A fact is that the hydrothermal vents are characterised by episodic activity (Lalou et al., 1993). For all of them, present-day activity tends to mask the past. For example in the Atlantic, TAG's current period of activity is less then 100 years (Lalou et al., 1993), while the current phase of activity at Lucky Strike approximates a (couple) hundred of years (Humphris et al., 2002). Contrastingly, active vent deposits at 21°N at the fast-spreading East Pacific Rise (EPR) exhibit ages from 20 to 60 years, and the fossil deposit an age around 4000 years (Lalou et al., 1984). The rate of spreading is often linked with the longevity of hydrothermal venting. Even though all vent sites are considered ephemeral habitats, some sites appear quite stable, possibly reaching a life span up to one or several decades (Desbruyères 1998; Tunnicliffe at al., 2003). Generally, the vents on slower spreading ridges appear to have a longer lifespan than those on the faster spreading ridges. Next to the difference in spreading rate and age of the vent fields on the different ridges, the spatial frequency of venting on the EPR can be as high as 1 active high

temperature site every 5 km of ridge axis (Haymon et al. 1991), while on the MAR it is on the order of 1 site every 100-350 km (Murton et al., 1994; German et al., 1996).

Around spreading centres, the ocean floor is highly permeable and cold, dense seawater penetrates the crust (Tunnicliffe, 1991). While deep-sea water percolates through the sea-bottom, it gets heated up by the underlying heat source (magma intrusions or chambers) and leaches the crust (Fig. 1.2) (Hannington et al., 1995). The hot water comes close to the boiling point and gets ejected into the cold surrounding deep-sea water where due to the temperature shock the dissolved chemicals start precipitating, slowly building chimneys and edifices (Fig. 2) (Tivey, 1995). Characteristic for the hydrothermal vents are the high temperatures (up to 400°C) and the elevated levels of sulfide, created

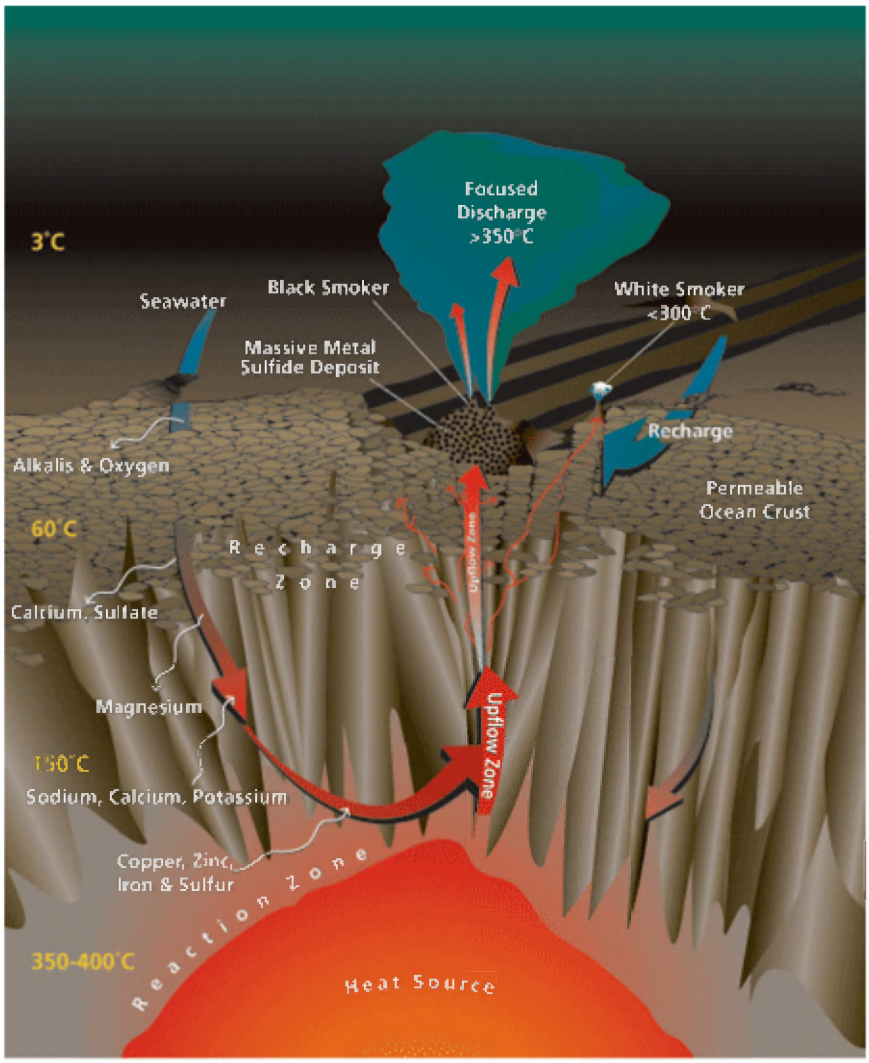

Fig. 1.2: Hydrothermal circulation at Mid-Ocean Ridges taken from Humphris & McCollum (1998). Cold seawater seeps through the permeable seafloor. It undergoes a series of chemical reactions with subsurface rocks at various temperatures to create hot hydrothermal fluid that eventually vents at the seafloor. The recharge zone is where seawater enters the crust and percolates downward, until it reaches the reaction zone at the maximum depth of fluid penetration, where the high-temperature reactions, that are thought to determine the final chemical characteristics of the hydrothermal fluid, take place. In the upflow zone, the buoyant hydrothermal fluids rise and are discharged at the seafloor.

by the geochemical interaction between hot rocks and seawater. End-member hydrothermal vent fluids are, when compared to surrounding bottom seawater, enriched in hydrogen sulfide (H_2S), hydrogen (H_2), methane (CH_4), manganese (Mn) and other transition metals (Fe, Zn, Cu, Pb, Co, Al). Mg and O are completely stripped from these end-member fluids (Alt, 1995).

A wide range of different styles of mineralization of seafloor venting has been found (Hannington et al., 2005). The simplest morphology is thus a single conduit, columnar black smoker chimney, which can form early in the evolution of a hydrothermal site (Haymon et al., 1993). However, where the individual structures coalesce, complex massive sulfide structures like edifices (Fig. 1.3) or sulfide mounds originate, which can contain multiple high temperature orifices and diffusion zones (Hannington et al., 1995). Examples of different venting styles and typical sulfide structures are the previously mentioned chimneys (the black, grey and white smokers), flanges, diffusion zones (see section 4.2, Fig. 8 for examples) and beehives. When hydrothermal fluid does not exit from a single orifice but through the entire chimney wall or from cracks or crevices, it rapidly mixes with seawater and is less concentrated. Consequently, it exhibits lower temperatures (<60°C) and is emitted as a transparent fluid. This type of venting is called a diffusion zone.

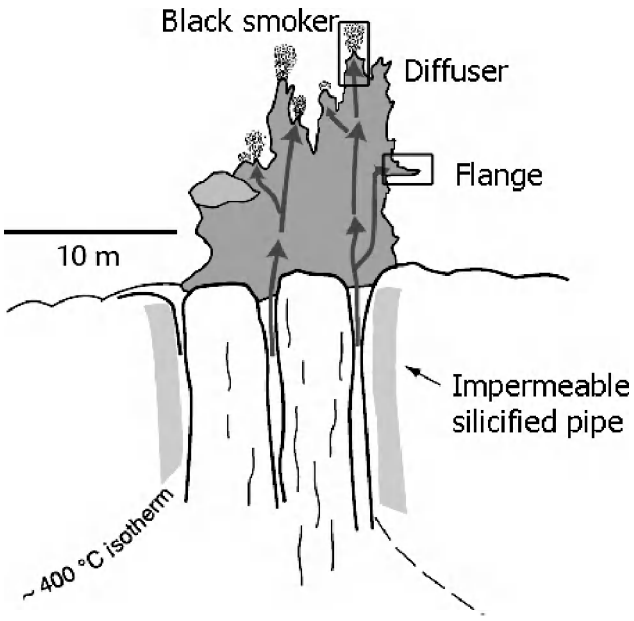

Fig. 1.3: An edifice formed by coalescence of various individual structures. Several black smokers are present as well as a flange and some diffusion. Adjusted from Tivey (2007).

Flanges and beehives are considered more complex structures of the actual black smoker morphology (Hannington et al., 1995). Flanges are accretionary structures that grow laterally from the large sulfide edifice walls (Fig. 1.3, Fig. 1.8). They tend to trap inverted pools of buoyant, high temperature hydrothermal fluid (Hannington et al., 1995), which makes them look like inversed pools or mirrors. Diffuse flow of much cooler fluids (30-80°C) happens through the top of the flange, while near ~350°C fluids overflow from the pools trapped in the flange (Hannington et al., 1995). At many other vents black smokers are capped by beehive structures featuring a bulbous outer shell with a porous interior filled by high-temperature hydrothermal fluid (Hannington et al., 1995).

When the temperature of ejected fluids is lower and fluids are not hot enough to carry sufficient metals and sulphur to the seafloor, white and grey smokers may grow at any stage in the development of a vent field (Hannington et al., 1995). It is mainly iron (Fe) (along with sulfides) that is needed to produce black smoke.

Throughout this PhD, the following terms are used to point out different scales of venting (based on Chevaldonné et al., 1997):
A "vent field" is a cluster of vent sites located a few 100 meters apart, containing several vent sites (e.g. Lucky Strike).
A "vent site" is a spatially continuous area of venting, constituted of several emissions only a few meters apart, emerging from a common network of fissures, this can be either in height or in width – edifice falls here-under (e.g. Eiffel Tower edifice)
A "vent" is a localised emission of hydrothermal fluids, often referred to as a fluid exit in this study

2. Hydrothermal vent fauna differences and specificities

2.1. Fauna

Once all the oceans were interconnected, and thus have a shared faunal history, which was followed by up to million years of ridge formation, separation and isolation (Van Dover, 1995; Tunnicliffe et al., 1996; Juniper & Tunnicliffe, 1997). These processes happened to such an extent that current day proximity of ridges and oceans might be deceiving (Juniper & Tunnicliffe, 1997). The major transform faults cutting through the ridges enhance the existing geographic separation and habitat heterogeneity. When studying the faunal composition of vent communities, the most basic pattern to emerge is an inverse relationship between faunal similarity and distance between vent fields (Hessler & Lonsdale, 1991).

Dissimilarities in vent endemic fauna are observed between the mid-ocean ridges, while only ~10% of the genera are shared between MAR and EPR. The East Pacific is characterised by the luxuriant and colourful populations of siboglinid tubeworms (*Riftia pachyptila* and *Tevnia jerichonana*, Siboglinidae), other polychaetes (Alvinellidae), limpets (Lepetodrilidae and others), clams (*Calyptogena magnifica*, Vesicomyidae) and mussels (*Bathymodiolus thermophilus*, Mytilidae) (Hessler et al., 1985; 1988; Shank et al., 1998a; Govenar et al., 2005; Lutz et al., 2008), while the Atlantic vent sites are dominated by mussels (*Bathymodiolus azoricus* and *B. puteoserpentis*), shrimps (Alvinocarididae: *Rimicaris exoculata, Mirocaris fortunata* and *Chorocaris chacei*) and polychaetes (*Branchipolynoe seepensis* and *Amathys lutzi*) (Van Dover, 1995; Desbruyères et al., 2001; 2006b) (Fig. 1.4a, c and d).

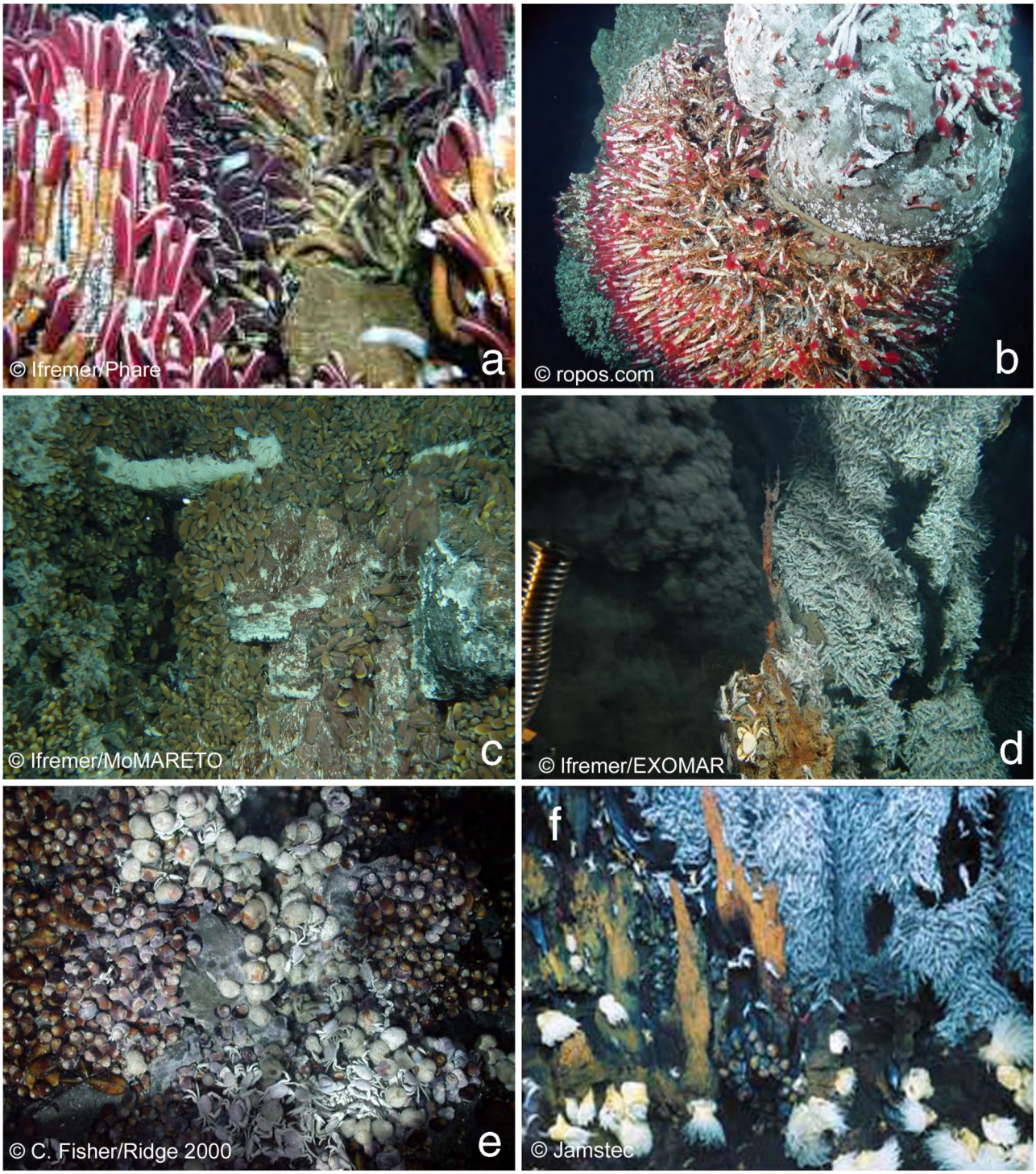

Fig. 1.4: Faunal domination at various Mid-Oceanic Ridges all over the world (a) East Pacific Rise (EPR) dominated by *Riftia pachyptila* tubeworms (b) Northern East Pacific featuring *Ridgeia piscesea* tubeworms and *Paralvinella sulfincola* alvinellid polychaetes (c) "Shallow" Mid Atlantic Ridge at 1700m of depth on the Lucky Strike vent field with the domination of *Bathymodiolus azoricus* and the presence of some alvinocaridid shrimp species (d) "Deep" MAR at TAG 3650m featuring the huge swarms of *Rimicaris exoculata* shrimps (e) Lau Basin in the West-Pacific featuring two species of snails (a hairy one: *Alvinoconcha hessleri* and a black one: *Ifremeria nautilei*) (f) Central Indian with the presence of anemones, gastropod snails and a *Rimicaris* shrimp species, showing affinity with the species from the other basins.

Western Pacific vents (e.g. Lau back-arc Basin) are characterised by hairy gastropods (*Alvinoconcha hessleri*), a black snail (*Ifremeria nautilei*) and barnacles (*Vulcanolepas* sp.) (Desbruyères et al., 2006a),

while those in the North-East Pacific are dominated by skinny tubeworms (*Ridgeia piscesea*, Siboglinidae) in association with alvinellid polychaetes (*Paralvinella sulfincola* and *P. palmiformis*) and gastropod limpets (Tunnicliffe et al., 1997; Sarrazin et al., 1997; Sarrazin & Juniper, 1999; Tsurumi & Tunnicliffe, 2001) (Fig. 1.4e and b respectively). The Central Indian ridge appears to be an intermediate between the western Pacific fauna (*Alvinoconcha*) and that of the deep Atlantic sites (*Rimicaris*) (Hashimoto et al., 2001) (Fig. 1.4f).

In many known vent sites the mussel *Bathymodiolus* sp. has a presence or even dominance in certain stage of succession (Hessler et al., 1985; Johnson et al., 1994; Gebruk et al., 2000b; Desbruyères et al., 2001; Lutz et al., 2008). It is the most wide-spread mollusc genus (Tyler & Young, 1999). It was thought to be absent at 21°N and Juan de Fuca (Tyler & Young, 1999), but McKinnes et al. (2005) reported the collection of 2 Bathymodiolinae specimens from Juan de Fuca. Although subsequent cruises did not observe any additional Bathymodiolinae, their presence does raise questions about their geographical range.

Due to these faunal dissimilarities, various numbers of biogeographic provinces have been proposed (Van Dover et al., 2002; Tyler et al., 2003; Tyler & Young, 2003; Ramirez-Llodra et al., 2007; Bachraty et al., 2009). When more provinces are considered, often the little-explored zones or missing pieces are included as "potential" new provinces (Bachraty et al., 2009). Even though the number of provinces tends to change, several distinctions are maintained throughout all the studies. The main recurring partition is the difference between the North-East Pacific and the East-Pacific Rise (Tyler & Young 2003; Ramirez-Llodra et al., 2007). Bachraty et al. (2009) take it even further and divide the East-Pacific Rise in a northern and southern part. The Indian Ocean is likely to be a new province as it shows affinities to two other provinces and it has new and unique species as well (Watabe & Hashimoto, 2002). Another difference in opinion is to divide or not divide the MAR in two biogeographic provinces (as proposed by Van Dover et al., 2002). Along the MAR, a shift in dominance with increasing depth from mussel domination to shrimp dominated vent sites is observed. Asides from the shift in dominance, there is also a shift in species composition. The mussels present in the deeper sites (>3000 m) are the species *Bathymodiolus puteoserpentis* while those present at the "shallower" sites (<2500 m) are identified as *Bathymodiolus azoricus*. There is a hybrid zone present at Broken Spur (3090 m), situated on an intermediate ridge segment almost devoid of mussels, where the mussels exhibit characteristics of both *B. azoricus* and *B. puteoserpentis* (O'Mullan et al., 2001). For the shrimps, the species (*Mirocaris fortunata* and *Chorocaris chacei*) can be present along the entire ridge (above the equator). However one species, namely *Rimicaris exoculata*, is

mainly and abundantly present at the deeper vent sites (starting at 2300 m depth) and has been sampled at one single edifice at the Lucky Strike vent field, be it in very low densities (Shank et al., 1998b; Desbruyères et al., 2001). Despite these noted differences, Bachraty et al. (2009) consider the North-Atlantic as one province based on the presence/absence of species and the proximity of the hydrothermal vent fields in a model that explained 23.3% of among-field variation.

Some remarks or nuances should be taken into account as it is very likely that in the near future our perceptions will change, definitely when new discoveries will be done on less accessible ridge systems (e.g. Arctic, East Scotia ridge etc.). In addition, increased intensity of sampling and identification of the, until now somewhat neglected, smaller faunal compartments (meiofauna) could create other perspectives for all biogeographic provinces as well, in the sense that a better knowledge about the communities is acquired possibly enlarging the variations.

2.2. Adaptations to the vent environment

Hydrothermal vents are extreme ecosystems, hence vent organisms need to be adapted to multiple varying conditions, which are mostly characterised by a broad range of fluctuations, as there are for instance high temperature fluctuations, toxic fluids and steep gradients. In addition, there are several constant "extremes", which are less of a threshold and not an extreme challenge for natural selection because of their constancy, e.g. fair depths (and consequently complete darkness (absence of sunlight) and low influx of photosynthesis-derived material). All these adaptations combined are cues for the existence of a unique vent-endemic fauna. Up to 85% of the fauna inhabiting hydrothermal vents is considered endemic (Ramirez-Llodra et al., 2007).

Temperature

The hottest temperature for vents (407°C) was recorded at 4.48°S in the South-Atlantic (Koschinsky et al., 2008). However, it is not for the warmth that vent communities concentrate around the vent openings but for nutrition (Hessler & Kaharl, 1995). In fact, most metazoans at vents live at temperatures below 20°C (Childress & Fisher, 1992; Van Dover & Lutz, 2004), which is nothing special for metazoans, but high when compared to the surrounding seawater temperature (2-4°C). Nevertheless, several vent organisms were shown to withstand high temperatures. *Alvinella pompejana* (an alvinellid polychaete) was considered to be one of the most thermotolerant eukaryotes on earth (Cary et al., 1998; Desbruyères et al., 1998). Arguably, the highest (registered) temperature limit for a macro-faunal organism was set at 105°C for *A. pompejana* (Chevaldonné et al., 1992), although later investigations and *in vitro* biochemical evidence did not support the idea of a suite of cellular

constituents adapted for life at continuously extremely high temperatures in this species (Chevaldonné et al., 2000). For other organisms, e.g. *Hesiolyra bergi* polychaetes (which live amongst alvinellid tubes), behavioural responses, such as escaping local heat pulses, rather than biochemical adaptations are thought to be sufficient (Shillito et al., 2001). Micro-organisms are most likely to withstand highest temperatures (Van Dover & Lutz, 2004), as shown by Kashefi & Lovley (2003) that put the limit of microbial thermotolerance to 121°C. Currently, the maximum pressure-temperature limits for a living organism are set at 20-120Mpa and 80-108°C for a *Pyrococcus* micro-organism (Zeng et al., 2009).

Chemosynthesis

Many organisms (e.g. non-vent deep-sea invertebrates) survive without sunlight. Organisms living at hydrothermal vents survive thanks to a mechanism called chemosynthesis whereby the oxidation of a chemical compound (sulfide or methane, etc) by micro-organisms drives chemosynthesis via creation of a proton gradient and synthesis of ATP, which is then used to drive the Calvin cycle and fix inorganic carbon (Fig. 1.5).

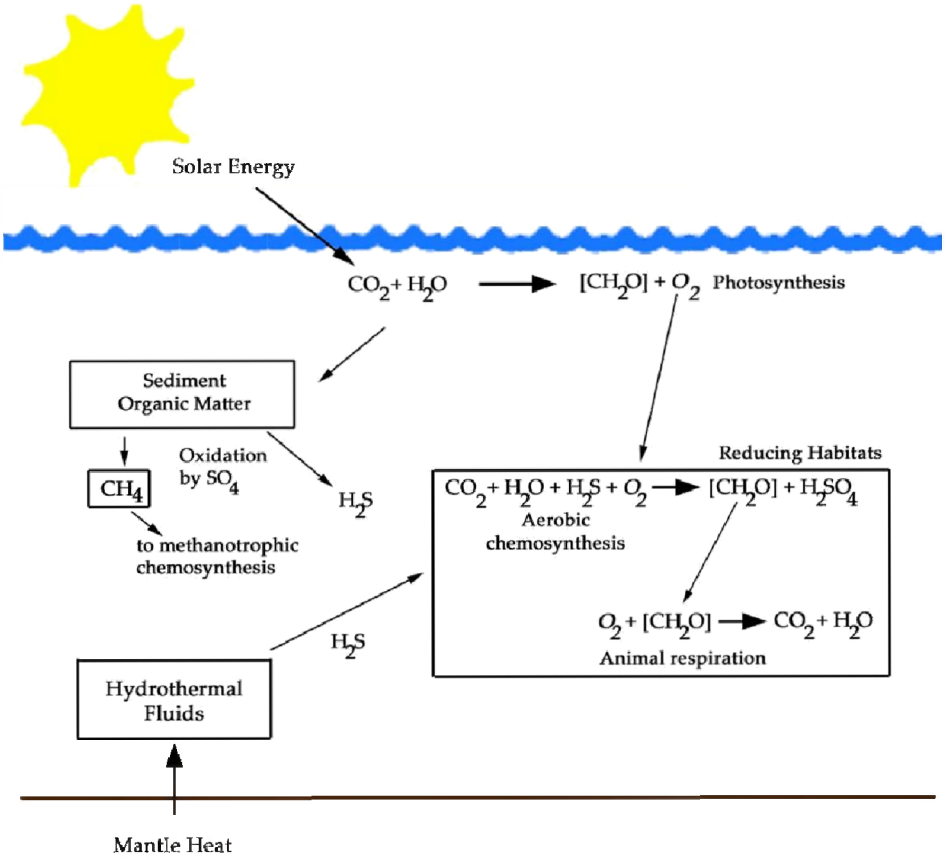

Fig. 1.5: Linking photosynthesis to chemosynthesis, showing the representative energy-consuming (chemosynthesis) and energy-producing (animal respiration) reactions in reducing habitat metabolism and their relation to solar and geothermal energy sources. Only chemosynthesis based on sulfide oxidation is shown. The requirement for dissolved O_2 links aerobic chemosynthesis and animal respiration to photosynthesis that happens in the sunlit surface ocean. Adjusted from Tunnicliffe et al. (2003).

Characteristic for hydrothermal vents are the microbial mats and microbial flocs which are responsible for the primary production by oxidizing chemical compounds (e.g. sulphur) and which form the corner stones of the local foodchain and population (Childress & Fisher, 1992). Moreover, microbes are abundant in the hydrothermal fluids, which also contribute significantly to the primary production available as food source for vent organisms. Invertebrates can be found wandering and grazing on the microbial mats. Various animals have associations with endosymbiotic bacteria which transfer H_2S in energy/ATP (Fisher, 1990). Even though these vent bacteria do not need sunlight as an energy source, they do need oxygen, which is a waste product of photosynthesis, to reduce inorganic material to organic matter (Hessler & Kaharl, 1995, see Fig. 1.5). There are also anaerobic chemoautotrophs (e.g. using tellurium as a terminal electron acceptor (Csotonyi et al., 2006)), although they do not appear to be particularly abundant in biomass and productivity.

At hydrothermal vents, there are several species that can certainly count as flagship species for these extreme ecosystems. Some examples follow.

One of the most famous vent organisms is the siboglinid tubeworm *Riftia pachyptila.* A very advanced form of adaptation to the hydrothermal vent ecosystem can be found in *Riftia,* which lacks an actual mouth and digestion system, but developed a unique organ called the trophosome which is packed with endosymbiotic, chemoautotrophic, sulphur-oxidizing bacteria (Cavanaugh et al., 1981). *Riftia* tubeworms form erect thickets when H_2S is abundantly available.

Bathymodiolus species also support a nutritional relationship with the bacterial symbionts in their gill tissue (Tunnicliffe, 1991; Colaço et al., 2002; Dupérron et al., 2006). The Atlantic species of these mytilids (*Bathymodiolus azoricus* and *B. puteoserpentis*) maintain a dual symbiosis as they have both methane-oxidizing and sulphur-oxidizing bacteria, which enlarge their feeding capacity and thus increase their niche space (Trask & Van Dover, 1999; Fiala-Medioni et al., 2002; Dupérron et al., 2006). The abundance of these two types of endosymbionts might shift depending on the microhabitat the mussels occupy and the composition of the local hydrothermal fluid (Halary et al., 2008). In addition are these mytilids capable of filter-feeding (Page et al., 1991; Tunnicliffe, 1991; Colaço et al., 2002), which allows them to survive until 5 years after vent disruption (Fisher, 1995; Copley et al., 1997). Mussel beds are also capable of diverging fluids laterally thus expanding the spatially limited zone where sulfide is available (Johnson et al., 1994).

In contrast with the vent mytilids, the other bivalve taxon present at vents, namely Vesicomyidae (*Calyptogena* spp.), have a mouth but a reduced digestive system, indicating that they largely depend on their symbionts for nutrition (Le Pennec et al., 1990) and that they seemed to have lost the capability of filter-feeding.

Species of Gastropoda (e.g. *Alvinoconcha*) have been encountered with atrophied oesophagus and digestion system but well developed (hypertrophied) gills housing symbiotic bacteria, implying chemosynthesis (Warèn & Bouchet, 1993). The limpet *Lepetodrilus fucensis*, on the other hand, has a well-developed digestive tract, but hosts a filamentous episymbiont on its gill lamellae that may be ingested directly by the gill epithelium (Fox et al., 2002; Bates, 2007).

Rimicaris exoculata is a shrimp that has episymbiotic bacteria growing on their mouthparts and on the inner surface of its branchial chamber (Van Dover et al., 1988; Segonzac et al., 1993; Van Dover, 1995; Zbinden et al., 2004). It also has a fully developed digestive system, thus they are not chemoautotrophic, but they rather graze upon their own episymbiotic or free-living bacteria (Van Dover et al., 1988; Colaço et al., 2007). These shrimp are thus dependent of exposure to hydrothermal fluid, to sustain the chemosynthetic primary production on their mouthparts or of substratum bathed in hydrothermal fluid (Copley et al., 1997). Zbinden et al. (2008) showed the presence of three metabolic types of epibionts on the scaphognathites of *Rimicaris exoculata*. As this shrimp colonises chemically contrasted environments, the relative contribution of each metabolism-type is thought to differ according to the local fluid chemical composition (Zbinden et al., 2008).

Depth

Hydrothermal vents are often situated at intermediate to great ocean depths. Shallow hydrothermal venting has been described as well (e.g. Cardigos et al., 2005) but there seem to be many differences in structure, function, evolution and biogeographical history separating the faunal communities inhabiting the shallow vents (<200m) from the deeper sites (>200m) (Tarasov et al., 2005). In other words, there seems to be little or no "vent endemic" fauna in the shallow vents (Desbruyères et al., 2006b). The deepest, populated by macrofauna, vent encountered to date is situated in the Cayman Trough at a depth of 5000m (J.T. Copley & P. Tyler, pers. comm.).

Great depths are associated with high pressure. The local pressure–temperature characteristics determine the phase separation of the seawater occurring in the ocean crust (vapour and brine) and its boiling temperature. Consequently, it also influences the rate of precipitation of dissolved and

particulate metals and sulfide and thus will have an effect on the toxicity of the vent fluids. In addition are both pressure and temperature very important for biological processes as they tend to interact (Childress and Fisher, 1992). Modifications in many biochemical systems, notably protein and lipid-based systems permit vent animals to live under conditions of high pressure (Somero, 1992). Hydrothermal vent animals thus have adaptations as to allow the physiological processes to take place under the potentially interacting extremes (McMullin et al., 2003).

Distance

If all of the above is not enough, hydrothermal vents are isolated ecosystems; they are hotspots of biomass in the otherwise "barren" deep-sea landscape. Distances in-between vent fields are large and intersected by transform faults and cannot be easily bridged. Even so, after an eruption or complete destruction of a local vent habitat and associated populations, nascent vent sites get (re-)colonised in the first year to come (Tunnicliffe et al., 1997; Shank et al., 1998a; Tsurumi & Tunnicliffe, 2001; Marcus et al., 2009). The dispersal stage of most vent organisms is a pelagic larva, as for most marine invertebrates (Tunnicliffe et al., 2003). However, there are also several vent species that brood, show direct development or have demersal larvae (reviewed by Tyler & Young, 1999). Most vent larvae are very small and free-drifting, with relatively little ability to propel themselves over significant distances by swimming; they thus appear to rely on hydrographic processes. Some marine larvae can survive for months in the water (column) and thus have a broad distribution (Tunnicliffe et al., 2003). Overall, two types of feeding behaviour exist in larvae: lecithotrophic (feeding on its proper yolk) and planktotrophic (feeding on plankton) larvae which impact dispersal potential with the plankton-feeding larvae being the most dispersive (Young, 2003). Herring & Dixon (1998) collected alvinocaridid postlarvae up to 100km's from the Broken Spur hydrothermal vents. The rising water of the smoker plumes is a buoyant plume, which is likely to transport eggs, zygotes and larvae (Tyler & Young, 2003; Mullineaux et al., 2005). Depending on the local topography it can be advected in any direction (e.g. EPR), or it can be constrained (e.g. MAR) to flow along the axis of the ridge (Tyler & Young, 2003). However, few species transgress the biogeographic provinces, let alone different ridges and ocean basins (Tunnicliffe et al., 2003).

Other

Supposedly, hydrothermal vent animals do not need eyes as there is no light penetrating that deep in the ocean. Even so, most of them do have eyes, except for the eyeless shrimp, *Rimicaris exoculata*. Meanwhile, hydrothermal vents have been shown to "glow" and to emit some kind of light (from thermal radiation, Van Dover et al., 1996a; White et al., 2002). In stead of a pair of eyes, *Rimicaris*

shrimp have a dorsal photoreceptor which could help them in finding faint sources of light (Van Dover et al., 1989). In this context, the high-intensity of submersible lights may irreversibly damage the photoreceptors of *R. exoculata* (Herring et al., 1999). However, it is impossible to measure the actual ecological impact of submersible lighting on shrimp populations without a 'dark control'. The results presented by Copley et al. (2007a) suggest no immediate effect of submersible lighting on the shrimp populations over time or threat to its survival at the TAG sulfide mound.

Next to higher temperatures and H_2S, the hydrothermal fluids also contain toxic elements like heavy metals or radionuclides that could have an impact on the faunal assemblages (Kadar et al., 2005; Sarradin et al., 2009; Charmasson et al., 2009). Hydrothermal vent organisms seem to be able to accumulate large amounts of metals without an apparent deleterious effect (Cosson & Vivier, 1997; Colaço et al, 2006; Cosson et al., 2008; Sarradin et al., 2009). Crustaceans tend to store these metals in their exoskeleton which they then shed upon moulting or ecdysis (Cosson & Vivier, 1997). *Bathymodiolus* store the trace metals (e.g. Ag, Cd, Cu, Fe, Hg, Mn and Zn) in various tissues (Colaço et al, 2006; Cosson et al., 2008). Polychaetes, on the other hand, are likely to sequestrate trace elements in insoluble, membrane-bound vesicles (Cosson & Vivier, 1997; Desbruyères et al., 1998).

3. Temporal variation and Succession at vents

A similar overview was written for Glover et al. (2010) 'Temporal Change in Deep-Sea Benthic Ecosystems: A Review of the Evidence from Recent Time-Series Studies'. *Advances in Marine Biology* **58**, 1-95

Due to their remoteness and quite often fair depths, most time-series at vents are not based on continuous monitoring but on an annual or pluriannual visits that were carried out with ROV's or submersibles. Several vent fields, however, are considered quite accessible, and often it is for those sites (e.g. the Atlantic vents) that time-series exist, be it not yet investigated. Overall, time-series studies at vents are scarce and restricted to several relatively well-known sites, mainly situated in the Pacific Ocean. There is only a single decadal-scale temporal study on the Mid-Atlantic Ridge (MAR) (Copley et al., 2007a).

Temporal evolution studies at hydrothermal vents can be divided in two types: those that started during or following an eruption (called T_0 for vents) and those that took place under continuous venting. Until now, no nascent vent development study is available for the slow-spreading Atlantic, while for the faster spreading Pacific and North-East Pacific several eruptive events were observed,

which initiated nascent vent development studies (Baker et al. 1989; Haymon et al. 1993; Tunnicliffe et al., 1997; Shank et al. 1998a; Levesque et al., 2006; Marcus et al., 2009). Several other vent fields were visited regularly, allowing a study of temporal evolution under continuous venting conditions (Hessler et al., 1985, 1988; Fustec et al., 1987; Sarrazin et al., 1997; Copley et al., 2007a).

3.1. Post-eruptive nascent vent studies

Galápagos

Rose Garden at the Galápagos Rift was the first discovered hydrothermal vent site (Lonsdale, 1977). During its first visit in 1977 with submersible Alvin (Corliss et al., 1979), this site was called "Rose Garden" because of its thickets of tubeworms, which looked like long-stemmed red roses (Fig. 1.6). In the course of the 80s, many scientific investigations were carried out on this vent field. In 2002, after 13 years of absence (i.e. without visits or sampling), Rose Garden was visited again, only to find out that its well-developed faunal communities had disappeared and apparently were buried by fresh basaltic sheet flows (Fig. 1.6, Shank et al., 2003). Ca. 300 m towards the north-west of the last known position of Rose Garden a new, nascent, low temperature site (named Rosebud) was discovered in 2002 at 2470 m depth. It contained young vent faunal assemblages, featuring small siboglinids (<6cm), bathymodiolid mussels, amphianthid anemones and vesicomyid clams that colonised cracks within a fresh, glassy basaltic sheet flow (Shank et al., 2003).

East Pacific Rise

9°50'N

In April 1991, submarine volcanic eruptions initiated the formation of numerous hydrothermal vents between 9°45 and 9°52N along the crest of the East Pacific Rise (EPR). Since this eruption, many cruises visited this region known as 9.5°N (Fig. 1.6). This eruptive event covered a large proportion of the ridge crest with a fresh basaltic sheet and wiped out the entire or a huge part of the established vent communities e.g. "Tubeworm Barbecue" (Desbruyères 1998; Lutz et al., 2001). Old vents had been buried by lava, and new ones, devoid of megafauna, were developing. One of the first temporal variation studies for nascent vents, starting from T_0 was carried out along a Biologic-Geologic transect of 1.37km long on a segment of the axial summit caldera (Shank et al., 1998a). Extensive bacterial mats surrounded new venting areas, and blanketed the fresh lava flows. The water was cloudy with apparent "floc" of bacteria (Daniel Desbruyères, pers. comm.; Haymon et al., 1993; Shank et al., 1998a). Large populations of *Bythograea thermydron* and other mobile species were observed which probably fed on increased biological production (Desbruyères, 1998). Nine months later, the "microbial" coverage had decreased (~60%) and the venting focused on restricted areas.

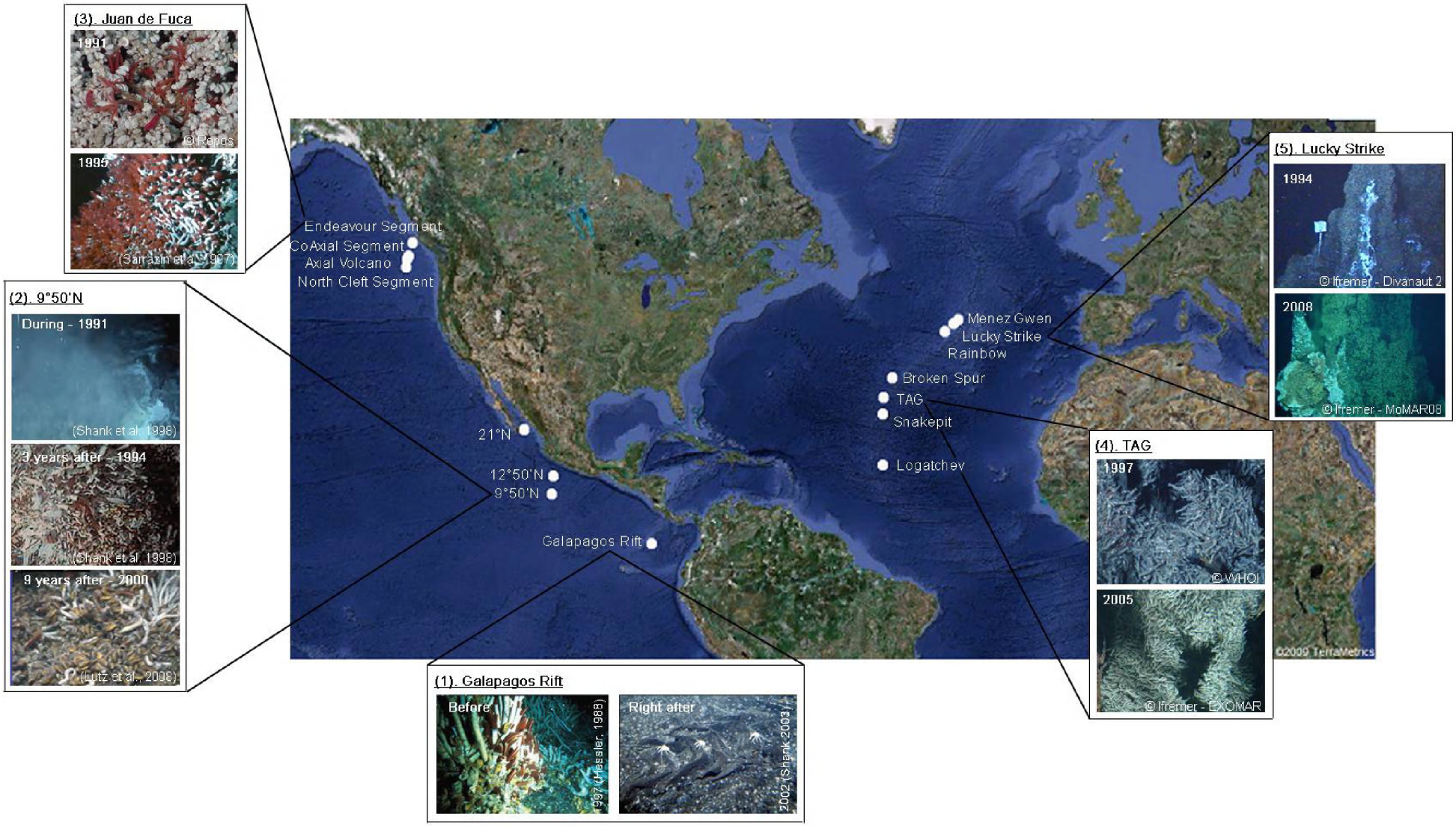
(3). Juan de Fuca
1991
© Ridge
1995
(Sarrazin et al. 1997)
(2). 9°50'N
During - 1991
(Shank et al. 1998)
3 years after - 1994
(Shank et al. 1998)
9 years after - 2000
(Lutz et al. 2008)
Endeavour Segment
CoAxial Segment
Axial Volcano
North Cleft Segment
21°N
12°50'N
9°50'N
Galapagos Rift
Menez Gwen
Lucky Strike
Rainbow
Broken Spur
TAG
Snakepit
Logatchev
(5). Lucky Strike
1994
© Ifremer - Divanaut 2
2008
© Ifremer - MoMAR08
(4). TAG
1997
© WHOI
2005
© Ifremer - EXOMAR
©2009 TerraMetrics
(1). Galapagos Rift
Before
1997 (Hessler, 1988)
Right after
2002 (Shank 2003)

Fig. 1.6: An overview of the main vent fields featuring temporal variation studies. (1) The first discovered vent site at the Galápagos Rift contained luxuriant populations of *Riftia* and was subject to a short temporal study between 1979 and 1985 (Hessler et al., 1988). However, after 13 years of absence, it was completely wiped out and covered by lava (Shank et al., 2003). (2) The first T_0 study for hydrothermal vents took place at 9°50'N on the EPR. Following an eruption in 1991, 4 years of nascent vent development were studied (Shank et al., 1998a). Settlement of pioneering tubeworms was described as well as the invasion of the mussels. It continued monitored and was subject to biological experiments until 2006 when it was obliterated by a new eruption (Lutz et al., 2008). (3) The Endeavour segment on the Juan de Fuca Ridge hosted a temporal evolution under continuous venting conditions between 1991 and 1995 (Sarrazin et al., 1997). The figure shows one of the transfers occurring between 1991 and 1995 from different assemblages dominated by 2 different species of *Paralvinella* to an assemblage featuring *Ridgeia* and large palm worms (Sarrazin et al., 1997). (4) The TAG mound on the MAR is the longest studied vent field in the Atlantic and hosted a decadal study comparing 1994 with 2004 in population densities and distribution (Copley et al., 2007a). Decadal-scale constancy was described and constancy over 20 years was hypothesised (Copley et al., 2007a). Images used are from later years, but show no significant differences in the shrimp population. (5) The Lucky Strike vent field features a photograph of the Sintra edifice in 1994 and in 2008 from a slightly different point of view, 2008 rotated about 45° counter clockwise when compared to 1994. The edifice remains active and dominated by mussels.

Numerous venting fissures were occupied by dense populations of the siboglinid tubeworm *Tevnia jerichonana* (Desbruyères, 1998; Shank et al., 1998a). By the 32nd month, extensive *Riftia pachyptila* colonies were present in each of the pre-existing *Tevnia*-colonies (Fig. 1.6) and extensive microbial mats had disappeared. Small *Bathymodiolus thermophilus* mytilids were first observed adjacent to these siboglinid clumps 10 months after *Riftia* establishment and affixed to the *Riftia* tubes 13 months later (Shank et al., 1998a). Later in the sequence, 55 months after venting initiated, the mussel *Bathymodiolus thermophilus* surrounded every surviving siboglinid colony (Shank et al., 1998a) and ultimately displaced the Siboglinidae, most likely by laterally diverging the fluids and causing H_2S depletion to the tubeworms (Lutz et al., 2008). This temporal sequence was hypothesized to correspond to a change in the temperature and chemistry of vent fluids (Shank et al., 1998a). *Tevnia jerichonana* was thus identified as a pioneering species which got replaced by thickets of *Riftia pachyptila* and later on these tubeworms were out-competed by *Bathymodiolus thermophilus* (Fig. 1.6) (Shank et al., 1998a; Lutz et al., 2008). Successful colonisation of vesicomyid clams was not observed per se, although Mullineaux et al. (1998) reported finding two individuals. A second extensive volcanic eruption occurred in January 2006 literally obliterating the entire vent site around marker 119 (deployed by Shank et al., 1998a) at 9.5°N (Lutz et al., 2008). While most of the hydrothermal vent system at 9°50'N was mussel-dominated prior to the 2006 eruption, subsequently, the vent system changed back to a tubeworm-dominated field (Nees et al., 2008). *Tevnia jerichonana* quickly colonised the newly formed vents, characterised by increased temperatures and sulfide concentrations, however it is anticipated that mussels will once again populate the local vent habitats as sulfide concentrations decrease to levels observed before the eruption (Nees et al., 2008).

North East Pacific

More up north from the EPR respectively the Gorda Ridge, the Juan the Fuca Ridge and the Explorer Ridge can be found. The Juan de Fuca Ridge (JdF) has hosted several decades of hydrothermal vent research. It is formed of seven different segments, most of them harbouring active vent sites (Baker & Hammond, 1992).

Coaxial segment

On the CoAxial Segment of the Juan de Fuca Ridge, an eruption and the consequent colonisation of a new hydrothermal vent site was observed over a two-year period (1993-1995) by Tunnicliffe et al. (1997). The eruption was caused by a dike intrusion (Dziak et al., 1995) and was characterised by a large blow-out of subsurface microbes (Juniper et al., 1995). This microbial population was shown to play a key role as macrofauna recruitment was highest at the sites with the highest microbial concentrations (Tunnicliffe et al., 1997). Seven months after the eruption, several species had colonised the active sites, despite the absence of adjacent vent communities (Tunnicliffe et al., 1997). The most abundant colonisers were *Ridgeia piscesae* tube worms, alvinellid polychaetes (*Paralvinella pandorae*) and nemertean worms. Within two years, one third of the regional pool of vent organisms was present at the site (Tunnicliffe et al., 1997). This new colonisation was linked with an increase in temperature and H_2S over the same time interval. However, not all sites seemed to thrive within the two years after the eruption, as there were also several dying sites. The suite of species where venting ceased differed from the suite observed in active areas, as the alvinellid populations were going extinct and predators (e.g. majid crabs and octopus) were observed (Tunnicliffe et al., 1997).

North Cleft segment

The northern portion of the Cleft segment, which is the southernmost segment of the Juan de Fuca Ridge, was subject to a seafloor-spreading episode during the mid-1980s, which was originally discovered by the occurrence of megaplumes and later confirmed by the formation of pillow mounds (Embley & Chadwick, 1994). A huge plume of hot water rose 800m off the bottom in 1986 and disappeared within one month and a second megaplume was identified the following year (Baker et al. 1989). This 1986 eruption provided the opportunity to observe potential successional patterns of vent fauna between 1988 and 1994 (Tsurumi & Tunnicliffe, 2001). The communities encountered in 1988 at north Cleft were very similar to those observed at the post-eruptive vents on CoAxial segment (Tunnicliffe et al., 1997) at two years after eruption: extensive microbial mats, large *Ridgeia piscesae* forming thick bushes, abundant and well-dispersed *Paralvinella pandorae* and cracks in the basalt featuring floc particulates (Tsurumi & Tunnicliffe, 2001). By 2 years post eruption, more than half of

the Cleft species pool was present on north Cleft. From 1988 to 1990, the coverage by microbial mats decreased, tubeworms became long and skinny, *P. pandorae* became smaller in size and localised, and floculated particles disappeared (Tsurumi & Tunnicliffe, 2001). Five years after the eruption, most low-temperature vents were extinguished and by 1994 all were gone. High temperature venting was maintained, nevertheless, the biological communities diminished in visual extent (Tsurumi & Tunnicliffe, 2001). Despite dramatic visual changes over time, vent sites investigated between 1988 and 1994 did not cluster by year, nor by geographic locality. It was thus hypothesised that local habitat-scale features (such as sulfide supply, food availability and competition) were determinant (Tsurumi & Tunnicliffe, 2001). It is likely that the species pool of North Cleft is adapted to episodic and frequent eruptive events on the segment. Major changes in fluid composition, resulted in no detectable community changes other than habitat loss due to a large decrease in dissolved-sulfide availability (Tsurumi & Tunnicliffe, 2001).

Axial Volcano

In 1998, intense earthquakes were observed at Axial Volcano and in the summer of the same year a new lava flow, which paved over the known faunal assemblages, was encountered (Embley et al., 1999). New venting activity of warm hydrothermal fluids (80°C) attracted a suite of hydrothermal species (Embley et al., 1999). The "nascent" post-eruptive vents were sampled for the next four years (Marcus et al., 2009). The basaltic seafloor was covered with white microbial mats, on which alvinellid and polynoid polychaetes were feeding. In June 1999, *R. piscesae* tube worms and additional consumer species started colonising the site (Levesque & Juniper, 2002). Contrary to the expectations and to what was observed on the CoAxial segment (Tunnicliffe et al., 1997), *Ridgeia piscesae* tubeworms took up to three years to recruit to all new vent sites and this despite the close presence of a source population (Marcus et al., 2009). The polychaete *Paralvinella pandorae* dominated all the present tubeworm assemblages in the first year. 30 months post-eruption, i.e. in year 3, all new vents had established tubeworms and 64% of the known Axial vent macrofaunal species had arrived (Marcus et al., 2009). Causes of the delayed and variable tubeworm recruitment remain unidentified, however mean H_2S/heat was higher at pre-tubeworm vents than at vents with first year tubeworm bushes and tended to decrease over the three years (Marcus et al., 2009). In year 2, limpets (*Lepetodrilus fucensis*) became more numerous, ending up taking over the highest abundance from *P. pandorae* in year 3 and thus dominating the communities (Marcus et al., 2009).

3.2. Temporal evolution studies under continuous venting

Galápagos

After a first visit in 1979, this site was re-visited in 1985. In this interval of five-and-a-half years' absence, considerable faunal change was revealed even though the venting pattern remained much the same (Hessler et al., 1988). Siboglinid tubeworms of *Riftia pachyptila* were luxuriant and dominated nearly every vent opening in 1979, but in 1985 their dominance got reduced to 10% of the abundance (Hessler et al., 1988). On the other hand, the mytilid *Bathymodiolus thermophilus* seemed to thrive as it became dominant in the vent community (Hessler et al., 1988). The galatheid *Munidopsis subsquamosa* also increased considerably in numbers, although it also lives on the non-vent terrain so the increase could have been the result from immigration (Hessler et al., 1988). Same goes for the whelk *Phymorhynchus* sp., which lives in the periphery and at dying vent fields and whose density increased as well (Hessler et al., 1988). By 1985, the clam population increased and by 1988, the population of *Calyptogena magnifica* had grown dramatically and surrounded the mussel beds probably due to a decrease in fluid flow (clams are able to insert their foot in cracks to pump the sulfide) (Desbruyères, 1998). A decrease in the filter-feeders (anchored siphonophores, serpulids, and anemones) between the subsequent visits was observed (Hessler et al., 1988; Desbruyères, 1998). Between 1985 and 1990, the community changed very little, although the peripheral fauna had moved increasingly into the active area (Desbruyères, 1998).

East Pacific Rise

12°50'N

This vent field at 12°50'N is often referred to as 13°N and contains a complex set of active vent sites. Temporal variations between 1982 and 1984 were analysed by Fustec et al. (1987) on 3 sites. The main variations noticeable were growth or regression of *Riftia* and of the active sulfide edifices, the disappearance of individuals (not quantified), lava collapses (Fustec et al., 1987) and migration of *Alvinella pompejana* along the edifice walls (Desbruyères, 1998). Between 1984 and 1987, a rearrangement of subsurface circulation led to the collapse of two active sites and the reactivation of a previously dead area, while some sites situated within 100m were not affected (Desbruyères, 1998). In 1984 the Genesis edifice showed no temperature anomaly and only featured a small clump of small-sized mussels and some groups of rusty and empty tubes of the siboglinid *Tevnia jerichonana*. By 1987, however, it seemed reactivated with warm water venting (<23°C) and extensive microbial mats surrounded the vent opening. The fauna was dominated by the vent crab *Bythograea thermydron* and widespread populations of *T. jerichonana* mixed with young individuals of *Riftia pachyptila* (Desbruyères, 1998). Three years later, the extensive *T. jerichonana* population had collapsed and was

replaced by small clumps of *R. pachyptila*. Active sulfide edifices up to 5 m high developed and were colonised by large alvinellid populations dominated by *Alvinella pompejana* (Desbruyères, 1998). In 1991 and 1992 stabilisation of venting conditions was observed and the previously described characteristics did not fundamentally change (Desbruyères, 1998). By 1996, several chimneys did collapse, emphasizing the rather short lifespan (ca. 5 years) of smokers in this vent field (Desbruyères, 1998).

21°N

A 21°N site, called Clam Acres was visited in 1979, 1982 and 1990 (Desbruyères, 1998). As the name suggests, this site was dominated by *Calyptogena magnifica*, which lived together with *Riftia pachyptila* in varying proportions, while *Bathymodiolus thermophilus* was missing (Hessler et al., 1985). The clams tended to dominate the flat parts of the vent field, where the individuals were concentrated in cracks between basalt pillows (Hessler et al., 1985). The vent openings of the chimneys of this site were populated by dense stands of large *Riftia*, sometimes incrusted with limpets. The main shaft of the edifices were colonised by the mineralised tubes of the *Alvinella pompejana* polychaete (Hessler et al., 1985). According to the dissolution rates of the clam shells originating out of beds of dead clams, the segment has been active for at least 300 years (Kennish & Lutz, 1999). Peripheral venting areas yielded higher percentages of dead shells (Hessler et al., 1985). The comparison of venting patterns and community distribution between 1979 and 1990 demonstrates temporal stability at a decadal scale (Desbruyères 1998).

North-East Pacific

Axial Volcano

Vent species on the Axial Volcano appear to be distributed along a horizontal gradient that lies from the centre to the periphery of the vent site (Marcus & Tunnicliffe, 2002). This zonation changes with increasing distance from the vent openings. Along this gradient *Ridgeia piscesae* is more typical for the centre flow areas and the alvinellid polychaetes, *Paralvinella pandorae* and *Paralvinella palmiformis* tend to disappear towards the peripheral zones, while the gastropods (*Lepetodrilus fucensis* and *Depressigyra globulus*) are distributed quite evenly although the relative abundance of *L. fucensis* tends to increase towards the periphery (Marcus & Tunnicliffe, 2002). In 1986, a time-lapse camera was deployed over periods of 1, 5 and 26 days on the Mushroom vent, a venting area on the Axial seamount. The most striking phenomenon was the rapid growth and collapse of anhydrite spires which may have caused the mortality of 44% of the *Ridgeia piscesae* tube worms studied within the 26-day period (Tunnicliffe,

1990). Mass removal of animals by falling chimney fragments or landslides may be common in the vent habitat and significantly impact the vent communities (Tunnicliffe, 1990; Sarrazin et al., 1997).

Endeavour

On a large hydrothermal edifice of the Main Endeavour field, called S&M, six distinct faunal assemblages were recognised, which formed repeating mosaics according to changing physico-chemical conditions (Sarrazin et al., 1997; 1999). Four communities contained the siboglinid tubeworm *Ridgeia piscesae*, which differed one from another in tube length and associated species (Gastropoda and Polychaeta) and two communities contained only alvinellid polychaetes (*Paralvinella sulfincola* and *P. palmiformis*) (Sarrazin et al., 1997). Community dynamics were monitored over 4 years (between 1991 and 1995, during which five visits were carried out, 2 in 1991, 1 in 1994 and 2 in 1995) (Fig. 1.6). The relative abundance or percentage coverage of the different communities varied over the different time intervals (3 and 1 year), in which several communities colonised previously inhabited surfaces. Dense patches of *P. palmiformis* with *Lepetodrilus fucensis* limpets and snails (*Provanna vanabilis* and *Depressigyra globulus*) (Fig. 1.6) as well as the assemblage of apparently dead or unhealthy brown-coloured tubeworms increased substantially (Sarrazin et al., 1997); the latter might be an indication of a local waning fluid supply. *Paralvinella sulfincola* is considered a primary coloniser of new high-temperature surfaces (Juniper et al., 1992; Sarrazin et al., 1997). All the identified assemblages appear to represent different successional stages where the transfers are primarily initiated by variations in hydrothermal fluid flow and substratum porosity. The progressive mineralization of hydrothermal edifices thus contributes to fluid flow modification at small spatial scales and faunal succession proceeds as the substratum matures (Sarrazin et al., 2002). As mineralization and succession progress on the edifice, the influence of other biotic factors such as predation and competition, are thought to become more apparent (Sarrazin et al., 2002). Throughout the succession patterns, abiotic factors appear to predominate in the early stages, i.e. in the assemblages characterised by the presence of *Paralvinella* polychaetes, while biotic factors seem to modulate later stages such as the *R. piscesae* tubeworm assemblages, where the tubes can be regarded as a secondary surface for other organisms to occupy (Tunnicliffe et al., 1997; Sarrazin & Juniper, 1999; Sarrazin et al., 2002). Biotic processes interact with the abiotic conditions thus driving succession patterns (Sarrazin et al., 1997; 2002).

Mid-Atlantic Ridge

TAG sulfide mound

The TAG (Trans-Atlantic Geotraverse) sulfide mound lies within the deep Mid-Atlantic (3600m depth) and was the first discovered hydrothermal vent in the Atlantic Ocean. Consequently, it hosts the

longest-studied vent community on the MAR (Rona et al., 1986) as well as the only Mid-Atlantic long-term variation study. Decadal-change was assessed between 1994 and 2004 of the distribution and abundance of the fauna that occupies the central chimneys and the periphery on the upper terrace of the mound (Copley et al., 2007a). No significant difference in the coverage and abundance of the shrimp *Rimicaris exoculata* (characteristic for the central chimneys, Fig. 1.6) and the sea anemone *Mariactis rimicarivora* (distributed more peripherally) were observed over that period. Hence decadal-scale constancy in community structure was displayed at TAG (Copley et al., 2007a). Although not quantified, similar distributions of these species were also noted in 1985 (Rona et al., 1986), suggesting this constancy may have persisted over two decades. This decadal constancy coincides with a steadiness in physical parameters at similar timescales: the geochemistry of high-temperature vent fluids appears to have been invariant over 10 years (Parker et al., 2005). In 1994, a time-lapse video camera was deployed for 9 months in the NE quadrant of the TAG mound, where it assessed shorter time-scale changes as well as the effects of an ODP drilling (Copley et al., 1999). The drilling operation induced a rise in seafloor temperature and dense aggregations of vent shrimps appeared in this quadrant while the distribution of sessile species remained more or less the same (Copley et al., 1999). This trend, however, was transient and shrimp densities returned to 'baseline' densities even before the temperature returned to pre-drilling levels and the central black smoker complex remained the focal point of high-temperature hydrothermal discharge at TAG (Copley et al., 1999). By 2004, the NE quadrant of the mound had returned to relative quiescence, with aggregations of shrimp no longer present (Copley et al., 2007a).

Broken Spur

Contrarily to the dense aggregations of *Rimicaris exoculata* observed at the TAG and Snake Pit sites, the Broken Spur vent field (3100m depth) revealed *R. exoculata* to be present but not in such dense "swarms". The possible restricting factor in shrimp densities appeared to be the presence of suitable substratum exposed to hydrothermal fluid flow (Copley et al., 1997). Such a habitat was not available at individual chimneys, where the fluid is expelled at the summit and consequently appears to lead to absence or reduced *R. exoculata* aggregations (Copley et al., 1997). Similar observations were made at the Logatchev vent field, which is also situated in the deep Atlantic (Gebruk et al., 2000b). When such habitat was available, for example at the Bogdanov site (Broken Spur), where the summit was broad and flat and the substratum gets washed by the hydrothermal fluids, "swarms" of shrimps were found (Copley et al., 1997). It was hypothesised that low faunal abundances in an otherwise active and established hydrothermal field might be due either to a recent reactivation after a period of quiescence, or to a catastrophic event which reduced faunal abundance drastically (Murton et al.,

1995). Within this last scenario, the vent community would still be recovering from such a disturbance, with animals just arriving to recolonise the system (Van Dover, 1995). The interannual variation in the faunal distribution at Broken Spur did not immediately suggest that the community was recovering from a disturbance but rather that the low population density of shrimp represented a "climax" state in the sense that there was little optimal habitat available (Copley et al., 1997). However, this did not remove the possibility that Broken Spur had undergone such a period, or several such periods, during its geological past (Copley et al., 1997).

Rainbow

Rainbow vent field (2300m) could be regarded as intermediate between deep and shallow MAR fields. It harbours tall sulfide chimneys which host *R. exoculata* aggregations and *B. azoricus* assemblages, but both in lower densities than in respectively deeper and shallower hydrothermal vent sites. More recently, hydrothermal activity within this vent field appeared to be waning. In 2006, most mussel beds were gone and shrimp aggregations were less abundant than in previous years.

Menez Gwen and Lucky Strike

Lucky Strike is the vent field on which lays the main focus in this study and is described more in detail in section 4.2. Fauna-wise, Lucky Strike and Menez Gwen are the most similar of all MAR vent sites (Desbruyères et al., 2001). Contrastingly to Lucky Strike, there are no real edifices at Menez Gwen and due to the shallower depth there is an increased invasion of surrounding bathyal fauna possible, e.g. the crab *Chaecon affinis* is observed (Colaço et al., 1998). Large amounts of limpets (among others *Lepetodrilus atlanticus* and *Protolira valvatoides,* Desbruyères et al., 2001; 2006b) are present on the mussel shells beds at Menez Gwen as well as on bare surfaces. Menez Gwen is thought to be younger than Lucky Strike (Charlou et al., 2000; Desbruyères et al., 2001) and might be regarded as an immature snapshot of the latter.

3.3. Nascent vs. continuous venting contrasts

When investigating community dynamics under conditions of continuous venting, i.e. not after a major disturbance or eruption, other factors intervening in the assemblage mosaics, like biotic interactions and small-scale, short-term abiotic changes tend to get highlighted. However, biotic interactions remain difficult to quantify and it is even harder to unravel the relative contributions of the different processes in shaping faunal communities when we only observe them at a certain point in time. Past environmental regimes have been shown to leave an imprint on the structure and succession of communities (Mullineaux et al., 2009). In addition, we still depend on – in the best case -

yearly visits, while sub-annual processes are likely to play a role as well, which is emphasised by the deployment of time-lapse cameras (Tunnnicliffe et al., 1990; Copley et al., 1999). Only high frequency investigations, with for instance cabled or year-round observatories, could enlighten us on natural change, successional patterns and possible anthropogenic impacts.

4. The Atlantic as a study site

4.1. Atlantic

The known hydrothermal vent fields on the MAR are often separated by several hundred kilometres and cut off by major transform faults. These faults enhance the existing geographic separation and habitat heterogeneity. A big part of the northern MAR (15-35°N) has been monitored for two years for seismic events (Smith et al., 2003). A significant variability in event rate along the axis of the MAR was observed and groups of neighbouring segments appeared to behave similarly, producing an along-axis pattern with high and low levels of seismic activity (Smith et al., 2003). Moreover, due to the differences in water depth, the geology of source rocks and the nature of the hydrothermal deposits, vent habitats among MAR fields vary in their fluid chemistry (including particulate content) and mineral deposit pattern (Desbruyères et al., 2000). This leads to a distinction between deeper (>3000m) and shallower vents (<2300m), described in section '2.1 Fauna'.

4.2. Lucky Strike

Lucky Strike vent field (37°17.5'N, 32°16'W) was discovered serendipitously during the French-American FAZAR cruise in 1992. Scientists dredged haphazardly along the MAR, looking for vents, and the dredge basket returned from a depth of 1600m filled with live mussels and fresh sulfide. Due to its remarkable random discovery it was named Lucky Strike. The subsequent year (1993) a return cruise was organised and a field of vents was found. Lucky Strike is situated within the Portuguese EEZ and can be considered rather accessible, as confirmed by the high numbers of returning visits, adding up to a total 20 cruises with submersibles or ROV's by 2009 (Table 1.1).

More in detail is Lucky Strike situated in the Azores Triple Junction area at a mean depth of 1700m. It consists of a large lava lake (ca. 200 – 300 m diameter) surrounded by three volcanic cones that form the present day summit of the volcano (Fig. 1.7; Ondréas et al., 2009). The numerous active vents are located mainly in the north-western and south-eastern zones around the lava lake (Fouquet et al., 1995; Charlou et al., 2000; Humphris et al., 2002; Ondréas et al., 2009; Fig. 1.7). It is a basalt hosted site (Langmuir et al, 1997; Fouquet et al., 1998; Desbruyères et al., 2000).

Table 1.1: Cruises and their underwater vehicles, with the exception of the discovery cruise, that have been diving to the Lucky Strike vent field. The cruises marked in grey were included in the presented study.

YEAR	Cruise	Research vessel	Underwater vehicle	Chief scientist(s)	Organising country
1992	FAZAR	Atlantis	-	C.H. Langmuir	US, FR
1993	ALVIN	Atlantis	Alvin	C.H. Langmuir	US
1994	DIVA 1	Nadir	Nautile	Y. Fouquet	FR
1994	DIVA 2	Nadir	Nautile	D. Desbruyères & A-M Alayse	FR
1996	LUSTRE '96	Knorr	Jason/ARGO II	D. Fornari & S. Humphris	US
1997	FLORES	L'Atalante	Nautile	D. Desbruyères & A-M Alayse	FR
1997	MAR'97	Atlantis	Alvin	B. Vrijenhoek & R. Lutz	US
1997	MARVEL	L'Atalante	Nautile	Y. Fouquet	FR
1998	PICO	Nadir	Nautile	D. Desbruyères	FR
2001		Atlantis	Alvin	C.L. Van Dover	US
2001	ATOS	L'Atalante	ROV Victor 6000	P.M. Sarradin	FR
2002	SEHAMA 1	L'Atalante	ROV Victor 6000	F. Barriga	PT, FR
2002		Akademik Mstislav Keldysh	Mir I & II		RU
2003	Meteor M58-3	Meteor	ROV Quest	Gerrit Meinecke	DE
2005	EXOMAR	L'Atalante	Nautile	A. Godfroy	FR
2006	GRAVILUCK	L'Atalante	Nautile	V. Ballu	FR
2006	MOMARETO	Pourquoi Pas?	ROV Victor 6000	P.M. Sarradin & J. Sarrazin	FR
2008	MAR2008 knoxrr18	R. Revelle	ROV JASON 2	A.-L. Reysenbach	US
2008	MoMAR08	L'Atalante	ROV Victor 6000	J. Escartin	FR
2009	Bathyluck	Pourquoi Pas?	ROV Victor 6000	J. Escartin, M. Cannat	FR
2009	LUSO-EMEPC	Gago Coutinho	ROV LUSO	N. Lourenço	PT

Slabs are present in this area with cracks from which vent fluids originate (Langmuir et al., 1997; Ondréas et al., 1997). Underneath these slabs, a subsurface circulation of hydrothermal fluids occurs, allowing a subsurface biological production. Flocs of bacterial mats have been observed, emerging from cracks and warm vent openings (Desbruyères et al., 2000). The vents grow mostly through the hydrothermally cemented volcanic breccia, referred to as "slab", while the surrounding seafloor is sedimented and cut by a dense network of fissures and scarps (Ondréas et al., 1997; 2009).

There are two sources of hydrothermal fluids separating the north-western and north-eastern vents (White Castle, Helene, Bairro Alto, Elisabeth, Y3, Statue of Liberty and Sintra) from those in the south-east (i.e. Isabel, Eiffel Tower and Montsegur, Fig. 1.7) (Langmuir et al., 1997; Von Damm et al, 1998; Charlou et al., 2000; Humphris et al., 2002). The south-eastern vents are significantly different from the others and show the lowest chlorinity values and significant differences in other chemical parameters (Von Damm et al., 1998; Charlou et al., 2000). Due to the depth and the phase separation Lucky Strike has metal depleted - gas enriched fluids except for H_2S and He_3 (Wilson et al., 1996; Charlou et al., 2000).

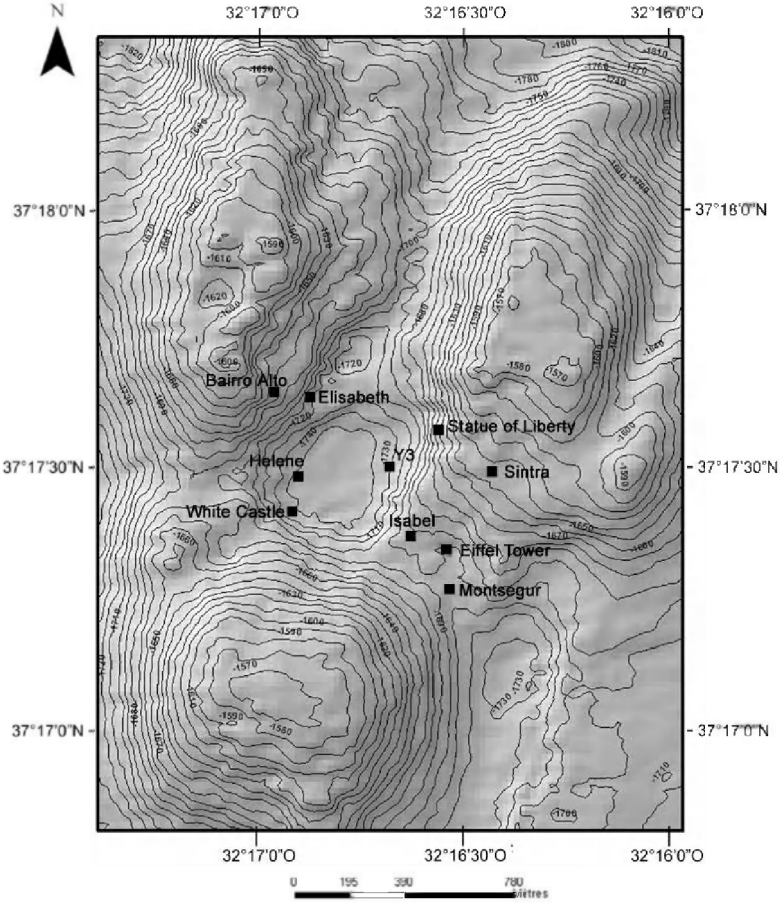

Fig. 1.7: Lucky Strike vent field, with the central lava lake and the summits of the seamount surrounding it. The main active edifices are indicated.

Lucky Strike vent fluid compositions are generally within the range observed elsewhere (Von Damm et al., 1998). The metal end-members (Fe, Mn, Cu, Zn & Si) as well as chloride and hydrogen in the hydrothermal fluids are low if compared with other deeper hydrothermal vent sites, as a consequence, Lucky Strike fluids are considered 'less toxic' (Desbruyères et al., 2000). They show most similarities to fluids from the Endeavour Segment and especially to those from Axial volcano (Von Damm et al., 1998), with whom Lucky Strike also shares an analogous geotectonic setting (Wilson et al., 1996; Humphris et al., 2002).

The activity features at Lucky Strike consist of black smokers (up to 324°C), active flanges (<200°C) and diffusion zones (~60°C), the latter is characterised by shimmering water (Langmuir et al., 1997; Sarradin et al., 1999; Charlou et al., 2000) (Fig. 1.8).

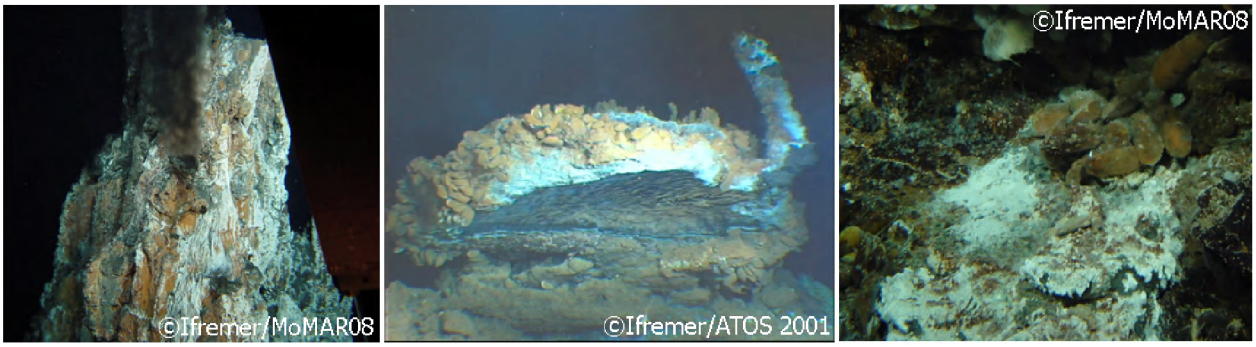

Fig. 1.8: The most common activity features of the Lucky Strike vent field going from (left to right) black smokers, to flanges and diffusion zones. For an explanation of these activity features see section 2.1.

Eiffel Tower is a well-defined and one of the most active hydrothermal edifices at Lucky Strike, located in the south-eastern region of the vent field (Fig. 1.7). It is a complex 11 m high sulfide edifice. During the French and Portuguese cruises, incorporated in this study (Table 1.1) over 744 hours of video footage and about 6175 high definition pictures, spanning 14 years of research cruises at the Lucky Strike vent field were available. From the 744 hours of diving and imagery recording time at Lucky Strike, ca. 297.5 hours (~40%) were solely attributed to Eiffel Tower.

The fauna of Eiffel Tower is considered to be representative for the entire vent field (Desbruyères et al., 2001). Similar to other hydrothermal active structures at shallower depths in the Atlantic Ocean, it is covered with dense mussel beds of the mytilid *Bathymodiolus azoricus* Cosel and Comtet, 1998 (Fig. 1.9, Van Dover, 1995; Langmuir et al., 1997; Comtet & Desbruyères, 1998; Desbruyères et al., 2000, 2001). In association with these mussel beds live several decapod species, namely alvinocaridid shrimps (*Mirocaris fortunata* (Martin and Christiansen, 1995), *Chorocaris chacei* (Williams and Rona, 1986), *Alvinocaris markensis* Williams, 1988) and a bythograeid crab (*Segonzacia mesatlantica* (Williams, 1988)) and many other less conspicuous species, like polychaetes and limpets (Desbruyères et al., 2006b) (Fig. 1.9).

Fig. 1.9: A photo showing the typical fauna harboured by the Eiffel Tower hydrothermal edifice and by the entire Lucky Strike vent field. It is dominated by *Bathymodiolus azoricus* mussels and alvinocaridid shrimp (in this photo: *Mirocaris fortunata*). It also features the crab *Segonzacia mesatlantica* and some polynoid polychaetes, which are recognisable by their red-pink colour.

5. Aims and thesis outline

The main objective of this PhD is to investigate the temporal variations in the community dynamics of chemosynthetic environments and more specifically of the hydrothermal vents of the Lucky Strike

vent field in the Atlantic. A unique time-series of more than 14 years of imagery is analysed, representing the first long-term high-resolution study on the hydrothermal vents along the Mid-Atlantic Ridge. The use of image analysis as a tool for assessing temporal change has already proven its value (e.g. Sarrazin et al., 1997; Shank et al., 1998a; Copley et al., 2007a). Since the discovery of hydrothermal vents in the late 1970s, research on these remarkable ecosystems evolved at a quick pace. Although our knowledge of the communities inhabiting these extreme environments has greatly improved; their long-term dynamics remain unclear.

The overall hypothesis, as defined by the gaps in our ecological knowledge of vent systems, is that the distribution and dynamics of hydrothermal faunal assemblages on a continuously-venting structure are invariant in settings of different spreading rates. This hypothesis breaks up in two parts, focusing on the spatial and on the temporal scale. For the temporal one, the main question is the following: are the community dynamics on a continuously-venting structure on a slow-spreading ridge the same as those deduced for faster-spreading ridges?

In **Chapter 2** the distribution and spatial variation of hydrothermal faunal assemblages at Eiffel Tower is presented. The identification of the faunal assemblages and substrata is explained in detail as well as the image analyses protocol developed for analysing faunal coverage. Possible drivers for the spatial variation are discussed. This chapter was published as **Cuvelier D., Sarrazin J., Colaço A., Copley J., Desbruyères D., Glover A., Tyler P., Serrão Santos R. (2009).** Distribution and spatial variation of hydrothermal faunal assemblages at Lucky Strike (Mid-Atlantic Ridge) revealed by high-resolution video image analysis. *Deep-Sea Research Part I – Oceanographic Research Papers* 56, 2026–2040

Chapter 3 describes the community dynamics over 14 years at the Eiffel Tower hydrothermal edifice. The method explained in detail in Chapter 3 is employed for all the years available in the time-series. Temporal variations of the faunal assemblages and substrata are described at various scales, going from the entire edifice to the different sides and small patch-dynamic scales. Consecutive years are compared as well as decadal scale changes. A first succession model for the "shallower" Atlantic vents is presented. This chapter was accepted for publication as **Cuvelier D., Sarrazin J., Colaço A., Copley J.T., Glover A.G., Tyler P.A., Serrão Santos R., Desbruyères D.** Community dynamics over 14 years at the Eiffel Tower hydrothermal edifice on the Mid-Atlantic Ridge. Manuscript accepted for publication in *Limnology & Oceanography*

Chapter 4 intends to characterise the previously imagery-based identified faunal assemblages at Eiffel Tower, and their associated microhabitats. It combines biological and chemical sampling, wielded to better characterise and discuss the previously delineated microhabitats based on the models presented in Chapters 2 and 3. This chapter has been accepted to be published as **Cuvelier D., Sarradin P.-M., Sarrazin J., Colaço A., Copley J.T., Desbruyères D., Glover A.G., Serrão Santos R., Tyler P.A (*in press*)**. Hydrothermal faunal assemblages and habitat characterisation at the Atlantic Eiffel Tower edifice (Lucky Strike vent field). *Marine Ecology*

Chapter 5 deals with species distribution over time within the Lucky Strike vent field. Various edifices within the vent field were repeatedly sampled over the years and picked-out samples lists have been stored in the Biocean database. The influence of both time and locality on the species composition is investigated and described.

In **Chapter 6** a general synthesis is presented, tying all the chapters together.

Chapter 2

Distribution and spatial variation of hydrothermal faunal assemblages at Eiffel Tower

Published as:

Cuvelier D., Sarrazin J., Colaço A., Copley J., Desbruyères D., Glover A., Tyler P., Serrão Santos R. (2009). Distribution and spatial variation of hydrothermal faunal assemblages at Lucky Strike (Mid-Atlantic Ridge) revealed by high-resolution video image analysis. *Deep-Sea Research Part I – Oceanographic Research Papers* 56, 2026–2040

CHAPTER 2
Distribution and spatial variation of hydrothermal faunal assemblages at Eiffel Tower

1. Introduction

Two decades of research on deep-sea hydrothermal vents in the Atlantic Ocean have led to a reasonably good knowledge of the mega-and macro-fauna inhabiting these chemosynthetic habitats. Rather less is known about the community structure and the spatial and temporal distributions of the fauna in relation to abiotic and biotic factors. In particular, small-scale and detailed spatial distribution studies for the Atlantic hydrothermal vents have been scarce. On the other hand, large-scale variations between Atlantic vent fields, have already been investigated (Desbruyères et al., 2000; 2001).

The most important structuring factor for the composition, distribution and dynamics of deep-sea hydrothermal vent assemblages appears to be the high spatial variability of biotic and abiotic factors related to hydrothermal vent activity and more specifically, the chemical composition and flow intensity of the vent fluids (Hessler et al., 1988; Tunnicliffe, 1991; Sarrazin et al., 1997; Shank et al., 1998a; Desbruyères et al., 2001; Luther et al., 2001; Govenar et al., 2005). Consequently, alteration of fluid composition or cessation in fluid flow causes small-scale disturbances on short time-scales and can initiate significant faunal changes (Hessler et al., 1985; 1988; Fustec et al., 1987; Tunnicliffe, 1991; Sarrazin et al., 1997; Shank et al., 1998a). Biological interactions are also thought to affect the hydrothermal vent community composition (Fustec et al., 1987; Hessler et al., 1988; Tunnicliffe, 1991; Johnson et al., 1994; Shank et al., 1998a; Sarrazin et al., 1999; Mullineaux et al., 2003; Govenar et al.; 2005). Typical examples of biological interactions are predation and competition based, for instance, on trophic (e.g. access to hydrogen sulfide or other resources) and topographic (optimal positioning on the structure or limitation in available space) grounds (Hessler et al., 1985; Fustec et al., 1987; Comtet & Desbruyères, 1998). Food partitioning is likely to play a significant role (Levesque et al., 2006; Limen & Juniper, 2006).

For the Pacific Ocean, spatial distribution and high degrees of patchiness and heterogeneity at hydrothermal vents have been described by many authors (e.g. Jollivet, 1993; Sarrazin et al., 1997; Tsurumi & Tunnicliffe, 2001; 2003; Govenar et al., 2005); these observations are quite often based on

imagery data (e.g. Hessler et al., 1985; 1988; Chevaldonné & Jollivet, 1993; Jollivet, 1993; Grehan & Juniper, 1996; Sarrazin et al., 1997). To date, only a few studies have investigated spatial variation in fauna coverage through video imagery in the Atlantic. These studies took place at Broken Spur (3090m depth, Copley et al., 1997), Menez Gwen (850m depth, Colaço et al., 1998) and TAG (3650m depth, Copley et al., 2007a).

The present study assesses spatial variation and distribution patterns of faunal assemblages of a large sulfide edifice located on the Mid-Atlantic Ridge (MAR). A continuous overview of the Eiffel Tower edifice at the Lucky Strike vent field is provided, including flow features, community composition and the scale of the geological structural features observed. The overall aim was to test the following hypothesis: the proximity to sources of visible fluid flow strongly influences faunal distribution, regardless of the orientation of the edifice. Using a new faunal mapping technique and high-resolution imagery, we aim to provide the first insights into small-scale heterogeneity and zonation patterns on a MAR vent edifice. This up-to-date approach will serve as a reference basis for future studies of temporal trends at dynamic and extreme deep-sea environments such as hydrothermal vents.

2. Material and methods

2.1. Study site

Lucky Strike vent field (37 °17.5'N, 32° 16'W) was discovered serendipitously in 1992, and has been visually observed since 1993. It is situated in the Azores Triple Junction area at a mean depth of 1700m (Fig. 2.1a). It is a basalt-hosted site (Langmuir et al., 1997 ; Fouquet et al., 1998 ; Desbruyères et al., 2000), consisting of a large lava lake (ca 300 m diameter) surrounded by numerous active vents located mainly in the north-western and south-eastern zones (Charlou et al., 2000; Humphris et al., 2002; Ondréas et al., 2009) (Fig. 2.1b). Eiffel Tower is a well-defined hydrothermal edifice and one of the most active at Lucky Strike (Fig. 2.1c), located in the south-eastern region of the vent field. Slabs are present in this area with cracks from which vent fluids originate (Langmuir et al., 1997; Ondréas et al., 1997; 2009). This irregular edifice hosts some intense black smokers (up to 324°C), active flanges and diffusion zones (<200°C), with shimmering water seeping through (Langmuir et al., 1997; Sarradin et al., 1999; Charlou et al., 2000). The fauna of Eiffel Tower is considered to be representative for the entire vent field (Desbruyères et al., 2001). Like other active hydrothermal structures at shallower depths in the Atlantic Ocean, it is covered with dense mussel beds of the mytilid *Bathymodiolus azoricus* (Van Dover, 1995; Langmuir et al., 1997; Comtet & Desbruyères, 1998; Desbruyères et al., 2000; 2001).

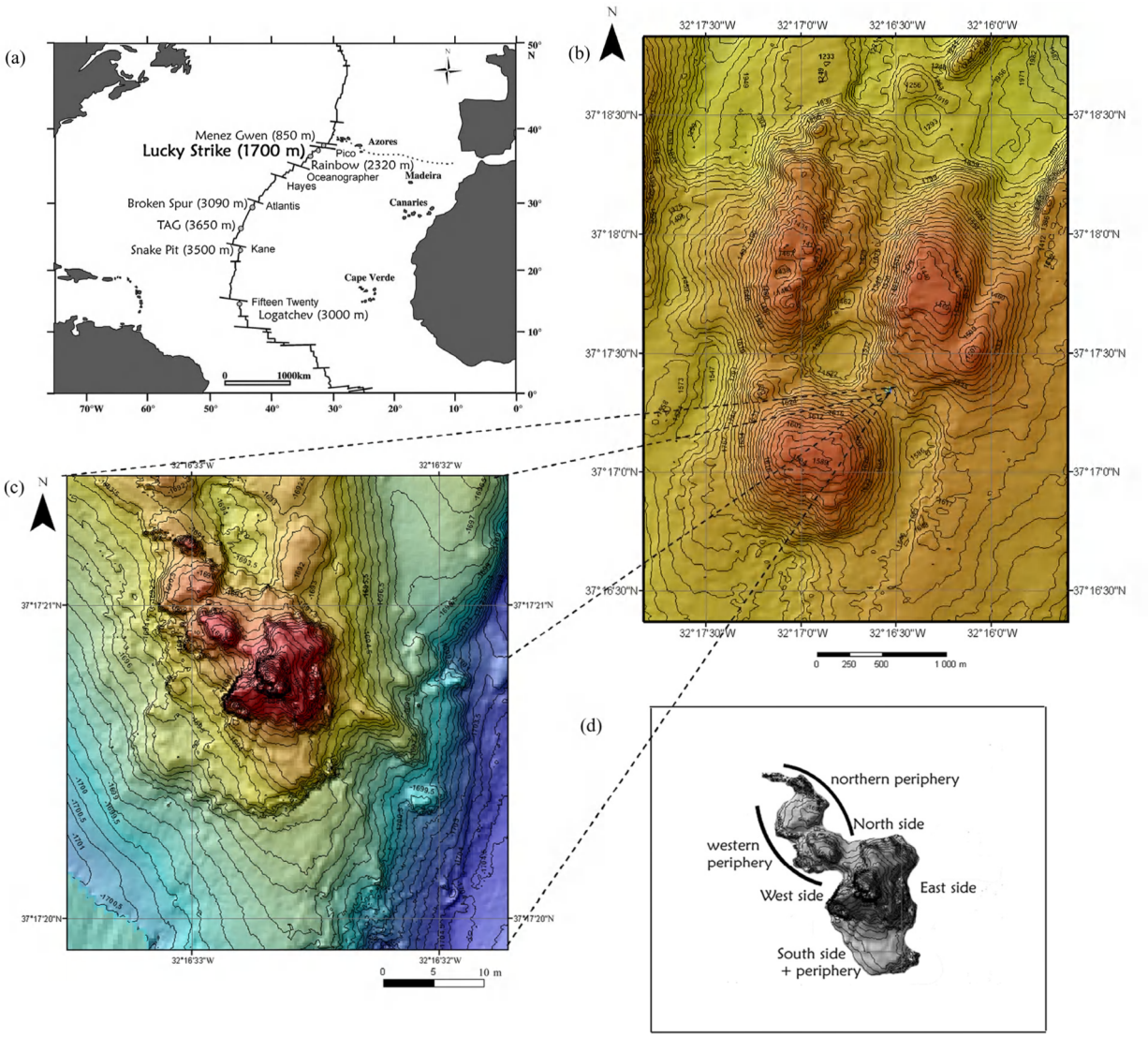

Fig. 2.1. (a) Hydrothermal vent fields of the northern Mid-Atlantic Ridge. The major transform faults are shown as well. Image modified from Desbruyères et al. (2001). (b) Bathymetric map of the Lucky Strike vent field area at a mean depth of 1700m (Flores 1998©Ifremer, resolution: 20m). The Lucky Strike vent field consists of one seamount of which the three cones surround a lava lake. (c) Microbathymetric map of Eiffel Tower (MoMARETO 2006©Ifremer, resolution=20cm), which is situated in the south-eastern region, on the saddle between two seamounts. (d) Terminology of the different sides used in this study.

2.2. Image acquisition

During six (out of eleven) dives to the Eiffel Tower edifice (MoMARETO cruise 2006) video transects were carried out by the ROV Victor 6000 which was equipped with a 3-CCD camera, 2 piloting cameras and 5 additional colour cameras. A total of approximately 10 hours of video transects were dedicated to acquiring complete imagery coverage of this well-defined edifice. Two types of video transects were carried out. (1) Vertical video transects were executed from bottom to top and started at a distance of 4 to 5 m from the structure, to allow reconstruction of the entire edifice, heading North, East, South, West and their intermediates (see Fig. 2.1d for terminology used to identify the different sides). (2) Transects were then repeated at a distance of 1 m from the edifice. For each side the same heading was

maintained and the pan and tilt of the principal camera was set to zero. Zoom levels were kept constant (wide open) during the video sampling, in order to generate similarly scaled and comparable images. Video transects were collected in colour imagery, which allowed a visual study of the assemblages and their distributional patterns. Screen-stills from video imagery had a resolution of 696 x 576 pixels. High-definition photographs were taken with a digital still camera (Sony, Cybershot), which was mounted above the principal camera of the ROV and had a resolution of 2048 x 1536 pixels.

2.3. Video Analysis

Faunal assemblages and substrata were identified based on high definition photographs and video images (Fig. 2.2 and Table 2.1). Observations and identifications from on-screen individuals were ground-truthed with samples taken during the same cruise and with historical sample lists present in the Biocean database (©Ifremer, Fabri et al., 2006). For each assemblage, mussels were measured on screen to confirm the observed difference between larger- and smaller-sized individuals in order to allow a better distinction to be made between assemblage types.

Screen stills were taken from video transects with 'Adelie video' (version 1.8, ©Ifremer 2005) and were used to reconstruct the hydrothermal structure through mosaicing. Mosaics per edifice side and for zoomed-in regions were created manually in Adobe Photoshop Elements 2.2©; pixel lengths were measured and images adjusted one to another and superimposed. The mosaics were used as a template to map the different types of fluid exits (black smokers, active flanges and zones of diffusion) as well as the different assemblages. Visually recognizable geological features on the edifice were used as reference points to localize emissions or assemblages. Vertical transects were studied with different viewing angles (intermediate headings), to make sure no detail was missed and to minimize the distortion effects of protruding rocks, relief and uneven surfaces. Contours were drawn and video transects were watched repeatedly in order to map the fluid exits and the assemblages on the mosaic templates using colour coding, so they could be digitized. Visually interpretable maps were created for each side of the tower and the periphery. Sampling instruments present on the structure or visible parts of the ROV, when in the same focal plane, were used to scale the mosaics. The proximity (distance and direction) of the assemblages and substrata to fluid exits was measured, as well as the mean patch size for all assemblages and substrata. Patterns and gradients in assemblage distribution were analysed. Systematic transfer patterns between the different neighbouring assemblages were investigated. Counts were made of the number of times that a patch of assemblage X was bordered by a patch of another type of assemblage (Y). A patch was defined as an enclosed surface occupied by a certain type of assemblage or an uncolonised surface (substratum).

Table 2.1. Composition of the faunal assemblages and substrata as well as several physico-chemical and topographic characteristics, all based on visual observations. Since the identification of the assemblages was based on video imagery, only mega- and macro-faunal species are represented here. Ophiuroids and fish were not included because there was no discernable pattern to their occurrence ++ Abundant, + present, () occasional, - absent. (Ass = Assemblage, Sub = Substratum)

			Ass 1	Ass 2a	Ass 2b	Ass 3	Ass 4a	Ass 4b	Sub 1a	Sub 1b	Sub 2
Fauna											
Bivalvia	Mytilidae	*Bathymodiolus azoricus* (Larger sized)	++	(+)	(+)	-	-	-	-	-	-
		Bathymodiolus azoricus (Smaller sized)	(+)	++	++	-	+	+	-	-	-
		Bathymodiolus azoricus (New recruits)	+	+	+	-	+	+	-	-	-
Decapoda	Alvinocarididae	*Mirocaris fortunata*	+	(+)	(+)	++	(+)	(+)	-	(+)	(+)
		Chorocaris chacei	+	(+)	(+)	++	(+)	(+)	-	(+)	(+)
		Alvinocaris markensis	(+)	(+)	(+)	(+)	-	-	-	-	(+)
	Bythograeidae	*Segonzacia mesatlantica*	(+)	(+)	(+)	(+)	(+)	(+)	(+)	(+)	(+)
Gastropoda		Limpets (*Lepetodrilus atlanticus*,*Pseudorimula midatlantica*, *Protolira valvatoides*, etc)		+	+	-	++	++	-	-	-
Cnidaria		Hydroids	-	-	-	-	++	-	(+)	-	-
Micro-organisms		Visible microbial mats	(+)	-	++	(+)	-	++	-	++	+
Flow features											
proximity of black smoker			++	+	+	++	-	-	-	-	++
proximity of flange/diffusion zones			++	+	+	++	++	++	-	+	++
in flow			No	No	No	Yes	No	No	No	No	Yes
Habitat characteristics			possibly everywhere	possibly everywhere	possibly everywhere	possibly everywhere, rougher substrata	Mainly edifice base and periphery	Mainly edifice base and periphery	Mainly edifice base and periphery	possibly everywhere	possibly everywhere

All image analysis operations, i.e. length/distance measurements and surface calculations, are pixel-based and were carried out by the Image analysing program IP Lab Spectrum®. Each patch surface was measured 3 times to reduce error from online tracing (in analogy with Sarrazin et al., 1997).

2.4. Statistics

Statistical analyses of percentage cover and distances were carried out both in R (version 2.7, Multicore team 2008) and in Statistica 6 (StatSoft Inc 2001). Ordinations in R were performed with the Vegan package (Oksanen et al., 2008). Data used in the multivariate analyses were linearly distributed hence PCA (Principal Component Analysis) and RDA (Redundancy Analysis) were used. For the cluster analysis Ward's method was used for Euclidean distances. The Friedman's test is the non-parametric equivalent of a two-way ANOVA used to compare multiple dependent samples, in this case the size of the patches between the sides. Factorial ANOVA's and the Tukey HSD post-hoc test were used to compare minimum and maximum distance to the fluid exits between the different assemblages and substrata. Correlations (Spearman Rank) were calculated between the number of visible black smokers, flanges and diffusion zones and between the assemblages and substrata, between all sides (n=7, degrees of freedom=5).

3. Results

3.1. Eiffel Tower morphology and activity

The Eiffel Tower edifice extends 11 m in height and at most 20 m in width and was divided into two parts, a 'tower' structure consisting of the upper 8 m (summit at 1681 m of depth) and a 'periphery' including the lower 3-4 m until the seafloor is reached at a depth of 1692 m. The overall Eiffel Tower morphology did not change drastically during the MoMARETO cruise. However, several structural differences were noted between the dives; black chimneys of freshly precipitated minerals grew more than 0.5m per night (structures were sampled for certain experiments and grew back after one night, sometimes overgrowing sampling devices, D. Cuvelier, pers. obs.).

The number of black smokers and the number of diffusion zones were positively correlated (R^2=0.944, p=0.001): their numbers increased proportionally one to another. Flanges were not correlated with either black smokers or diffusion zones. The hydrothermal activity spread out towards the periphery since highly-active black smoker chimneys were observed at the base of the edifice, on the southern periphery and on the structure between North and West sides (Fig. 2.1d). No activity was observed, however, on the eastern periphery, and no associated life was present. Therefore this part of the structure was not included in the analyses.

3.2. Faunal composition of the Eiffel Tower edifice

The taxonomic composition of the vent fauna inhabiting Eiffel Tower was determined through the use of both video imagery, still photography and past and ongoing faunal sampling (Table 2.1). The resolution of video precludes the identification of smaller organisms; however, larger macro- and mega-fauna could be identified in most cases to species level. The main species associated with the vent were the mussel *Bathymodiolus azoricus,* and three species of alvinocaridid shrimp, namely *Mirocaris fortunata, Chorocaris chacei* and *Alvinocaris markensis*. Bytograeid crabs (*Segonzacia mesatlantica*) and many other less conspicuous species lived in association with these mussel beds (Desbruyères et al., 2006b). *Bathymodiolus azoricus* was the most abundant component of 2 out of the 4 assemblages, creating a microhabitat for other accompanying organisms (Table 2.1). Of the three species of shrimps present on Eiffel Tower, *A. markensis* was the most solitary, followed by *C. chacei,* which lived in small groups of low numbers. The smallest species, *M. fortunata*, was the most gregarious and abundant over the entire edifice; it co-occurred with *C. chacei*. *Alvinocaris markensis* was occasionally seen on top of or in between the larger-sized mussel beds. The mobility of all these alvinocaridids decreased when close by or in the actual warm water flow. If present in warm shimmering water, they were almost immobile, in contrast to the rapid movements when moving between and over mussels.

Segonzacia mesatlantica (Bythograeidae, Decapoda) is a typical vent species on the MAR and occurred anywhere on the edifice, in shimmering water, crawling in between and over mussel beds and clumps, hiding underneath them or crossing bare surfaces, etc. Sometimes they were observed traversing the microbial mats.

Towards the base and periphery of the edifice, ophiuroids were observed. Although difficult to identify from the video imagery, the species is most likely to be *Ophioctenella acies* (P. Tyler, pers. obs.), which seems to show an affinity for *Bathymodiolus* beds (Desbruyères et al., 2006b). Gastropod grazers (Lepetodrilidae and other families) were observed on mussel shells and bare rocks, also mostly towards the base of the structure (Table 2.1). A diverse associated ichthyofauna was also associated with the edifice. These fish were observed making regular predatory incursions (e.g. *Hydrolagus pallidus* (Chimaeridae), *Synaphobranchus sp.* (Synaphobranchidae), *Coryphaenoides armatus* (Macrouridae)) or living in cracks and crevices of the chimney (*Gaidropsarus* sp. (Moridae)). *Cataetyx laticeps* (Bythitidae) was observed almost every time a video transect was executed, lying immobile at the base of the edifice. This species often occurred in pairs.

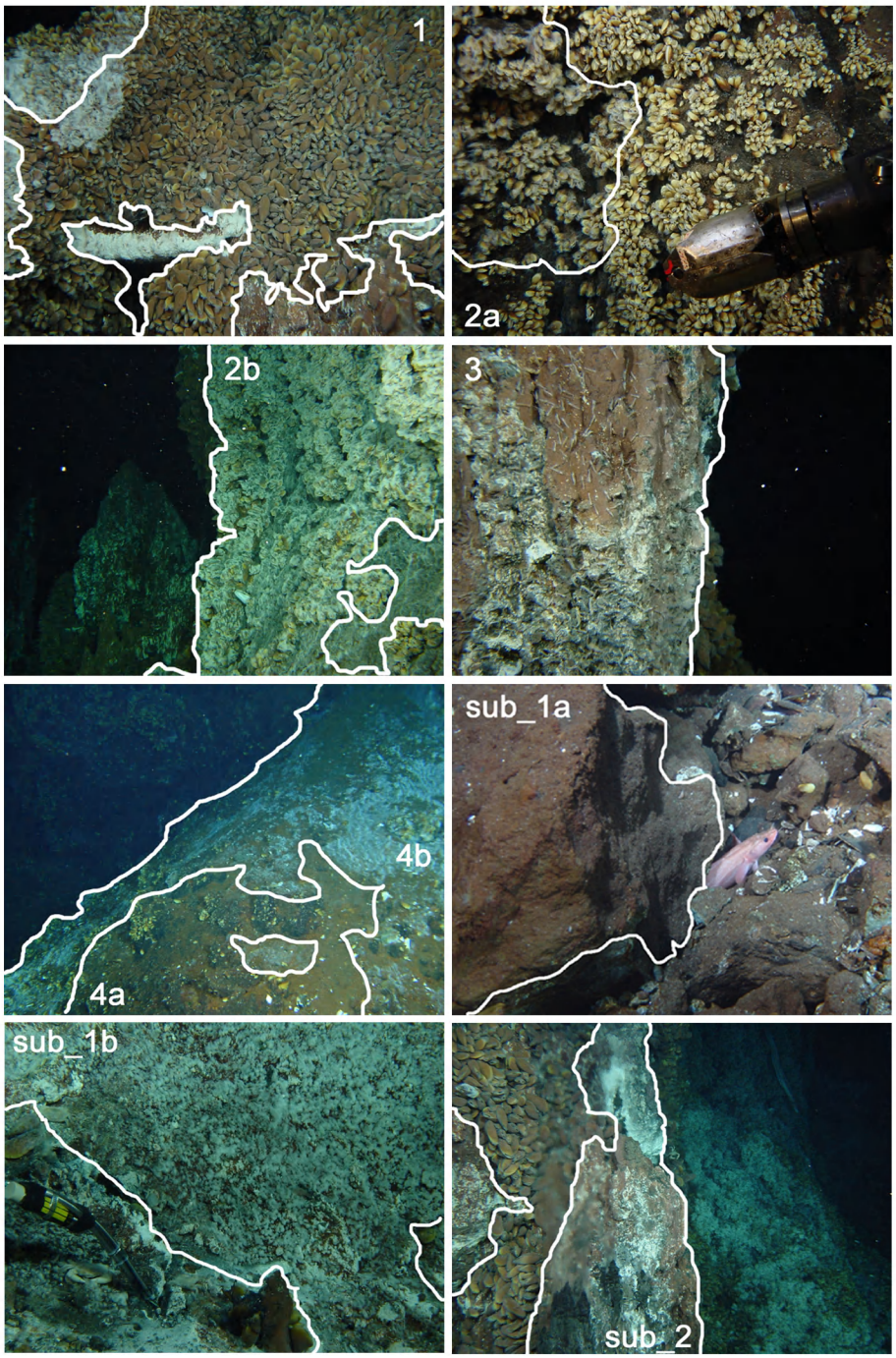

Fig. 2.2. Faunal assemblages identified at Eiffel Tower hydrothermal edifice. (a) Assemblage 1: Dense *Bathymodiolus azoricus* beds (the mussels are of the larger size class, in general > 4cm), occasionally patchy microbial mats can be present. (b) Assemblage 2a: *Bathymodiolus azoricus* clumps (in this case the mussels are almost always less than 4cm in length) separated by bare surface without visible microbial mats or (c) Assemblage 2b: with visible microbial mats. (d) Assemblage 3: Bare surface 'colonised' by Alvinocarididae (*Mirocaris fortunata* and/or *Chorocaris chacei*). (e) Bare surface with mussel "veins" and very small mussels (possibly new recruits) without visible microbial mats (Assemblage 4a) and with visible microbial mats (Assemblage 4b). (f) Substratum 1a represents bare dark brownish, sometimes slightly reddish surfaces (with on the image the fish *Gaidropsarus* sp. hiding in a crevice). (g) Substratum 1b represents bare surfaces with visible microbial mats. (h) Substratum 2 represents bare surfaces with clear mineral precipitation (whitish, greyish) and with possible microbial presence as well (cf. Table 2.1). Predators and scavengers (*Segonzacia mesatlantica* (Bythograeidae), *Mirocaris fortunata, Chorocaris chacei* and *Alvinocaris markensis* and some fishes) can be present on top of these assemblages. Scales were not put on the individual pictures due to malfunctioning of the laser pointers during the 2006 cruise. The surface covered by each image depends on the zoom-level, proximity to the edifice and irregularity of the edifice.

3.3. Assemblages

To understand small-scale heterogeneity on the vent edifice, we identified and quantified distinct assemblages defined by the presence or absence of key taxa, their size and their coverage. Distinct substratum types were also identified based on the type of mineralization and, in some cases, microbial cover.

Four distinct assemblages and two substratum types were identified (Fig. 2.2) of which two assemblages and one substratum had two subordinate forms ("a" without and "b" with visible microbial coverage). Assemblage 1 consisted of dense mussel beds (the mussels are of the larger size class, in general > 4 cm) often with shrimps crawling over and between them. Some limpets were present on the mussel shells. Assemblage 1 mussel beds were found in the neighbourhood of fluid exits, but they were never present in the hot water flow (Fig. 2.2a). Assemblage 2 comprised clusters of mussels (clumps) with bare surface visible between them (Fig. 2.2b and c, respectively without and with microbial cover). In this case, the mussels were almost always less than 4 cm in length. Alvinocaridid shrimps were observed, but they were not as abundant as in Assemblage 1. Uncovered surfaces colonised by shrimps constituted Assemblage 3 (Fig. 2.2d). *Mirocaris fortunata* was always present, quite often accompanied by less numerous *Chorocaris chacei*. Assemblage 3 was found mostly in the direct proximity of the warm water flow from the fluid exits, or within the flow itself. Assemblage 4 was characterized by dispersed small mussels and/or new recruits on bare surface (the latter prevails). Assemblage 4a had no microbial cover (Fig. 2.2e), and scattered hydroids and limpets were present next to the newly recruited mussels. Assemblages 4b, with microbial cover, lacked hydroids, but limpets were encountered (Fig. 2.2e). Assemblage 4 was often situated at the base of the tower (or in the periphery), often with large dead mussel shells below the base, possibly fallen from the wall of the structure.

In addition to the assemblages, two substratum types were detected. The main visual difference between these two substrata is their colour. Substratum 1a was a bare, brownish to reddish uncolonised surface (Fig. 2.2f) while Substratum 1b represented a similar surface covered by whitish filamentous bacteria (Fig. 2.2g). Occasionally, decapods were present. Substratum 2 had a white-mottled surface due to anhydrite deposits; patchy microbial mats were sometimes also present (Fig. 2.2h). This substratum often occurred in very hot regions with the presence of black smokers, shimmering water and/or diffusion. Black chimneys composed of freshly deposited minerals were never colonised permanently, but were sometimes visited by shrimps and crabs from surrounding patches (Table 2.1).

3.4. Spatial distribution and size of the assemblages

The visually interpretable maps showing the spatial assemblage and substratum distribution are presented in Fig. 2.3. Assemblages 4a and 4b were considered as 'uncolonised' surface because bare surfaces largely predominate. Counts (number m^{-2}) of visible active features (black smokers, flanges and diffusion zones) showed variations between structure sides as well (Table 2.2).

Table 2.2. Percentage of the edifice that is colonised by fauna and the number of active features (n=black smokers, flanges and diffusion zones) per m^2 for each side. The least colonised side of the tower (upper 8 m) is the most active one and vice versa. The peripheral zones (lower 3 m until sea bottom is reached) show similar trends. Highest activity and degree of colonisation values are marked in bold.

Tower	% coverage/colonisation	# active features (n/m^2)
East	28.11	**0.84**
South	49.17	**0.60**
West	**82.82**	0.19
North	**58.85**	0.36
Periphery	% coverage/colonisation	# active features (n/m^2)
East periphery	0	0
South periphery	12.75	**0.53**
West periphery	**54.10**	**1.16**
North periphery	**64.54**	0.39

The East and South sides, which were the least strongly colonised (Fig. 2.3e and g), had quite large proportions of Assemblages 1 and 3 and Substratum 2 (Fig. 2.3h) compared to the other sides, and also showed the highest level of visible hydrothermal activity (Table 2.2). Conversely, the North and West sides, which were colonised most intensively (Fig. 2.3a and d), were dominated by Assemblages 2a and 2b (Fig. 2.3h) and showed the lowest level of activity (Table 2.2). The peripheral zones (Fig. 2.3b, c and f) demonstrated similar trends of high activity, low degree of colonisation, and vice versa. The southern peripheral zone was the least colonised (Fig. 2.3f) and dominated by Assemblages 4a and 4b (Fig. 2.3h). It showed a large amount of activity, but this was limited to a few highly-active high-temperature exits (Table 2.2). The western periphery was the most active, with the highest number of active venting structures in proportion to its surface (Table 2.2), but the fluid flow was visibly less intense than that on the South side.

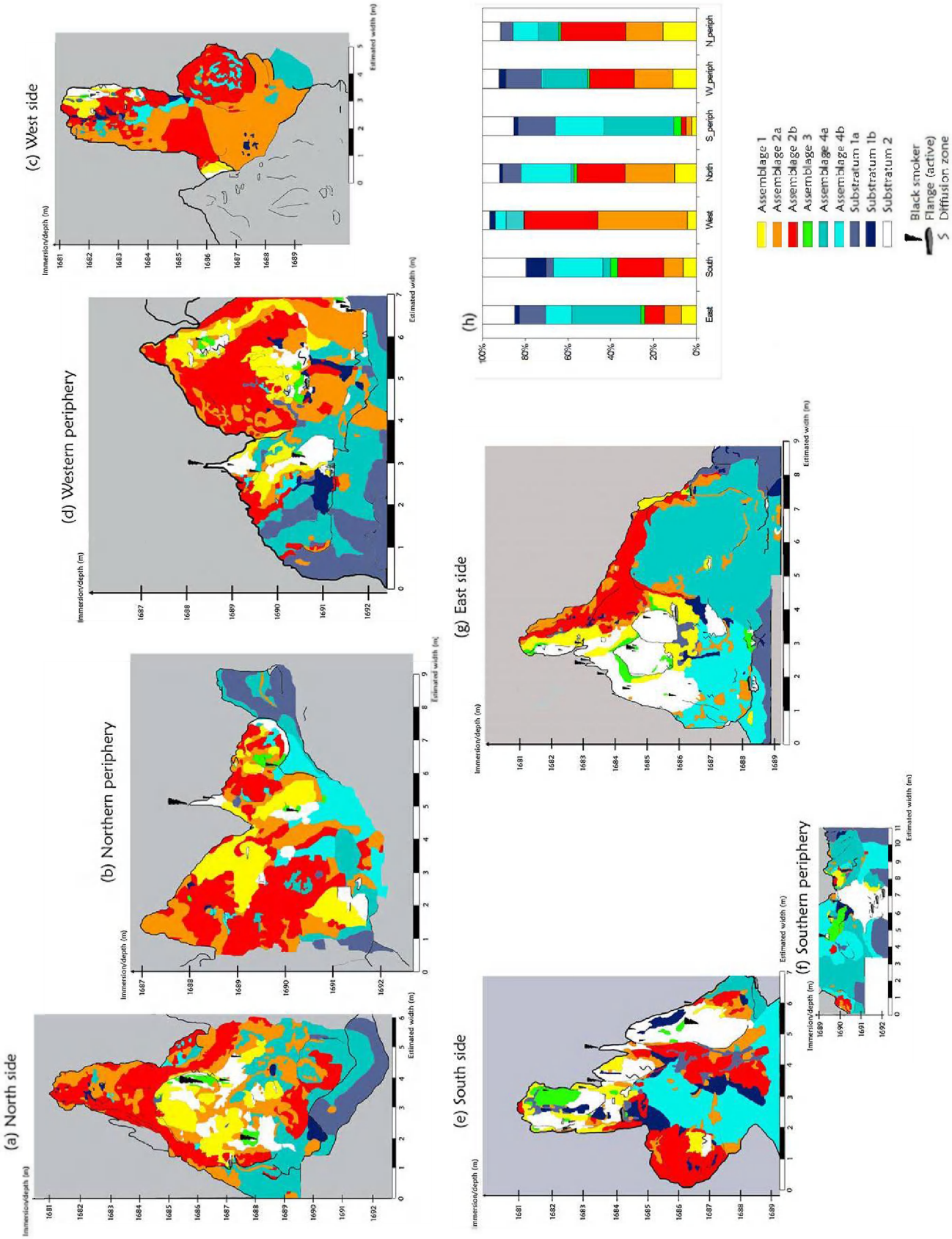

Fig. 2.3. Spatial distribution of faunal assemblages and substrata on each side of the Eiffel Tower hydrothermal edifice (Lucky Strike vent field, MAR). (a) North side, (b) Northern periphery, (c) Western periphery, (d) West side, (e) South side, (f) Southern periphery, (g) East side and (h) stacked histogram representing the % of coverage per assemblage.

The number of patches (see description above in '2.3. Video Analysis') occupied by the different assemblages differed between the sides. Assemblage 2a had always the highest number of patches, regardless of the side it occurred on. However, the total number of patches did not necessarily reflect the total surface covered by an assemblage since the sizes of the patches was variable. For example, while Assemblage 2a had 46 patches on the North side, the surface it covered was estimated to be 4.50 m^2 on this side of the edifice, while Assemblage 4b with only 16 patches covered 4.54 m^2.

In most cases, the mean size of a single patch varied between 0.002 and 1 m^2 for each assemblage across the sides. This must be interpreted with caution, since one big patch can significantly enlarge the mean patch size. The significance of these assumptions was tested with a Friedman's test for all patch sizes across sides and periphery. For Assemblages 1, 2b, 4a and the substrata, there was no significant difference in patch size between the sides ($p>0.05$, $df=6$). Outliers were removed for Assemblages 3 and 4b, after which they did not show a significant difference. Assemblage 2a, however, showed significant differences between the sides ($p<0.001$, $df=6$). This was mainly due to the presence of very large patches on the West side and, to a lesser extent, to those present on the North side of the edifice.

Different correlations were observed between the percentage coverage of the assemblages. Substratum 1a was negatively correlated with Assemblage 2b ($R^2=0.73$, $p=0.014$). Substratum 2 was negatively correlated with Assemblage 2a ($R^2=0.67$, $p=0.023$), but positively correlated with Assemblage 3 ($R^2=0.73$, $p=0.014$). Assemblage 2a was positively correlated with Assemblage 2b ($R^2=0.67$, $p=0.023$) and negatively correlated with Assemblage 3 ($R^2=0.73$, $p=0.014$). The other correlations were not significant.

The ordinations (Fig. 2.4) showed the same trends as observed on the faunal distribution maps. The different sides were plotted based on the relative percentage coverage of the different assemblages and substrata. The constraints added in the ordinations were the number of visible active features per square meter. Major trends were maintained in both PCA and RDA analyses (therefore only RDA is shown, Fig. 2.4a). On the RDA, almost 62% of the variance was explained by the two axes, with axis 1 explaining 51.8% of the variance. The first axis was able to discriminate the more active (East side, southern periphery (S_periph)) from the less active (North side, northern periphery (N_periph) and West side) sides (RDA-plot was not significant, $F=2.119$ $p=0.1587$). The main separation in the ordination plot was caused by Assemblages 2a and 2b on the one hand and Assemblage 4a, 4b and Substratum 1a and 2 on the other. The activity features (black smokers, flanges and diffusion zones)

also confirmed the separation of the active and less active sides (Fig. 2.4a). Two sides of the edifice appeared to be in the middle of the ordination plot, namely the South side and the western periphery (W_periph). The cluster analysis, based on Ward's method, clarified this (Fig. 2.4b), showing that the western periphery is more similar to the North side, the northern periphery and the West side. The South side grouped with the East side and the southern periphery, although the similarity was quite low.

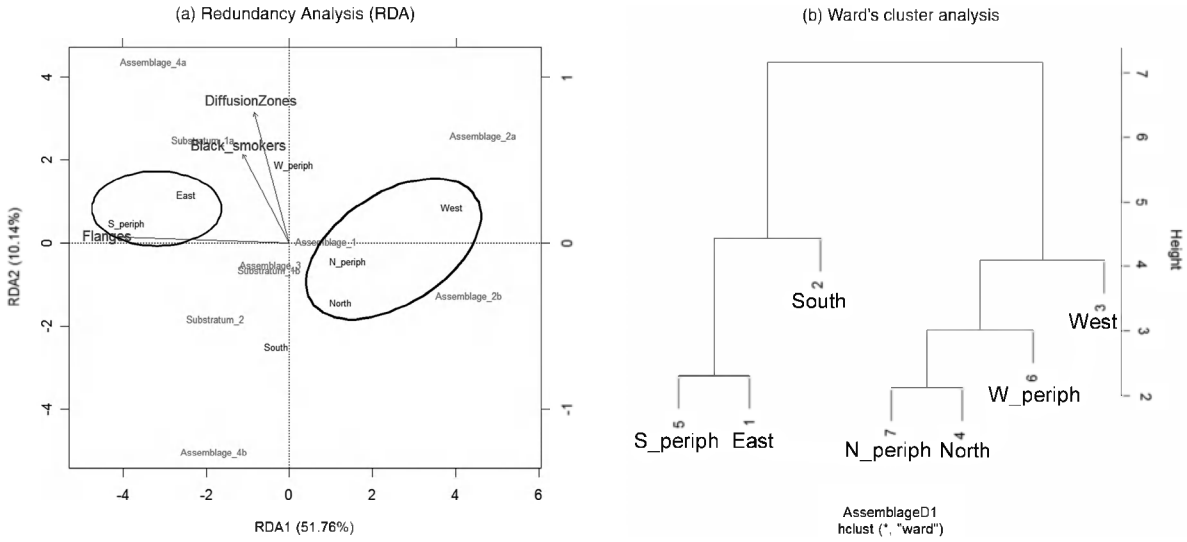

Fig. 2.4. Ordinations based on the relative percentage coverage of each assemblage and substratum on each side of the Eiffel Tower structure. PCA showed exactly the same tendencies as the RDA and is therefore not shown. (a) Redundancy Analysis (RDA), where the number of visible active features ($n.m^{-2}$) acted as constraints. The horizontal and vertical axes together take into account 61.9% of the variation between the sides, although the horizontal axis is clearly more important. (b) Ward's cluster analysis. Clustering of the different sides of Eiffel Tower based on assemblage coverage. The agglomeration method used was Ward's method which minimizes the Sum of Squares between two formed clusters (the most similar sides cluster together first). The patterns are similar to those revealed by the canonical analysis. The positioning of the South side and the western periphery, which were difficult to interpret in the RDA, are clarified in the cluster analysis (S_periph=southern periphery, N_periph=northern periphery, W_periph=western periphery).

Analysis of video images revealed some preliminary trends regarding which assemblages thrive in or can tolerate warm water flows. Most of these trends were confirmed when the distance from a fluid exit to a patch was measured (Fig. 2.5). A selection of assemblages was found in close proximity (< 1 m) to the fluid exits. However, only Assemblage 3 and Substratum 2 seemed to prevail in the warm water flow. Assemblage 1 was always present in the surroundings of fluid exits, but was rarely seen in the warm water flow itself. The minimum distances of these three assemblages to the closest fluid exit were significantly different from the other assemblages (ANOVA, R^2=0.38, p=0.00). Assemblages with smaller mussels (2a and 2b) were situated further away from the fluid exits. However, for all the sides of the edifice, the assemblage covered with microbial mats (2b) was closer to the fluid exits than the one without (2a). In general, larger patches had a greater probability that their borders are surrounded

by different fluid exits.

If a division was made between the different types of fluid exits, black smokers (up to 324°C) and flanges and diffusion zones (<200°C) (Fig. 2.5 a-b respectively), it was clear that they showed the same trends. Assemblage 3 was found closest to all three types of fluid exits. Assemblage 1 and Substratum 2 showed a similar distribution. The minimum distance of these three assemblages in relation to black smokers was significantly different from that of the other assemblages, while for the flanges and diffusion zones the differences were less obvious. Overall, the minimum distance to flanges and diffuse emissions was half of that to black smokers.

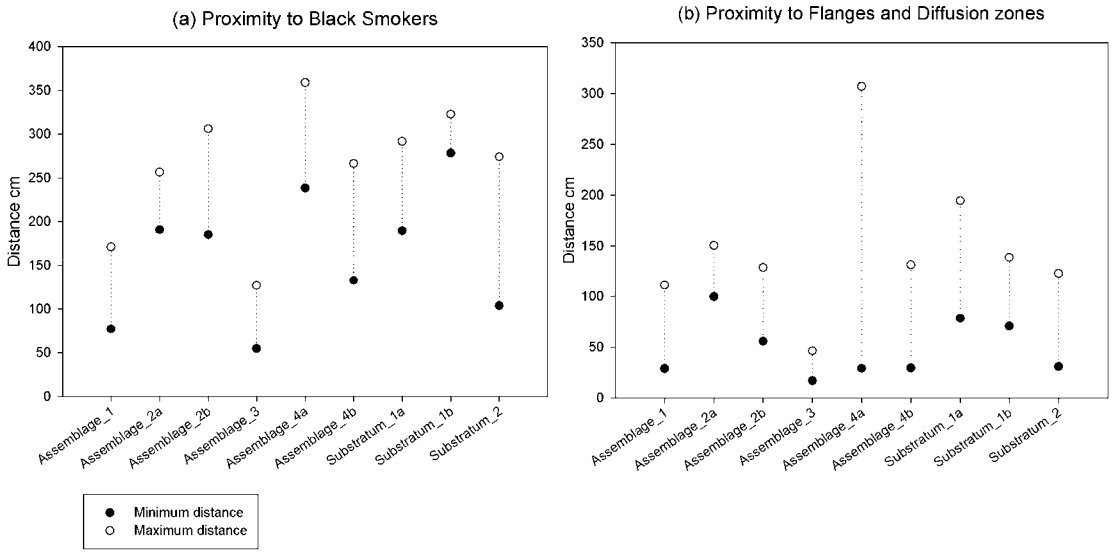

Fig. 2.5. Minimum and maximum distances of the assemblages (n=6) and substrata (n=3) were measured to the different activity features and their associated temperature regimes; (a). black smokers (324°C) and (b). flanges and diffusion zones (<200°C).

3.5. Neighbouring patterns

Based on video observations, systematic patterns between different neighbouring assemblages appeared to be present. This was confirmed with the analysis of adjacent patches. For the "mussel-based" assemblages, a clear gradient from bare surface with new recruits and scattered mussels (Assemblages 4a and b) to mussel clumps (Assemblages 2a and b) and dense mussel beds (Assemblage 1) was noted. This coincided with an increase in temperature measured in these mussel-based assemblages, respectively ranging from 4.7°C to 12.5°C (Sarrazin et al., in prep).

Each assemblage had at least 2 "preferred" or dominant neighbours, accounting for the occupancy of ca. 50% and more of the adjacent patches (Table 2.3). The other ca. 50% was divided between the other assemblages and substratum types (n-2=7 with n=9 being the total number of assemblages and

substrata). For example, newly formed surface (Substratum 2) was more often bordered by Assemblage 1 and 2a, while Assemblage 3 was more often bordered by Substratum 2 and Assemblage 1. For Assemblages 4a and b, Assemblages 2a and b are the most frequent neighbours.

Table 2.3. Representation of the dominant neighbouring patches (2 for each assemblage), responsible for an occupancy of ca. 50% of the adjacent patches.

	Dominant neighbours	%	∑
Assemblage 1	Substratum 2	30.8	61.9
	Assemblage 2a	31.1	
Assemblage 2a	Assemblage 2b	20.9	48.8
	Substratum 2	27.9	
Assemblage 2b	Assemblage 2a	40.5	55
	Assemblage 1	14.5	
Assemblage 3	Substratum 2	34.5	64.1
	Assemblage 1	29.6	
Assemblage 4a	Assemblage 2a	32.9	55.9
	Assemblage 2b	23.0	
Assemblage 4b	Assemblage 2a	34	60.4
	Assemblage 2b	26.4	
Substratum 1a	Assemblage 2a	25.7	45.1
	Assemblage 4a	19.4	
Substratum 1b	Assemblage 2a	29.3	55.8
	Assemblage 2b	26.5	
Substratum 2	Assemblage 2a	29.2	56.5
	Assemblage 1	27.3	

4. Discussion

In contrast to the diverse assemblages of tubeworms, clams and polychaetes found at hydrothermal vents on the East Pacific Rise (EPR), the shallower vents of the slow-spreading MAR (< 2300 m depth) are dominated visually, on macrofaunal scales, either by an assemblage of Bathymodiolin mussels (Van Dover, 1995; Turnipseed et al., 2003) or Alvinocaridid shrimps (Desbruyères et al., 2001). Due to the shallower depth of some of these Atlantic vents (e.g. Lucky Strike) and the associated phase separation (i.e. the local pressure-temperature characteristics that determine the rate of precipitation of dissolved and particulate metals and sulfide), the hydrothermal fluids lose part of their toxicity, which allows non-vent bathyal fauna to make predatory incursions (Desbruyères et al., 2000). Fishes have

been observed to feed on shrimps, crabs and mussels (Saldanha & Biscoito, 1997; Marques & Porteiro, 2000; Desbruyères et al., 2006b).

Crucial to our understanding of global macro-ecological patterns are small-scale ecological forcing factors. In particular, the relationships between the substrata, vent activity, fluid flow, temperature and biological tolerances are important. Mid-Atlantic vents differ substantially from those on the EPR in the nature of their abiotic variables. Elucidating the influences of these variables on composition and zonation patterns is one of the main goals of this study. Using a high-resolution video imaging technique, assemblages were identified and mapped on a typical MAR vent edifice, revealing the potential spatial patterns in relation to visible abiotic factors.

4.1. Spatial and zonation patterns

When the spatial patterns of the assemblages and substrata were analysed, a systematic lateral zonation between the patches was observed, transforming one assemblage into another over distance. Analyzing the occupancy of neighbouring patches was considered the most appropriate way to quantify the number of transfers. A zonation model, summarising the way that assemblages and substrata change across the edifice, is presented in Fig. 2.6a. The overall driver of this spatial shift in faunal composition is the decrease in fluid flow, i.e. the presence of high temperature fluid exits and proximity to fluid exits (Fig. 2.6b). Associated with this decrease in flow is the probable decrease in temperature, sulfide and other associated chemicals. Thermal conditions and associated factors like fluid flow play a role in habitat selection, spatial partitioning and distribution of vent animals (Sarrazin et al., 1999; Bates et al., 2005; Levesque et al., 2006; Mills et al., 2007). An idealized scenario of faunal distribution and zonation at Eiffel Tower is shown in Fig. 2.7.

Faunal assemblages can be divided into three groups (Fig. 2.6). Assemblages 3 and 1 are associated with the harshest environment. Assemblages 2a and 2b, the most abundant on the edifice, are associated with intermediate conditions and are found at moderate distances from fluid-flow exits. Assemblages 4a and 4b can be regarded as the "recolonisation pools" for the rest of the sulfide structure, hosting new recruits and small mytilids. This sequence of assemblages creates a gradient in mussel densities. Among the substrata, Substratum 2 is characterized by the co-occurrence of precipitated anhydrite and shimmering water suggesting the presence of a high permeability. Substratum 1b is colonised by microbial mats and is more abundant at a greater distance from the fluid exits. A spatial segregation between different microbial communities (present in Assemblages 2b, 4b, Substratum 1b and 2) may be a response to a temperature gradient. In addition, the existence of

intra-specific (between mussels) and inter-specific (bacteria and mussels, mussels and shrimp) competition for access to resources (e.g. sulfide) could play a role in structuring the spatial distribution of the different communities.

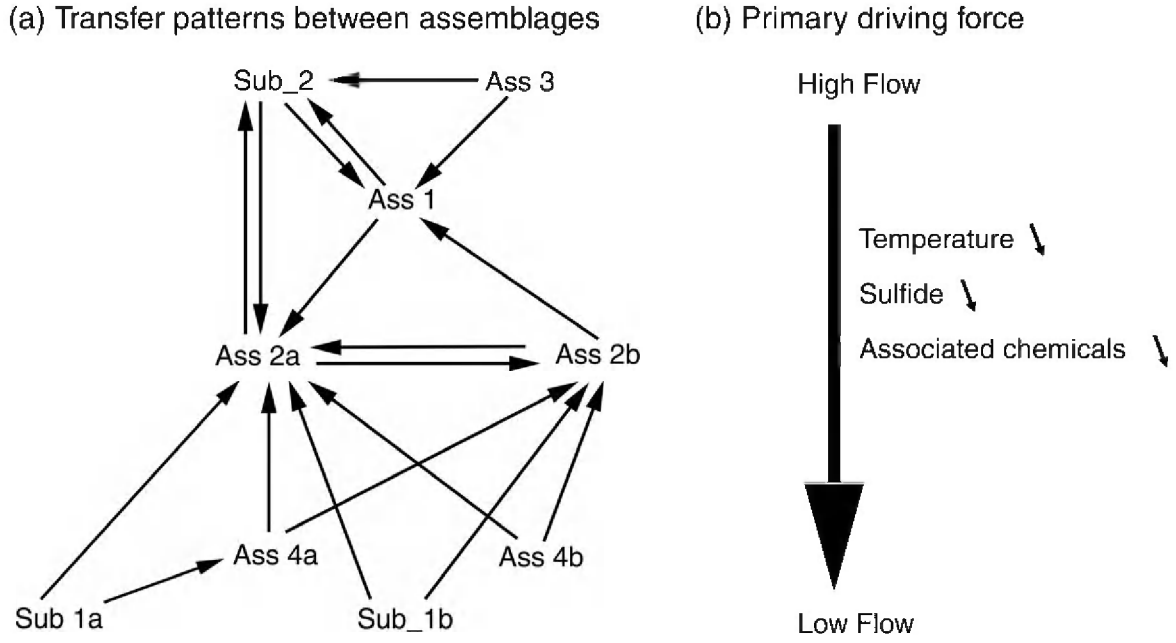

Fig. 2.6. The neighbour transfer patterns between assemblages and substrata are presented in a zonation model (a). For each assemblage the adjacent patches were analysed. This resulted in 2 'favourite' neighbours (2 arrows) accounting for more than 50% occupancy of the adjacent patches (cf. Table 2.3). The primary driving force (b) that coincides with this zonation pattern is shown as well.

The main interacting factors likely to drive the observed assemblage and substratum distribution and zonation are thus twofold, namely abiotic constraints and biotic interactions. Based on experimental manipulations, abiotic gradients and biotic interactions are believed to act jointly to shape benthic vent communities (Micheli et al., 2002; Lenihan et al., 2008). Abiotic constraints include the geomorphology, porosity and composition of the substratum as well as the presence/absence and proximity of fluid exits. Although they were not tested in the present study, biotic interactions must exert an important control on the observed distribution of the fauna (Shank et al. 1998a; Sarrazin et al. 2002; Mullineaux et al. 2003). They include the community induced changes in microhabitat, e.g. changes in sulfide concentrations resulting from biological uptake and dilution (Johnson et al., 1994), competition and predator-prey interactions (Micheli et al., 2002). Their exact role and importance, however, is difficult to asses based on imagery.

Mussels may out-compete other sessile chemosynthetic macrofauna for access to vent fluid (Lenihan et al., 2008). They have several advantages over other vent animals. For example, dense mussel beds are able to redirect the fluid flow horizontally (Johnson et al., 1994) explaining the existence of vast mussel

beds. In addition, their motility enables them to escape from unfavourable environmental conditions or to colonise newly formed habitats. Species of *Bathymodiolus* have been observed moving 0.74cm per hour (Govenar et al., 2004). Temporal evolution studies and manipulative experiments are needed to test these hypotheses and to enhance our knowledge with regard to assemblage dynamics.

4.2. Assemblages on the Eiffel Tower edifice

4.2.1. Mussel-based assemblages

The dominant megafaunal species, and the main constituent of Assemblages 1, 2a and 2b, is *Bathymodiolus azoricus*. *Bathymodiolus* is the most widespread genus in deep-sea chemosynthetic environments, present in both cold seeps and hydrothermal vents (Tyler & Young, 1999). The definition of the assemblages is partially based on a visible difference between big and small mussels that was confirmed by length measurements. In the case of Eiffel Tower, the mussels belonging to a larger size class form dense mussel beds (Assemblage 1) and are relatively more abundant, compared to Assemblages 2a and 2b (mussel clumps), on the more active sides. On all sides of the edifice, a spatial segregation of the assemblages based on their proximity to fluid exits is observed.

Larger mussels (Assemblage 1) are found in the close proximity of a fluid exit, suggesting that they may be able to survive a somewhat more hostile environment than the smaller-sized mussels (Desbruyères et al., 2001). The observations presented here support a spatial segregation of mytilid sizes at Eiffel Tower as described previously (Comtet & Desbruyères, 1998; Sarradin et al., 1999; Desbruyères et al., 2001). In contrast to the present observations, the mussels in the Lau Basin (SW Pacific) live further away from the fluid exits. Zonation studies show *Bathymodiolus brevior* to have a low thermal tolerance but a high autotrophic capacity. Like *B. azoricus*, *B. brevior* avoids direct contact with vent fluids, although it can stand high concentrations of sulfide (Henry et al., 2008; Waite et al. 2008).

Mytilids use their byssus threads to attach to the substratum, which allows them to grow almost everywhere on the edifice and to connect to other individuals, resulting in 'stacking' several layers deep (Johnson et al., 1994). In this regard, the permeability of the substratum and the thermal tolerance of the animals appear to play a significant role in the faunal distribution observed. Shrimps (Assemblage 3) can get closest to the fluid exits. They are very mobile, are not attached to the substratum and have a temperature resistance up to 36°C (Shillito et al., 2006). Therefore they can survive on the highly permeable substrata close to the fluid exits (e.g. Substratum 2). This is supported by the positive correlation between Substratum 2 and Assemblage 3. Mussels, on the other hand, are not observed on newly formed surfaces, either because they have more difficulties attaching to this

substratum or they are less tolerant of warm fluid flows.

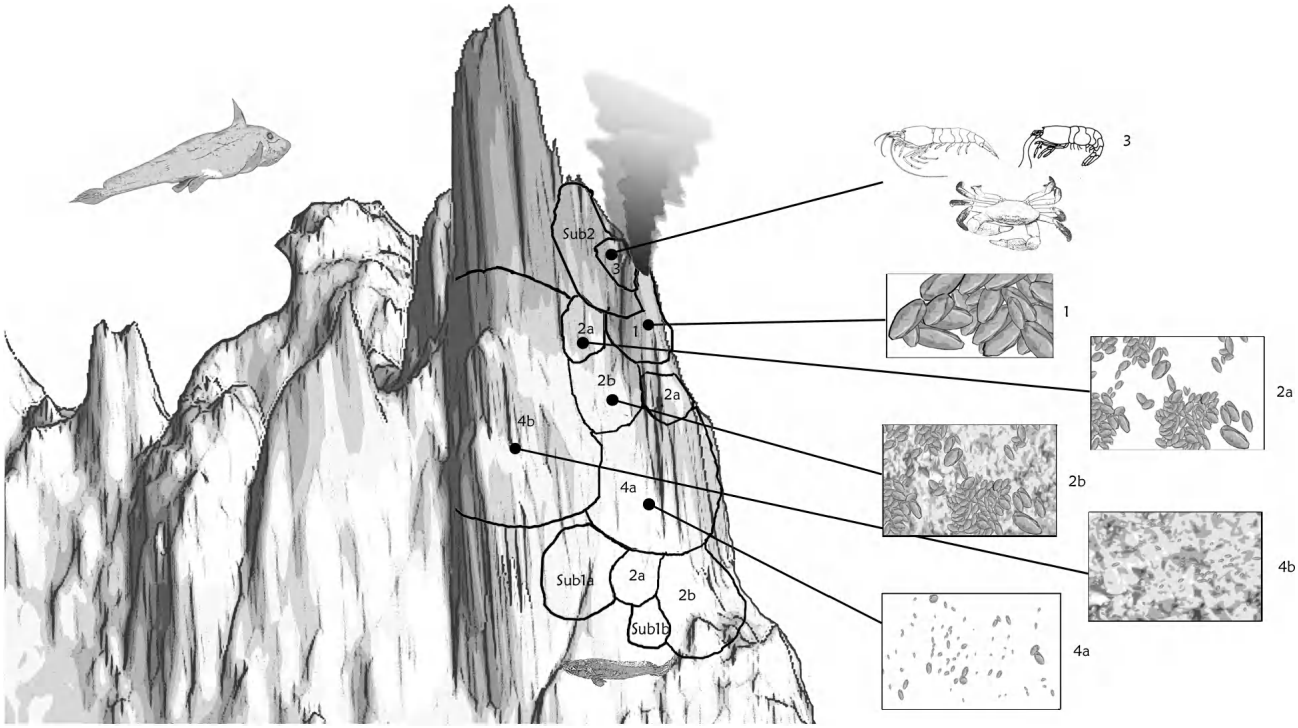

Fig. 2.7. A conceptual model representing an idealized biological zonation of assemblages and substratum distribution at Eiffel Tower, taking into account all results presented this study. Patches occupied by assemblages and substrata are positioned on the structure in a way that represents their relative size and positions relative to other assemblages and to the fluid exit. Mean patch sizes are in proportion as well as the relative distance to the fluid exit. Faunal assemblages (1, 2a, 2b, 3, 4a, 4b) are represented by a sketch, substrata are named on the patch itself (Sub 1a, Sub 1b, Sub 2). Some predators are represented as well; *Cataetyx laticeps* (Pisces) is lying at the bottom of the structure, and *Hydrolagus pallidus* (Pisces) is passing by left of the sulfide structure. The presence of the crab, *Segonzacia mesatlantica*, is mostly driven by the presence of a food source.

The dependence of the mussel community on the lateral dispersion of vent fluids by the physical structure of the community makes individuals at the boundaries vulnerable to a disruption in reduced chemical supply. A limit to autotrophy would constrain the growth rates within the vent environment, enhancing the spatial segregation between large and small sizes and their proximity to fluid exits. We speculate that individuals living closer to fluid exits could have a faster growth rate, or are able to attain larger sizes because there is no limit to sulfide and methane (see Bergquist et al., 2004 on *Bathymodiolus childressi* at cold seeps).

In the Pacific hydrothermal vents *Bathymodiolus* species are regarded as the final survivors in waning vent fields. When the activity decreases they tend to out-compete the siboglinid tubeworms (Hessler et al., 1985). Mussel beds offer a complex secondary surface and interstitial microhabitats for associated species (Van Dover & Trask, 2000). The provision of complex physical structures by foundation species plays a role in the composition and diversity of vent communities. It contributes to

altering the physico-chemical environment, and thus influences the physiology of the organisms (Bergquist et al., 2004; Govenar & Fisher, 2007). Although naturally high densities of mussels can directly or indirectly inhibit recruitment of invertebrates at deep-sea hydrothermal vents (Lenihan et al., 2008), gastropod grazers are found on the mussel shells, possibly feeding on the microbial cover. In addition, some gastropod species at other vent sites have been observed to (re)position themselves along thermal gradients, looking for the ideal temperature regime (Bates et al., 2005; Mills et al., 2007).

New mytilid recruits occur on the mussel shells in the other assemblages and in larger numbers on bare substratum in Assemblage 4, which is present on all sides, tower and periphery, of the edifice, mostly at the base. Assemblage 4 can be either closer to lower temperature exits (e.g. flanges, diffuse flow) or further away from high temperature black smokers. Often dead mussel shells can be encountered in the immediate vicinity. A change in the porosity of the substratum or local (de)activation might explain this observation.

Decapod predators and scavengers (*Segonzacia mesatlantica, Mirocaris fortunata, Chorocaris chacei* and *Alvinocaris markensis*) are all very mobile and can occur anywhere on the edifice, but they are most abundant in the more hydrothermally-active zones. *Segonzacia mesatlantica* appears to require rougher vertical substrata onto which they can grip, or horizontal platforms from which they cannot slip off, or mussel beds that provide ample support.

4.2.2. Shrimp assemblage

The occurrence of shrimp (Assemblage 3) is an indication for the proximity of vent fluid exits since they are usually present in the warm water flow. The higher abundance of Alvinocarididae on the more active East and South sides and the peripheral zones can be explained by the higher hydrothermal activity observed there. At Eiffel Tower, the shrimps may be predators and/or scavengers, consuming free-living bacteria present in the hydrothermal solution flows or ingesting other small invertebrates (Gebruk et al., 2000a; Colaço et al., 2002). Shrimps also exhibit a more opportunistic behaviour as they can be observed feeding on broken mussel shells. *Segonzacia mesatlantica* consumes shrimps and other small invertebrates (Voight, 2000; Colaço et al., 2002) and were also abundantly present at broken mussel shell sites. *Mirocaris fortunata* is present in almost all samples taken at Eiffel Tower (Sarrazin et al., in prep.) suggesting that they live in the interstitial spaces between the mytilids or hidden in the cracks and crevices from which fluids enriched in micro-organisms can be emanating.

4.3. Comparison between the edifice sides

The hydrothermally most active sides of Eiffel Tower show a lower degree of colonisation and share a similar composition. Analogously the less active sides display a high degree of colonisation with a comparable composition. However, if there is no hydrothermal activity there is no visible vent-associated fauna. While carrying out video-transects, the temperature sensor on the ROV Victor registered up-welling clouds of hot fluids present at East and South sides and the highest temperature was reached at the top of the edifice. Similar patterns were observed for the North and West sides but the temperature differences were considerably smaller than on the more active sides (ca. 1.2°C for the North and West sides compared to 4°C for the East and South sides). The sides that were considered the most active showed the highest temperatures, linking temperature with flow vigour as already suggested by Sarrazin et al. (1997) for the Pacific.

The highest percentage of colonisation can be found on the West side of the edifice. The mussel shells are mostly of a smaller size range than on the other sides (dominance of Assemblages 2a and 2b; Fig. 2.3h). Many mussels on the West side were observed with their siphons opening upwards. This might be explained by the fact that *Bathymodiolus azoricus* is capable of filter feeding, in addition to supporting a nutritional relationship with the bacterial symbionts in its gill tissue (Tunnicliffe, 1991; Colaço et al., 2002). The limited supply of hydrothermal fluids and reduced chemicals on the West side might constrain their growth, explaining the high abundance of smaller sized individuals on this side. According to a carbon-flux model developed by Martins et al. (2008), small mussels depend more on filter feeding than big mussels, which rely mostly on chemosynthesis.

The western periphery is fairly active compared to the tower. We suggest that the West side tower is less permeable since there are almost no fluid exits. Fluids may have been redirected towards the periphery because the main tower was partially clogged. The south peripheral zone is very active and shows a low degree of colonisation. The percentage of colonisation is equally divided between the different faunal assemblages (1, 2a, 2b and 3 – Fig. 2.3(h)). Individuals of *B. azoricus* living in this zone are quite large (≥4cm). Most likely these adults originate from the main tower 1 or 2 m away.

4.4. Habitat and substrata

Hydrothermal vent fields and sites are very changeable environments. Unlike the high frequency of eruptive events on fast-spreading ridges, drastic changes in the Atlantic Ocean are rather rare (Van Dover, 1995), but a certain degree of (sulfide) accretion is responsible for some structural changes (Haymon et al., 1983), providing additional substrata for fauna to occupy (Copley et al., 1997; Sarrazin

et al., 1997; Butler et al., 1998). Some of these rapid accretions are responsible for certain over-night changes in the appearance of the Eiffel Tower edifice.

The presence of shimmering water and even black smokers at the base and the peripheral zones could be explained by the redirection of the fluids. During the life span of a hydrothermal vent, the edifice can become clogged by mineral precipitation. Sulfide deposition causes loss of pore connectivity in the sediment, thus drastically reducing the substratum permeability and fluid flow rate (Zhu et al., 2007). The fluids may be redirected towards the periphery, as observed on Juan de Fuca Ridge (Sarrazin et al., 1997).

The colour of the substratum can depend on the nature of the minerals precipitating from the vent fluids. Substratum 1a has no visible mineral precipitation and is unable to support vent-endemic fauna, probably because it is not permeable, i.e. no hot fluids can seep through. It can be present as small patches between the faunal assemblages or as larger patches further away from the fluid exits and nearly always at the base of the structure. In contrast, Substratum 2, which is characterised by obvious anhydrite precipitation, appears to be permeable, letting warm fluids flow through. It often seems to act as a buffer zone between the fluid exits and the faunal patches. Substratum 1b can be covered by thick microbial mats that can serve as a feeding ground for grazing organisms further away from the fluid exits. The nature of the substratum (porosity, composition and instability) may play an important role in structuring vent assemblages and its importance should not be underestimated (Tunnicliffe, 1991; Grehan & Juniper, 1996; Copley et al., 1997; Shank et al., 1998a; Sarrazin et al., 2002; Tsurumi & Tunnicliffe, 2003; Zhu et al., 2007).

5. Conclusion

A patchy zonation of biological assemblages around fluid exits on the Eiffel Tower hydrothermal construct was revealed (Fig. 2.7). A fluid exit is always bordered by Substratum 2 that can be colonised by shrimps (transforming into Assemblage 3) followed by larger-sized mussels (Assemblage 1). Beyond this point, a decrease in mussel densities and sizes occurs with increasing distance from the fluid exits (Assemblages 2 to Assemblages 4) as well as an increase in the area of bare surface between the mussel clumps. A gradient is thus created by the presence or absence of fluid exits and the fluid flow dynamics. This implies a spatial segregation of assemblages based on proximity to fluid exits and correlated environmental factors. As a result, there is a greater similarity in the percentage coverage of faunal assemblages and substrata between the highly active sides of the hydrothermal edifice. The same relationship applies to the less active sides. The influence of factors such as geomorphology and porosity of the substrata on assemblage distribution should not be underestimated. These can

constrain the ability of fauna to colonise certain regions. Biological interactions are another likely factor influencing faunal distributions, although their importance is difficult to verify based on imagery.

Acknowledgments

I would like to thank Captain P. Guillemet of the R/V Pourquoi pas? and his crew for their collaboration indispensable to the success of the MoMARETO cruise. I also acknowledge the Victor 6000 ROV pilots for their patience and constant support. I am grateful to P-M Sarradin, second chief scientist on the MoMARETO cruise for his help and ideas and to H. Ondréas for the kind assistance with the creation of the maps of the MAR and Eiffel Tower.

Chapter 3

14-years of community dynamics at the Eiffel Tower hydrothermal edifice

Submitted as:

Cuvelier D., Sarrazin J., Colaço A., Copley J.T., Glover A.G., Tyler P.A., Serrão Santos R., Desbruyères D. Community dynamics over 14 years at the Eiffel Tower hydrothermal edifice on the Mid-Atlantic Ridge. Manuscript accepted for publication in *Limnology & Oceanography*

CHAPTER 3
14-years of community dynamics at the Eiffel Tower hydrothermal edifice

1. Introduction

Despite over 30 years of research since the first hydrothermal vent discoveries (Lonsdale, 1977), the functional ecology of these remarkable deep-sea ecosystems is only gradually being revealed. Although our understanding of the faunal assemblages inhabiting vents is growing, their long-term dynamics remain unclear. Many recent discoveries of hydrothermal venting have taken place in the South Atlantic, Arctic, West Pacific and Indian Oceans, but time-series studies, however, are scarce and restricted to several well-known and more accessible sites in the East Pacific and the North Atlantic Oceans. Ecological temporal variations studies have been carried out on the Galápagos Rift (Hessler et al., 1985, 1988), the East Pacific Rise (EPR: Fustec et al., 1987; Desbruyères, 1998), the Juan de Fuca Ridge (JdF: Sarrazin et al., 1997), and in some cases, monitoring started right after or during an eruption (Shank et al., 1998a (9.5°N, EPR); Tunnicliffe et al., 1997; Tsurumi & Tunnicliffe, 2001 and Marcus et al., 2009 (JdF); Shank et al., 2003 (Galápagos Rift)). Each of these studies attempts to disentangle community dynamics and assess or propose a succession model. There is only a single long-term temporal dynamics study available for the Mid-Atlantic Ridge (MAR) (Copley et al., 2007a). For all these time-series studies, imagery analysis was an important tool.

Individual vent fields provide ephemeral habitats for faunal assemblages, but based on sulfide geochronology (Lalou et al., 1991), hydrothermal activity on slower-spreading ridges (e.g. MAR) appears to have a longer lifespan than on faster-spreading ridges (e.g. EPR). While catastrophic perturbations seem to occur on time-scales of years to decades on fast-spreading ridges, they would be far less common on slow-spreading ridges, where a relative "stability" is observed (Lalou et al., 1991; Desbruyères et al., 2001). Spreading rate influences faunal assemblage stability on long-term, while local site- or vent field specific factors appear more significant on shorter time-scales. The geological history of the local seafloor, which varies among ocean basins, is probably the most important factor in determining changes in fluid composition and temperature on short-term scales (Von Damm et al., 1998). This fluid composition is one of the most important factors, as its chemical composition and fluid flow intensity have a large impact on the composition, distribution and dynamics of

hydrothermal vent assemblages (Fustec et al., 1987; Hessler et al., 1988; Sarrazin et al., 1997; 2002; Shank et al., 1998a; Desbruyères et al., 2000).

In post-eruption studies, the original fauna inhabiting the vents is massively removed as a consequence of the destructive events linked with the eruption (e.g. paving, edifice collapse). Changes in community dynamics of the pioneers and subsequent colonisers are linked with variations in temperature, sulfide supply and fluid composition (Shank et al., 1998a; Tunnicliffe et al., 1997; Tsurumi & Tunnicliffe, 2001). In studies under continuous venting conditions, the de- and reactivation of fluid exits, chimney collapse and progressive mineralization of hydrothermal edifices contribute to fluid flow modification at small spatial scales, which impact the faunal distribution and dynamics (Tunnicliffe, 1990; Sarrazin et al., 1997; 2002; Desbruyères, 1998). Biological interactions also play an important role in explaining the assemblage mosaic distribution and composition along environmental gradients (Hessler et al., 1988; Sarrazin et al., 1997; 2002; Mullineaux et al., 2000; 2003; Micheli et al., 2002).

Under conditions of continuous venting, Copley et al. (2007a) assessed decadal change at the Atlantic TAG sulfide mound (3600 m of depth), based on 2 sampling cruises. The first cruise took place in 1994 with the Russian submersible Mir, while the other occurred in 2004 with the American ROV Jason 2. Over 10 years, TAG displayed decadal-scale constancy in community structure, without significant differences in shrimp and anemone populations. This decadal constancy coincides with a steadiness in physical parameters on decadal time-scales (Copley et al., 2007a). Such a physical constancy cannot be assumed for the other Atlantic vent fields, as a significant variability in seismic event rate along the axis of the MAR was observed (Smith et al., 2003). Additional differences between the various Atlantic vent fields have already been demonstrated, as water depth changes, the geology of source rocks and the nature of the hydrothermal deposits vary as well, causing the vent habitats to differ in their fluid chemistry (Desbruyères et al., 2000). This alteration with depth is associated with a shift in faunal dominance from deeper alvinocaridid shrimps to shallower mussel-dominated sites (Desbruyères et al., 2001). Whether these alterations have an impact on the community dynamics at the shallower Lucky Strike vent field will be evaluated.

Studies investigating both long-term (>10 years) variations in community structure and dynamics on shorter time-scales (1 to 4 years) are non-existent for the Atlantic vents. The present study is the first high-resolution long-term ecological variations study on the Mid-Atlantic Ridge. Our main objectives were to investigate if: (1) faunal assemblage composition and their relative proportions on the edifice

change significantly between the years, (2) alterations in hydrothermal activity affect community dynamics, (3) the rate of change in community dynamics is lower on a slow-spreading ridge than on fast(er)-spreading ridges, (4) a recognisable succession can be identified.

2. Material & Methods

2.1. Study Site

In the Azores Triple Junction area, several hydrothermal vent fields can be found within the Portuguese EEZ. One of them, the Lucky Strike vent field (37 °17.5'N, 32° 16'W) is situated on the Mid-Atlantic Ridge, south of the Azores at a mean depth of 1700m. Following its discovery in 1992, 20 scientific cruises (by 2010) dived to this vent field, of which 10 had imagery available for this study (Table 1). One of the most visited edifices is Eiffel Tower, where ~40% of all diving time was spent. This well-defined and active 11 m-high sulfide edifice is the focus of this ecological time-series study. Eiffel Tower is situated in the south-eastern sector of Lucky Strike between two of the three volcanic cones surrounding the central lava lake, characteristic to this vent field. These 3 cones form the present day summit of the volcano (Ondréas et al., 2009, Fig. 3.1). Lucky Strike is one of the MAR sites considered of importance for conservation (Santos et al., 2003) and it was included in the OSPAR network of MPAs in 2007 and accepted by the EC as a Site of Community Importance [SCI] under the Natura 2000 network in 2009.

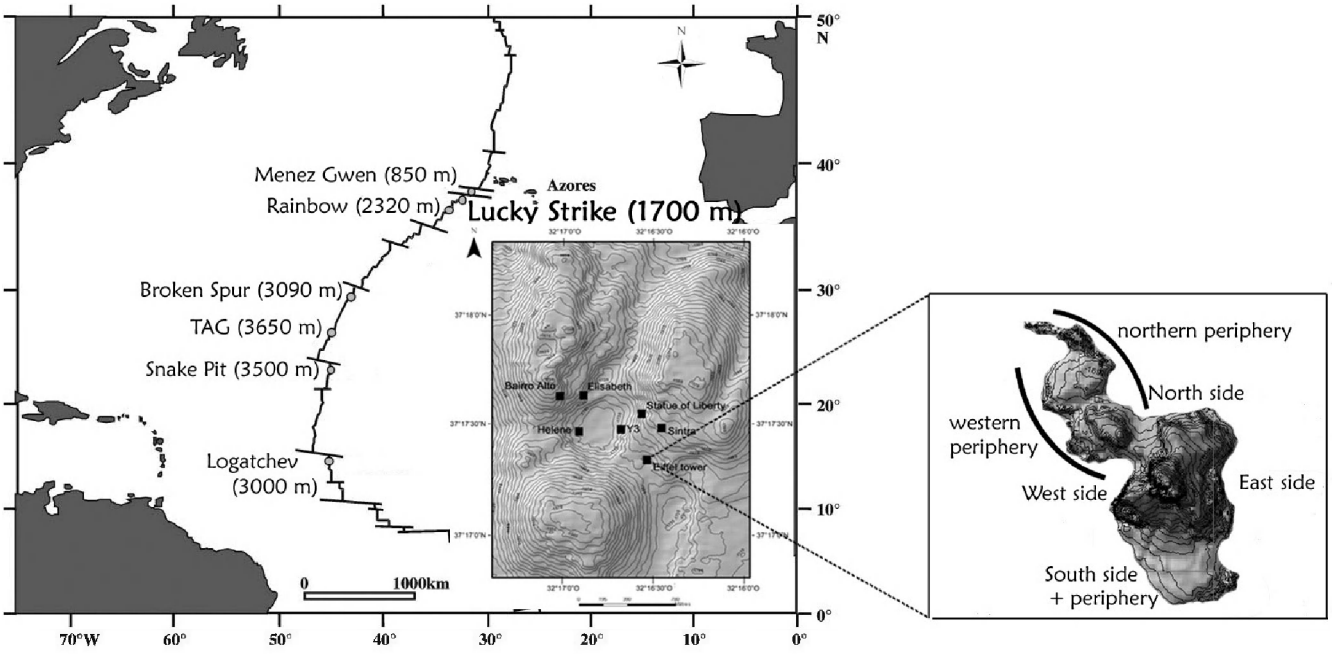

Fig. 3.1. Major vent fields on the northern Mid-Atlantic Ridge are shown, with as inset the Lucky Strike vent field. The location of the Eiffel Tower edifice is shown next to a zoom-in on this sulfide structure together with the terminology used according to the orientation of the different sides of the edifice.

2.2. Video analyses

This study encompasses both analysis of historical VHS analogue video footage going back to 1994 as well as newly carried-out digital video transects (for an explanation of the term "transect", see Material & Methods of Chapter 2). This implies the use of images that were recorded without the explicit purpose of creating an imagery overview of the site or without the repetition of defined videographic transects which would have facilitated a temporal variation study. The dives of the cruises available were carried out with either the submersible Nautile (1994, 1997 and 1998) or the ROV Victor 6000 (2001, 2002, 2005, 2006 and 2008). First of all, the use of manned submersibles leads to a different acquisition of imagery. When not acquired intelligently, images are in danger of becoming of secondary importance during manned submersible dives, while for remotely operated engines, the real-time imagery arriving on board is of primary importance, first of all to pilot the vehicle and secondly, to gather scientific information. This drawback is particularly evident for the 1997 Marvel and Flores cruises (Table 3.1), where the compiled imagery was insufficient to allow reconstruction of the Eiffel Tower edifice. Therefore the year 1997 was omitted in this study. However, when video or imagery transects are carried out methodologically, manned submersibles are as efficient as ROV's.

Table 3.1. Overview of all the available cruises, research vessels and submersible platforms (submersible Nautile or ROV Victor 6000) used in data collection, as well as the chief scientists. The Eiffel Tower edifice was divided in different sides according to their orientation (Fig 1.) and the side reconstructions possible with the available imagery are shown. X=complete imager coverage available, /=no imagery data available, Partially=Partial reconstruction of the side in question (over 85% was reconstructed).

Cruises	Research Vessel	Engine	Chief Scientist	Years	North	East	South	West	N_Periph	S_Periph	W_Periph
DIVA1	Nadir	Nautile	Y. Fouquet	1994	Partially	X	X	X	X	X	X
DIVA2	Nadir	Nautile	D.Desbruyères A-M Alayse								
MARVEL	L'Atalante	Nautile	D.Desbruyères A-M Alayse	1997	Partially	Partially	Partially	/	Partially	/	Partially
FLORES	L'Atalante	Nautile	Y. Fouquet								
PICO	Nadir	Nautile	D.Desbruyères	1998	X	Partially	X	X	X	X	X
ATOS	L'Atalante	Victor	P.M. Sarradin	2001	X	X	X	X	X	X	X
SEHAMA	L'Atalante	Victor	F. Barriga	2002	X	X	X	X	Partially	Partially	Partially
EXOMAR	L'Atalante	Victor	A. Godfroy	2005	X	X	X	X	Partially	X	X
MOMARETO	Pourquoi pas?	Victor	P.M. Sarradin J. Sarrazin	2006	X	X	X	X	X	X	X
MOMAR08	L'Atalante	Victor	J. Escartin	2008	X	X	X	X	X	X	X

There was a difference in resolution for the high-definition pictures, where the resolution was lower for the images taken with the Nautile submersible, varying between 736x576 pixels and 1024x768 pixels. Images taken with ROV Victor in the later years had a higher resolution: 2048x1536 pixels.

Screen stills taken from video imagery all had a resolution of 696x576 pixels independent whether they were collected with Nautile or Victor, although inevitably the video quality was different due to the recording year.

Because of the utilisation of two different submarine engines and cameras, several features, like for example the overall growth of Eiffel Tower edifice, were impossible to assess. Another disadvantage of image analyses is the exclusion of smaller fauna, not visible on the images, as well as the underestimation of the thickness or actual density of the faunal assemblages. Notwithstanding these disadvantages, studying temporal variations based on imagery is far more unbiased than discrete sampling. In addition, it allows us to recreate a larger scale overview and it is a non-invasive technique.

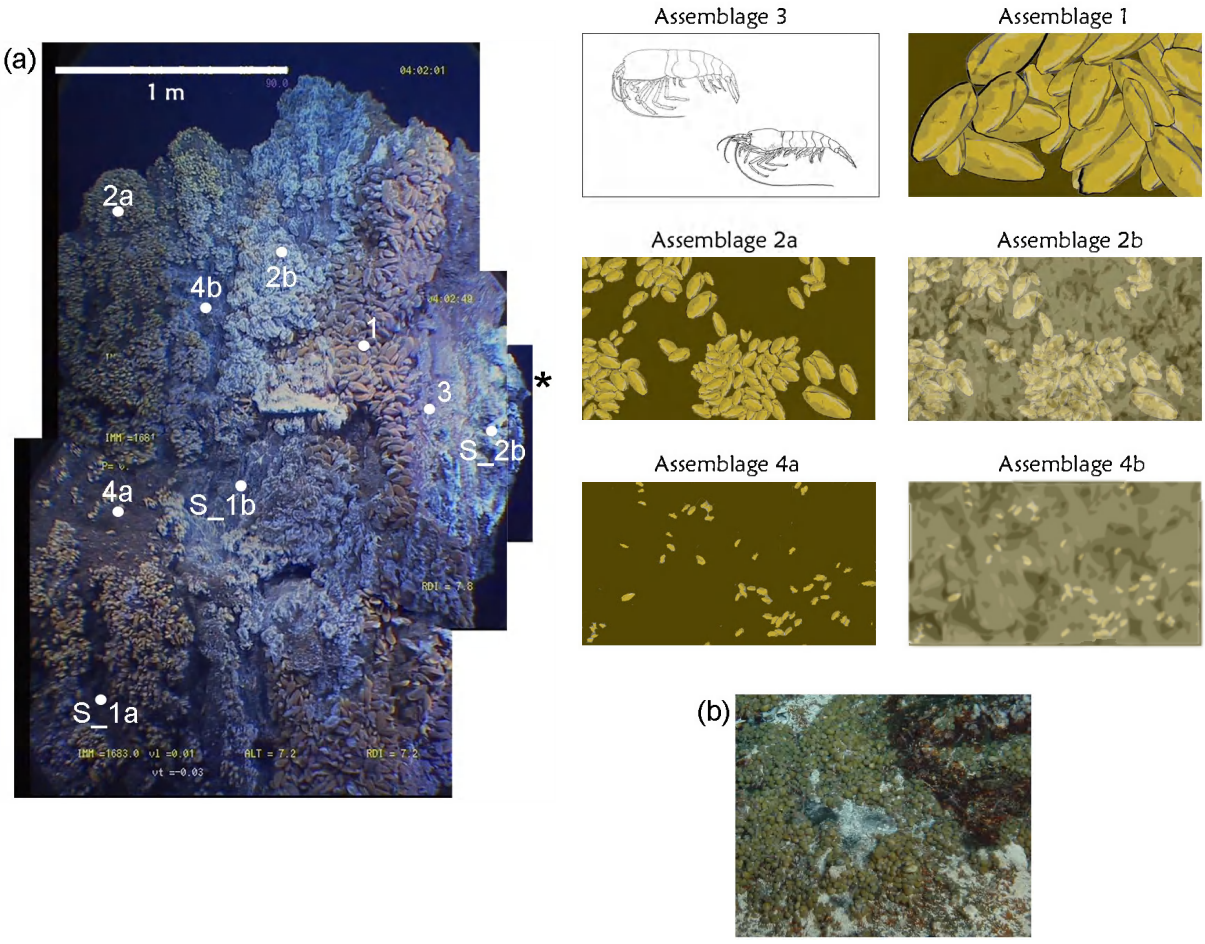

Fig. 3.2. (a) A mosaic of the West side of Eiffel Tower (MoMAR08) is presented with the distribution of the assemblages (1, 2a, 2b, 3, 4a and 4b) followed by a schematic drawing or explanation (from Cuvelier et al., 2009). The substrata are marked with their name on the mosaic with Substratum 1a (S_1a): red-brown substratum, Substratum 1b (S_1b): brown bare substratum with filamentous microbial cover and Substratum 2 (S_2): bare substratum with anhydrite precipitation and patchy microbial cover. Zonation patterns are representative of the reality, with the black smoker (*) surrounded by Substratum 2, which gets colonised by shrimps (Assemblage 3) and larger-sized mussels (Assemblage 1). A decrease in mussel size and density (Assemblage 2 to Assemblage 4) is observed with increasing distance from the source of hydrothermal fluid. (b) A unique assemblage was observed in 1994, consisting of alvinocaridid shrimp and the limpet *Peltospira smaragdina*.

Image mosaics of all sides of the hydrothermal edifice (see Fig. 3.1 for the different sides of the edifice and see Fig. 3.2a for an example of a partial mosaic) were constructed using the protocol described by Cuvelier et al. (2009): screen stills were taken from the videos, pixel lengths of an object or part of the edifice present on 2 subsequent images was measured and adjusted to one another to be equal in length, allowing superimposition and merging in order to create one mosaic per side (Table 3.1). On these mosaic templates, the assemblages and substrata were mapped (Fig. 3.3), digitized and the area they covered measured through pixel-based image analysis software (IP Lab Spectrum®). To partially counteract the degree of distortion caused by the use of two different submersible platforms and camera systems, we chose to work with the percentages of coverage of each assemblage and substratum for subsequent analyses. Three types of fluid exits (black smokers, flanges and diffusion zones), visible on the video images, were also identified and mapped on the mosaics (Fig. 3.3).

The faunal assemblages and substratum types were defined based on high-definition photographs and video imagery (Fig. 3.2a, Chapter 2, Cuvelier et al., 2009). These ranged from dense larger-sized *Bathymodiolus azoricus* mussel beds, which can contain an occasional patch of microbial cover (Assemblage 1) to smaller (medium)-sized mussel clumps (without visible microbial cover: Assemblage 2a, and with microbial cover: Assemblage 2b) to bare surface with very small dispersed mussels (Assemblages 4a and 4b, respectively without and with microbial cover) and alvinocaridid shrimps (Assemblage 3). In addition, two types of substrata were identified, varying from red-brown surface (Substratum 1a) with a white filamentous microbial cover (Substratum 1b) to substratum with anhydrite precipitations (Substratum 2). The latter also contains patches of microbial cover (Fig. 3.2a). In addition to the assemblages described by Cuvelier et al. (2009) (see Chapter 2), the presence of a unique assemblage was detected in 1994, consisting of small gastropods (limpets) and alvinocaridid shrimps, and was characterised by the presence of smokers or shimmering water, originating from cracks on the surface (Fig. 3.2b). After 1994, this assemblage was no longer observed at Eiffel Tower, and was thus not considered in the statistical analyses.

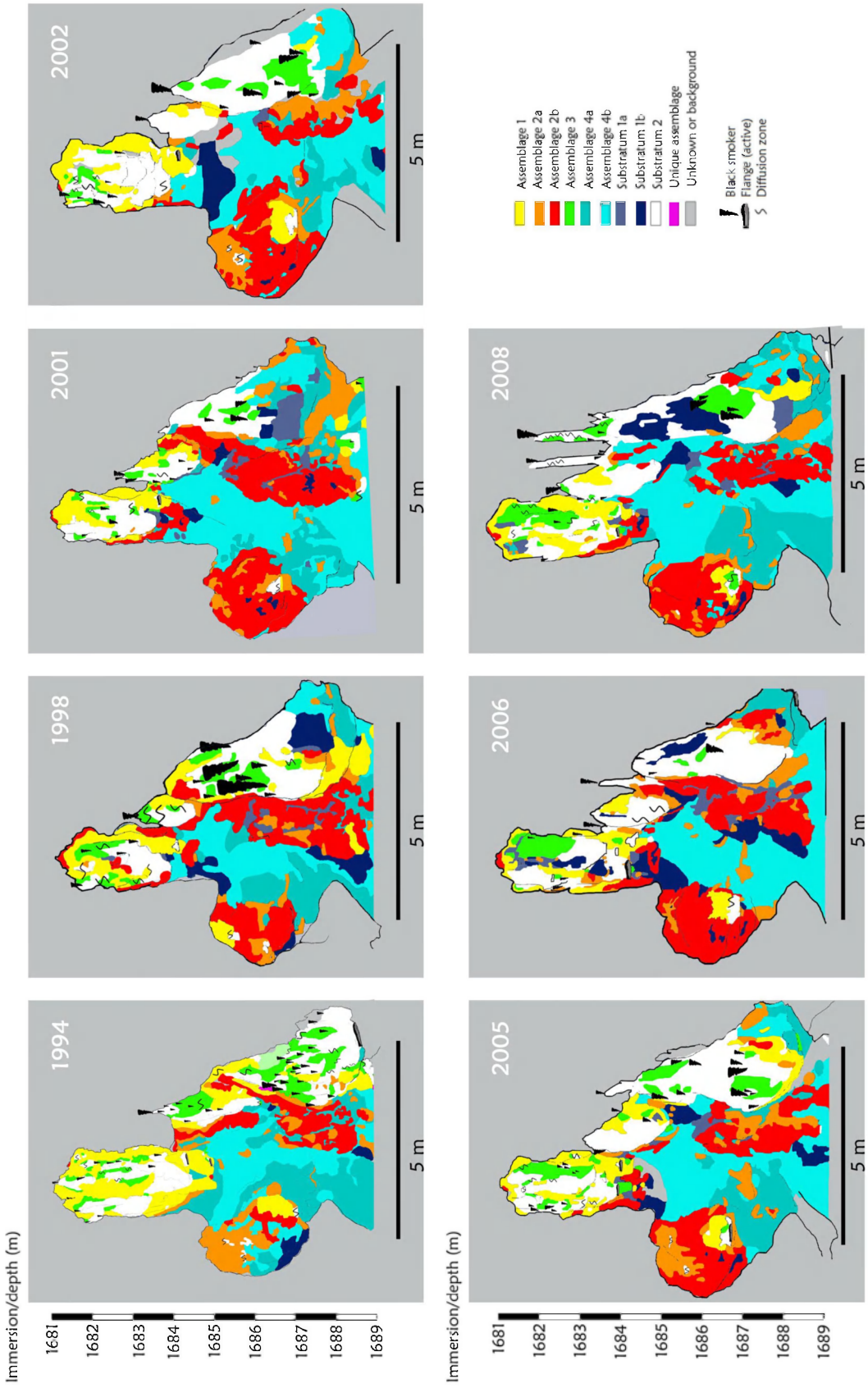

Fig. 3.3. The South side of Eiffel Tower is represented for the years available, showing its variations over time. The assemblages and substrata are colour-coded, while the different activity features are portrayed by symbols. A 'unique assemblage', only observed as a small patch in 1994, is presented in pink. The 'unknowns' are grey patches; they represent zones for which it was impossible to attribute an assemblage or substrata, mostly due to the lack of images. Differences in overall surface/shape of this South side are either due to sulfide precipitation, accretion and chimney collapse. There are also small deformations due to the use of different cameras and

submersibles as well as to the often random ways of acquiring images while diving. For characterisation of the assemblages see Fig. 3.2.

2.3. Detailed community dynamics

To assess community dynamics, the maps of the edifice sides, as presented in Fig. 3.3, were divided in smaller parts. A selection of similar and equally-sized regions of the Eiffel Tower edifice were thus obtained for all the years available. These selected regions showed a high degree of comparability between the consecutive years concerning their surface size. Based on the size of the surface covered by the selected region, a grid of points, equally spaced 25 cm apart, was overlaid (Fig. 3.4). Each of these points represented the centre of a grid cell, so theoretically a digitally generated grid with 25x25cm mesh size was superposed (see Fig. 3.4). To each point the feature of the underlying assemblage or substratum was assigned.

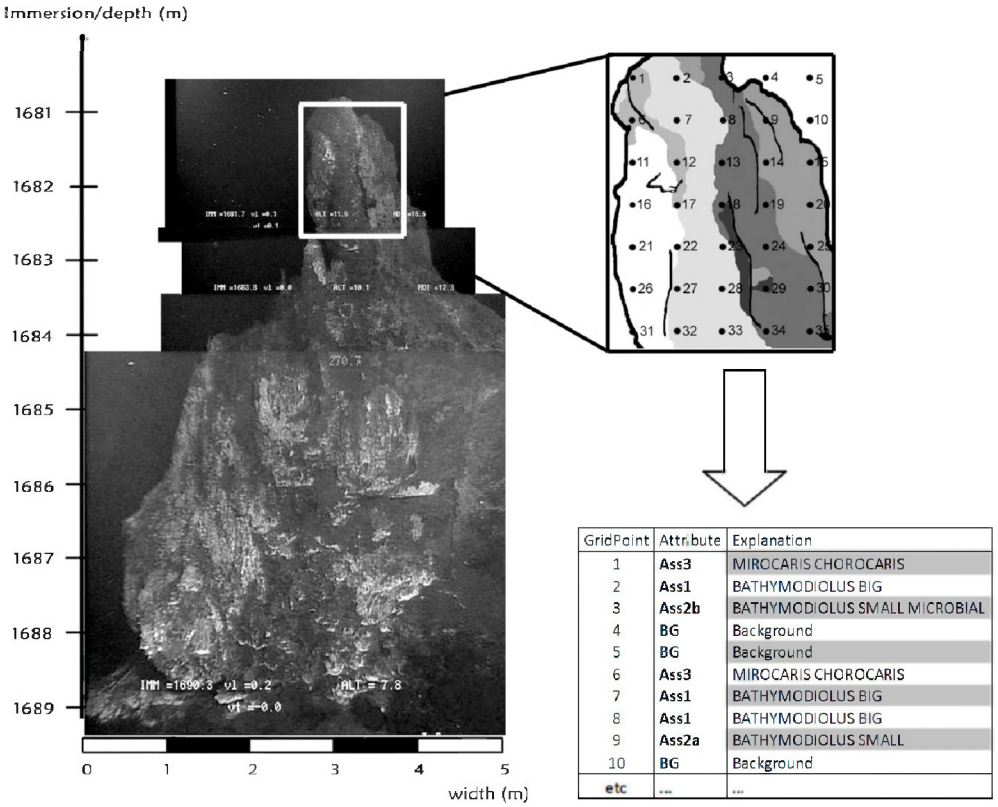

GridPoint	Attribute	Explanation
1	Ass3	MIROCARIS CHOROCARIS
2	Ass1	BATHYMODIOLUS BIG
3	Ass2b	BATHYMODIOLUS SMALL MICROBIAL
4	BG	Background
5	BG	Background
6	Ass3	MIROCARIS CHOROCARIS
7	Ass1	BATHYMODIOLUS BIG
8	Ass1	BATHYMODIOLUS BIG
9	Ass2a	BATHYMODIOLUS SMALL
10	BG	Background
etc	...	...

Fig. 3.4. Illustration of grid-overlay and attribution of assemblages on a selected region of the edifice.

The grid-overlay and the attribution of assemblages and substrata were done in CPCe (Coral Point Count with Excel extensions, Kohler & Gill, 2006). A specific code file was created to be used within this program, allowing assemblage and substrata assignment to the grid-points. Attributes included the (a) type of assemblages and (b) substrata, (c) background, i.e. points that fell outside of the edifice scope and were thus not located on the edifice and (d) "unknown". Grid-points with the same location among the years had the same number. This procedure was repeated for each year and the same

numbered grid-points between the years were compared. The frequencies of changes from assemblage x to assemblage y was quantified for all the years. Changes between the consecutive years were analysed as well as over the entire time span of 14 years (1994-2008). Recurrent patterns over this 14-year period were revealed, by identifying the most frequent transitions for each assemblage and/or substratum type into another.

2.4. Statistics

NMDS (Non-metric Multi-Dimensional Scaling) and cluster analyses were performed with the Vegan package (Oksanen et al., 2008) in R (version 2.8, Multicore team 2008), while correlations and significance tests were carried out in Statistica 6 (StatSoft Inc. 2001). Percentage assemblage and substratum coverage data were ArcSine transformed (Sokal & Rohlf, 1995). We used NMDS because, in addition to its robustness, it can find non-linear relationships. The NMDS plots carried out in this study were based on Bray-Curtis calculations, which computed dissimilarity indices. Environmental variables were added as vectors and a summarising environmental variable was fitted as a surface on the plot. The latter was based on GAM (General Additive Model) predictor and smoothing functions. For the cluster analyses, Bray Curtis distances were used together with Ward's clustering methods and clustering happened agglomerative.

For the parametric significance tests (ANOVA) between the years, the assemblages, the sides and the activity features were analysed to investigate if the variation between them was significantly larger than the natural variation occurring within. The untransformed data were used, unless the assumptions to correctly carry out an ANOVA were violated. If after transformation the assumptions were still not met, non-parametric testing (Kruskal-Wallis and Mann-Whitney U tests) was carried out. To determine variation in hydrothermal activity, the counts of black smokers, flanges and diffusion zones were used, since the same sides of the edifice were compared between the years. For the overall (entire edifice) degree of activity, the means of these counts per year were used. Correlations were calculated between activity features, assemblages, sides and years, to investigate their relation to one another. We chose to use Spearman Rank correlations, as these are less sensitive to outliers and do not assume normality of the data.

3. Results

Temporal dynamics of vent assemblages were investigated from three different perspectives (1) for the entire edifice, where all the sides were added up to compare the entire structure between the individual years. Error bars therefore reflect variation between the different sides; (2) on different

sides of the edifice separately (an overview of the South side is given in Fig. 3.3); and (3) at the level of small-scale assemblage dynamics over 14 years.

3.1. Temporal variations on the entire edifice

3.1.1. Variations in hydrothermal activity

The numbers of black smokers, flanges and diffusion zones, and thus overall degree of hydrothermal activity, increased and decreased among the years analysed (Fig. 3.5). Some de- and re-activation of fluid exits were observed but the differences between the numbers were not significant (Kruskal-Wallis-test, $p=0.423$, $df=6$). The activity features were all positively correlated one to another (for all sides available, $df=43$). Black smokers and diffusion zones showed the strongest correlation ($r=0.76$, $p<0.05$), followed by black smokers and flanges ($r=0.63$, $p<0.05$). The correlation between flanges and diffusion zones was less pronounced ($r=0.38$, $p<0.05$). The activity on the tower was negatively correlated with that of the periphery for all types of fluid exits (r-values between -0.39 and -0.36, $p<0.05$), suggesting that when the activity on the tower increased, it decreased in the periphery and vice versa. The differences between tower and periphery were significant for all activity features (Mann-Whitney U test, $p<0.021$), with the overall activity being lower in the periphery. Flanges were the only activity features that were significantly and positively correlated with the years ($r=0.35$, $p<0.05$).

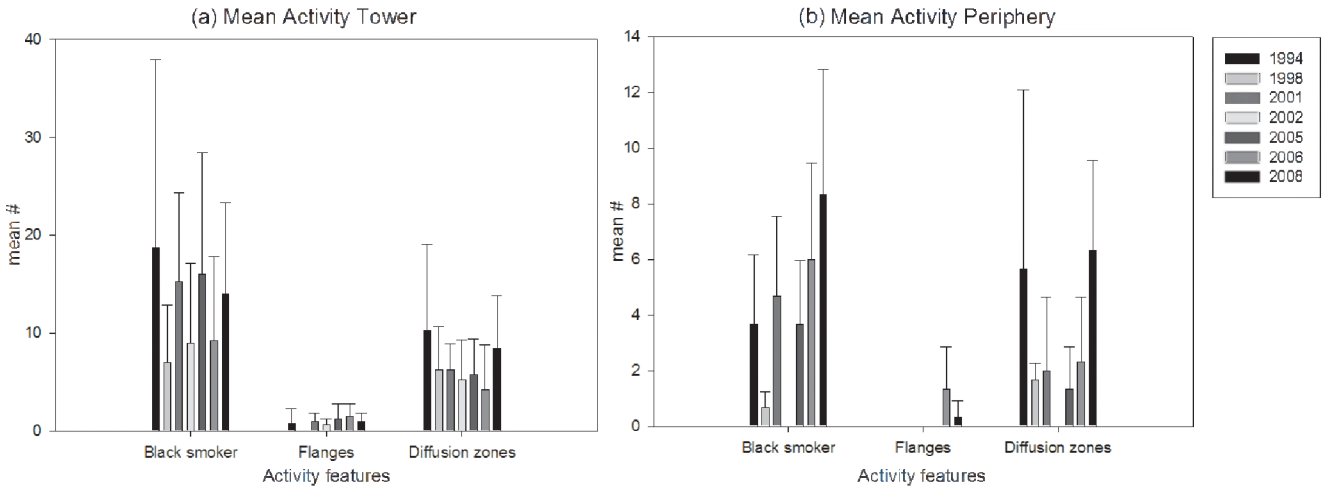

Fig. 3.5. Variation of hydrothermal activity on the Eiffel Tower edifice throughout the years, consisting of the mean counts of different visible hydrothermal activity features such as black smokers, flanges and diffusion zones (a) on the edifice, (b) on the periphery.

3.1.2. Variations in faunal assemblages and substrata

Over the 14 year time-scale, the percentage colonisation of Eiffel Tower edifice remained constant occupying about 50% of the edifice surface (Fig. 3.6a). No significant differences in the percentage of colonisation occurred between the years (Mann-Whitney U test, $p=0.65$). The assemblages used to

calculate the overall percentage colonisation were Assemblages 1, 2a, 2b, 3 (featuring a faunal coverage >50%) representing about 43-48% and Substratum 1b representing an additional 1-3%. Assemblages 4a and 4b were omitted because bare substratum largely dominates (>50%) these assemblages and the fauna is scattered and present in low visible densities. Small variations in the degree of colonisation or coverage among the years correspond to changes in hydrothermal activity (Fig. 3.6b). In 1998 and 2006, a decrease in activity coincided with an increase in percentage coverage. Conversely, in 1994 and 2008, the degree of colonisation decreased in relation with an increase in hydrothermal activity. A significant negative correlation existed between the percentage coverage and hydrothermal activity (r=-0.86, p=0.013, df=7).

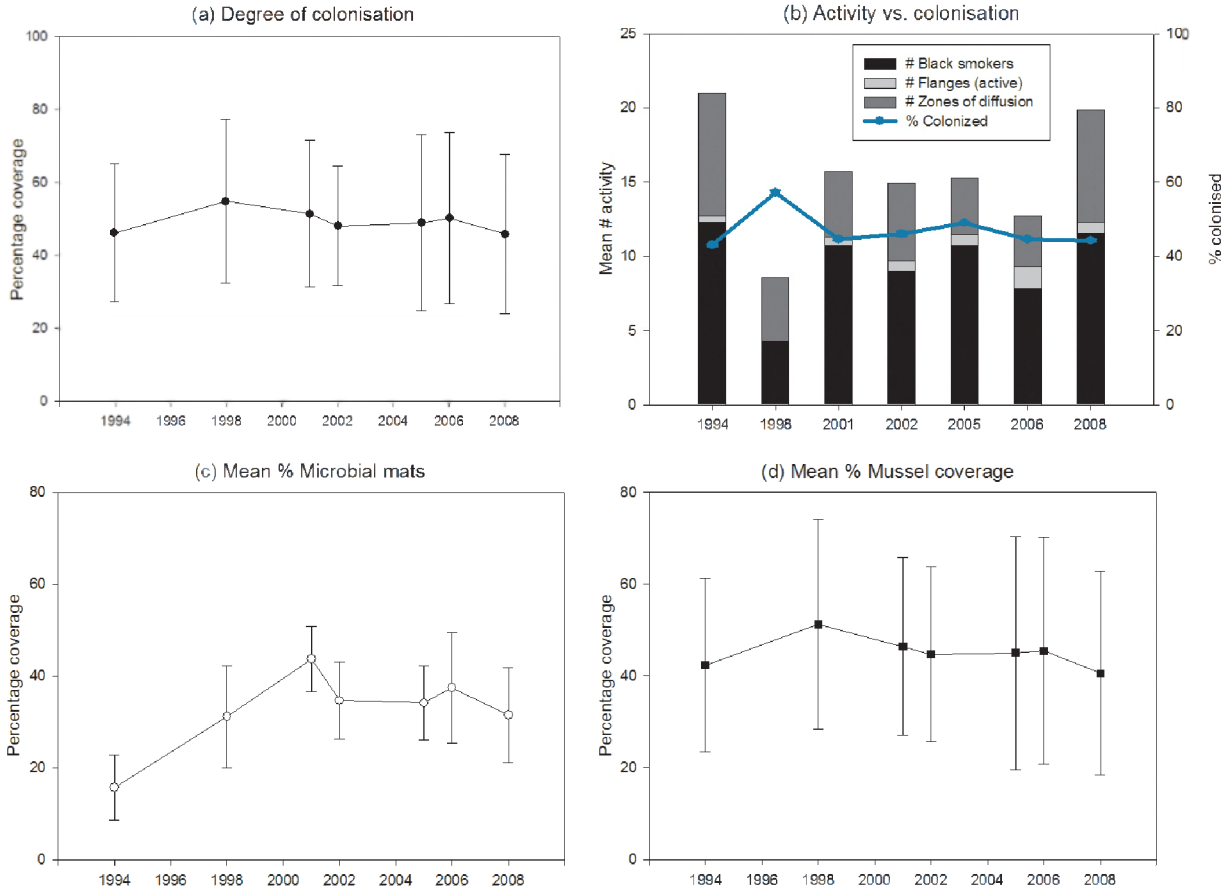

Fig. 3.6: (a) Variations in the degree of colonisation (% coverage) of faunal assemblages + substratum (those with a faunal coverage >50%, Assemblages 1, 2a, 2b, 3 and Substratum 1b), (b) variations in hydrothermal activity, in relation to variations in percentage coverage, (c) variations in the percentage of coverage of all assemblages and substrata with microbial mats (Assemblages 2b, 4b and Substratum 1b) and of (d) all mussel-based assemblages (Assemblages 1, 2a, 2b).

Coverage by visible microbial mats (consisting of Assemblages 2b, 4b and Substratum 1b) increased steadily over the time-intervals until it reached a peak in 2001 (Fig. 3.6c). However, the augmentation in microbial cover did not persist, as it was followed by a decrease in the subsequent years. Significant differences were observed (ANOVA, R^2=0.46, p=0.0006, df=6), which occurred because 2001, 2005 and

2006 were significantly different from 1994 (Tukey's HSD Post-Hoc test). No significant differences in microbial cover were observed between consecutive years. For the mussel coverage (consisting of Assemblages 1, 2a and 2b), a small peak was observed in 1998 that was followed by a decrease the subsequent year (Fig. 3.6d). The increase coincided with a decrease in activity features (see Fig. 3.6b), but no significant differences were observed for the overall mussel coverage between the years (ANOVA, R^2=0.022, p=0.99, df=6).

Even though the overall degree of colonisation stayed constant, the percentages of cover of the faunal assemblages (Fig. 3.7a) and substrata (Fig. 3.7b) did differ between the years and the sides. The decrease in percentage cover of an assemblage or substratum seemed to open up space for other assemblages to occupy, resulting in an increase in percentage cover for certain assemblages. However, the differences in percentage coverage between two consecutive years for a certain assemblage were rarely significant (Kruskal-Wallis tests, df=6). Only Assemblage 4a was shown to be significantly different between the years (p=0.009) as was Substratum 1a (p=0.03). Assemblage 4a showed a steep decrease, reaching a lowest value in 2002 after which it increased again (Fig. 3.7a). The larger-sized mussels of Assemblage 1 showed some small fluctuations, but overall they remained constant over the years, as did the alvinocaridid shrimp of Assemblage 3 (Fig. 3.7a). An increase of assemblages with microbial cover (Assemblage 2b and 4b) was also noticeable (but not significant), while the same assemblages without visible microbial cover (Assemblage 2a and 4a) tended to decrease over time, be it non significantly for Assemblage 2a.

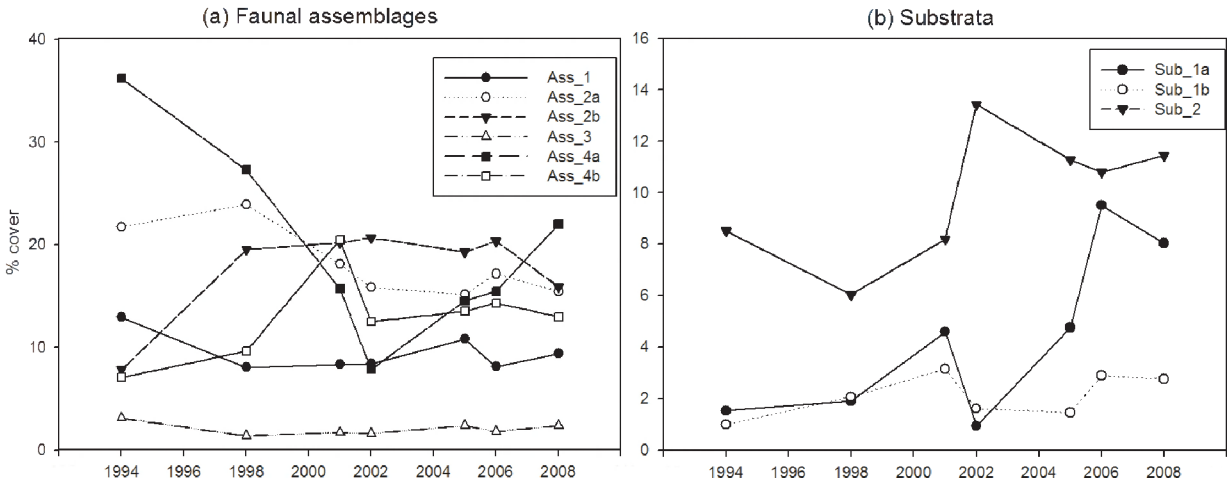

Fig. 3.7. Shifts in percentage coverage of the different (a) faunal assemblages and (b) substrata over time on the entire Eiffel Tower edifice. Error bars were omitted as the graph would have been difficult to interpret. The differences for the assemblages (Ass) and substrata (Sub) were mostly non-significant, with the exception of Assemblage 4a (Ass_4a) and Substratum 1a (Sub_1a) that showed significant differences between the years. For a characterisation of the assemblages see Fig. 3.2.

To unravel co-occurrence or exclusion tendencies between the assemblages and substrata over the years, correlations were calculated (df=43, Table 3.2). The correlations mentioned below were all significant and when positive, they implied that the assemblages and/or substrata tended to increase or decrease together. Negative correlations showed an inverse relationship: when one assemblage or substratum increased, the other decreased. Assemblages 1, 3 and Substratum 2 were positively correlated, and Assemblage 1 and Substratum 2 were negatively correlated with Assemblage 4a (Table 3.2). Assemblages 2a and 2b were positively correlated, but significant negative correlations existed with Assemblages 3, 4b, Substratum 1a, 1b and 2 for Assemblage 2a. For Assemblage 2b, these negative correlations were limited to Assemblage 4a and 4b. In addition to the correlations previously mentioned, Assemblage 3 was also positively correlated with Assemblage 4b and Substratum 1b. Positive correlations with Substratum 1a, 1b and Substratum 2 were observed for Assemblage 4b. Lastly, Substratum 2 had a positive correlation with Substratum 1b (Table 3.2).

Table 3.2. Spearman Rank correlations between the assemblages and substrata over time. The correlations marked bold are significant at $p<0.05$ (light grey=positive correlation, dark grey=negative correlation).

	As_1	As_2a	As_2b	As_3	As_4a	As_4b	Sub_1a	Sub_1b	Sub_2
As_1	1.00	0.14	0.22	**0.35**	**-0.33**	-0.14	-0.11	-0.15	**0.35**
As_2a	0.14	1.00	**0.56**	**-0.40**	-0.13	**-0.67**	**-0.45**	**-0.33**	**-0.54**
As_2b	0.22	**0.56**	1.00	-0.22	**-0.58**	**-0.36**	-0.28	-0.07	-0.23
As_3	**0.35**	**-0.40**	-0.22	1.00	-0.14	**0.39**	0.04	**0.33**	**0.77**
As_4a	**-0.33**	-0.13	**-0.58**	-0.14	1.00	-0.17	0.19	-0.15	**-0.31**
As_4b	-0.14	**-0.67**	**-0.36**	**0.39**	-0.17	1.00	**0.36**	**0.36**	**0.51**
Sub_1a	-0.11	**-0.45**	-0.28	0.04	0.19	**0.36**	1.00	0.19	0.14
Sub_1b	-0.15	**-0.33**	-0.07	**0.33**	-0.15	**0.36**	0.19	1.00	**0.44**
Sub_2	**0.35**	**-0.54**	-0.23	**0.77**	**-0.31**	**0.51**	0.14	**0.44**	1.00

3.2. Temporal variations on the different sides of the edifice

Variations in hydrothermal activity and changes in the percentage of colonisation on the Eiffel Tower edifice showed similar trends among the sides as on the entire edifice. Sides with a lower degree of activity (e.g. North and West sides) had a relative higher percentage of colonisation and vice versa (Table 3.3). The only side that does not really comply with this statement is the southern periphery, which showed a rather low degree of activity together with a low degree of colonisation.

Overall edifice - Evidence from the NMDS analysis indicated that the assemblage composition on the edifice sides was related to orientation rather than year (Fig. 3.8a). The southern periphery pooled apart due to the higher percentage cover of Substratum 1a and to a lesser extent of Assemblage 4a. The addition of environmental vectors (numbers of visible fluid exits per side) to the NMDS plot (Fig. 3.8b), confirmed that the South and East sides were the most active over the studied time-intervals

and were characterised by a higher percentage cover of Assemblage 3. Due to their positioning close to each other in the cluster, sides with high activity shared a similar faunal composition, while for the less active sides, the results were less clear. Assemblages 2a, 2b and 4a had a higher percent cover over the years on these less active sides.

Table 3.3. Percentage of colonisation (%) and activity (sum of activity features) on each side of the edifice and periphery. The dashed bars stand for a shortage of data or an incomplete reconstruction of the side in question – no extrapolation could be made due to the high patchy nature of the edifice (Chapter 2, Cuvelier et al. 2009).

Years	North		N_periph		West		W_periph		South		S_periph		East	
	%	Activity	%	Activity	%	Activity	%	Activity	%	Activity	%	Activity	%	Activity
1994	/	/	**62.71**	5	**45.81**	4	59.32	19	46.66	**70**	11.34	4	46.56	**32**
1998	**67.04**	20	**63.87**	2	**73.62**	4	54.10	3	50.34	**24**	11.83	2	/	/
2001	**66.48**	27	**60.45**	4	**77.12**	7	61.98	13	44.62	**24**	19.41	3	33.16	**32**
2002	**60.39**	5	/	/	**62.24**	4	/	/	40.35	**24**	/	/	28.53	**26**
2005	**64.29**	16	/	/	**76.06**	2	57.25	6	43.27	**36**	9.12	8	38.01	**38**
2006	**58.85**	7	**64.54**	5	**82.82**	3	61.10	16	49.17	**15**	12.75	8	28.11	**35**
2008	**58.70**	24	**47.40**	19	**73.31**	3	62.84	17	40.62	**35**	6.75	9	33.47	**32**

To better resolve such differences, a surface plot representing the mean activity, was added (Fig. 3.8b). A clear gradient in visible activity can be observed. Sides with the same degree of visible activity did not necessarily share a similar faunal composition, for example West98 and S_periph05 and S_periph08. This was more pronounced for the sides with a lower degree of mean visible activity. The cluster analysis clarified and corroborated the NMDS analyses, showing that South and East sides were more similar to the southern periphery than to West and North sides and their respective peripheries (Fig. 3.8c). The tree was divided in three classes, based on the hierarchy of the clustering and these were plotted on the NMDS (Fig. 3.8a). Classes were significant for flanges only ($F_{1,41}$=4.6984, p<0.05).

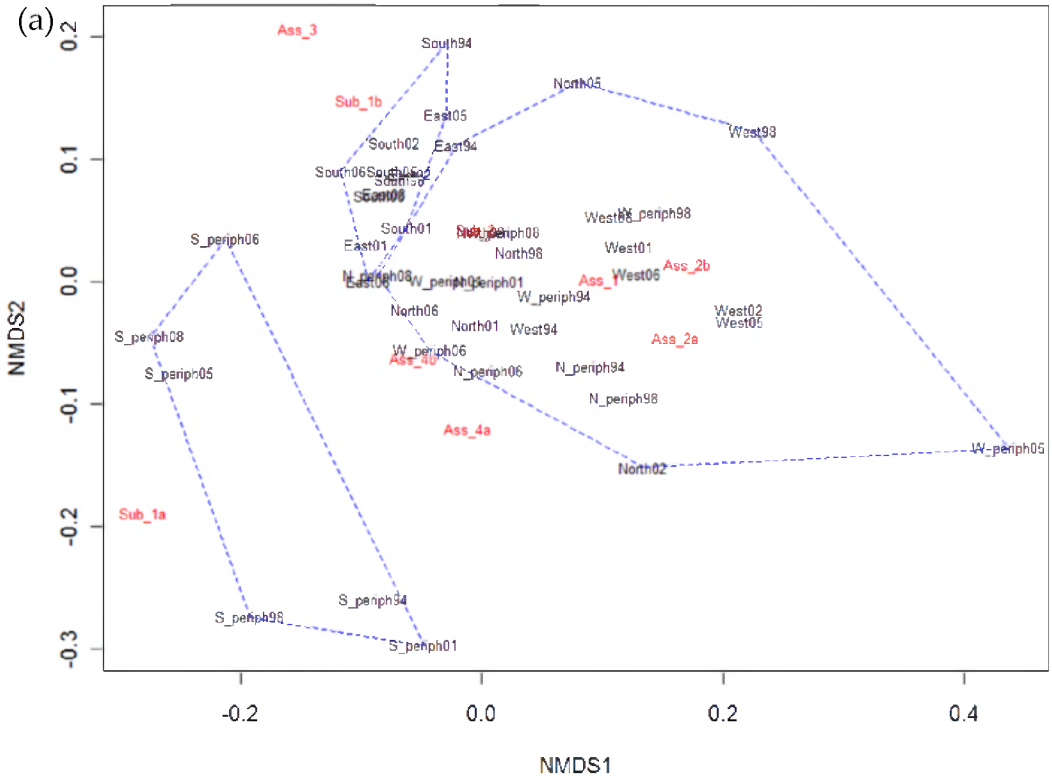

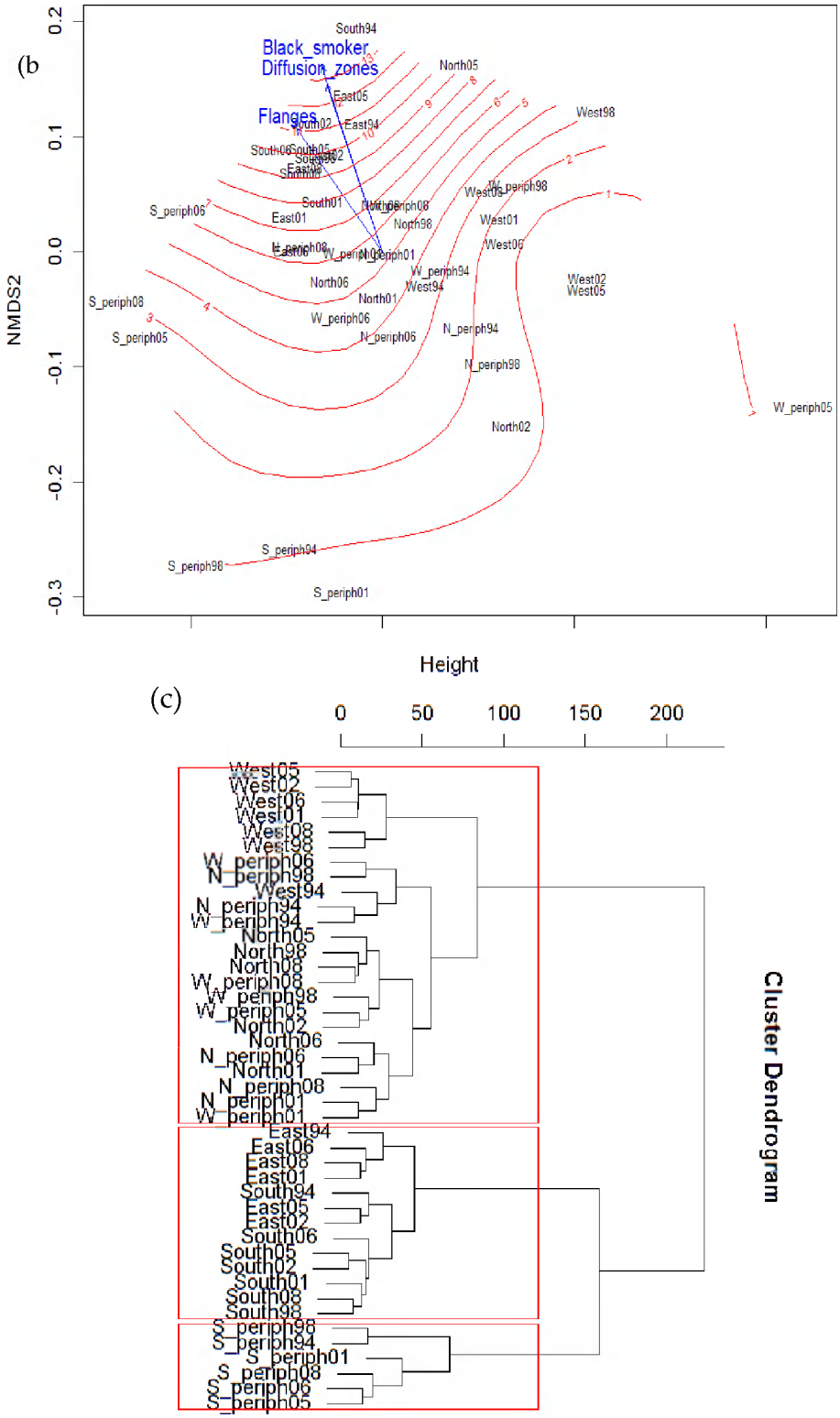

Fig. 3.8. Non-metric Multi-Dimensional Scaling plots based on Bray-Curtis dissimilarity index for all the sides over the years. (a) NMDS-plot with the sides followed by the year (e.g. South94) as well as the assemblages and substrata on which the clustering was based. Three clusters were identified, grouping the southern periphery (S_periph), the East and the South sides and the West and North sides with their respective peripheries (W_periph and N_periph) over time. (b) Environmental variables, i.e. the activity features "black smoker, flange and diffusion zone", were added as vectors (arrows). A surface based on the mean activity (curved lines), connected the sides with the same mean activity. An activity gradient was thus generated on the plot. (c) The

cluster-analysis corroborated the clusters recognised in the NMDS-plots and clarified the position and relation of several sides of the edifice.

Tower - When focusing on the tower alone, similar patterns were observed as for the entire structure, which is clustering of the sides according to their orientation (East and South side group, as well as West and North sides). The division in 2 groups gives a significant difference in mean activity ($F_{1,24}$=20.557, p<0.001) as well as for the separate activity features (black smokers: $F_{1,24}$= 22.74, p<0.001; flanges: $F_{1,24}$= 19.05, p<0.001; diffusion zones: $F_{1,24}$=9.0296, p<0.01), separating the active and less active sides.

Periphery - The southern periphery is separated based on the relative higher presence of Substratum 1a in the later years (2005, 2006 and 2008). Assemblages 4b and 4a appear more predominant in the earlier years: 1994, 1998 and 2001. The northern and western peripheries show a higher degree of colonisation mainly consisting of mussel beds (Assemblage 1) and clumps (Assemblage 2). In contrast to the tower, the sides with a relative higher degree of colonisation were also the more active sides (Table 3.3). With the mean activity fitted as a surface, there is a more pronounced difference in relative assemblage composition for the less active sides (e.g. W_periph05, S_periph08, S_periph01 and S_periph94) even though they share the same degree of activity. Instead, sides facing the same direction of the edifice share a higher degree of similarity independent of the time component. As there is no significant difference, visible activity cannot explain the discrepancy between the clusters of the periphery.

3.3. Community dynamics

A total of 2020 points of the overlaid grid were compared between all the years. Grid-points that did not correspond in locality between the years (ca. 5%) were excluded from further analysis. For each assemblage, the transition of a grid-point into another assemblage or substratum was registered and its frequency was assessed (Fig. 3.9). Recurrent patterns were examined in order to identify the most common and frequent transfers, which are presented in Fig. 3.10. In general, individual assemblages and substrata remained primarily stable, i.e., the relatively highest frequency (~40%, Table 3.4) of grid-points featured the same assemblage or substratum between the studied time-intervals, except for Assemblage 3 and Substratum 1b (Fig. 3.9). The other ~50-60% of grid-points did change (Table 3.4) and were divided over the other assemblages and substrata, replacing (transfer) one assemblage or substrata by another (Fig. 3.9). The most common transfers are described here. Assemblages 1 and 3 were most often replaced by Substratum 2. Assemblage 2a changed into Assemblage 2b, while the contrary was true for Assemblage 2b, although less frequently. Assemblages 4a and 4b transferred

into assemblages with mussel-clumps, i.e., Assemblages 2a and 2b. Substratum 1a was colonised by mussels (Assemblages 2a and 2b and to a lesser extent Assemblages 4a and 4b, with a higher frequency of the assemblages with microbial cover (b)). Substratum 1b got replaced by mussel-based assemblages, although the ones with a microbial cover (Assemblages 2b and 4b) had a higher frequency. Substratum 2 changed very little, however, when it did, it was generally colonised by larger-sized mussels (Assemblage 1) and shrimps (Assemblage 3).

The periphery was more stable over the years, as it exhibited a lower percentage of change for either the same or longer time periods (Table 3.4). An increase in stability was noticeable over time, with the highest degree of change occurring between 1994 and 1998 for the tower and between 1998 and 2001 for the periphery. When comparing 1994 with 2008 (a 14-year time span), a higher overall degree of change (70%) was observed.

Table 3.4. Percentage of grid-points that stayed the same or changed between the consecutive years on the tower and the periphery of the Eiffel Tower edifice. Data were ordered in decreasing order according to the time interval between consecutive years.

Tower				Periphery			
Interval	**Years compared**	**Stay the same**	**Change**	**Interval**	**Years compared**	**Stay the same**	**Change**
4	1994-1998	30.67	69.33	4	1994-1998	42.22	57.78
3	1998-2001	40.39	59.61	4	2001-2005	50.00	50.00
3	2002-2005	42.53	57.47	3	1998-2001	35.04	64.96
2	2006-2008	43.23	56.77	2	2006-2008	71.21	28.79
1	2001-2002	42.01	57.99	1	2005-2006	41.36	58.64
1	2005-2006	45.20	54.80				

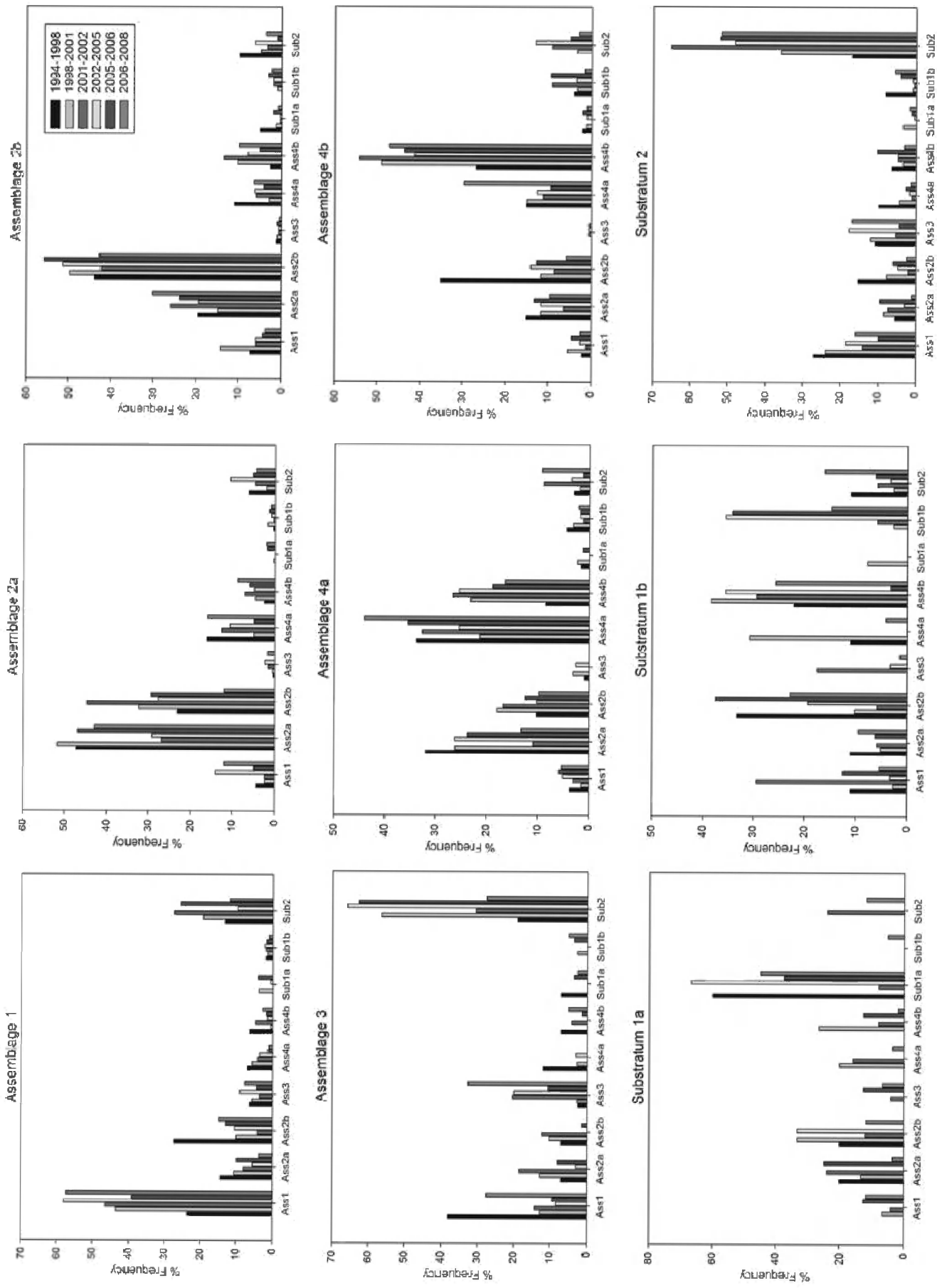

Fig. 3.9. Frequencies of transfers (%) in grid-points of assemblages between the years analysed. For assemblage identification: see Fig. 3.2.

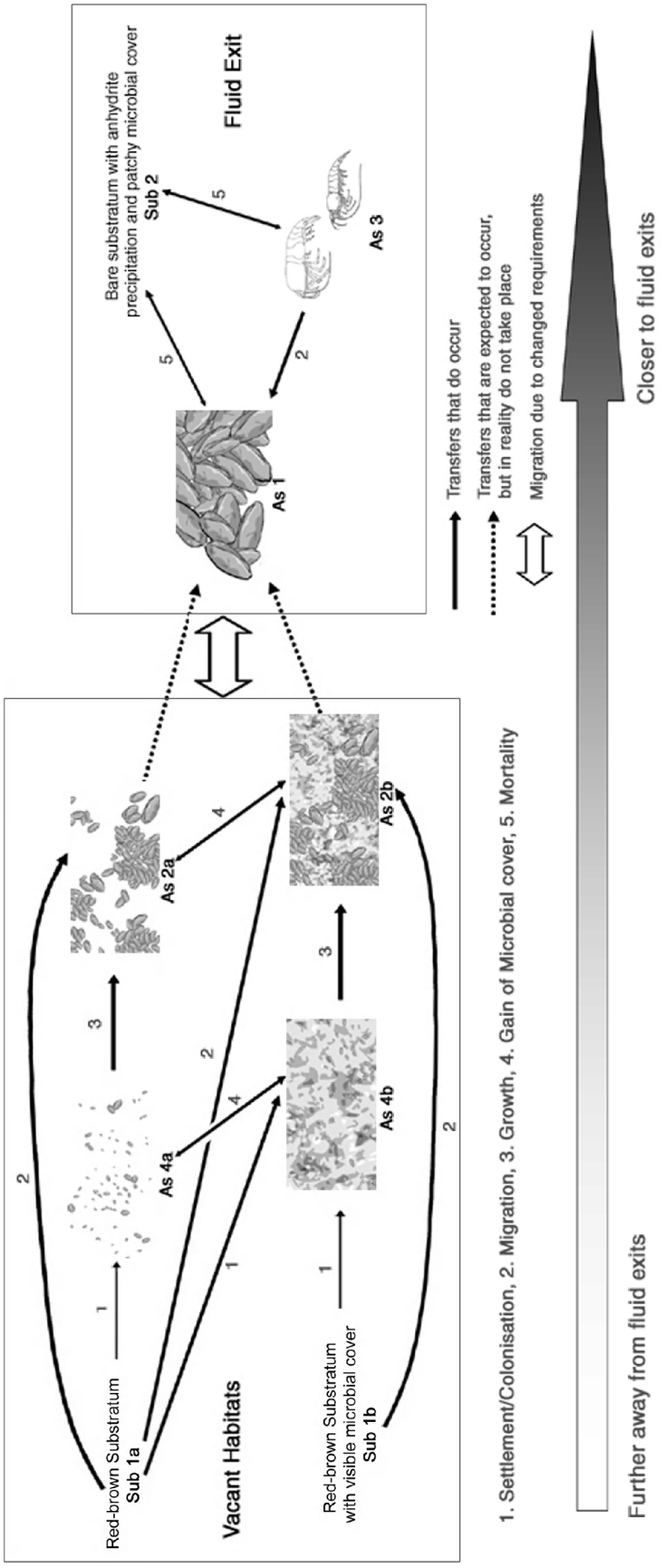

Fig. 3.10. This "Succession model" represents the most frequent transfers from one assemblage or substratum into another over time. It is based on the recurrent patterns over the years on the Eiffel Tower edifice, hence identifying the most important transfers. The directions of the arrows show the direction of the transfer: from x to y. The

number on top of each arrow points to the possible mechanism responsible for the transfer. The thickness of the transfer arrows points to the relative frequency, i.e. the bolder the more frequent. Double pointing arrows mean that the transfer occurs in both direction, but the heaviest arrowhead is pointing towards the net-transfer. The separation in 2 separate cycles is noticeable. (Ass=Assemblage, Sub=Substrata).

4. Discussion

Our results show some considerable temporal changes in assemblages on the Eiffel Tower edifice within a 14 year time-series, both at the scale of the entire edifice, between the sides and at small patch-scales. The influences of the years and hydrothermal activity in these processes were evaluated, as well as the possible role of other factors.

4.1. Succession?

4.1.1. Eiffel Tower succession model

The most frequent transitions between the assemblages and substrata are presented as a succession model (Fig. 3.10). Initially, bare substrata are colonised by *Bathymodiolus azoricus* mussels. Substratum 1a is colonised by Assemblages 4a and 4b and by Assemblages 2a and 2b. The medium-sized mussels of Assemblage 2 have slightly more success in occupying this type of bare substratum as the frequency of transfers is a little more elevated (Fig. 3.9). Overall, Substratum 1a vacant habitats are more readily colonised by mussels and microbial cover. However, there is no difference in physiology detected between mussels with or without (visible) microbial cover (Martins et al., 2009). Bare substratum with microbial mats (Substratum 1b) is readily colonised by small mussels and mussel clumps (Assemblages 2b and 4b). There are also transfers between the sub-forms (without (a) and with microbial cover (b)) of the same assemblage (4a-b and 2a-b). The net-transfers between these sub-forms point to the gain of microbial cover.

Small mytilids (from Assemblages 4a and 4b) grow and proliferate in visible and countable densities, forming clumps (Assemblages 2a and 2b, Fig. 3.9 and 3.10). We would then expect these mussel clumps to grow and proliferate into dense mussel beds of larger-sized individuals (Assemblage 1), but these transfers occur only rarely (Fig. 3.9). This suggests either mortality for the larger mussels and transfer in Substratum 2 (dead mussel beds can be observed at the base of the edifice) or a migration of the Mytilidae when they attain a certain size to another locality which can sustain their (feeding) requirements (Fig. 3.10). Alternatively, we could argument that the mussels living close to the fluid exits grow faster, however, we deem the migration hypothesis as more likely, as large mussels are not subsequently present at certain locations. In addition, shell increment studies from mussel shells collected at the same location show that these individuals wandered different paths along their life

and recorded different sequences of environmental conditions (J. T. Copley, pers. comm.). It thus remains difficult to asses the growth of the *B. azoricus* individuals. Without marking single individuals, however, we can never be sure that it is the same individual encountered at locality x in year y1 and y2. In fact, it seems to be even more complicated for the larger-sized individuals, as their mobility seems higher and indispensable for their survival. Larger mussels (Assemblage 1) are also capable of recolonising Substratum 2 (Fig. 3.9 and 3.10), probably when activity decreases, though the net transfer is one of mortality and relocation. Mussels seem to have more difficulties to invade these bare patches as long as the disturbance persists, probably because of substratum instability and permeability and associated difficulties for attachment and elevated temperatures. The same observations of recolonisation vs. mortality were made for the shrimp assemblage (Fig. 3.9 and 3.10). Shrimps are likely to be the first to recolonise this type of substratum (2). Large mussels also invades the patches of the shrimp Assemblage 3 (Fig. 3.10), which does not necessarily mean that they out-compete the shrimps, since these can live on top and in-between the mussel-beds.

Our observations suggest that there are two different cycles in community dynamics with little overlap between the two (Fig. 3.10), which suggests the existence of two different micro-environments. Assemblages 1 and 3 and Substratum 2 can be found close to the fluid exits (Cuvelier et al., 2009, Chapter 2), while the other faunal assemblages (2a, 2b, 4a and 4b) can be found further away from the fluid exits which is likely to correspond to a less harsh environment (see Chapter 4.). Following the definition of succession, defined as a proper directional and predictable change in community composition, i.e. one community being replaced by another community, often following a perturbation, it can be confirmed that the cycle featuring the assemblages closer to fluid can indeed be labelled as succession. This succession starts with the shrimps being the first colonisers while mussels move in later on and take over in visible faunal dominance, when the perturbation diminishes. Taking into account the same definition and/or prerequisites for succession to occur in examining the second identified cycle, i.e. the transfers between the mussel-based assemblages featuring smaller-sized mussels with bare surface in between, it becomes clear that these community dynamics cannot be appointed as succession as there is as no apparent alteration in community composition. Rather, it seems that these identified assemblages are different stages or variations of one and the same faunal assemblage. The community dynamics observed here and the change in distribution of the mussels according to their size (Comtet & Desbruyères, 1998) seems to confirm the previously proposed link between size and mobility. Larger mussels may have a higher physiological adaptability or tolerance to environmental conditions and fluctuations than smaller individuals (Company et al., 2007; Martins et al., 2008; De Busserolles et al., 2009) and might thus be able to survive closer to the fluid exits.

4.1.2. Comparison with other succession models

The situation at Lucky Strike can be described as a phase of either a facilitation model or an inhibition model (*sensu* Connell & Slatyer, 1977). The facilitation model requires that in the earlier history of Eiffel Tower, the edifice was colonised by a pioneer or earlier successional species that prepared the environment for later colonisers. This succession pattern would then be analogous to what is described at the EPR. At 9.5°N *Tevnia jerichonana* (a siboglinid tubeworm) was identified as a pioneering species that was gradually replaced by thickets of *Riftia pachyptila* (another siboglinid tubeworm) (Shank et al., 1998a). Later in the sequence, the mussel *Bathymodiolus thermophilus* colonised the vents and ultimately displaced the siboglinids (Hessler et al., 1988; Lutz et al., 2008). This sequence appears to correspond to a change in the temperature and chemistry of vent fluids (Shank et al., 1998a), although species succession under conditions of continuous venting has been documented as well (at EPR and other sites), highlighting other potential cues as for example biotic interactions (Hessler et al,. 1988; Sarrazin et al., 1997; 2002; Mullineaux et al., 2000; 2003).

If the inhibition model is considered, the mussels at Eiffel Tower would be required to inhibit the successful settlement of other organisms, as shown for *Bathymodiolus thermophilus* at EPR (Lenihan et al., 2008). Later successional species would only colonise the habitat when the first colonisers, i.e. the mussels, disappear. The likelihood of this model somewhat diminishes when visual observations of Statue of Liberty, another Lucky Strike edifice, revealed that the death of the mussel assemblages was not followed by colonisation of later successional species (Langmuir et al., 1997; D. Cuvelier, pers. obs.). The degree of tolerance in the mussel beds cannot be underestimated either, as there are shrimps that live on top and in between the mussel beds, and limpets and other small organisms that live on top of or among the mussel shells (up to 60 species, Sarrazin et al., in prep.). These are likely tolerated because they do not represent an imminent threat for the mussels, and the chance that the latter will be out-competed by one of the former appears to be rather small. The capacity of the mytilids to divert the hydrothermal fluids laterally (Johnson et al., 1994) gives them the advantage to maintain vast mussel beds and possibly starve large organisms that tower above the beds (example of *Riftia* at EPR is given by Lutz et al. (2008) and at the Galápagos by Johnson et al. (1994)). If this is combined with an inhibiting effect of some kind on the settlement of other vent fauna, e.g. mussels filter small larval forms out of the water column (Comtet & Desbruyères, 1998), this will lead to stable communities that are resistant to invasion and thus to persistence of the mussel beds.

In summary, it seems that the *Bathymodiolus azoricus* mussels at Eiffel Tower (and the whole of Lucky Strike) represent a climax community, either because environmental or biological constraints exclude

other dominant fauna or because they are the strongest competitors under this hydrothermal regime and habitat.

4.1.3. Comparison with the history of other sites and Mid-Oceanic Ridges

Most of the existing temporal variations studies from the Pacific started after or during a monitored eruption, which can be regarded as T_0 (T zero) for hydrothermal vents, and which accordingly give a description of nascent vent development (e.g. Shank et al., 1998a; Tsurumi & Tunnicliffe, 2001; Tunnicliffe et al., 1997; Marcus et al., 2009). These stochastic events are reported to be far more frequent on faster-spreading ridges than on slow-spreading ridges, often cause quite dramatic changes and can have drastic consequences for the local fauna (Fustec et al., 1987; Shank et al., 2003). Because of the dynamics of fast-spreading ridges, most vent communities probably fail to reach stable conditions (Juniper & Tunnicliffe, 1997). Such stable periods, which are more frequent at slow-spreading ridges, would tend to favour colonisation by *Bathymodiolus* mussels (Desbruyères, 1998), if they are available from the regional pool of potential colonists. *Bathymodiolus* is present in both hydrothermal and cold seep environments all over the world, making it one of the most widespread molluscan genera (Tyler & Young, 1999). In EPR vents, mussels out-compete the siboglinid tubeworms, ending up as the last survivors at low activity - and possibly waning - vent fields (Hessler et al., 1985; Lutz et al., 2008). However, distribution of mussels on vertical surfaces of upright edifices is only observed at the hydrothermal vents in the shallower Atlantic (Lucky Strike and Menez Gwen) and in the North Fiji Basin (Desbruyères et al., 1994), while on the East-Pacific Rise and elsewhere mussels are present or even dominant in certain phases of the succession, though not in the same extent as to what is observed here.

At the EPR vents, periods of relative stability during which competition between species prevails (e.g. *Riftia* vs. *Bathymodiolus*), alternate with highly unstable periods. Such periods tend to favour the settlement and dominance of fast-growing opportunistic species such as siboglinids. Contrastingly, periods characterised by a higher stability appear to favour the slow growing clams and mussels (Desbruyères, 1998). Depending on which species are available in the regional species pool we could apply it to different localities. As a relative stability is observed at the MAR, it could explain the mytilid dominance. Once faunal communities are established, the succession does not necessarily have to be completely rewound (i.e. from first pioneers to later settlers) when the local habitat is not completely destroyed. Later colonisers could die and immediately recolonise the vacant habitats again (secondary vs. primary succession), explaining the persistence of a certain dominant species.

Until now, there is no record at the Atlantic vent fields of siboglinid tubeworm presence, which are identified as pioneer species at the Pacific vent sites, while they are present in Atlantic cold seeps and ship wrecks (Tyler et al., 2003; Cordes et al., 2009; Olu et al. 2009). One might wonder if tubeworms ever were present in the Atlantic vents as pioneers and that we are currently looking at a later succession stage. It could be that these tubeworms did not adapt to the Atlantic hydrothermal regime and they became extinct because they could not bridge the great distances and transform faults separating the Atlantic vent fields, except that until now no fossil records are known from siboglinids in the Atlantic (L. Génio, pers. comm.). Similar theories existed about the absence of vesicomyid clams along the MAR, until in 1997 clams were found at the Logatchev vent field (Gebruk et al., 2000b).

A nascent vent development study in the Atlantic would help understanding the history that preceded the current situation. The T_0 or nascence of the current phase of activity at Lucky Strike can only be estimated and probably goes back a couple of hundred years (Humphris et al., 2002). The Lucky Strike field is likely to be older as its activity, with alternating periods of activity and senescence, has occurred for possibly thousands of years (Langmuir et al., 1997; Humphris et al., 2002). As past environmental regimes leave an imprint on the structure and succession of communities (Mullineaux et al., 2009), the lack of knowledge on possible earlier colonisers represents quite an impediment. As an example we would like to reiterate the presence of a unique assemblage in 1994 featuring gastropods (most likely *Peltospira smaragdina*) and shrimps, but no bivalves. This assemblage was also found at the base of Y3 in 2008, another active edifice of the Lucky Strike vent field, where there are no mussel beds present on the actual edifice, only Alvinocarididae and a few small patchy mussel clumps at the base. But without the observation of a post-eruptive phase, we remain speculative about its role and stage in succession.

4.1.4. Rate of change

The rate of change for 1- to 3-year periods at Eiffel Tower is between 55-60% while a similar study carried out at the S&M edifice (Endeavour Segment, Juan de Fuca Ridge, North-East Pacific) demonstrated a rate of change between 68-88% for a same time period (Sarrazin et al., 1997). This lower rate of change is likely to be linked to the rate of spreading, as the MAR is known as a slow-spreading ridge (full spreading rate at Lucky Strike=22mm/yr) and the faster spreading Juan de Fuca Ridge (55mm/yr). The hypothesis that spreading rates, and the associated frequency of disturbances, might affect hydrothermal community dynamics (Tunnicliffe & Juniper, 1990; Van Dover, 1995) is thus corroborated. More studies on various different edifices would be needed for confirmation and more detailed quantification.

4.2. Role of physical disturbance

In the majority of natural communities, succession is frequently interrupted by major disturbances, starting the process all over again (Connell & Slatyer, 1977). However, if not interrupted, the community can eventually reach a stage in which further change is on a small-scale, as individuals die and are replaced. If replacement happens by a member of their own rather than by another species, stability is assured (Connell & Slatyer, 1977). This seems to be the case for the mytilids (Fig. 3.10) which reinforces the perception of mussels being a climax community.

In a space-limited ecosystem, bare substrata represent a vacant habitat. In intertidal mussel beds it is the exposure to waves which creates gaps and bare substrata, for which a "mussel disturbance dynamics model" was developed (*Mytilus californianus* based) (Guichard et al., 2003). The mussel beds bordering this newly created gap either recover and recolonise the available space or the unstable borders collapse and the disturbance spreads. If we compare this with hydrothermal ecosystems, the habitats or bare substrata at vents can be vacant for a number of reasons: either because the local habitat became unfavourable to sustain life (too harsh or no access to fluids) or because the organisms were removed from their patches. Because of the steep gradients in environmental factors, the high degree of species endemism and patchiness in both ecosystems, parallels have already been drawn between community development at hydrothermal vent and rocky intertidal habitats (Johnson et al., 1994; Van Dover & Trask, 2000; Mullineaux et al., 2003). In the model of Guichard et al. (2003), disturbance is initiated when mussels are removed. The mussel beds bordering this newly created gap either recover and recolonise the available space or the unstable borders collapse and the disturbance spreads.

When applying these shallow-water derived mechanisms as a reaction to physical disturbance to the vent environment, different scenarios are possible. Firstly local de-activations can create a gap and subsequently a cascade in assemblage degeneration as the local resource can run dry and the disturbance spreads. Bathymodiolinae still have the capacity of filter feeding and can survive for some time without the chemical supply of fluids (Page et al., 1991; Shank et al., 1998a), but if the de-activation persists and the habitat/substratum continues to be unsuitable they are likely to die or relocate. Secondly, an increase or re-activation of a fluid exit can cause mortality and render a patch (or local habitat) inhospitable and uninhabitable, which has been observed on the EPR (Desbruyères, 1998). Thirdly, when mussels are removed from their locality by predation or sampling, which is most comparable to the gaps created by waves (Guichard et al., 2003), these newly exposed bare substrata (1a and 1b) get rapidly (as fast as 1 year after sampling) re-colonised by mussels (called recovery in the *Mytilus*-model), as suitable substrata at hydrothermal vents are limited.

4.3. Temporal variations at Eiffel Tower

4.3.1. General tendencies over time

The peak in microbial cover observed in 2001 coincides with a dike intrusion that occurred on this MAR segment in March of the same year (Dziak et al., 2004). This earthquake was reported as being the biggest seismic event in 20 years, after which, in the subsequent summer months, there was an increase in microbial cover and diffuse flow (Dziak et al., 2004). The microbial increase reported for the summer of 2001 can thus be confirmed, although there was no corresponding increase in diffuse flow noted at Eiffel Tower.

The overall percentage of mussel coverage at Eiffel Tower does not vary significantly between successive years. However, an augmentation is noticeable in 1998, which coincides with a temporal decrease in visible activity. *Bathymodiolus* spp. does not appear to be that tolerant to high temperatures as they seem to avoid the fluid flow (Van Dover, 1995; Henry et al., 2008; Cuvelier et al., 2009), so the change (decrease) in activity might explain the increase in mussel coverage observed in the same year. After all, the overall % coverage, of which the mussels represent the biggest part, is negatively correlated with the hydrothermal activity. Despite some of the changes observed, the overall degree of colonisation fluctuates around 50%. It is thus possible that Eiffel Tower, under the current hydrothermal regime and as a space-limited ecosystem, has reached its carrying capacity. Carrying capacity can be defined as the quantity of "life" an ecosystem can support at any moment in time. It largely depends on the resources available, the size of the population, the surface available and the amount of resources each individual is consuming. Consequently, the carrying capacity of an ecosystem affects everything that lives in it. Even if the overall degree of life might have reached its carrying capacity, the individual faunal assemblages who add up to this total, change in relative proportion. To a certain extent an exchange of the fauna between the different sides and regions of the edifice can be postulated.

4.3.2. Faunal assemblages and substrata over time

The more active sides of the edifice (i.e. East and South sides) are characterised by a higher percentage of coverage of Substratum 2, as well as Assemblages 1 and 3, which are all three positively correlated. Overall, these sides show a lower degree of colonisation as well. On the other hand, the less active sides (West and North sides) show a higher percentage coverage of Assemblages 2a and 2b, which are also positively correlated one to another, and a higher degree of colonisation. A spatial segregation based on mussel sizes is observed at Lucky Strike. Moreover, a decrease in mussel size with increasing distance from the fluid exit has already been observed (Comtet & Desbruyères, 1998; Sarradin et al.,

1999; Cuvelier et al., 2009). In addition, the size of the mussels at Eiffel Tower was shown to be positively correlated with the temperature of their microhabitats (De Busserolles et al., 2009; see Chapter 4), which suggests larger-sized mussels can survive closer to high temperature fluid-exits. Even though correlation does not mean causality, the absence of correlation, is sufficient to abandon the hypothesis of a causal link between 2 variables (Legendre & Fortin, 1989).

As clustering occurs according to orientation, not according to the years, the characteristics inherent to the sides and their orientation seem to be more important in determining faunal occupation. Inherent characteristics can comprise hydrothermal activity (including substratum permeability), exposure to hydrodynamic factors, such as currents and local turbulence, larval settlement and biotic interactions. Similar patterns were described at Juan de Fuca Ridge, where vent sites investigated between 1988 and 1994 did not cluster by year either, nor by geographic locality, and where local habitat-scale features are thought to be determinant in explaining species distribution patterns (Tsurumi & Tunnicliffe, 2001).

As previously stated, the West and North sides share a higher percentage of smaller-sized mussels (i.e. Assemblages 2a and 2b). These sides are theoretically more exposed to the currents and the associated supply of particles and organisms. The local currents are directed toward the South-East at Lucky Strike and are generally strongly influenced by the local topography (Khripounoff et al., 2008). An 11 m high edifice, such as Eiffel Tower, is thus likely to act as an obstruction, creating local vortices or divergent patterns in the regular current pattern. The orientation of the edifice could also cause settling of larvae primarily on the sides exposed to the currents and thus a higher water flow (Genin et al., 1986) or conversely influence settling on the other sides. Cuvelier et al. (2009) hypothesised, that the higher percentage coverage of Assemblage 2 on these sides could be due to the possibility of smaller mussels being more dependent on filter-feeding (Martins et al., 2008) which would make them more dependent of the supply of organic matter. On the other hand, the larger mussels would rely more on chemosynthesis (Martins et al., 2008) which would explain their increased abundance/proportion on the more active East and South sides over the years. These suggestions however, are not supported by stable isotope analysis (Trask & Van Dover, 1999; Colaço et al., 2002; De Busserolles et al., 2009). Another explanation could be the possibility of the occurrence of a more intense mixing process on the sides exposed to the currents. Higher currents may cause more intense mixing and thus rapid dilution of hydrothermal fluids, which get carried away by these currents. This could restrict the availability of sulfide and other substances for the mussels, and thus restrain growth. Possibly, there could be a limit to autotrophy on the more exposed sides where smaller individuals

prevail and where larger-sized mussels are restricted to localities close to the fluid exits. The higher abundance of shrimps on the East and the South sides could be, next to the more abundant activity features, due to the currents as well.

4.3.3. Variations in hydrothermal activity

The main pattern in the variations over the years of the activity features is the variability in the number fluid exits. A link between the number of fluid exits, temperature and flow vigour has already been established (Cuvelier et al., 2009, Chapter 2). All three activity features show similar trends. One of the most striking observations, however, is the increase of black smokers in the periphery and the corresponding decline in activity on the tower. The increase in black smokers in the periphery corresponds to similar observations made at the North-East Pacific vent sites, where deactivation of the main tower edifice and expansion of activity towards the periphery was reported (Sarrazin et al., 1997). After years of hydrothermal activity, the sulfide edifice may become clogged by the mineral precipitation from the hot fluids (Tivey, 1995). Hence, the warm fluids are diverted to cracks in the periphery, creating small chimneys and black smokers. This "clogging" effect can be illustrated by a series of photos of the actual summit (1681 m of depth) of the Eiffel Tower that showed signs of activity in 1994, that somewhat diminishes by 1998, while no more fluid was expelled in 2001 and later (Fig. 3.11).

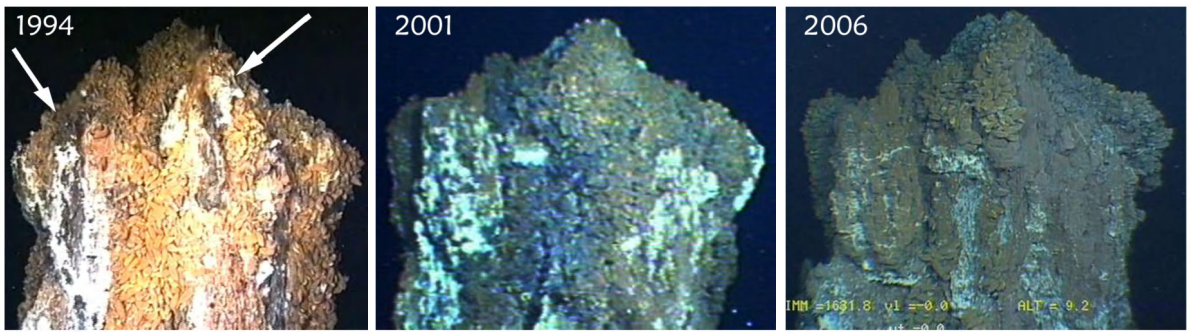

Fig. 3.11. The summit of the South side of the Eiffel Tower edifice over the years, from 1994 to 2006. The 2 arrows on the 1994 photo indicate the fluid exits. By 2001, these are no longer active, while small diffusion zones and black smokers are detectable below the summit along the flank of the edifice. Between the years, other tendencies are noticeable such as the decrease and re-organisation of the mussel beds, the change in the colour of the substrata and the redistribution of shrimp (not visible here).

Visible activity does not explain all the variation occurring between the sides with different orientation, but may be used as a proxy. However, when the tower and the periphery are separated, trends do emerge. The differences in clustering for the tower are significantly different for the visible activity. East and South sides are more active, independent of the years studied and cluster together, while the less active West and North sides do the same. For the periphery however, the activity does

not explain the division occurring there. The periphery may be more influenced by the hydrodynamic processes.

4.3.4. Others cues-biotic interactions

As visible activity does not explain all variations, biotic interactions can be a potential underlying cue in influencing assemblage distribution over time. However, it is arduous to assess or quantify the importance of these biotic interactions, particularly when restricted to video imagery transects. Several experimental manipulations have already shown the underlying structuring strength of inter- and intra-specific interactions in temporal evolution studies at vents (Mullineaux et al., 2000; 2009; Micheli et al., 2002; Lenihan et al., 2008; Lutz et al., 2008). In any given ecosystem with limiting factors, it is likely for competition to occur between the organisms based on access to resources, optimal habitats and exposition to predation or physico-chemical stress. However, demonstrating that contemporary competition is occurring requires manipulative field experiments, and cannot simply be inferred from niche differentiation or assemblage distribution or displacement. Studies carried out on vent sites with constant venting (i.e. not after an eruption) already mentioned the likelihood of biological interactions intervening in the assemblage mosaics distribution and composition along environmental gradients (Hessler et al., 1988; Sarrazin et al., 1997; 2002; Mullineaux et al., 2000; 2003). In addition, the importance of the non- or less visible fauna in the observed mechanisms was impossible to estimate based on the image analysis methodology as many of them cannot be identified nor quantitatively assessed. These include the organisms living in the interstitial spaces between the mussel beds, the limpets and polychaetes grazing on the mussel shells, on the bare substrata or on the microbial mats, not even to mention the even smaller meiofaunal species.

4.3.5. Decadal-scale stability?

At Eiffel Tower, no significant differences were observed in the overall percentage mussel coverage, not on a decadal scale, nor between the consecutive years, which could point to decadal constancy. However, there are significant differences, both on decadal scales and shorter time scales, for the overall microbial cover. For individual assemblages, more complicated patterns lie at the base, as these tend to change between the years and between sides. Often these short-term and local changes get masked in the overall view of the edifice.

5. Conclusion

14 years of community dynamics were investigated both at the scale of the entire edifice, between the sides and at small patch scales. The mytilid *Bathymodiolus azoricus* can be considered a climax-

community at this vent edifice, as its dominance is undisputed over this 14-year time-interval. At first sight, decadal-scale stability appears to persevere for the overall edifice, however, on shorter time-scales changes do occur, as well as on smaller spatial scales. Significant differences in the microbial cover were revealed as well as in the individual assemblages, which do tend to change between the years. The small fluctuations in the rather constant overall degree of colonisation (~50%) were explained by subtle changes in hydrothermal activity. Because of the steadiness of the degree of colonisation, it can be that Eiffel Tower has reached its carrying capacity. Hydrothermal activity and the number of fluid exits cannot explain all variations that occur between the assemblage coverage fluctuations on the various sides of the edifice and between the years, although it might give a good first interpretation. The years analysed were shown not to have a consistent influence on similarities in the community structure, while the orientation of the edifice appeared to play an important role. Characteristics inherent to the orientation are e.g. activity, exposure to currents, suitable habitats and substrata.

A succession model is proposed for the shallow MAR fields, in addition to a first quantification of the rate of change in community dynamics at a slow-spreading ridge. This rate of change is about 15% slower than that observed on sulfide edifices from faster-spreading ridges in the North-East Pacific.

Acknowledgments

I would like to thank J. Escartin, chief scientist of the MOMAR08 cruise for attribution of diving time to collect an extra year of imagery, as well as all GENAVIR crews and submersible pilots that cooperated throughout the years. Thanks to P.-M. Sarradin for his engagement and involvement to this subject and his kind assistance during the cruises and at Ifremer. I would like to acknowledge Ifremer for granting access to past and present imagery.

Chapter 4

Hydrothermal faunal assemblage and habitat characterisation at Eiffel Tower

Published as:

Cuvelier D., Sarradin P.-M., Sarrazin J., Colaço A., Copley J.T., Desbruyères D., Glover A.G., Serrão Santos R., Tyler P.A. (*2011*). Hydrothermal faunal assemblages and habitat characterisation at the Eiffel Tower edifice (Lucky Strike, Mid-Atlantic Ridge). *Marine Ecology* (*in press*)

CHAPTER 4
Hydrothermal faunal assemblages and habitat characterisation at Eiffel Tower

1. Introduction

Hydrothermal ecosystems are extremely variable environments, characterised by elevated temperatures relative to ambient deep-sea water. However, with only a few exceptions, the temperatures most vent-endemic species live at are no different from those in shallow water habitats and it is the actual chemistry and composition of the fluids that sustain the chemosynthetic life (Jannasch, 1985). Steep thermal and chemical gradients exist and turbulent mixing occurs between the hydrothermal fluids and cold surrounding seawater, resulting in high local variability, on a scale of a few centimetres (Johnson et al 1988a; Chevaldonné et al., 1991; Le Bris et al., 2006; Sarrazin et al., 1999; 2006). The region wherein sulfide and oxygen co-exist, both indispensable for chemosynthesis, is thus restricted to the interface between reduced chemicals from the hydrothermal fluids and oxygenated seawater (Johnson et al., 1988b; Sarradin et al., 2009). Attempts to define the microhabitats where species live and characterising the local faunal composition have taken place on the hydrothermal vents of various Mid-Ocean Ridge segments: at the East Pacific Rise (EPR: Fisher et al., 1988; Johnson et al., 1988b; 1994; Sarradin et al. 1998; Bates et al., 2005; Dreyer et al., 2005; Govenar et al. 2005; Mills et al., 2007; Lutz et al., 2008; Matabos et al., 2008), at the Juan de Fuca Ridge (JdF: Sarrazin and Juniper, 1999; Sarrazin et al., 1999; Tsurumi & Tunnicliffe, 2003; Urcuyo et al., 2003), at Lau Basin (Henry et al., 2008; Podowski et al., 2009) and at the Mid-Atlantic Ridge (MAR: Sarradin et al., 1999; Desbruyères et al., 2000; 2001). Evidence for the close association of vent community development with physicochemical conditions has already been demonstrated (Luther et al., 2001). According to changing physico-chemical conditions, hydrothermal vent edifices may be inhabited by faunal assemblages that form repeating mosaics (Sarrazin et al., 1997; 1999).

The Eiffel Tower edifice of the Lucky Strike vent field (1700 m depth) is located on the shallower part of the MAR. It is visibly dominated by Bathymodiolus azoricus that forms extensive mussel beds (Desbruyères et al., 2001). A variety of taxa live in association with these mussel beds, including alvinocaridid shrimps and a decapod crab along with less conspicuous fauna such as polychaetes, gastropods, amphipods and pycnogonids etc. (Desbruyères et al., 2006). At the Eiffel Tower hydrothermal edifice, Cuvelier et al. (2009, Chapter 2) identified 4 visibly different faunal assemblages

of which 2 had a sub-form. Assemblage 1 was visibly dominated by dense beds of larger-sized mussels, while Assemblage 2a featured mussel clumps with bare surface in between. Assemblage 2b was similar to Assemblage 2a but contained visible microbial mats. Assemblage 3 represented bare surfaces colonised by shrimps. Assemblage 4a resembled bare substrata with small dispersed mussels, whereas Assemblage 4b was similar to Assemblage 4a but with visible microbial mats.

Using image analysis, a faunal zonation model around a fluid exit has been proposed for the Eiffel Tower edifice (Chapter 2, Cuvelier et al., 2009). Subsequently, a succession model, based on recurring community dynamics, was elaborated using 14 years of time-series data acquired on the Eiffel Tower edifice (Chapter 3). Based on the distribution patterns, proximity to the fluid exits and two separate cycles in succession of the faunal assemblages, the existence of at least two microhabitats was hypothesised. These microhabitats were thought to correspond to a "harsher" (higher temperature, higher sulfide) environment, inhabited by shrimps and larger-sized mussels, while the other assemblages, featuring smaller-sized mussels and a less dense coverage, were thought to be characterised by lower levels of T°C and sulfide. However, since these models were primarily based on video imagery, it requires confirmation through biological sampling. Hence the primary objectives of this study are: (a) to examine macrofaunal composition in visibly different assemblages, (b) to identify the microhabitats inhabited by the different faunal assemblages, (c) to evaluate if variability in physico-chemical factors corresponds to visible faunal differences (size of mussels, presence of microbial cover and species composition/dominance) and (d) to analyse if the microhabitats identified correspond to the previously hypothesised microhabitats.

2. Material & methods

2.1. Study site

Lucky Strike is a basalt-hosted vent field (Langmuir et al., 1997; Fouquet et al., 1998; Ondréas et al., 2009) situated on the shallow part of the MAR, at a mean depth of 1700 m, and was visually observed for the first time in 1993 (Fig. 4.1). It is characterised by a central lava lake, around which the hydrothermal vent edifices are localised (Ondréas et al., 2009). The Eiffel Tower sulfide structure is situated in the south-eastern sector, on the saddle between two volcanic cones. It is an 11 m high active edifice and one of the most visited sites within this vent field. Its fauna is considered representative for the entire vent field (Desbruyères et al., 2001).

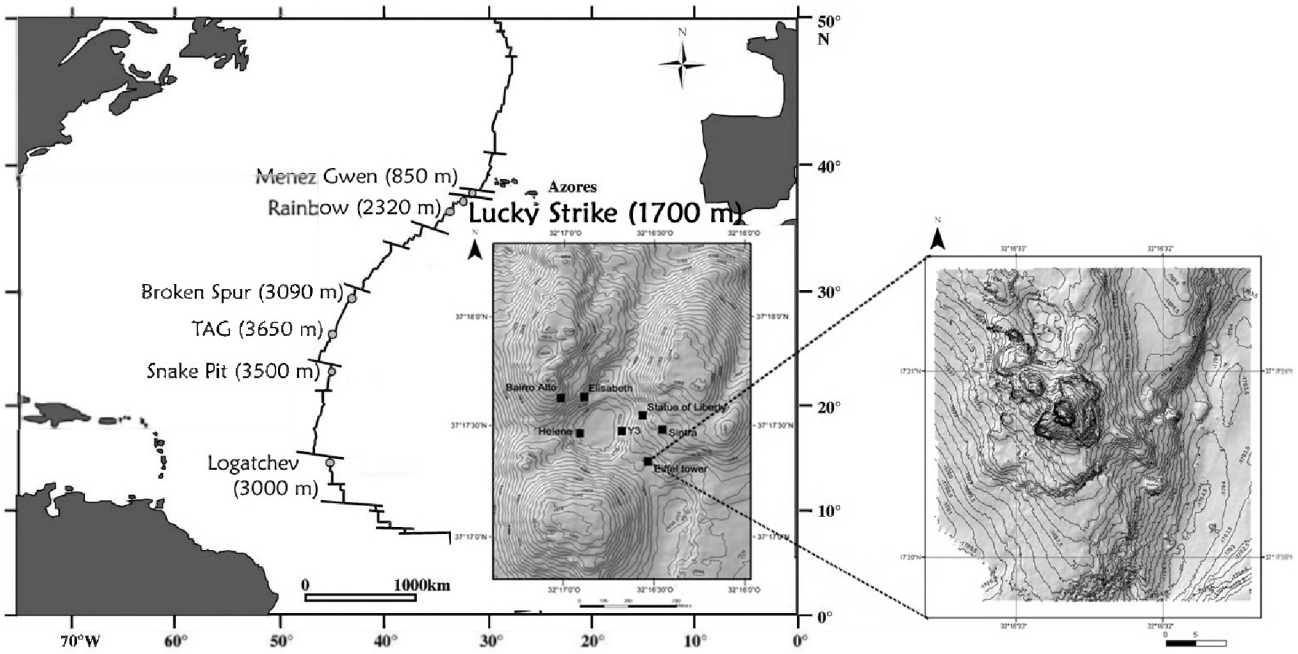

Fig. 4.1: Major known vent fields and their respective depths are shown along the Mid-Atlantic Ridge. The inset shows the Lucky Strike vent field with several of its most well-defined edifices. The 11 m high Eiffel tower is one of them, situated in the south-eastern sector of the vent field.

2.2. Assemblage sampling

During the MoMAR08 cruise (August 2008, NO l'Atalante), semi-quantitative biological samples were taken with the Remotely Operated Vehicle (ROV) Victor 6000 on visibly different assemblages, which correspond to those identified by Cuvelier et al. (2009) (Fig. 4.2 and Fig. 4.3). Biological sampling was undertaken to investigate the macrofaunal species composition of these assemblages. To facilitate the description of the results, we will refer to the samples taken using the name of the assemblages they correspond to. Accessibility and manoeuvring space for the ROV were prime determinants in choosing a sampling location. Sampling sites and images from where and how the sampling was carried out can be found in Fig. 4.3. Samples (three to four grabs, see Fig. 4.3) were taken with the manipulator arm of the ROV and placed in a sampling box, followed by a clearing of the sampled surface with the slurp gun/suction sampler. The faunal sampling of Assemblage 4b failed due to a hydraulic problem of the ROV, and was therefore left out of the analyses.

When the biological samples arrived on board, the macro-and megafauna received the highest attention and organisms were immediately identified to the lowest taxonomic level possible. Specimens were subsequently fixed in seawater buffered formalin (10%) and after 48 hours transferred to 70% ethanol. The surfaces sampled were measured with pixel-based image analysis software IPLAB Spectrum® as described in Sarrazin et al. (1997), in which the manipulator arm of the

ROV was used as a scale (Table 4.1). The crab *Segonzacia mesatlantica* was not considered in the statistical analysis, because this species is highly mobile and tends to escape when approached with sampling equipment, hence it could not be considered representative. Finally, the empty gastropod shells of *Shinkailepas briandi* present in two different samples were noted in the density table but were not considered in the statistical analyses, since these appeared to be remnants of a senescent population. Chemical sampling was carried out in a consecutive dive.

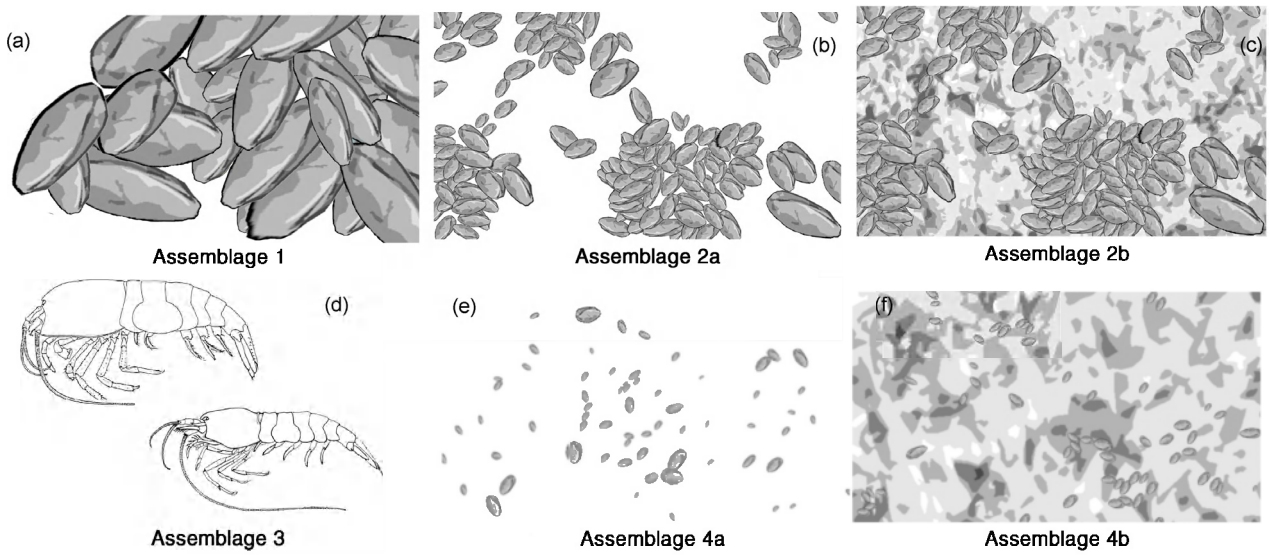

Fig. 4.2: Assemblage identification based on imagery as described by Cuvelier et al. (2009), varying in visibly dominant species (mussels and shrimp), in mussel size and in density of mussel coverage. Each assemblage is represented by a sketch: (a) Assemblage 1: dense *Bathymodiolus azoricus* mussel beds of larger-sized mussels (~6 cm); (b) Assemblage 2a: mussel clumps of smaller sized mussels (2–5 cm) with bare substrata inbetween; (c) Assemblage 2b: Assemblage 2a but with a microbial cover; (d) Assemblage 3: alvinocaridid shrimp colonising bare surface (mostly *Mirocaris fortunata*, other shrimp species can be recognised on imagery); (e) Assemblage 4a: scattered small mussels (~1 cm) with prevailing bare surface; and (f) Assemblage 4b: Assemblage 4a but with a microbial cover.

2.3. Chemical sampling

The CHEMINI (CHEmical MINIaturised) analyser was used to measure in situ concentrations of sulfides among the fauna (Vuillemin et al., 2009). The inlet of the analyser was directly mounted on the temperature probe manipulated by the ROV Victor 6000. Hence temperature and total dissolved sulfides (ΣS=H2S, HS-, S2-), hereafter referred to as ΣS, were measured during 10 minutes among the different assemblages. Chemical sampling was carried out in an undisturbed region of each sampled assemblages. A reference sample was taken away from the hydrothermal active area, to calibrate the sensor against bottom seawater. Calibration of the analyser was done in situ, at the beginning and at the end of the dive. Sampling time stamps were noted during the dive and afterwards measurement results were refined by looking at the video imagery. Data from when the CHEMINI probe was not touching the fauna (due to involuntary ROV movements caused by currents) were eliminated to avoid

measurements of surrounding seawater. Total concentrations of CH_4 were calculated from these in situ values, using a T°C vs. CH_4 regression curve obtained for Eiffel Tower hydrothermal fluids during the same cruise (Sarradin et al., in prep.).

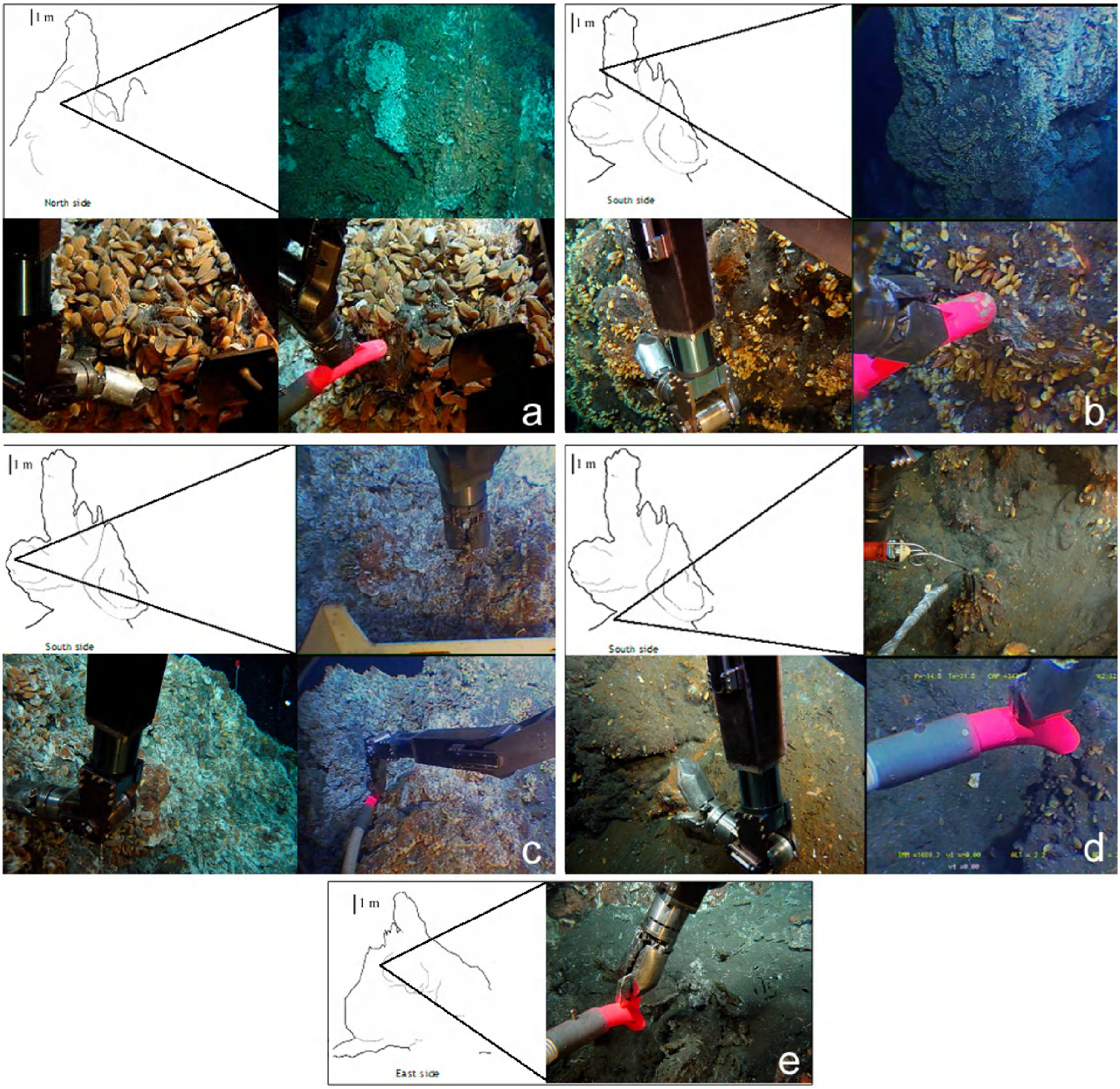

Fig. 4.3. Representation of the faunal assemblages sampled and their localities. Grabs were taken followed by an aspiration with the slurp gun. Assemblages sampled are (a) large mussel beds (Assemblage 1, grabs + aspiration) (b) smaller-sized mussel clumps (Assemblage 2a, grabs + aspiration) (c) mussel clumps with microbial cover (Assemblage 2b, grabs + aspiration) (d) bare substrata with discarded small mussels (Assemblage 4a, grabs + aspiration) (e) shrimp assemblage (Assemblage 3, aspiration).

2.4. Statistics

Principal Component Analysis (PCA) was carried out with the Vegan package (Oksanen et al., 2008) in R (version 2.8, Multicore team 2008) based on species abundance data. The species abundance-matrix was subject to a Hellinger-transformation prior to statistical analyses. Hellinger transformation is calculated by taking the square root of observed values divided by the row (site) totals and is very useful for community data, making them suitable for linear ordinations (Legendre & Gallagher, 2001). Taxonomic richness and rarefaction were also calculated with the Vegan package, while Spearman Rank Correlations among the chemical factors were carried out in Statistica 6 (StatSoft Inc. 2001). Preference was given to Spearman Rank Correlations as these are less sensitive to outliers and do not require normality of the data. As the data matrix did not meet the assumptions for parametric testing, not even after transformations, differences between the environmental variables (T°C and $\sum S$) were analysed with non-parametric tests (Kruskal-Wallis followed by post-hoc Wilcoxon pairwise testing), which were performed in R. Since CH_4 was estimated based on the temperature values, it was not used in the statistical analyses.

3. Results

3.1. Faunal assemblage composition

The visible assemblage identification at Eiffel Tower is given in Fig. 4.2, while an overview of the fauna present in the sampled assemblages is presented in Table 4.1. The density data showed that samples from Assemblages 2a and 4a were dominated by the same four species, starting with *Bathymodiolus azoricus*, the gastropods *Protolira valvatoides* and *Lepetodrilus atlanticus* and the polynoid polychaete *Branchipolynoe seepensis*. Assemblage 1 was also dominated by *B. azoricus* but the second dominating species was the shrimp *Mirocaris fortunata*, followed by *B. seepensis* and *Amathys lutzi* polychaetes. Assemblage 3 was almost exclusively dominated by *Mirocaris fortunata* shrimps, which was also very abundantly present in Assemblage 2b. The second dominant species for both assemblages was the amphipod *Luckia striki*, together with an undetermined polynoid polychaete in Assemblage 3. *Luckia striki* had the highest abundance in Assemblage 2b.

The mytilid individuals showed significant differences in mussel lengths (Kruskall Wallis, $H=41.71$, $p<0.001$, $df=3$). Assemblages 2a and 2b measured between 2 and 5 cm (no significant differences between them, but significantly different from Assemblages 1 and 4a $p<0.05$) while the mean size of the individuals in Assemblage 4a was about 1 cm (significantly different from Assemblages 1 and 2, $p<0.05$). The mussel length in Assemblage 1 was significantly higher ($p<0.001$), with a mean of 6 cm. The size or length distribution of the mussels was as followed: Assemblage 4a < Assemblage 2 < Assemblage 1. There were no mussels in Assemblage 3. Gastropods were only present in the

assemblages with smaller to medium-sized mussels without visible microbial cover (Assemblages 2a and 4a), while polychaetes had the highest abundance in the larger-sized mussel beds (Assemblage 1). *Branchipolynoe seepensis* lives inside the mussel shells of the Bathymodiolinae. This commensal polychaete had the lowest abundance when the size of the mussels was smallest (i.e. in Assemblage 4a), however its abundance did not increase in proportion to the mussel shell size. The ratio of the number of *B. seepensis*/number of mussels was highest in the medium-sized mussels of Assemblage 2b followed by Assemblage 1 with the larger mussels. Assemblage 4a had a unique presence of the pycnogonid *Sericosura heteroscela*. The crab *Segonzacia mesatlantica* was present in 3 samples: 4 individuals were sampled in Assemblage 1, 2 in Assemblage 2b and 2 in Assemblage 3.

Table 4.1: Species densities (ind/m²) and total taxonomic richness in the different faunal assemblages sampled. The undetermined species are also considered in the taxonomic richness calculations as these were definitely different from the other determined species. Highly mobile *Segonzacia mesatlantica* (Bythograeidae, Decapoda) was left out of the table.

		Density (ind/m²)				
Group	**Species**	**As_1**	**As_2a**	**As_2b**	**As_3**	**As_4a**
Mollusca						
Bivalvia						
Mytilidae	*Bathymodiolus azoricus*	952	5027	569	0	3260
Gastropoda						
Lepetodrilidae	*Lepetodrilus atlanticus*	0	340	0	0	104
	Pseudorimula midatlantica	0	0	0	0	21
Skeneidae	*Protolira valvatoides*	0	1155	0	0	1121
Orbitestellidae	*Lurifax vitreus*	0	68	0	0	0
Phenacolepadidae	*Shinkailepas briandi* (empty)**	0	0	44	0	21
Polychaeta						
Polynoidae	*Branchipolynoe seepensis*	385	544	350	0	332
	Branchinotogluma mesatlantica	18	0	0	0	0
Ampharetidae	*Amathys lutzi*	330	68	219	0	249
	Polychaeta indet.	37	0	88	0	21
	Polynoidae indet.	0	0	0	27	21
Arthropoda						
Amphipoda						
Eusiridae	*Luckia striki*	0	136	832	27	21
	Amphipoda indet.	0	68	0	0	0
Decapoda						
Alvinocarididae	*Mirocaris fortunata*	604	0	3065	3406	62
Pycnogonida						
Ammotheidae	*Sericosura heteroscela*	0	0	0	0	123
Total densities		2326	7406	5167	3460	5356
Surface sampled cm²		546.12	147.21	228.41	369.98	481.66
Taxonomic richness		6	8	6	3	11

**Not considered in statistical analyses or diversity calculations

Taxonomic richness and rarefaction were calculated to evaluate which sample of which assemblage was the most diverse (Table 4.1). The highest richness was found in Assemblage 4a with 11 taxa present, while Assemblage 3 was the least diverse (Table 4.1). In these calculations the undetermined species also counted as species, as they were different from the determined species. When calculating the expected number of species (Es) present in a sub-sample of size 100 (rarefaction or Es(100)), similar trends were apparent (Table 4.1). Mussel sizes showed negative relationships with taxonomic richness (R^2=0.67) and Es(100) (R^2=0.81).

3.2. Physical and chemical characterisation

Overall, a narrow temperature range (<2°C) was observed between the different assemblages (Fig. 4.4). However, some variability was noticeable as the temperature tended to oscillate, resulting in a broader temperature range for certain assemblages (Fig. 4.4). The minimum temperature measured was 4.44°C in Assemblage 2b, i.e. very close to the seawater temperature (4.4°C) (Table 4.2).

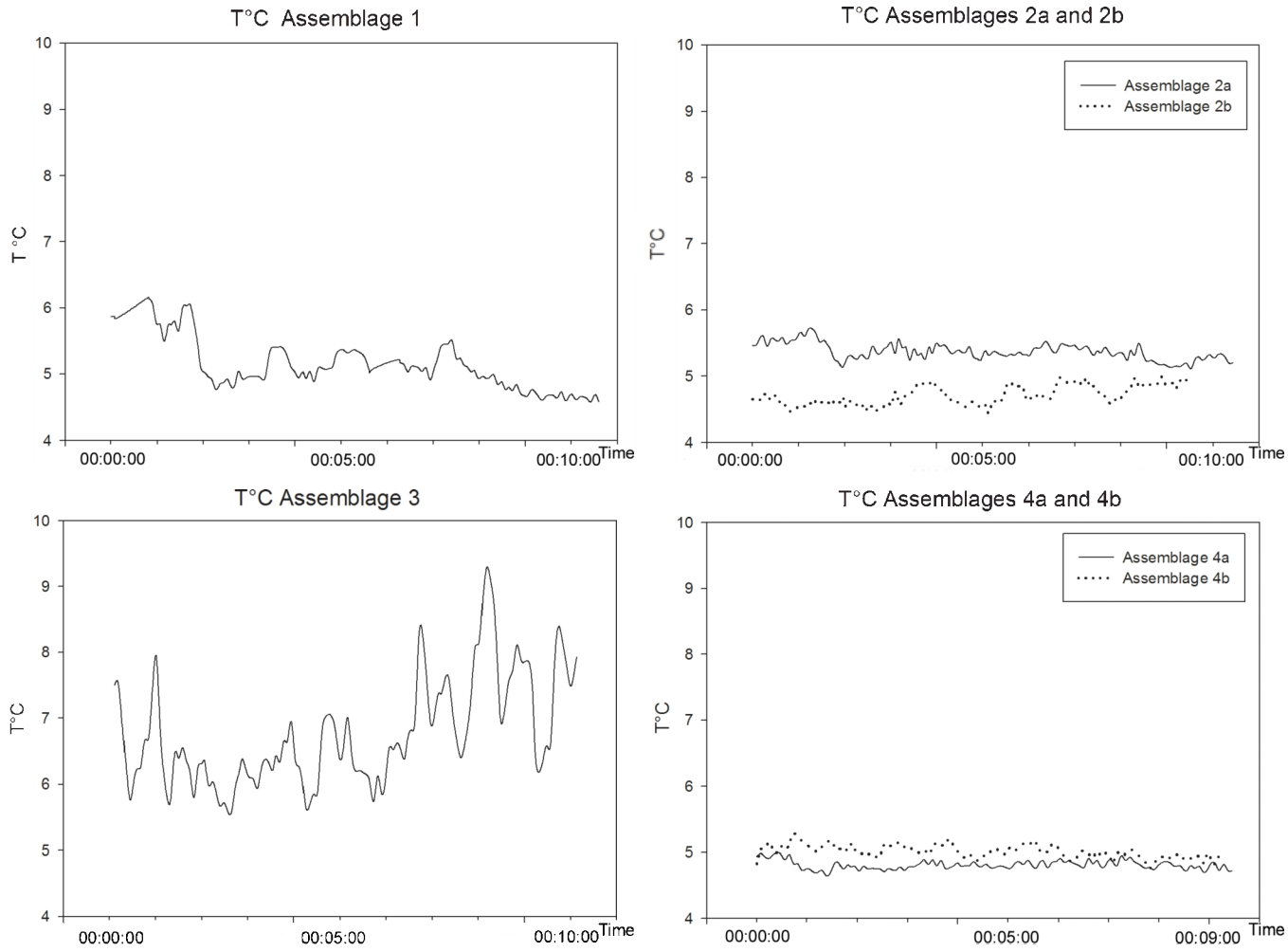

Fig. 4.4. Temperature fluctuations over a 10 minute time period on the different assemblages sampled.

The highest temperature (9.54°C) was measured in Assemblage 3. The shrimp assemblage (Assemblage 3) thus tolerated the highest temperatures recorded and the highest degree of temperature fluctuations (up to ~4.4°C), while both Assemblages 4a and 4b were very stable, exhibiting the lowest degree of fluctuations (Fig. 4.4). Of the mussel-based assemblages, Assemblage 1 with the larger-sized mussels had the broadest range (~1.56°C) and the highest maximum temperature (6.14°C) (Fig. 4.4).

Table 4.2: Mean values of T°C, ∑S and CH_4 and their standard deviations (stdev) measured or estimated on the different faunal assemblages. T°C and ∑S were measured *in situ*, n=number of samples, which is absent for CH_4 as this factor was calculated from the *in situ* T°C values, using a T°C vs. CH_4 regression curves. Maximum values are highlighted in grey. Ass=Assemblage

	T°C		∑S total µM		CH_4 total µm (estimated)
	n	Mean ± stdev	n	Mean ± stdev	Mean ± stdev
Ass_1	120	5.12 ± 0.39	7	1.72 ± 0.73	5.59 ± 0.75
Ass_2a	129	5.37 ± 0.13	6	1.40 ± 0.37	6.20 ± 0.17
Ass_2b	116	4.71 ± 0.15	7	0.81 ± 0.29	4.76 ± 0.28
Ass_3	128	6.79 ± 0.88	8	9.00 ± 11.81	8.73 ± 3.10
Ass_4a	117	4.81 ± 0.07	6	4.47 ± 0.83	4.96 ± 0.08
Ass_4b	115	5.01 ± 0.10	4	3.64 ± 0.87	5.61 ± 0.11

Among the different environmental factors, temperature and ∑S were positively and significantly correlated ($r=0.42$, $p<0.05$, $df=38$). As CH_4 was estimated based on the temperature, it showed exactly the same trends. We will not go in further detail on the latter. A non-parametric Kruskal-Wallis test confirmed significant variations in both temperature ($H=576.55$, $p<0.001$, $df=5$) and ∑S values ($H=26.16$, $p=0.001$, $df=5$) on the different faunal assemblages (Fig. 4.5).

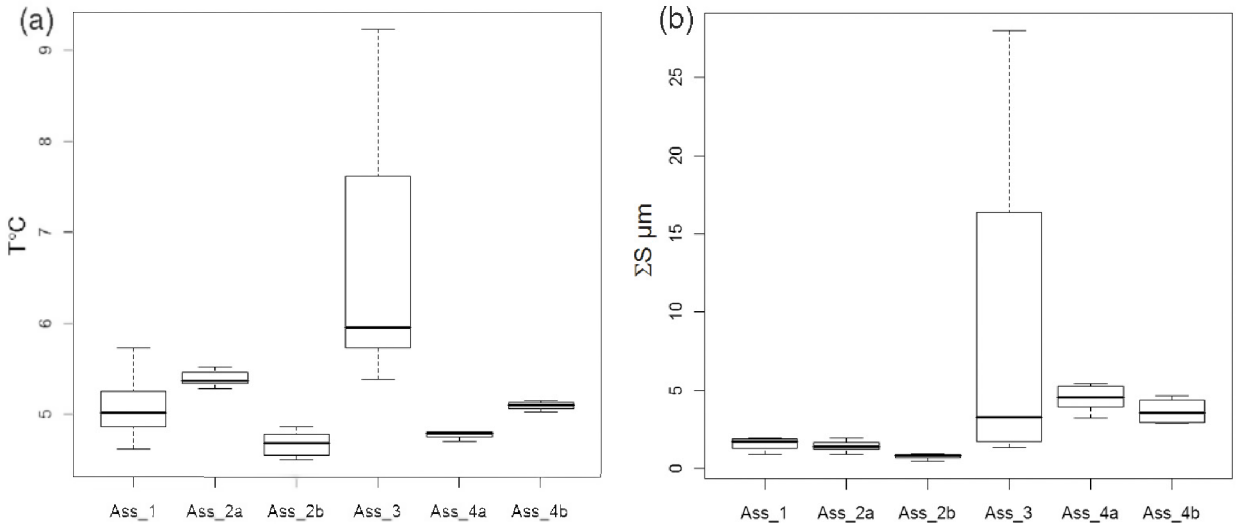

Fig. 4.5: Boxplots of environmental variables per assemblage. (a) Temperature and (b) ∑S were measured in situ. Black horizontal lines within the boxes represent the median.

The temperature values measured in Assemblage 1 showed the largest variations, when compared to the other mussel-based assemblage values (Fig. 4.5a). The mussel clumps of Assemblage 2a had a higher mean temperature than Assemblages 1 and 2b. Assemblage 4b had a significantly higher temperature than Assemblage 4a ($p<0.001$), a trend opposite to that observed between Assemblages 2a and 2b (Fig. 4.5a). Post-hoc testing revealed that differences in the temperature values between all the assemblages were significant ($p<0.001$) except between Assemblages 1 and 4b ($p>0.05$).

For the ∑S values, the differences between the different assemblages were less pronounced (Table 4.2, Fig. 4.4b), with concentrations ranging from 0.4 to 28 μM. Assemblage 3 exhibited the broadest range and the highest values. Assemblages 4a and 4b exhibited higher ∑S values than the other mussel assemblages, while ∑S concentrations were lower in Assemblages 1, 2a and 2b (Fig. 4.4b). Contrary to their temperature values, the ∑S-values of Assemblages 4a and 4b were closer to those of Assemblage 3 than the other assemblages. The differences between Assemblages 1 and 2 were not significant for ∑S ($p>0.1$). Significant differences are found between Assemblage 2b and Assemblage 3 ($p<0.05$), between Assemblage 4a and Assemblages 1, as well as between Assemblages 4a and 2b ($p<0.05$).

3.3. Habitat characteristics

When plotting the temperature vs. the concentrations of ∑S measured within the different faunal assemblages, all the points are limited to quite a narrow range (Fig. 4.6) with a strong curvature in the smoothed dilution curve. Assemblage 3 clearly had the broadest temperature range and the highest concentrations of ∑S. The microhabitats of the larger- and medium-sized mussels (Assemblages 1 and 2) were consistent. The T°C-∑S values measured in the larger-sized mussel beds of Assemblage 1 were positioned on a gentle slope (slope of curve=1.92). The mussel clumps with microbial mats (Assemblage 2b) had slightly lower ∑S-values than the mussel clumps without microbial cover (Assemblage 2a), which also had a higher temperature than the former (Table 4.2, respective slopes are 1.67 and 3.02). The plotting of Assemblages 4a and 4b above the observed dilution curve (Fig. 4.6), highlights their elevated levels of ∑S compared with the temperature and the ratios of the other mussel-based assemblages (Table 4.2). Both had steep slopes in the T°C-∑S curve, for which the slope of their curves are 7.19 for Assemblage 4a and -13.19 for Assemblage 4b. Even so, the assemblage with microbial cover (4b) had lower ∑S-values for higher temperatures than the same assemblage without visible microbial mats (Assemblage 4a).

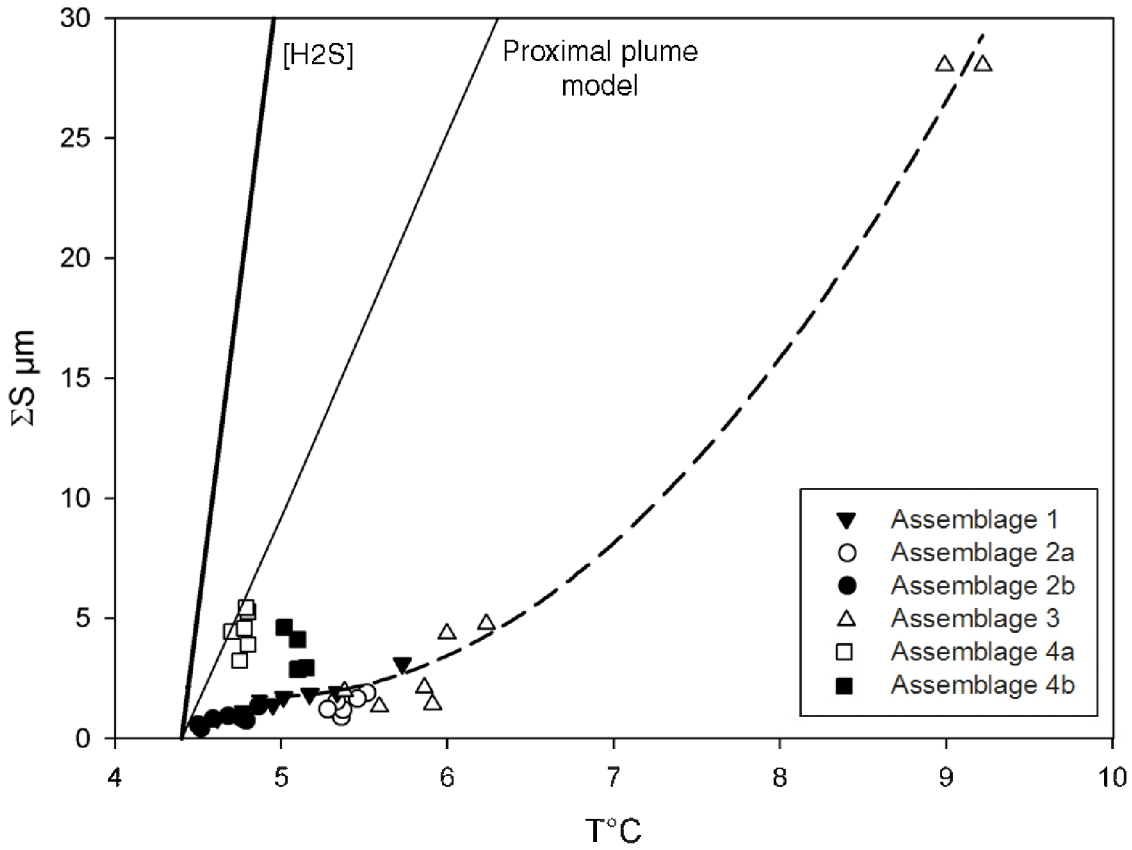

Fig. 4.6: Total sulfide concentration versus temperature on the different assemblages of the Eiffel Tower edifice. The curve between the assemblages is the best fitting polynomial curve (R^2=0.95) and can be considered as a non-linear dilution curve. [H2S] is the theoretic sulfide value, based on the end-member fluid concentrations at Eiffel Tower (Charlou et al., 2000). The "proximal plume model" represents the T°C vs. ΣS values based on the measurements made on uncolonised areas, in the vicinity of a black smoker (Sarradin et al., in prep.). See Fig. 4.2 for the assemblage identification.

3.4. Fauna-Habitat relations

Ordinations with Hellinger-transformed species abundances were used to unravel patterns between species and assemblages (Principal Component Analysis (PCA)) as well as relationships between species and environmental variables (Redundancy Analysis = RDA). Both plots were rather similar, as was the % variance explained, but since the RDA with chemical factors included in the analysis as constraints, did not show significant results (F=0.478, p=0.81), we chose to discuss only the PCA-plot (Fig. 4.7). A total variation of 92.4% was explained by the first two axes, of which the first axis accounted for 79.6% (Fig. 4.7). Assemblages for which the distance separating them equals zero are considered similar. Therefore Assemblages 1, 2b and 3 were considered more similar regarding their species composition and abundance as were Assemblages 2a and 4a. The positioning of Assemblages 1, 2b and 3 was largely due to the abundance of *Mirocaris fortunata* in these assemblages. Assemblages 2a and 4a were considered similar due to the shared abundance of *Lepetodrilus atlanticus* and *Protolira valvatoides* gastropods. In addition to *Bathymodiolus azoricus*, the mussel-based assemblages (i.e. Assemblages 1, 2a, 2b and 4a) are characterized by the presence of different polychaete taxa.

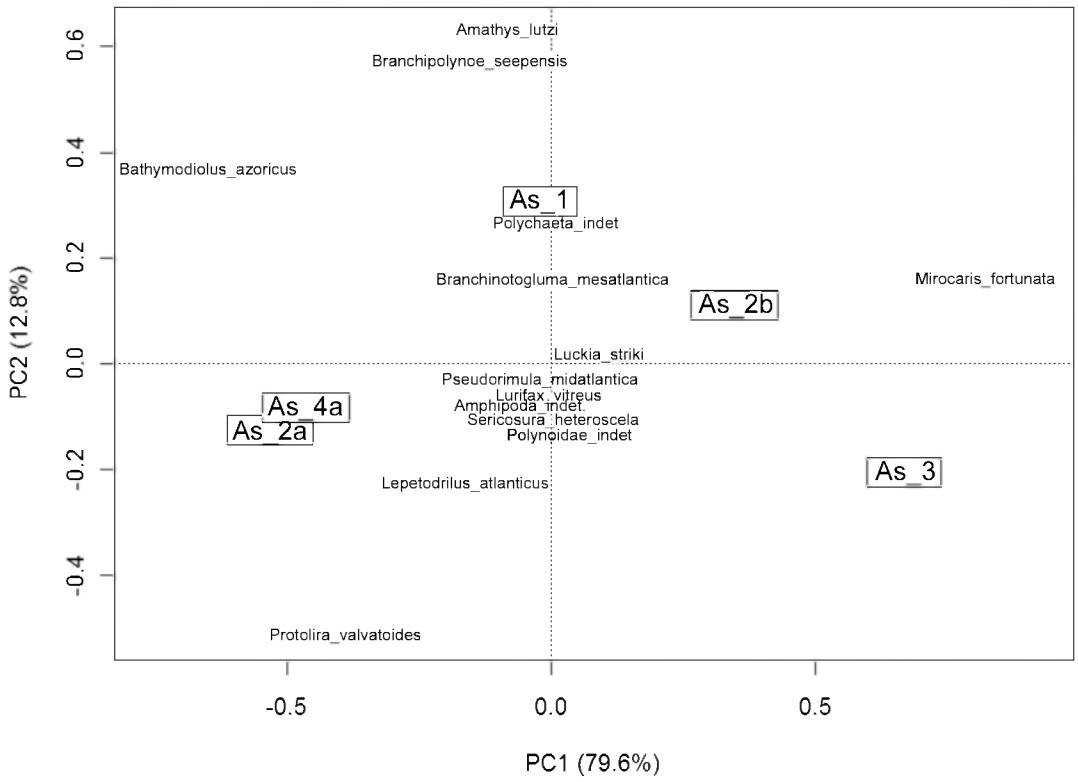

Fig. 4.7: Principle components analysis (PCA) based on the Hellinger transformed species abundance data. A total variation of 92.4% is explained by the PCA plot, where the first axis accounts for 79.6% and the second for 12.8%. As, Assemblage.

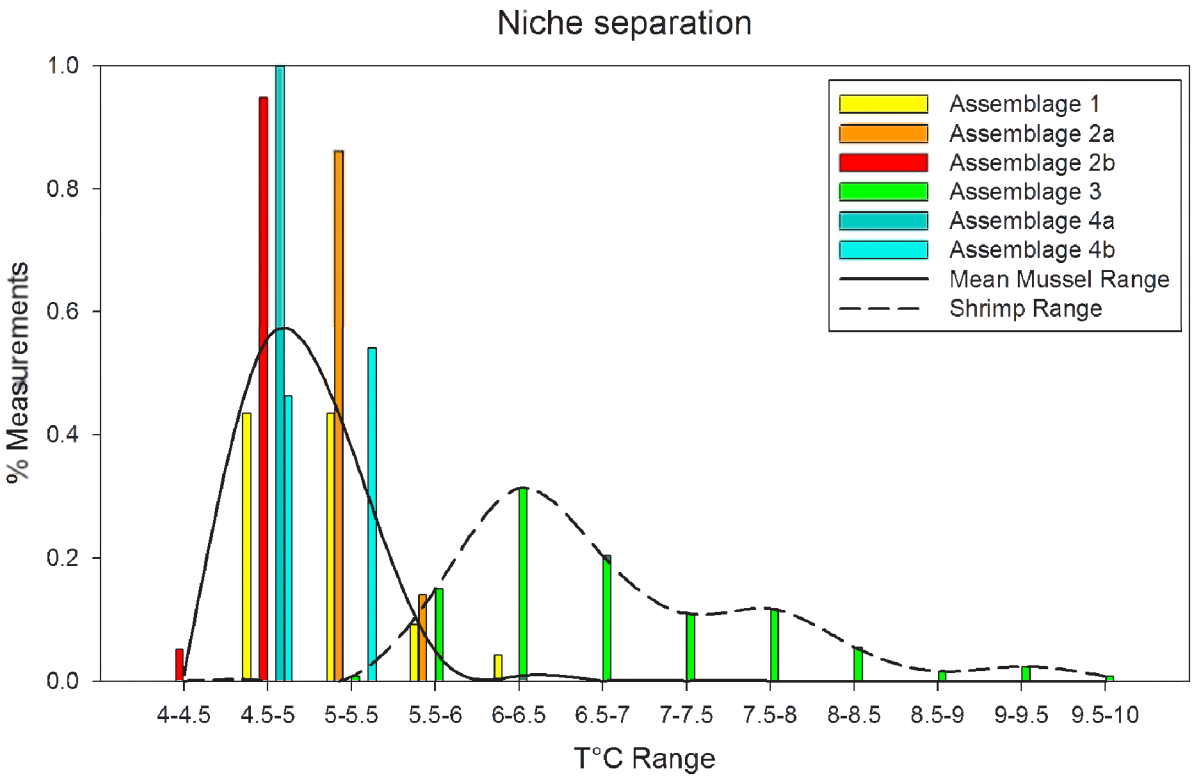

Fig. 4.8. Histogram featuring the percentage of T°C measurements in 0.5°C intervals for each assemblage. Two temperature-niches are revealed, one for the mussel-based assemblages (mean frequency of the mussel-based assemblages measurements) and the other for the shrimp assemblage.

When plotting histograms of the percentage of temperature measurements in categories separated by 0.5°C, preference for a certain temperature regime was revealed for each assemblage (Fig. 4.8). All mussel-based assemblages grouped together in the colder temperature array (4.4°C - 6.2°C), while the shrimp assemblage had the broadest range in the warmer temperatures (5.18°C - 9.54°C). Two temperature niches were thus revealed. In addition, there was a significant positive correlation between the mussel size and the temperature, where the increasing mussel size corresponded to increasing temperature (R^2=0.9986, p=0.00, df=27). This could be deduced from Fig. 4.8 as well. The larger-sized mussels of Assemblage 1 had the broadest range and the highest temperature, overlapping in temperature with the beginning of the shrimp-niche. Assemblage 2a is present in the 5-6°C range, while Assemblage 2b spanned 4-5°C, with a higher numbers of measurements between 4.5-5°C. Assemblage 4a had 100% of its measurements in the range 4.5°C - 5°C, while Assemblage 4b featured higher temperatures.

4. Discussion

4.1. Physico-chemical characteristics of the assemblages

Widest temperature and ∑S ranges are found in the shrimp assemblage (Assemblage 3). The second largest temperature variations are encountered in the larger-sized mussel-beds of Assemblage 1. In the remaining assemblages, composed of medium and smaller-sized mytilids, a narrower range of temperature values is observed. The ∑S measurements show different results, as wider ranges are encountered in the assemblages featuring small dispersed mussels on predominating bare surface (Assemblages 4). In other words, the ∑S concentration of Assemblage 4a, and to a lesser extent Assemblage 4b, is higher than for other mussel-based assemblages with similar or higher temperatures, e.g. Assemblages 1 and 2b. This might result from the preponderance of bare surface and consequently a lower biological uptake by the small and dispersed animals. In fact, what we measure in the vicinity of the fauna results from what is supplied by the fluids and what disappears through precipitation and organism consumption.

Assemblage 3 inhabits localities with relatively high temperatures and associated high levels of ∑S, which should be a common feature since these abiotic factors are positively correlated. Within vent mussel beds, however, temperature and chemistry do not necessarily conform to a conservative mixing model (Le Bris et al., 2006). The concave curvature we observe in the T°C-∑S plot is indicative for sulfide removal (Johnson et al., 1988b). This suggests that mussels may influence chemistry by removing H_2S through their endosymbionts (Fisher, 1990), altering the already existing gradients (Johnson et al., 1988b). The presence of the animals might also result in a higher degree of

precipitation of chemicals (Sarradin et al., 1999). When plotting temperature vs. ∑S, the medium to larger-sized mussel beds (Assemblages 1, 2a and 2b) tend to group together. The ∑S-values in Assemblage 1, associated with a broad T-range, are positioned on a gentle slope, which can imply that larger mussels consume more H_2S. Assemblage 2b has a gentler T-∑S slope than Assemblage 2a suggesting that mussel-assemblages with, in addition to their endosymbionts, a microbial cover on their shells also have a higher H_2S consumption (Le Bris et al., 2006). Assemblages with the predominance of bare surface (Assemblages 4a and 4b) tend to cluster above the dilution curve, approaching a proximal-plume model at Eiffel Tower (Sarradin et al., in prep., Fig. 4.6). Nonetheless, the measurements of the majority of mussel-based assemblages are coherent with the mussel microhabitat measurements from 2006 (De Busserolles et al., 2009; Vuillemin et al., 2009), except for Assemblage 4a.

At Eiffel Tower, shrimps (Assemblage 3) live closest to the fluid exits, followed by larger sized-mussels (Assemblage 1) and with further increasing distance, by the smaller-sized mussels in the mussel-clumps of Assemblage 2 (Comtet & Desbruyères, 1998; Sarradin et al., 1999; Cuvelier et al., 2009). The distance to the fluid exits increases even more for the small mussels from Assemblages 4a and 4b (Cuvelier et al., 2009). The gradient of decreasing mussel size with increasing distance from the fluid exit observed at Eiffel Tower was suspected to correspond to a decline in temperature (Comtet & Desbruyères, 1998; Sarradin et al., 1999; Desbruyères et al., 2001), which was confirmed here, as a significant positive correlation is observed between mussel size and temperature. Overall, we discern two temperature niches, distinguishing the mussel-based assemblages from the shrimp assemblage. Despite the overlap in temperature niche and range of the larger-sized mussels of Assemblage 1 and the shrimps, mussels generally thrive in the colder regions as opposed to the shrimps that prefer warmer localities.

Subtle differences in spatial zonation (i.e. different spatial niches) can be sufficient for species coexistence when species have similar adaptations to the local environmental regime (Chesson & Huntley, 1997). Environmental fluctuations provide opportunities for niche partitioning. As the different mussel-assemblages appear to occupy the same temperature niche, the individual assemblages do show differences in overlap among each other. Assemblages with microbial cover and the ones without are significantly different from each other regarding their temperature values (see Assemblages 2a-2b and 4a-4b). We could hypothesise that the microbial cover has an effect on the local environment or on the mussels either by increasing sulfide consumption or by supplying energy from chemosynthesis to the mussels. However, until now, no physiological (no significant differences

in lipids, carbohydrates or total proteins) nor toxicological (no significant differences in metals and metallothioneins) differences were found between mussels with or without microbial cover (Martins et al., 2009). Additionally, the differences observed are not consistent between the sub-forms of assemblages, as Assemblage 2a has higher temperature values than Assemblage 2b while it is the other way around for Assemblages 4a and 4b. Overall, Assemblage 2a has a relative high mean temperature compared with the other mussel-based assemblages, as do Assemblages 4a and 4b, although their maximum temperature is lower than that of Assemblages 1 and 3. There are two possible explanations for this feature; the first is the ability of the mussels to divert the flow horizontally, which allows them to expand the spatially limited, redox-transition zone (Johnson et al., 1988a; 1994). As a consequence, higher temperatures tend to occur at the edges of the mussel clumps (Johnson et al., 1988b). The second explanation is that during sampling the temperature sensor touched the (underlying) rocky, thereby measuring conductive heatflow from subsurface circulation of hot hydrothermal fluids.

Previous studies have hypothesised the existence of different physico-chemical microhabitats at the Eiffel Tower edifice (Sarradin et al., 1999; Cuvelier et al., 2009, Chapter 2 and 3), supposedly dividing it in a "harsh" (higher temperature, higher sulfide) and a "less harsh" (lower temperature, lower sulfide) environment, with the shrimps and larger-sized mussels inhabiting the harshest one, and the smaller-sized mussels occupying the other one. Based on the data acquired for this study, these two microhabitats are characterised by variability rather than harshness, although they also feature the highest and lower maximum temperatures. All values of temperature, ΣS and CH_4 presented in this study are in concordance with previously published values for this edifice and MAR mussel beds (Sarradin et al., 1999; 2009).

4.2. Faunal characteristics

Mirocaris fortunata, the most abundant shrimp at Eiffel Tower, can tolerate warm fluids at the MAR vents (36°C; Shillito et al., 2006), which explains their presence in the warmer regions. This shrimp species is an opportunist and feeds on a great variety of food items, such as microbial mats and tissues of other invertebrates (Gebruk et al., 2000; Colaço et al., 2002). They can be found in several mussel-based assemblages, mostly where there is a microbial cover present as well as on bare substrata, with no mussels. In addition, the less gregarious *Chorocaris chacei* and the more solitary *Alvinocaris markensis* also occur at Lucky Strike and Eiffel Tower (Desbruyères et al., 2006). Of the latter two species, there were no individuals present in our samples, even though video imagery of Assemblage 3 showed that *M. fortunata* co-occur with low abundances of *C. chacei* (Cuvelier et al., 2009). The absence of certain

'expected' species can be explained by the 'patchy' nature of the hydrothermal vent edifices along with our limited number of samples (n=5).

Bathymodiolus azoricus is the dominant species of the Eiffel Tower edifice and for the entire Lucky Strike vent field, representing a climax-community. *Bathymodiolus* can be regarded as an engineering species, offering secondary surfaces and interstitial microhabitats for other organisms to occupy (Van Dover & Trask, 2000). Structurally complex localities may allow the coexistence of many more species through competition-induced habitat specialization or through moderation of predation (Menge & Sutherland, 1976). In this way, mytilids promote biodiversity by enhancing habitat complexity and altering the local physico-chemical habitat. Gastropods (mainly *Protolira valvatoides*, *Lepetodrilus atlanticus* and *Pseudorimula midatlantica*) and even new mytilid recruits of Bathymodiolinae can be found on top of the mussel shells, although gastropod presence is limited to the smaller-sized mussel-based assemblages without microbial cover (2a and 4a). The microbial presence appears to exclude gastropod fauna. These gastropods probably feed on the detrital layer and biofilms covering these mussel shells without microbial cover, while filamentous bacteria might cause difficulties for attachment and movement of the gastropods. Larger-sized mussels could filter a larger amount of gastropod larvae out of the water column, inhibiting settlement. Presence and abundance of polychaetes differed from that of the gastropods. The gastropods are exclusively present in the smaller-sized mussel assemblages without microbial cover. While several polychaete species are clearly associated with the mussels, such as *Amathys lutzi* and *Branchinotogluma mesatlantica,* which live in the interstitial spaces between the mussels and are present in all mussel-based assemblages. At Eiffel Tower, polynoid polychaetes are often visible on the mussel beds and microbial mats. One of them, the commensal polychaete *Branchipolynoe seepensis* lives in the mantle cavity of the mussels. The abundance of *Branchipolynoe* is lowest in the very small mussel-based assemblages (Assemblages 4a and 4b), which is also visible in the PCA-plot.

Assemblage 2b is visibly dominated by *Bathymodiolus azoricus*, however, the high densities of *M. fortunata* could cast a new angle on the previous proposed models (Chapter 2 and 3) as well as on the assemblages identified based on imagery. This specific sample of Assemblage 2b (mussel clumps with microbial cover) was not actually dominated by mussels, but yes by shrimp. In this perspective Assemblage 2b cannot be regarded as being Assemblage 2a with an additional microbial cover as proposed in Chapter 2 and 3. Nevertheless, the elevated presence of the highly mobile shrimp could represent a sampling bias. Additional and more thorough, replicate sampling would be advisable and could change results as presented here.

4.3. Sample/assemblage similarity

The highest similarity in faunal abundances and species composition is observed between Assemblages 2a and 4a, which could be a different stage of the same assemblage. It is Assemblage 3 that stands out, while Assemblages 1 and 2b are more similar to one another as well. Due to this high faunal similarity between the latter two, there is no clear boundary between the assemblages able to withstand the highest environmental fluctuations (1 and 3) and those tolerating smaller environmental variable ranges (2a, 2b and 4a). This feature of species crossing the borders delineated by the variability in microhabitats is due to the existence of two temperature niches wherein the mussel-based assemblages group together under a colder temperature regime (4.44°C-6.14°C).

4.4. Diversity

The least diverse assemblage is the shrimp assemblage (Assemblage 3) and is also found closest to the fluid exits (Cuvelier et al., 2009). This corresponds to the most variable environment and could be considered the most stressful. At first sight there seems to be an increase in taxonomic richness with distance from a fluid exit with Assemblage 4a, situated the furthest away from a fluid exit, showed the highest richness. The expected number of species corroborated this, although differences were less pronounced. This increasing distance is hypothesised to correspond to a decrease in variability/stress as well. This is confirmed as there is a significant negative relation between Es(100) and the standard deviations of the temperature, which are a measure for the variability. Richness is likely to be subject to the surface area sampled, while rarefaction tends to mitigate this artefact. However, caution should be taken as our observations are based on a small number of samples and that the evaluation of species richness is largely dependant on this number of samples and the surface area sampled (Gauthier et al., 2010).

5. Conclusion

At Eiffel Tower, variability rather than differences in mean conditions distinguishes two microhabitats, in which temperature is proposed as being a more limiting factor than ∑S. The first and most variable microhabitat (broadest ranges in temperature values), also features the highest maximum temperatures, is inhabited by the alvinocaridid shrimps (Assemblage 3) and the larger-sized mussels (Assemblage 1). The second, more stable habitat, is inhabited by the smaller-sized mussels in clumps (without and with microbial cover respectively Assemblages 2a and 2b) and dispersed small mussels (without and with microbial cover respectively Assemblages 4a and 4b).

Hydrothermal vent animals such as mussels modify the local environment as we measure and perceive it. Larger mussels (present in Assemblages 1 and 2) appear to consume more ∑S than smaller-sized

individuals (~1 cm, Assemblage 4). A higher ∑S consumption can also be postulated for the mussel clumps that have an additional microbial cover on their shells (Assemblage 2a). The mussel size was also shown to be positively correlated to the temperature and negatively with the associated macrofauna richness. There is no evidence of the microbial cover being associated to specific environmental conditions or of its influence on the local chemistry, though its presence excluded gastropod fauna. The distinction between the two microhabitats is less clear when looking at species abundances. Despite several marked differences in presence and abundance of species between the visibly different faunal assemblages, there are species (e.g. *Mirocaris fortunata* and several polychaete species) that cross the boundaries delineated by the microhabitats. This was explained by the existence of two temperature niches: one for the mussel-based assemblages in the colder temperature areas and the other for the shrimps in the warmer regions, with an overlap in temperature-niche between the larger-sized mussels and the shrimps. A more thorough sampling at Eiffel Tower, both biologically (including replicates, meiofauna assessment and different sampling efficiency) as chemically (consideration of other electron donors, time-series measurements) is needed to validate our findings or highlight possible other factors at play, which we were unable to assess at this point. Additional sampling of similar faunal assemblages originating from other edifices within Lucky Strike would be the next step in testing the consistencies of the differences in faunal assemblages at this vent field.

Acknowledgments

I would like to thank Javier Escartin, chief scientist of the MoMAR08 cruise, for his collaboration and attribution of diving time. Thanks as well to the captain, Michel Houmard of l'Atalante, and his crew for their collaboration, indispensable assistance and availability. A huge thank you for the pilots of ROV Victor 6000 for their patience, expertise and willingness. A big thank you to Patrick Briand and Marie Morineaux for their valuable and much appreciated help in preparing the cruise.

Chapter 5

Temporal variations in faunal sampling and species composition at Lucky Strike

CHAPTER 5
Temporal variations in faunal sampling and species composition at Lucky Strike

1. Introduction

In 1985, hydrothermal vents were discovered in the Atlantic Ocean. The first discovered site along the Mid-Atlantic Ridge (MAR) was TAG (at 3600 m depth, Rona et al., 1986). It was populated by dense aggregations of shrimp. When in the early nineties the shallower parts of the MAR were screened for hydrothermal vents, it became clear that with depth the dominant fauna tended to change, going from shrimp-dominated sites in the deeper regions to mussel-dominated edifices at the shallower part (Desbruyères et al., 2001). At its discovery, the Lucky Strike hydrothermal community, largely dominated by dense beds of mussels, was visually distinct from most other known vent communities (Van Dover et al., 1996). Until then, distribution of mussels on vertical surfaces of upright edifices had only been observed at the hydrothermal vents in the North Fiji Basin (Desbruyères et al., 1994), while on the East Pacific Rise and elsewhere mussels were all but dominant and characterised the diffuse flow areas and lower regions of sulfide mounds (Van Dover et al., 1996).

Along with the discoveries of these new deep-sea ecosystems, the occurrence of species new to science was rather frequent. While species identification may take up to 5 to 10 years after a cruise, a centralised database was created at Ifremer to help manage the several steps between sampling and species identification, as well as allowing comparisons among the years (Biocean, Fabri et al., 2006). Similar databases have been created by ChEss (Chemosynthetic Ecosystem Science, a Census of Marine Life project) and InterRidge (Promoting international cooperation in ridge-crest studies). On another note, the first steps in studying temporal variations at hydrothermal vents were initiated following an eruption at 9°50′N along the East Pacific Rise, where the nascence of hydrothermal vents and first insights in vent community development were described by Shank et al. (1998a).

2. Material & methods

2.1. Study site

Lucky Strike vent field is situated in the Azores Triple Junction area, along the Mid-Atlantic Ridge (MAR), at a mean depth of 1700m (Fig. 5.1). It can be regarded as a large volcano or seamount, with a central lava-lake on its summit dividing it in 3 volcanic cones (Ondréas et al., 2009, Fig. 5.2).

Hydrothermal vents are situated around this lava lake. The south-eastern sector is one of the most active sectors hosting many venting areas and some of the largest edifices (Fig. 5.2). The hydrothermal edifices in the north-western and north-eastern sectors are thought to be the first-formed edifices within the vent field, while the south-eastern and south-western vents are younger as they are located around, what are believed to be, more recent faults (Ondréas et al., 2009, Fig. 5.2). The present-day distribution of exposed hydrothermal deposits and active vents at Lucky Strike is proposed to be controlled by the spatial distribution of eruptive products which may have covered pre-existing sulfide deposits, and by the faults which provide reactivated pathways for hydrothermal fluids (Ondréas et al., 2009). Lucky Strike edifices are dominated by *Bathymodiolus azoricus* mussel beds, although a few sites exist without mussel coverage. Even though the Atlantic is considered being one biogeographic province (Bachraty et al., 2009), there are considerable changes in the dominant fauna with depth along the MAR, differentiating the deeper sites from the shallower sites (Desbruyères et al., 2001). This vent field is part of the shallower venting sectors along the Mid-Atlantic Ridge.

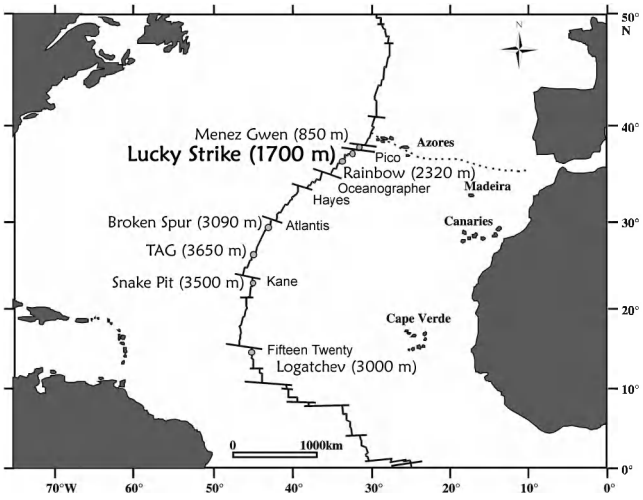

Fig. 5.1: Major known vent fields along the MAR and their depth. The major transform faults, separating the various vent fields, were added as well.

2.2. Biocean database

Early 1980 the first onset for the Biocean database was given, with as main objectives the gathering, compiling and centralising of lists of samples taken in the deep sea (Fabri et al., 2006). Biocean contains cruise metadata (scientific objectives, localities, cruise details and participants, samples taken) as well as species lists, densities, chemical environmental variables and so on. Currently, it contains data going back to the sixties, covering over 40 years of French deep-sea oceanographic research and including 114 cruises. For this study the species lists, densities and sampling localities of 6 cruises taking place at the Lucky Strike vent field between 1994 and 2006 were queried by Marie-Claire Fabri (©Ifremer, Département Etudes des Ecosystèmes Profonds).

Isabel
Sintra
Y3
Eiffel Tower
Statue of Liberty
Montsegur
Elisabeth
White Castle
Helene
Bairro Alto
Nuno
32°16'0"O
32°16'30"O
32°17'0"O
37°18'0"N
37°17'30"N
37°17'0"N
Statue of Liberty
Sintra
Y3
Isabel
Eiffel Tower
Montsegur
Elisabeth
Bairro Alto
Nuno
Helene
White Castle

Fig. 5.2: The Lucky Strike hydrothermal vent field, featuring the central lava lake and most of the well-known and well-defined sulfide structures that can be found surrounding it. Mosaics created represent one side of the structure or a part that can be considered characteristic for the structure and which can be used to recognise it. Mosaics are not to scale relative to one another. For more explanation on the individual sites see section 3.4. Images used to create the mosaics originate from ATOS (Bairro Alto), MoMARETO (Eiffel Tower), Knox18rr (Y3, Elisabeth and Statue of Liberty) and MoMAR08 (Sintra, Isabel, Montsegur, Nuno, Helene and White Castle).

2.3. Sampling bias

A representation of the data used in analyses is given in Table 5.1. For individual species and site assessments, presence/absence data was used to restrain the bias of the uneven sampling effort. Several species were left out of the analyses and discussion as their presence/absence was a misrepresentation of the reality (Table 5.1). For example, fish (*Cataetyx laticeps* and *Gaidropsarus* sp.) were left out because they represented a huge sampling effort and were therefore undeniably biased. The same strategy was applied for the anemone *Maractis rimicarivora*, as it was only sampled once but it was observed more often on video footage. Species only determined to the genus-level were left out as well, as we can never be sure that species x in year 1 is the same as species y in year 2. Samples present in Biocean were collected either with the suction sampler or with the manipulator grab. Total numbers of grabs and suction samples are known for each year and edifice, though the exact species composition of each separate sample was not known. More about sampling bias can be found in the discussion section.

2.4. Statistics

Statistical analyses were carried out with R (version 2.8, Multicore team 2008). Preference was given to working mainly with presence/absence data as this would mitigate the unevenly distributed sampling effort. When species abundance was used, it was Hellinger transformed prior to analyses. This transformation has been suggested to be very useful for community data. It is calculated by taking the square root of data divided by the row (site) totals (Legendre & Gallagher, 2001). The sites that were sampled only once were left out of the more detailed statistical analyses. The cluster analyses as well as Kendall's coefficient of concordance (Legendre, 2005) calculations were both executed within the Vegan Package (Oksanen et al., 2008). They were carried out to investigate the species associations and their significance. Method used to unravel the groups was the Sørensen index (also referred to as the binary Bray-Curtis index), which was used as a distance measure in the cluster analyses that delineated the different groups. When used as a distance measurement (1-x), Sørensen index equals the Bray-Curtis dissimilarity index. As binomial data were used, calculation of this index was preferred and due to the fact that there are no scales (size of samples) at play, results are thought to give more useful and intuitive information. The Kendall's coefficient of concordance was calculated

between these delineated groups, to see if they formed a significant species association. *A posteriori* tests were carried out to test the contribution of each species to the concordance of its group.

Table 5.1: Species presence/absence on the various sites for which sample lists were present in Biocean and the years collected, listed alphabetically. Species marked in grey were eliminated out of the statistical analyses as these were not considered representative. For higher taxonomy see Table 5.3.

sites	Bairro Alto				Chimiste	Elisabeth	Helene	Isabel		Sintra		
Year sampled	1994	1997	1998	2001	1994	1998	1994	1994	1997	1994	1998	2001
Alvania sp.												
Alvania stenolopha												
Alvinoceris markensis												
Amethys lutzi	*	*	*	*		*		*	*	*	*	*
Aphotaeontius atlanteus	*							*		*		
Archinome sp.												
Asbestopluma infundibulum												
Bathymodiolus azoricus	*	*		*				*	*	*	*	*
Bouvierella curtirama				*								
Branchinotopluma fisheri												
Branchinotopluma mesatlantica	*	*		*		*			*	*	*	
Branchinotopluma sp.		*						*	*			
Branchipolynoe seepensis	*	*	*	*		*		*	*	*	*	*
Candelabrum phrygium										*		
Choroceris chacei				*				*	*			
Cladorhiza primeldi										*		
Copidognathus alvinus												
Dendronotus comteti												
Eudendrium olanum												
Eunice sp.											*	
Glycera sp.	*		*			*			*	*	*	
Glycera tesselata												
Glyptelasma hamatum												
Harmothoe sp.												
Heteromesus sp.												
Krithe sp.								*				
Leeviphitus desbruyeresi	*	*	*	*								
Leonice asaccata				*					*		*	
Lepetodrilus atlanticus	*	*	*	*		*		*	*	*	*	*
Lepetodrilus sp.		*										
Lepidonotopodium jouinae	*	*		*		*		*	*	*	*	
Lepidonotopodium sp.											*	
Levensteiniella iris			*						*			
Levensteiniella sp.												
Lirapex costellata	*	*	*	*								
Luckia striki												
Lurifax vitreus	*			*							*	
Marectis rimicarivora												
Mesotaneis sp.	*											
Mirocaris fortunata	*	*	*	*		*		*	*	*		
Munneurycope sp.												
Ophioctenella acies			*	*					*			
Ophryotrocha fabriae												
Ophryotrocha sp.				*								
Paralepetopsis ferruginea					*						*	
Paralepetopsis sp.												
Peltospira smaragdina	*	*			*	*			*	*	*	*
Phymorhynchus ovatus				*							*	
Prionospio unilamellata	*			*		*			*	*	*	
Propontocypris sp.	*							*		*		
Protolira sp.												
Protolira thorvaldssoni	*	*	*	*		*			*	*		*
Protolira valvatoides	*	*	*	*		*			*		*	*
Pseudorimula midatlantica	*	*	*	*		*		*	*	*	*	
Pseudorimula sp.												
Pseudotaneis sp.	*											
Rimiceris exoculata												
Segonzacia mesatlantica	*	*		*				*	*	*	*	
Sericosura heteroscele	*	*	*	*			*		*			
Shinkailepas briandi	*	*	*	*				*	*	*	*	*
Shinkailepas sp.												
Storthyngura sp.										*		
Stygiopontius rimivagus	*									*		
Thalassarachna alvina	*											
Thermichione sp.												
Torometopa seldenhae			*									
Typhlotanais sp.	*		*						*	*	*	
Xylodiscula analoga	*		*	*								
Fish												
Cataetyx laticeps												
Geidropserus sp.												

sites	Statue of Liberty	Eiffel Tower						US6	US7	Y3	
Year sampled	1994	1994	1997	1998	2001	2005	2006	1994	1994	1994	1998
Alvania sp.				*							
Alvania stenolopha		*									
Alvinocaris markensis						*					
Amathys lutzi		*	*	*	*	*	*	*	*		*
Aphotopontius atlanteus	*	*							*		
Archinome sp.		*									
Asbestopluma infundibulum		*									
Bathymodiolus azoricus	*	*	*	*	*	*	*		*		
Bouvierella curtirama					*						
Branchinotogluma fisheri		*			*		*				
Branchinotogluma mesatlantica		*	*	*	*	*	*		*		
Branchinotogluma sp.		*	*	*	*		*				
Branchipolynoe seepensis		*	*	*	*	*	*		*		
Candelabrum phrygium		*									
Chorocaris chacei		*	*	*	*	*	*				*
Cladorhiza grimaldi											
Copidognathus alvinus		*									
Dendronotus comteti		*									
Eudendrium planum		*									
Eunice sp.		*									
Glycera sp.		*									
Glycera tesselata							*				
Glyptelasma hematum		*									
Hermothoe sp.					*						
Heteromesus sp.		*									
Krithe sp.											
Laevilitus desbruyeresi		*		*	*	*	*			*	
Leonice aseccata					*		*				
Lepetodrilus atlanticus	*	*	*	*	*		*		*		
Lepetodrilus sp.			*				*				
Lepidonotopodium jouinae		*	*	*	*	*	*				
Lepidonotopodium sp.											
Levensteiniella iris			*		*						
Levensteiniella sp.				*							
Lirapex costellata		*	*	*	*	*	*				
Luckia striki					*						
Lurifex vitreus		*	*	*	*		*		*		
Maractis rimicarivora						*					
Mesotenais sp.											
Mirocaris fortunata		*	*	*	*	*	*			*	*
Munneuryopsis sp.		*									
Ophioctenella acies			*		*						
Ophryotrocha fabriee							*				
Ophryotrocha sp.		*		*							
Paralepetopsis ferrugivora		*	*		*			*			
Paralepetopsis sp.						*					
Peltospira smaragdina		*		*			*	*			
Phymorhynchus ovatus											
Prionospio unilamellata			*				*				
Propontocypris sp.	*	*							*		
Protolira sp.							*				
Protolira thorvaldssoni	*	*	*	*	*				*		
Protolira valvatoides			*	*	*	*	*				
Pseudorimula midatlantica		*	*	*	*	*	*				
Pseudorimula sp.					*		*				
Pseudotenais sp.		*									
Rimicaris exoculata				*	*						*
Segonzacia mesatlantica	*	*	*	*	*	*	*				
Sericosura heteroscela		*	*	*		*	*				
Shinkailepas briandi	*	*	*	*	*		*	*	*		*
Shinkailepas sp.						*	*				
Storthyngura sp.		*									
Stygiopontius rimivagus											
Thalassorchina alvina			*								
Thermiphione sp.							*				
Torometopa seldenhee											
Typhlotenais sp.		*									
Xylodiscula enaloga				*	*	*					
Fish											
Cataetyx laticeps		*	*								
Geidropserus sp.					*						

Generalized linear models were carried out in R on the binomial presence/absence data of individual species to investigate if they were significantly influenced by time and/or locality. Time was used as a continuous variable in these models, while the sample locality was a categorical variable. Preference was given to work with quasi-binomial models, as binomial models assume that the dispersion parameter equals one, meaning that individuals are thought to be randomly distributed. A quasi-binomial GLM will estimate the same regression coefficients as the binomial GLM, but will estimate the dispersion parameter and use this dispersion parameter to provide different estimates of standard errors and significance levels (Kindt & Coe, 2005). Prior to GLM analyses, *Phymorynchus ovatus* and *Candelabrum phrygium* were left out, as their presence and more peripheral positioning on the venting edifices was not considered representative for a specific vent site and their sampling required a specific sampling effort.

Triangle plots were used to assess beta-diversity between the edifices sampled, allowing 6 pair-wise comparisons and using the following calculations: (a) the number of species shared, (b) the number of species gained, i.e. present in the focal quadrant but not in the neighbouring and (c) species lost (i.e. species absent in the focal quadrant but present in the neighbouring) (Koleff et al., 2003).

3. Results

3.1. The Lucky Strike vent field

3.1.1. Sampling sites

Sampling was not equally distributed across the vent field nor was it over the years. In other words, biological and other sampling was biased in a certain way that it was restricted to several well-known and easily-accessible (with manoeuvring space) sites. In the early years, when the vent field was first discovered, the most number of different edifices were sampled (n=10, Table 5.2), while in the later years the focus of faunal sampling tended to shift to one specific edifice, namely Eiffel Tower (Table 5.2). Depending on the objective of a cruise, other kinds of sampling occurred, as for example fluid, temperature or substratum sampling, explaining the visits to certain sites over the years. In addition the cruises which were not led by a chief scientist of Ifremer, but by a scientist from another institute and/or nationality, did not add their picked-out sample data to the Biocean database (cruises present in the Biocean database are listed in Table 5.2, while all cruises to Lucky Strike are listed in Chapter 1: Table 1.1).

Table 5.2: Sites visited at the Lucky Strike vent field during the cruises occurring in the specified years. Sites, for which a biological picked-out sample and species list was available in Biocean, are marked in grey. The sites visited did not necessarily correspond to the sites that were biologically sampled.

1994 (DIVANAUT 2)	1997 (MARVEL)	1998 (PICO)	2001 (ATOS)	2005 (EXOMAR)	2006 (MoMARETO)
Bairro Alto	Bairro Alto	Bairro Alto	Bairro Alto	Bairro Alto	
Eiffel tower	Eiffel Tower	Eiffel Tower	Eiffel Tower	Eiffel Tower	Eiffel Tower
Elisabeth	Elisabeth	Elisabeth		Elisabeth	
	Fantôme	Fantôme			Fantôme
Helene		Helene			
Isabel	Isabel			Isabel	
Montsegur					
Nuno					
Petit Chimiste	Petit Chimiste				
Sintra	Sintra	Sintra	Sintra		
US4	US4	US4	US4	US4	
US6	US6	US6	US6	US6	
US7		US7	US7	US7	
	L'aiguille/M. Soares				
Y3		Y3	Y3		

Along the years, various markers have been deployed to assign zones of active venting or zones of possible interest. Some of them still count today as point of reference. Nowadays, the most recognisable markers are the Flores-markers (deployed during the FLORES cruise in 1998), the American markers (deployed in the 1993 and Lustre 1996 cruises) and the French Petit Poucet markers (PP, deployed over the years) (Fig. 5.3). With residence time at the hydrothermal vent fields, these markers can get overgrown with microbes, sometimes rendering them difficult to decipher or even illegible. Records are also known of burned and completely destroyed markers, e.g. the Diva-markers (1994). Desbruyères et al. (2001) and Ondréas et al. (2009) gave an overview of the most common or conventional names of the hydrothermal vent sites known at Lucky Strike along with their markers. Marker names are mentioned next to the sampled sites in section 3.4.

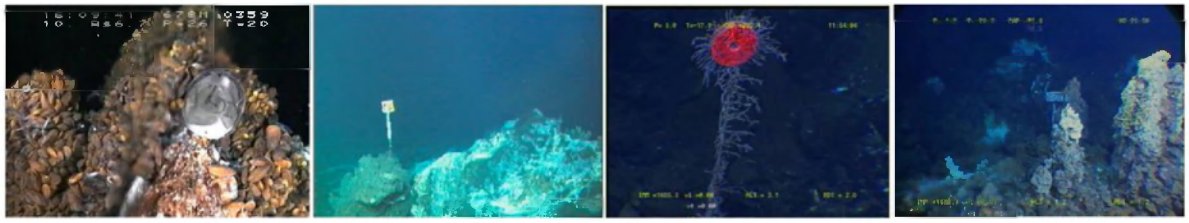

Fig. 5.3. Examples of the variety of markers that can be found at Lucky Strike, from left to right: the ancient DIVA-markers, only a couple of months after deployment, needless to say there are only very few present today. The square US markers, the round French PP-markers and the rectangular Flores-markers, covered with microbial mats.

Several venting structures were not well delineated and tended to coalesce with other edifice structures, which at certain moments in time were given other names and multiple markers. This was more the case in the south-eastern sector, closer to the lava lake. An example of this was Isabel and the region surrounding it, which contained various markers (PP23, FLORES 2x (last cipher is illegible)), as well as the Montsegur/US4 complex.

3.1.2. Sample or edifice similarity?

Comparing the different hydrothermal structures within the vent field turned out to be more complicated than expected, mainly because the samples taken did not always reflect the real situation. For example, Bairro Alto is dominated by mussels (Fig. 5.2 and Fig. 5.8). However in 1998 no mussels were sampled at this site (see Table 5.1), which clearly does not mean they were not present. As mussels were undoubtedly present, this was easily resolved, however for less visible species, such a correction could not be made. Nevertheless, there were several sites within Lucky Strike, namely Y3 edifice, White Castle and US6 that had no presence, let alone dominance of mytilids. White Castle was never biologically sampled during the cruises present in the Biocean database.

To study sampling behaviour over time, or in the best case edifice similarity, cluster analyses were carried out with Hellinger transformed abundance data (Fig. 5.4). Clustering distance used was the Bray-Curtis dissimilarity index and clustering method was Ward's. In a first attempt all sites (n=11) were withheld (Fig. 5.4a). Secondly, all sites that were only sampled once in the history of cruises to Lucky Strike were eliminated out of the analysis (Fig. 5.4b), in order to create more clarity for the repeatedly sampled sites (n=5). When all sites were considered Hélène, Chimiste and US6, exclusively sampled in 1994, pooled apart, because no mussels were sampled and only a few gastropods were present in the samples. US7 is an exception as it also was only sampled in 1994, but showed a species composition similar to the other sampled sites (Fig. 5.4a). When eliminating single visits, the sites visited and sampled in 1998 clustered apart, mostly because overall low faunal abundances sampled that year and the absence of mussels in the samples (despite their presence and dominance). In all clusters, Y3 stands out independent of the year sampled, as it showed some peculiarities, this time because no mussels were present and over all very few organisms (some shrimps and few other species) were sampled. For the other sites no distinct trend of year or locality could be revealed, resulting in a large cluster. Neither the types of samples (suction sample/grab) taken at each site and year could explain the clustering observed.

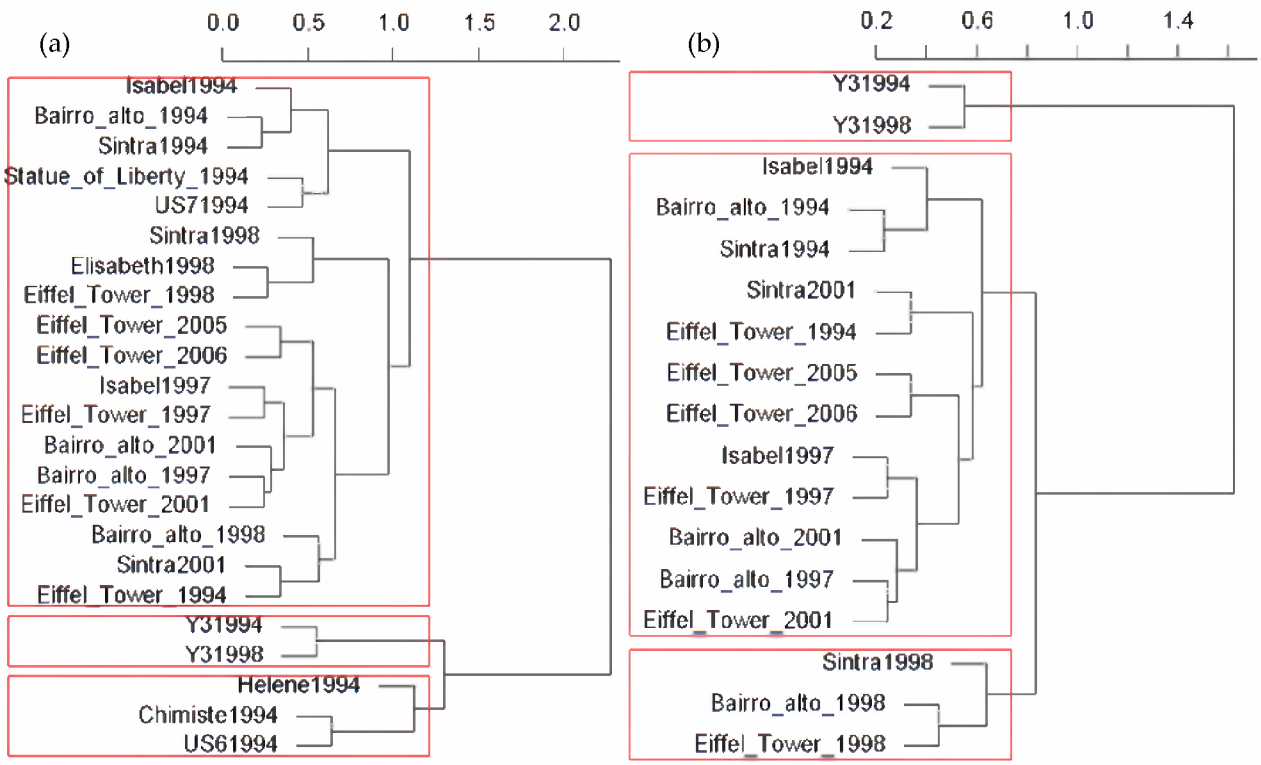

Fig. 5.4. Cluster analyses based on the Bray-Curtis dissimilarity index and the Hellinger transformed abundance of species at the sampled vent sites. (a) All sites ever sampled were included, which resulted in a high number of unique vent sites in 1994. (b) Only repeatedly visited sites ($n \geq 2$) were included in the analyses, in order to shed a light on similarity between sites and years sampled.

The rank/abundance (in this case rank/proportion) curves for the species in the samples show that *Bathymodiolus* mussels were the most abundant, representing a proportion of about 45% in the samples (Fig. 5.5). The second most abundant species was the shrimp *Mirocaris fortunata*, followed by the limpet *Protolira thorvaldsoni* and the polychaetes *Branchipolynoe seepensis* and *Amathys lutzi*. As the curve is steep, species are unevenly distributed, implying either several less abundant organisms in the samples and possibly in the Lucky Strike vent field or, several less sampled species.

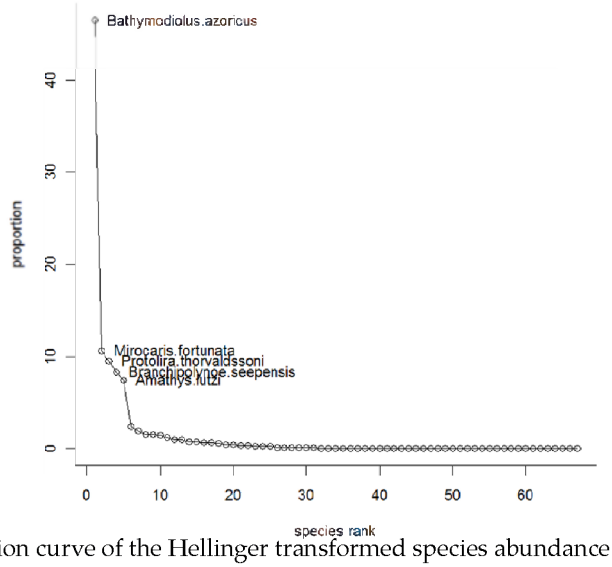

Fig. 5.5. Rank/proportion curve of the Hellinger transformed species abundance data matrix. The steepness of the

curve implies the presence of many less abundant species, while *Bathymodiolus azoricus* is without a doubt the most abundant or most sampled animal, followed by *Mirocaris fortunata*, *Protolira thorvaldssoni*, *Branchipolynoe seepensis* and *Amathys lutzi*.

3.1.3. Species list and sampling effort

A total species richness (no undetermined species) of 52 was encountered in Biocean for the Lucky Strike vent field, which is 67% of the total species pool thought to exist at Lucky Strike (calculations based on Desbruyères et al., 2006b, Table 5.3). The first European cruise in 1994 had both the highest level of sampled individuals and unique recordings (n=17), which makes sense, since this was the first European cruise to this vent field and the human bias in sampling a newly discovered locality tended to take over. In 2006, meiofauna was analysed in detail for the first time, resulting in an additional 9 copepod species (not included here, one of which was just recently described (Ivanenko et al., accepted CBM), J. Sarrazin, pers. comm.). The species list present here was compared with the species list presented in the "Handbook of deep-sea hydrothermal vent fauna" (Desbruyères et al., 2006b) and by Bachraty et al. (2009) (Table 5.3). Over the years, 21 determined species had one single and unique recording, i.e. were only present once in the samples.

Table 5.3: Species list of the Lucky Strike vent field checked alongside the species list as compiled by Desbruyères et al. (2006b) and double-checked with Bachraty et al. (2009). Higher taxonomy was taken from the Handbook (Desbruyères et al., 2006b).

			Species	Biocean	Handbook	Remarks
Porifera - Demospongiae						
Poecilosclerida	Cladorhizidae		*Asbestopluma infundibulum*	*	*	
			Cladorhiza grimaldi	*		There are 2 other *Cladorhiza* species in the handbook and a *Cladorhiza* aff. *grimaldi* was reported by Desbruyères et al. (2001)
	Guitarridae		*Eucheliplumа pristina*	*	*	Single occurrence at Lucky Strike in 1994
Cnidaria - Anthozoa						
	Actiniaria	Actinostolidae	*Maractis rimicarivora*	*		Not listed as occurring at Lucky Strike in handbook. Listed as present at Ashadze, Snake Pit and TAG
Cnidaria - Hydrozoa						
	Anthoathecata	Eudendriidae	*Eudendrium planum*	*	*	
		Candelabridae	*Candelabrum phrygium*	*	*	

Mollusca - Bivalvia					
Pteriomorphia	Mytilidae	*Bathymodiolus azoricus*	*	*	
Mollusca - Gastropoda					
Caenogastropoda,	Elachisinidae	*Laeviphitus desbruyeresi*	*	*	
	Rissoidae	*Alvaniastenolopha*	*	*	
Heterobranchia	Orbitestellidae	*Lurifax vitreus*	*	*	
	Xylodisculidae	*Xylodiscula analoga*	*	*	
Neomphalina	Peltospiridae	*Lirapex costellata*	*	*	
		Peltospira smaragdina	*	*	
Neritimorpha	Phenacolepadidae	*Shinkailepas briandi*	*	*	
Nudibranchia	Dendronotidae	*Dendronotus comteti*	*	*	
Patelligastropoda	Neolepetopsidae	*Paralepetopsis ferrugivora*	*	*	
Prosobranchia	Turridae	*Phymorhynchus ovatus*	*	*	
Vetigastropoda	Lepetodrilidae	*Lepetodrilus atlanticus*	*	*	
		Pseudorimula midatlantica	*	*	
	Skeneidae	*Protolira thorvaldssoni*	*	*	
	Skeneidae	*Protolira valvatoides*	*	*	
Annelida - Polychaeta					
Eunicida					
	Dorvilleidae	*Ophryotrocha fabriae*	*		New species from the 2006 MoMARETO cruise, described by Paxton & Morineaux (2009)
Phyllodocida					
	Glyceridae	*Glycera tesselata*	*	*	Single occurrence at Lucky Strike in 2006
	Polynoidae	*Branchinotogluma mesatlantica*	*		Other *Branchinotogluma* species are present in the handbook but not these 2
		Branchinotogluma fisheri	*		
		Branchipolynoe seepensis	*	*	
		Lepidonotopodium jouinae	*	*	
		Levensteiniella iris	*	*	
Spionida					
	Spionidae	*Laonice athecata*		*	There is a record of *Laonice assacata* in Biocean - but nowhere else
		Prionospio unilamellata	*	*	
Terebellida					
	Ampharetidae	*Amathys lutzi*	*	*	
Arthropoda - Arachnida					
Acariformes	Halacaridae	*Copidognathus alvinus*	*	*	
		Halacarellus auzendei		*	
		Thalassarachna alvina	*		Synonym with *Halacarellus alvinus* Bartsch, 1994 , though not present in

					handbook
Arthropoda - Pycnogonida					
	Ammotheidae	*Sericosura heteroscela*	*	*	
Arthropoda - Crustacea					
Copepoda					
	Cyclopinidae	*Heptnerina confusa*		*	
	Dirivultidae	*Aphotopontius atlanteus*	*	*	
		Aphotopontius temperatus	*		Present in Bachraty et al. (2009). Species not present in handbook, but present in Van Dover & Trask (2000), next to *Aphotopontius atlanteus*
		Stygiopontius rimivagus	*	*	
	Laophontidae	*Bathylaophonte azorica*	*		
	Tegastidae	*Smacigastes micheli*		*	
Cirripedia					
Scalpellomorpha	Scalpellidae	*Arcoscalpellum michelottianum*	*		No record of this genus in handbook, but it is listed in the chEss database as well. This is a single occurrence at Lucky Strike in 1994
Lepadomorpha	Poecilasmatidae	*Glyptelasma hamatum*	*		No record of this genus in handbook, but listed as present at Lucky Strike by Young (2001). 9 individuals were sampled only in 1994
Cumacea					
	Bodotriidae	*Bathycuma brevirostre*		*	
Tanaidaceae					
	Colleteidae	*Leptognathiella fragilis*		*	
	Fam. indet.	*Armaturatanais atlanticus*		*	
	Pseudotanaidae	*Pseudotanais vulsella*		*	
	Leptocheliidae	*Mesotanais styxis*		*	There is a *Mesotanais* sp. in Biocean. This could be the same species
	Nototanaidae	*Obesutanais sigridi*		*	
		Typhlotanais incognitus		*	There is a *Typhlotanais* sp. in Biocean. This could be the same species

Isopoda					
	Haplomunnidae	*Munnela danteci*		*	
		Thylakogaster lobotourus		*	
	Haploniscidae	*Antennuloniscus simplex*		*	
		Haploniscus aduncus		*	
		Haploniscus borealis		*	
	Ischnomesidae	*Heteromesus calcar*		*	
		Heteromesus ctenobasius		*	
Amphipoda					
	Aoridae	*Autonoe longicornis*		*	
	Eusiridae	*Bouvierella curtirama*	*	*	
		Luckia striki	*	*	
	Stegocephalidae	*Steleuthera ecoprophycea*		*	
	Amphilochidae	*Gitanopsis alvina*		*	
	Ischyroceridae	*Bonnierella compar*		*	
	Stenothoidae	*Torometopa saldanhae*	*	*	Single occurrence at Lucky Strike in 1998
Decapoda					
	Alvinocarididae	*Alvinocaris markensis*	*	*	
		Chorocaris chacei	*	*	
		Mirocaris fortunata	*	*	
		Rimicaris exoculata	*	*	
	Bythograeidae	*Segonzacia mesatlantica*	*	*	
		Thylakogaster lobotourus		*	
	Haploniscidae	*Antennuloniscus simplex*		*	
		Haploniscus aduncus		*	
		Haploniscus borealis		*	
	Ischnomesidae	*Heteromesus calcar*		*	
		Heteromesus ctenobasius		*	
Echinodermata - Ophiuroidea					
Ophiurida	Ophiuridae	*Ophioctenella acies*	*	*	
		Ophiocten centobi	*		Sthor & Segonzac (2004) based on sampling in 1994 at Lucky Strike
Chaetognatha					
	Spadellidae	*Calispadella alata*		*	
Chordata - Chondrichthyes					
Chimaeriformes	Chimaeridae	*Hydrolagus affinis*		*	Always present on video imagery, never sampled
		Hydrolagus pallidus		*	Always present on video imagery, never sampled
Chordata - Osteichthyes					
Gadiformes	Lotidae	*Gaidropsarus indet*	*	*	
Ophidiiformes	Bythitidae	*Cataetyx laticeps*	*	*	

Species richness of the sampled sites tended to fluctuate over the years, without any distinct trends (Table 5.4). However, it was clear that several sites, although repeatedly sampled were "under"-sampled, i.e. they displayed a very small sampling effort (e.g. Y3, Sintra) when compared to others (Eiffel Tower), although this did not always reflect in the species richness (e.g. Sintra and Isabel). There is a small positive linear relationship between the number of samples and species richness (R^2=0.17).

Table 5.4. Species richness (S) of each site and the year it was sampled in, along with the number of samples taken that year (grabs and aspirations). Total species richness per site was calculated as well as the species richness per sampling year. All calculations are based on the determined species.

	Eiffel Tower		Bairro Alto		Sintra		Isabel		Y3		∑ of samples	# Sites sampled	S per year
	S	# samples	S	# samples	S	# samples	S	# samples	S	# samples			
1994	27	8	22	3	17	1	11	2	2	1	14	5	40
1997	21	8	16	15			19	5			28	3	24
1998	20	15	15	4	16	1			5	2	22	4	27
2001	25	23	23	17	8	1					41	3	29
2005	15	23									23	1	16
2006	22	66									66	1	22
Total	40	143	29	39	22	3	20	7	6	3			

3.2. Species distribution over time

The variation in presence/absence data of species over time and locality was low, which was expressed by patterns of under-dispersion for many species in the carried out generalized linear models (GLM). In other words, many species were present on many edifices over the years. In addition, sampling tended to focus more on the Eiffel Tower edifice, which influenced the results as it was impossible to test time in the same extent for all the sampled sites. Only the sites that were sampled more than once were statistically analysed. A representation of data analysed can be found in Table 5.1 and Appendix 1. A selection of species was present over all the years, including the shrimps *Chorocaris chacei* and *Mirocaris fortunata*, the polynoid polychaetes *Branchinotogluma mesatlantica*, *Branchipolynoe seepensis* and *Lepidonotopodium jouinae*, the polychaete *Amathys lutzi*, the mytilid *Bathymodiolus azoricus*, the gastropods *Laeviphitus desbruyeresi*, *Lirapex costellata*, *Pseudorimula midatlantica* and the pycnogonid *Sericosura heteroscela* (Table 5.1 and Appendix 1). Their presence/absence on the repeatedly sampled sites tended to fluctuate between the years present in Biocean. GLM's were used to try and unravel the significance of the influence of the sampling locality as well as the time/year sampled. However, for the majority of species, fluctuations were not so that a significant trend with time or locality could be detected. Dispersion parameters turned out very small in a number of cases, which pointed to under-dispersion, meaning that many species were more regularly distributed than "random". However, it is important to keep the uneven sampling effort in

mind (Table 5.4). The small degree of variation between the tested explanatory variables inflated p-values, ending up producing not very reliable results. Below species presence/absence over time and locality is described per taxon, when assumptions were met, GLM results are mentioned. For the other species, no statistical testing was undertaken due to the little variance and no testable influence of time or locality.

Mollusca (Table 5.1, Appendix 1, p. 157-160)

For the *Bathymodiolus azoricus* mussels there was no influence of time noticeable, it was present at all sites except for Y3, which is a non-mussel dominated site within Lucky Strike (it has no mussels on its main edifice, although some small mussel clumps were found at the base/periphery). *Laeviphitus desbruyeresi* gastropods were sampled each year, though they were never sampled at Sintra and Isabel. *Lirapex costellata* was never sampled at Isabel, Sintra and Y3, while it was present over all the years at Eiffel Tower and Bairro Alto. A significant difference in locality, explaining 100% of the variance, was thus revealed ($p<0.001$). *Lurifax vitreus* showed a more variable presence-absence pattern. However neither sites, nor year, despite its absence in the 2005 samples, showed a significant influence (respectively $p=0.16$ and $p=0.58$). Another gastropod, *Peltospira smaragdina* showed an absence in 2005 as well and was never sampled at the Y3 site. Again, there were no significant influences from time or locality. The two *Protolira* species showed similar site occupation, with an absence on Y3, but with a different distribution over the years. *Protolira thorvaldssoni* was absent in the 2005 and 2006 samples, while *P. valvatoides* was present. As time was used as a continuous variable, it was shown to significantly influence *P. valvatoides* as this species was little present in the samples from 1994 but established a more constant presence ($p=0.007$), but not so for *P. thorvaldssoni*. *Shinkailepas briandi* was absent in 2005 and at Y3 in 1994, further on it was present in all the samples taken. *Xylodiscula analoga* was only sampled at Eiffel Tower and Bairro Alto, nonetheless the influence of the site was not significant, although smallish ($p=0.07$). There was no influence of time noticeable.

The three limpet species were all absent at Y3. *Lepetodrilus atlanticus* was present at all other sites and in all years except for 2005. *Paralepetopsis ferrugivora* was sampled at 2 sites and over 4 consecutive years, however it was not present in the samples originating from 2005 and 2006. The influence of time as a continuous variable was, however, not significant ($p=0.74$). No distinct patterns were distinguished for *Pseudorimula midatlantica* neither, as it was present over all the years and was sampled at almost all the sites.

Polychaetes (Table 5.1, Appendix 1, p. 161-162)

Amathys lutzi was present at all sites in all years, except in 1994 at Y3. *Laonice assacata* was only present from 1997 to 2001, but was distributed over all the sites (except Y3). The number of samples was too small to deduce valuable trends. *Prionospio unilamellata* was present in the samples from all sites but one (Y3) and in all years but one (2005). None of the explanatory variables had a significant influence (site: p=0.63, year: p=0.94). The polynoid polychaetes were never present in samples originating from the Y3 site. Three of them, *Branchinotogluma mesatlantica, Branchipolynoe seepensis* and *Lepidonotopodium jouinae* were present over all the years, therefore no distinct influence of year was revealed (for all: p>0.3). *Levensteiniella iris* was only present in samples taken from 1997 to 2001 and consequently only at the sites sampled in those years, i.e. Eiffel Tower, Bairro Alto and Isabel (as said before it was absent at Y3 which was sampled in 1998 as well).

Arthropoda (Table 5.1, Appendix 1, p. 163-165)

The Alvinocaridid shrimps *Chorocaris chacei* and *Mirocaris fortunata* were present in samples taken in every year. Locality-wise, there were some differences noticeable between these two species. *M. fortunata* was present in almost all samples taken, except for samples taken at Sintra in 1998 and 2001. *C. chacei* was never sampled at Sintra, and however present in the Bairro Alto samples from 1994; it was not sampled anymore at this site in the later years. *Alvinocaris markensis* was only sampled once in 2005 at Eiffel Tower. *Rimicaris exoculata* was present in very few samples, originating from the Y3 edifice and limited to the year 1998. The copepod *Aphotopontius atlanteus* was only encountered in samples originating from the 1994 cruise, where it was found to be present in all the sampled sites. The other copepod, *Stygiopontius rimivagus* was also only sampled in 1994, but was only encountered in samples form Bairro Alto and Isabel. The pycnogonid *Sericosura heteroscela* was present in samples over all the years and more specifically in samples taken at Eiffel Tower, Bairro Alto and Isabel. *Talassarachna alvina* was only sampled twice in the first two years and sample size was too small to deduct any tendencies. The amphipod *Bouvierella curtirama* was only sampled in 2001 be it both at Bairro Alto and Eiffel Tower.

Echinodermata (Table 5.1, Appendix 1, p. 165)

The ophiuroid *Ophioctenella acies* was present in samples taken in 1997, 1998 and 2001, although it was observed more often on video imagery, specifically at Eiffel Tower. It was never sampled at Sintra and Y3.

3.3. Beta diversity

The comparison in species composition between the sites was done through a pair-wise comparison which is presented in the triangle plots presented in Fig. 5.6 (Koleff et al., 2003). Overall the different sites sampled had many shared species. Hence there grouping towards the apex of a in Fig. 5.6. The sites that show the highest similarity (and the lowest beta-diversity) are Isabel-Bairro Alto (6), followed by Sintra-Isabel (4) and Bairro Alto-Eiffel Tower (3) (Fig. 5.6). Further down are Sintra-Bairro Alto (5), Isabel-Eiffel Tower (2) with Sintra-Eiffel Tower (1) showing the lowest similarity and consequently highest beta-diversity (Fig. 5.6). For all sites compared with Eiffel Tower (1, 2 and 3) there was a trend of species loss (high c), and only a few species that were present on the other sites and not at Eiffel Tower (b), meaning that the latter was the most species rich.

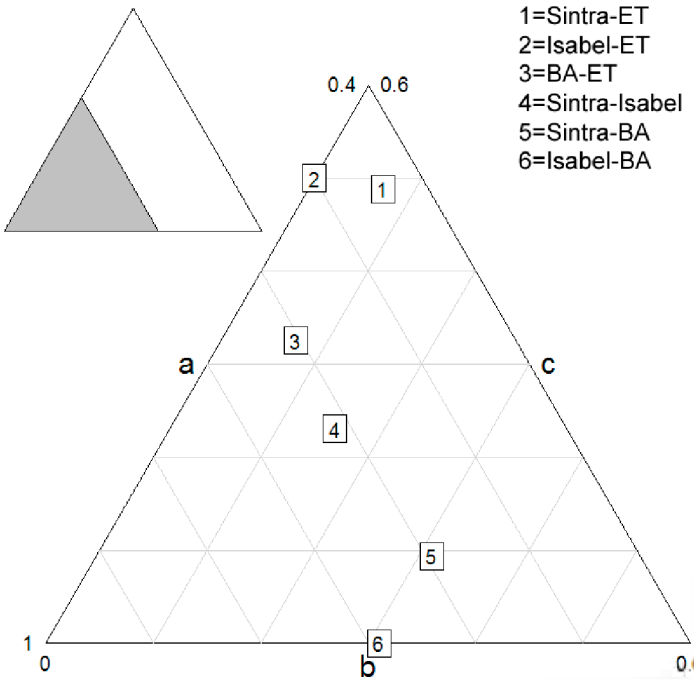

	a	b	c
1	19	3	21
2	20	0	20
3	26	3	14
4	16	4	6
5	19	10	3
6	20	9	0

Fig. 5.6. Triangle plots representing beta-diversity by pair-wise comparing the sites (Koleff et al., 2003). With a=species shared, b=the number of species gained, i.e. present in the focal quadrant but not in the neighbouring and c=species lost (i.e. species absent in the focal quadrant but present in the neighbouring).

3.4. Single vent edifices

3.4.1. Eiffel Tower (Flores 16, Diva II, IV, V, VI (burned))

Eiffel Tower is the only site that was sampled all the years (Table 5.2, Fig. 5.7), it was also the most sampled site (Table 5.4). In the more recent years it had become the centre of attention as it was often the only visited and sampled site during a cruise. Animals always present over all the years at Eiffel Tower were: the shrimps *Chorocaris chacei* and *Mirocaris fortunata*, the polychaetes *Branchinotogluma mesatlantica*, *Branchipolynoe seepensis*, *Lepidonotopodium jouinae* and *Amathys lutzi*, the mytilid

Bathymodiolus azoricus, the gastropods *Lirapex costellata* and *Pseudorimula midatlantica*. *Lepetodrilus atlanticus* was not sampled in 2005, nor was *Shinkailepas briandi*. The pycnogonid *Sericosura heteroscela* was not sampled in 2001. Despite these one-year absences of the latter three species, they are significantly associated with the ones that are always present (Group III, Table 5.5). All species within this group are significantly concordant with the others (p=0.004). Group I (Table 5.5) was significantly different from the other groups and contained species that were only sampled in 1994, later one they were no more encountered in the samples. Group II (Table 5.5) contained *Alvinocaris markensis* that was only sampled in 2005. Video imagery confirmed the unique high abundance of *A. markensis* in 2005 though it was observed in other years as well, be it more solitary and less abundant, but it was never sampled. The gastropod *Xylodiscula analoga* was present in samples taken 1998, 2001 and 2005. It was their presence in 2005 that groups them together. The species in Group IV are grouped because of the unique presence in 2001 of the amphipods *Bouvierella curtirama* and *Luckia striki*, the polynoid *Levensteiniella iris* and the ophiuroid *Ophioctenella acies* (Table 5.5). Group V is significantly different from the other delineated groups, even though not all species within show a significant association with each other (Table 5.5). The halacarid *Thalassarachna alvina* definitely stands out of this cluster and shows no concordance with the presence of the other species. It was only present in 1994 and 1997 samples, while the other species in its group in were associated due to their collective presence in 2006. Next to their presence in 2006, *Prionospio unilamellata* was also present in 1997, *Branchinotogluma fisheri* in 1994 and 2001, *Laonice assacata* was sampled in 2001 as well. *Segonzacia mesatlantica* crabs were always present at Eiffel Tower and always sampled, but were left out of analysis to allow comparability with the other sites where it was not always sampled, even though present.

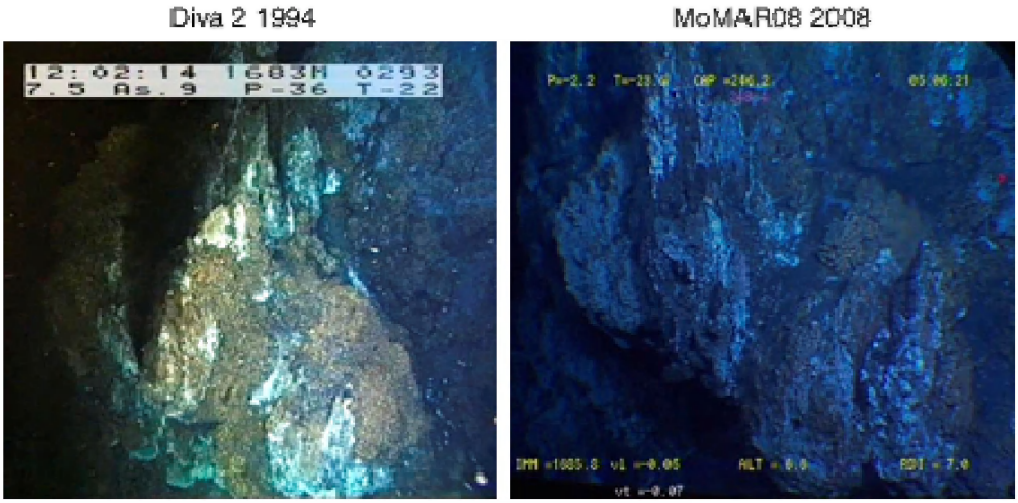

Fig. 5.7. The East-side of the Eiffel Tower edifice as observed over time. There is a reorganisation and relocation of the mussels noticeable and accretion of black smoker chimneys and some signs of de-activation and newly active smokers can be observed.

Table 5.5. Kendall's coefficient of concordance (W) calculations for the samples taken at the Eiffel Tower edifice. R=the mean of the Spearman correlations between a species and all the other species in the same group. Method used to unravel the groups was the Bray-Curtis dissimilarity index, which was used as distance measure in the cluster analyses that delineated the different groups. *A posteriori* tests were used to unravel which species were significantly concordant within the significantly different groups. In order to preserve a correct or approximately correct experiment-wise error rate, the probabilities of the *a posteriori* tests were adjusted for multiple testing: P_H = probability after Holm adjustment, based upon 999 random permutations.

	Eiffel Tower - Group I			
	Kendall's W = 1.00		p=0.005*	
		***A posteriori* tests**		
	r	**W**	**P_H**	
Alvania stenolopha	1	1	0.038	*
Aphotopontius atlanteus	1	1	0.038	*
Asbestopluma infundibulum	1	1	0.038	*
Candelabrum phrygium	1	1	0.038	*
Copidognathus alvinus	1	1	0.038	*
Dendronotus comteti	1	1	0.038	*
Eudendrium planum	1	1	0.038	*
Glyptelasma hamatum	1	1	0.038	*
	Eiffel Tower - Group II			
	Kendall's W = 0.90		p=0.005*	
		***A posteriori* tests**		
	r	**W**	**P_H**	
Alvinocaris markensis	0.80	0.90	0.038	*
Xylodiscula analoga	0.80	0.90	0.038	*
	Eiffel Tower - Group III			
	Kendall's W = 0.87		p=0.005*	
		***A posteriori* tests**		
	r	**W**	**P_H**	
Amathys lutzi	0.92	0.92	0.038	*
Bathymodiolus azoricus	0.92	0.92	0.038	*
Branchinotogluma mesatlantica	0.92	0.92	0.038	*
Branchipolynoe seepensis	0.92	0.92	0.038	*
Chorocaris chacei	0.92	0.92	0.038	*
Laeviphitus desbruyeresi	0.82	0.83	0.038	*
Lepetodrilus atlanticus	0.90	0.90	0.038	*
Lepidonotopodium jouinae	0.92	0.92	0.038	*
Lirapex costellata	0.92	0.92	0.038	*
Lurifax vitreus	0.90	0.90	0.038	*
Mirocaris fortunata	0.92	0.92	0.038	*
Paralepetopsis ferrugivora	0.56	0.58	0.038	*
Peltospira smaragdina	0.67	0.69	0.038	*
Protolira thorvaldssoni	0.80	0.81	0.038	*
Protolira valvatoides	0.86	0.86	0.038	*
Pseudorimula midatlantica	0.92	0.93	0.038	*
Sericosura heteroscela	0.83	0.84	0.038	*
Shinkailepas briandi	0.90	0.90	0.038	*
	Eiffel Tower - Group IV			
	Kendall's W = 0.87		p=0.005*	

	A posteriori tests			
	r	W	P_H	
Bouvierella curtirama	0.85	0.89	0.038	*
Levensteiniella iris	0.85	0.89	0.038	*
Luckia striki	0.85	0.89	0.038	*
Ophioctenella acies	0.85	0.89	0.038	*

Eiffel Tower - Group V

Kendall's W = 0.56 p=0.005*

	A posteriori tests			
	r	W	P_H	
Branchinotogluma fisheri	0.36	0.47	0.038	*
Glycera tesselata	0.60	0.67	0.038	*
Laonice asaccata	0.49	0.56	0.038	*
Ophryotrocha fabriae	0.60	0.67	0.038	*
Prionospio unilamellata	0.56	0.63	0.038	*
Thalassarachna alvina	0.20	0.33	0.89	

3.4.2. Bairro Alto (Flores 21, PP7, PP8)

Earlier on, this site was called Pagoda due to the unique form of the edifice structures. It hosted some large flanges, which gave it an overall view of a tiered tower with multiple eaves common in certain parts of Asia (Fig. 5.8). It was situated in the north-western sector of the vent field and it was last encountered during the EXOMAR cruise in 2005, however no samples were taken. During the 2006 and 2008 cruises (MoMARETO and MoMAR08, respectively) and despite the use of novel sonar techniques, the Bairro Alto structure was not encountered.

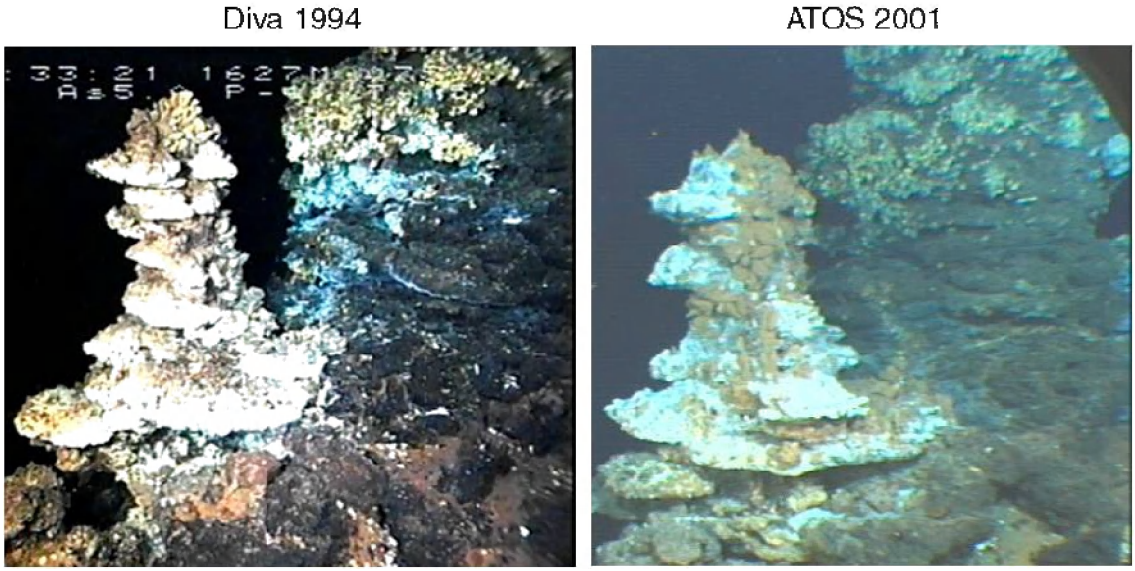

Fig. 5.8. Part of the Bairro Alto structure, as observed in 1994 and in 2001. The small mussels present on the left structure in 1994 seemed to have been replaced by larger–sized mussels that occupied different localities. Small-sized mussels continued to characterize the right-hand structure over the time-interval of 7 years, although the summit in 1994 was more heavily colonised.

Species present over the years sampled (1994, 1997, 1998 and 2001, Table 5.2) were the shrimp *Mirocaris fortunata*, the mytilid *Bathymodiolus azoricus*, the polychaetes *Branchipolynoe seepensis* and *Amathys lutzi*, the gastropods *Laeviphitus desbruyeresi*, *Lirapex costellata*, *Shinkailepas briandi*, *Protolira valvatoides*, *Lepetodrilus atlanticus*, *Pseudorimula midatlantica* and the pycnogonid *Sericosura heteroscela*. These were all grouped in Group I and showed indeed a significant association (p=0.028), in which no species stood out (Table 5.6). Group II was characterised by species that were only present in 1994 samples and which therefore were significantly concordant (Table 5.6). Group III species, on the other hand, were uniquely present in 2001 samples, also confirming a significant level of concordance (Table 5.6). The species present in Group IV were all present in the 1994 and 1997 samples and were all absent in the 1998 samples (Table 5.6). The two polychaete species (*Branchinotogluma mesatlantica* and *Lepidonotopodium jouinae*) did occur again in the 2001 samples, the gastropod *Peltospira smaragdina*, on the other hand, did not. Group V species were uniquely present in 1998 samples; they were not sampled before or after (Table 5.6). In the VIth Group (Table 5.6), the ophiuroid *Ophioctenella acies* did not show a significant association with the other species in the groups as it was only present in the two latest years, namely 1998 and 2001. The other 3 species were all absent in 1997, while *Lurifax vitreus* and *Prionospio unilamellata* were absent in 1998 as well.

Table 5.6. Kendall's coefficient of concordance calculations for the samples taken at the Bairro Alto edifice. R=the mean of the Spearman correlations between a species and all the other species in the same group. Method used to unravel the groups was the Bray-Curtis dissimilarity index, which was used as distance measure in the cluster analyses that delineated the different groups. *A posteriori* tests were used to unravel which species were significantly concordant within the significantly different groups. In order to preserve a correct or approximately correct experiment-wise error rate, the probabilities of the *a posteriori* tests were adjusted for multiple testing: P_H = probability after Holm adjustment, based upon 999 random permutations.

	Bairro Alto - Group I			
	Kendall's W = 1.00		p=0.006*	
		***A posteriori* tests**		
	r	**W**	**P_H**	
Amathys lutzi	1	1	0.028	*
Bathymodiolus azoricus	1	1	0.028	*
Branchipolynoe seepensis	1	1	0.028	*
Laeviphitus desbruyeresi	1	1	0.028	*
Lepetodrilus atlanticus	1	1	0.028	*
Lirapex costellata	1	1	0.028	*
Mirocaris fortunata	1	1	0.028	*
Protolira thorvaldssoni	1	1	0.028	*
Protolira valvatoides	1	1	0.028	*
Pseudorimula midatlantica	1	1	0.028	*
Sericosura heteroscela	1	1	0.028	*
Shinkailepas briandi	1	1	0.028	*

Bairro Alto - Group II

Kendall's W = 1.00 p=0.006*

	A posteriori tests			
	r	W	P_H	
Aphotopontius atlanteus	1	1	0.028	*
Stygiopontius.rimivagus	1	1	0.028	*
Thalassarachna alvina	1	1	0.028	*

Bairro Alto - Group III

Kendall's W = 1.00 p=0.006*

	A posteriori tests			
	r	W	P_H	
Bouvierella curtirama	1	1	0.028	*
Chorocaris chacei	1	1	0.028	*
Laonice asaccata	1	1	0.028	*
Phymorhynchus ovatus	1	1	0.028	*

Bairro Alto - Group IV

Kendall's W = 0.90 p=0.006*

	A posteriori tests			
	r	W	P_H	
Branchinotogluma mesatlantica	0.88	0.92	0.028	*
Lepidonotopodium jouinae	0.88	0.92	0.028	*
Peltospira smaragdina	0.76	0.84	0.028	*

Bairro Alto - Group V

Kendall's W = 1.00 p=0.006*

	A posteriori tests			
	r	W	P_H	
Levensteiniella iris	1	1	0.028	*
Torometopa saldanhae	1	1	0.028	*

Bairro Alto - Group VI

Kendall's W = 0.45 p=0.006*

	A posteriori tests			
	r	W	P_H	
Lurifax vitreus	0.35	0.51	0.028	*
Ophioctenella acies	0.0036	0.25	0.50	
Prionospio unilamellata	0.35	0.51	0.028	*
Xylodiscula analoga	0.38	0.53	0.028	*

3.4.3. Sintra (US3, Flores 15)

Species that were present over all the years sampled at Sintra (1994, 1998 and 2001, Table 5.2, Fig. 5.9) were the polychaetes *Branchipolynoe seepensis* and *Amathys lutzi*, the mytilids *Bathymodiolus azoricus* and the gastropods *Shinkailepas briandi*, *Peltospira smaragdina* and *Lepetodrilus atlanticus*, were all present in Group I and were joined by the two *Protolira* species (Table 5.7). All species were significantly associated to one another, although *Protolira valvatoides* was not present in the 1994 samples and *Protolira thorvaldssoni* was absent in the 1998 samples, therefore the value of the concordance coefficient was lower (W=0.66 and W=0.61 respectively). Group II (Table 5.7) featured the species that were only present in the samples taken in 1994. They were not encountered in samples of later years. Group III (Table 5.7) contained the species that were present in the samples from the first two years available, namely 1994 and 1998, none of these were present in the samples from 2001. Group IV contains all species exclusively present in 1998 (Table 5.7). The crab *Segonzacia mesatlantica* was sampled in all the years mentioned above.

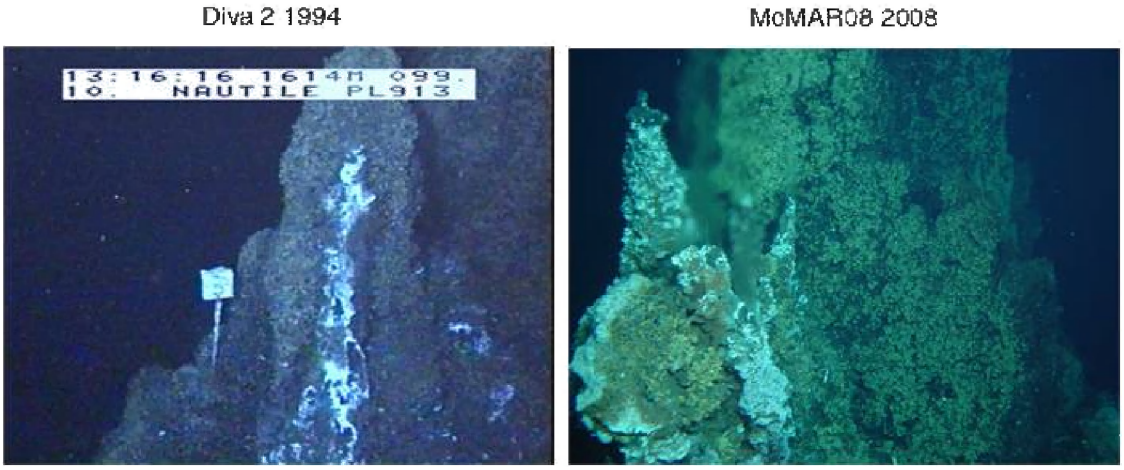

Fig. 5.9. Sintra as observed in 1994 and in 2008 from a slightly different viewing angle. The edifice continued to be dominated by small mytilids, the morphology of the active chimneys changed over the years.

Table 5.7. Kendall's coefficient of concordance calculations for the samples taken at the Sintra edifice. R=the mean of the Spearman correlations between a species and all the other species in the same group. Method used to unravel the groups was the Bray-Curtis dissimilarity index, which was used as distance measure in the cluster analyses that delineated the different groups. *A posteriori* tests were used to unravel which species were significantly concordant within the significantly different groups. In order to preserve a correct or approximately correct experiment-wise error rate, the probabilities of the *a posteriori* tests were adjusted for multiple testing: P_H = probability after Holm adjustment, based upon 999 random permutations.

	Sintra - Group I			
	Kendall's W = 0.84		p=0.004	
		***A posteriori* tests**		
	r	**W**	**P_H**	
Amathys lutzi	0.90	0.91	0.021	*
Bathymodiolus azoricus	0.90	0.91	0.021	*
Branchipolynoe seepensis	0.90	0.91	0.021	*

Lepetodrilus atlanticus	0.90	0.91	0.021	*
Peltospira smaragdina	0.90	0.91	0.021	*
Protolira thorvaldssoni	0.56	0.61	0.021	*
Protolira valvatoides	0.61	0.66	0.021	*
Shinkailepas briandi	0.90	0.91	0.021	*

Sintra - Group II

Kendall's W = 1 p=0.004

	***A posteriori* tests**			
	r	**W**	**P_H**	
Aphotopontius atlanteus	1	1	0.021	*
Cladorhiza grimaldi	1	1	0.021	*
Candelabrum phrygium	1	1	0.021	*
Mirocaris fortunata	1	1	0.021	*
Stygiopontius rimivagus	1	1	0.021	*

Sintra - Group III

Kendall's W = 1 p=0.004

	***A posteriori* tests**			
	r	**W**	**P_H**	
Branchinotogluma mesatlantica	1	1	0.021	*
Lepidonotopodium jouinae	1	1	0.021	*
Prionospio unilamellata	1	1	0.021	*
Pseudorimula midatlantica	1	1	0.021	*

Sintra - Group IV

Kendall's W = 1 p=0.004

	***A posteriori* tests**			
	r	**W**	**P_H**	
Laonice asaccata	1	1	0.021	*
Lurifax vitreus	1	1	0.021	*
Paralepetopsis ferrugivora	1	1	0.021	*
Phymorhynchus ovatus	1	1	0.021	*

3.4.4. Isabel (Diva VIII, Flores 22)

Isabel is a vast complex of different vent(ing) structures (Fig. 5.10). It could be that activity and associated fauna spread out, thus blurring the boundaries with previously separately identified sites, e.g. Fantôme (PP23). Species that were present over the years sampled (1994 and 1997, Table 5.2) were *Chorocaris chacei, Mirocaris fortunata, Branchipolynoe seepensis, Lepidonotopodium jouinae, Amathys lutzi, Bathymodiolus azoricus, Shinkailepas briandi, Lepetodrilus atlanticus* and *Pseudorimula midatlantica,* which were joined by the copepod *Aphotopontius atlanteus,* which was absent in 1997 in Group I (Table 5.8). Species were significantly associated and all individual species were concordant with the others in the group. Group II (Table 5.8) features all species that were absent in the samples from 1994 but present in those from 1997. *Segonzacia mesatlantica* was present in all the samples taken in the 2 years mentioned.

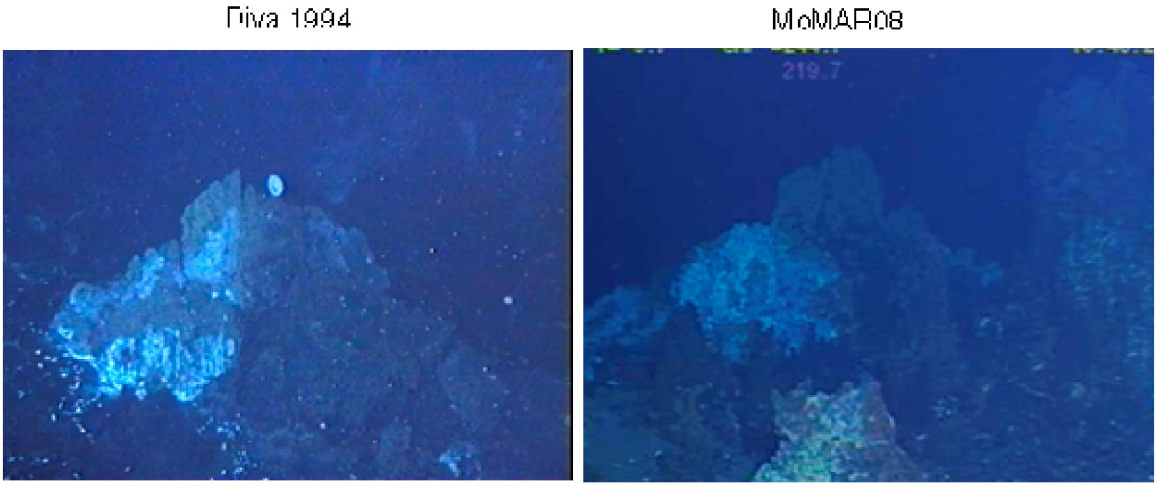

Fig. 5.10. Part of Isabel hydrothermal structure as observed in 1994 and in 2008.

Table 5.8. Kendall's coefficient of concordance calculations for the samples taken at the Isabel edifice. R=the mean of the Spearman correlations between a species and all the other species in the same group. Method used to unravel the groups was the Bray-Curtis dissimilarity index, which was used as distance measure in the cluster analyses that delineated the different groups. A posteriori tests were used to unravel which species were significantly concordant within the significantly different groups. In order to preserve a correct or approximately correct experiment-wise error rate, the probabilities of the a posteriori tests were adjusted for multiple testing: P_H = probability after Holm adjustment, based upon 999 random permutations.

	Isabel - Group I			
	Kendall's W = 0.96		p=0.002	
	***A posteriori* tests**			
	r	**W**	**P_H**	
Amathys lutzi	0.98	0.98	0.002	*
Aphotopontius atlanteus	0.78	0.8	0.002	*
Bathymodiolus azoricus	0.98	0.98	0.002	*
Branchipolynoe seepensis	0.98	0.98	0.002	*
Chorocaris chacei	0.98	0.98	0.002	*
Lepetodrilus atlanticus	0.98	0.98	0.002	*
Lepidonotopodium jouinae	0.98	0.98	0.002	*
Mirocaris fortunata	0.98	0.98	0.002	*
Pseudorimula midatlantica	0.98	0.98	0.002	*
Shinkailepas briandi	0.98	0.98	0.002	*
	Isabel - Group II			
	Kendall's W = 1.00		p=0.002	
	***A posteriori* tests**			
	r	**W**	**P_H**	
Branchinotogluma mesatlantica	1.00	1.00	0.002	*
Laonice asaccata	1.00	1.00	0.002	*
Levensteiniella iris	1.00	1.00	0.002	*
Ophioctenella acies	1.00	1.00	0.002	*
Peltospira smaragdina	1.00	1.00	0.002	*
Prionospio unilamellata	1.00	1.00	0.002	*
Protolira thorvaldssoni	1.00	1.00	0.002	*
Protolira valvatoides	1.00	1.00	0.002	*
Sericosura heteroscela	1.00	1.00	0.002	*

3.4.5. Y3 (Flores 14, Diva I)

Y3 is a 13-14 m high spire with black smokers ejecting fluid at the summit. It has no mussels present on the main spire-chimney, although there are some small patches present at the base of the edifice. This was the only site at Lucky Strike that showed presence of *Rimicaris exoculata* shrimp, however after 1998 *R. exoculata* was never observed again, except for in 2008 (MAR08 Knox 188rr cruise) where 1 individual was found in the samples. If this was a valid presence or a left-over in the sampling gear from sampling at Rainbow during the previous dive remained arguable as we were unable to confirm its presence by analysing video imagery. There were no mussels and no associated polychaetes, like *B. seepensis* and other polynoids sampled 1994 and 1998. Some polychaete species were sampled in 1998 e.g. *Amathys lutzi*. *Mirocaris fortunata* is the only species present over the two years for which sample lists were available.

3.4.6. Elisabeth (PP24, PP12, PP13)

Elisabeth is a hydrothermal structure situated in the north-western sector of the vent field. It is a 10 m high edifice which was also referred to as "the cathedral" (Fig. 5.11). Between 1997 and 1998, a time lapse camera was deployed at this structure (P. Tyler), which was programmed to record 30 seconds every 24 hours. Due to the high levels of activity and associated Fe-oxidation on the site of deployment and consequently on the camera lens, it was rendered opaque after 14 days, but it recorded a total of 18.5 min. Halfway through these 14 days of useable recorded footage, between day 8 and 9, the time lapse camera slid backwards, changing the viewing point and the surface monitored.

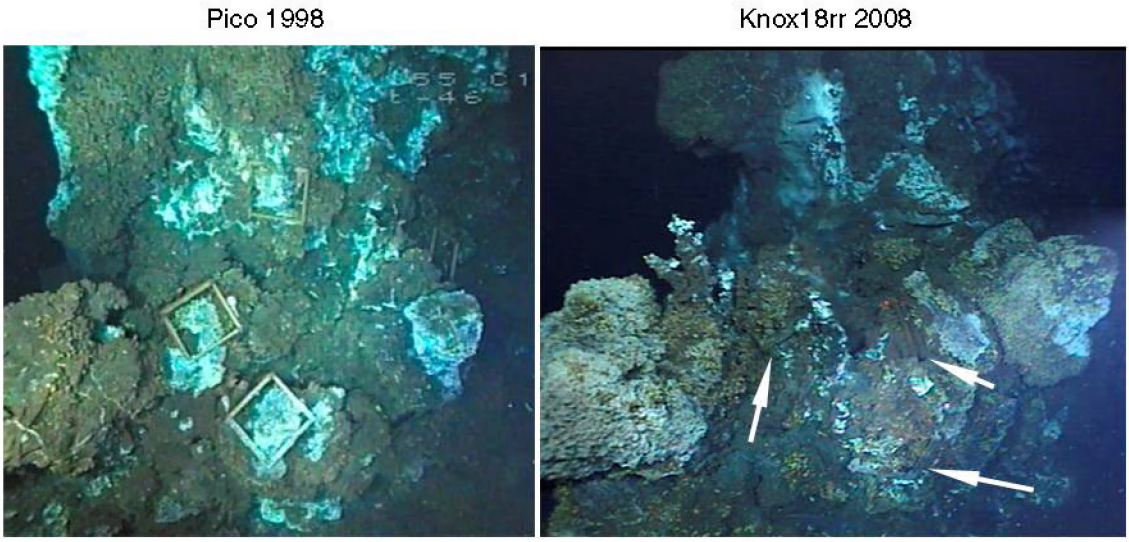

Fig. 5.11. Elisabeth as observed during 1998 and 2008. The arrows on the 2008 picture point to the frames visible on the 1998 picture, part of a sampling experiment in the same year, which were left there and are still visible 10 years later. They are overgrown with mytilids. Over this 10-year time interval there is an increase in microbial coverage noticeable as well as an increase or rather re-organisation/relocation of the mussel beds. A local increase in activity as can be observed on the images could lie at the base of these changing patterns.

In this short time window, no real movement (no distance covered) of the mussels was observed, although there was a hint of repositioning. The shrimps were more active, even though they tended to stay put on a certain mussel shell, only to dislodge or flee when a crab appeared. When standing still, *Chorocaris* individuals often stood upwards with their antennas up in the water and exposing their mouthparts to water- or fluid-flow. These mouthparts were moving as well, so they possibly were feeding on the microbial rich hydrothermal fluids. During the French cruises present in the Biocean database, Elisabeth was only biologically sampled in 1998.

3.4.7. Statue of Liberty (US1)

The Statue of Liberty structure was discovered and named during the first submersible cruise to Lucky Strike in 1993. It consisted of a large a 2 m wide active flange, inhabited with fauna in 1993 and 1994, containing mussels, new recruits and other life (Van Dover et al., 1996b; Langmuir et al., 1997; Comtet & Desbruyères, 1998) but with already some signs of senescence as its main chimney was inactive (Langmuir et al., 1997). By 1996, the structure was barely venting any fluids (Von Damm et al., 1998) and by 2008 there was hardly any fauna left (Fig. 5.12), possibly because the activity was waning or ceased. There was also the unique presence of a non-endemic sea-urchin, *Echinus alexandri* at Statue of Liberty in 1993 (Van Dover et al., 1996, Fig. 5.12) and a small population has been observed in 1997 (Desbruyères et al., 2006b). Later on, this species was never encountered again at the Lucky Strike hydrothermal vents. Its exact role in the assemblage and succession mosaics remains unclear. During the French cruises this site was only sampled in 1994.

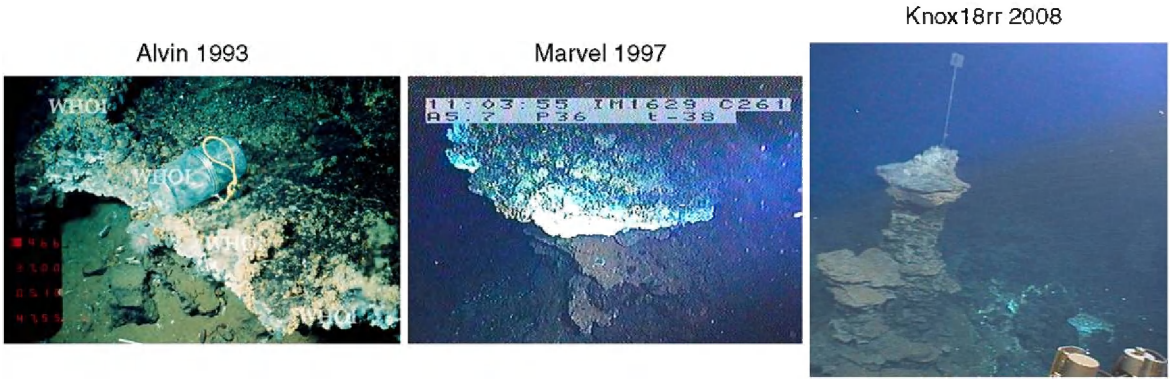

Fig. 5.12. Statue of Liberty flange, with the presence of the sea-urchin at the left and the changes it underwent over time, resulting in an inactive edifice with a small left-over of fauna in 2008.

4. Discussion

4.1. Limitations/Sampling Bias

Caution should be taken with the interpretation and extrapolation of these results, as these can be perilous if used to clarify generic tendencies. The fact that certain species are not present in the data matrix does not necessarily imply that they are absent. Due to the patchy nature of the fauna inhabiting the vent edifices, non-quantitative sampling (as almost inevitable when comparing (non-adjusted) sampling between the years) is difficult to call representative, especially concerning the smaller-sized animals. In addition, differences in sampling protocols and sieve sizes used can impact faunal compositions as determined in the lab and could give markedly different images of a community (Gauthier et al., 2010). Binominal presence/absence data tend to mask part of the problem as relative abundances are not taken into account.

The type of samples collected is also likely to have an influence on the species composition, as suction samples and manipulator grabs tend to collect different fauna. For example, large mussels are not sampled by the suction samples as these tend to clog the sampling device. On the other hand are smaller animals, such as small crustaceans, more effectively sampled with the slurpgun/suction sampler. Part of this is also countered with the use of presence/absence data. Often, both devices are used on the same sampling location to get a complementary picture. The total number of samples taken with each sampling device was available for each year and site, revealing no distinct trends; however, which specific sample was the result from which sampling device was unknown.

Characteristics inherent to certain species might also bias their sampling. For instance: visual observations describe the presence of numerous crabs and ophiuroids in the mussel beds (Desbruyères et al., 2001, D. Cuvelier, pers. obs.), while they are not always or not often present in the samples, due to their ability to escape. The different species of shrimps that are present within the vent field also have some peculiarities: *Mirocaris fortunata* is the most gregarious one and was consequently sampled every year at almost every site, *Chorocaris chacei* on the other hand was less sampled and is also less gregarious and abundant than *M. fortunata*. They usually occur in small groups of several (3-5) individuals, while *Alvinocaris markensis* is without a doubt the most solitary one. The latter can be found wandering around on the mussel beds. The year in which they were sampled (2005) they were surprisingly abundant on the sampling site in question, adding up to a total of ca. 5-7 individuals on a surface of about less than 1 square meter (m^2). Sessile species are much easier to sample quantitatively. Despite their ability to move, mussels and gastropod species or considered more "sessile" animals, in the way that they cannot escape when getting sampled,

contrarily to crabs, other crustaceans, ophiuroids, and most definitely fish. For these "less mobile" animals, it is of utmost importance not to underestimate the patchy nature of the hydrothermal edifices, for which the physico-chemical conditions change along the edifice walls, causing different assemblages to inhabit or colonise different localities with specific microhabitats. Many species (#17) were only sampled once or twice over all the years; so either they are rare species or our sampling devices and/or protocols are not adapted enough to sample this kind of species efficiently. Moreover, it is important to keep in mind that very few quantitative studies have been carried out in the Lucky Strike vent field.

The observed species richness is always an underestimation of the true species richness, as rare species require more sampling effort to be discovered than common species, unless we obtain a complete census (Gauthier et al., 2010). An illustration is given here as Eiffel Tower is the most species rich, but also the most sampled. The importance of a complete census becomes especially clear when the smaller faunal fraction (meiofauna) is taken into account (Sarrazin et al., 2006; Zekeley et al., 2006; Copley et al., 2007b) and many unknown species are encountered. For instance, the two copepod species only present in 1994 (*Aphotopontius atlanteus* and *Stygiopontius rimivagus*) were also abundantly encountered in the 2006 samples, when emphasis was put on analysing meiofauna (J. Sarrazin, pers. comm.) though these species were not yet present in the database. This smaller compartment of the fauna has received less attention (Copley et al., 2007b), thus significantly biasing the estimations of diversity (Gauthier et al., 2010).

4.2. Differences in faunal composition between edifices

For the most species there are no significant effects of time or locality demonstrable, with the exception of *Lirapex costellata* which is influenced significantly by the locality (it only occurs at Eiffel Tower and Bairro Alto) and *Protolira valvatoides*, which showed a significant influence of time (it increased in presence on various sites with time). Over the years, there is a rather strict species pool which is almost always present at all sites. The exact number of species present might shift, although there is an association of 4 species that are always and everywhere present (exception is Y3 edifice, which is also one of the least sampled edifices), combined with 10 other species that are nearly always present. This group consists off *Bathymodiolus azoricus*, *Branchipolynoe seepensis*, *Amathys lutzi* and *Mirocaris fortunata* which are most often joined by *Chorocaris chacei*, *Branchinotogluma mesatlantica*, *Lepidonotopodium jouinae*, *Lirapex costellata*, *Pseudorimula midatlantica*, *Lepetodrilus atlanticus, Shinkailepas briandi*, *Protolira valvatoides*, *P. thorvaldssoni* and *Sericosura heteroscela*. Several of the latter species were absent for single years, but nevertheless they are a significant part of the consistent species pool. These

single absences can be a result of sampling, rather than a significant scarcity or absence, as for example very few gastropod species have been sampled in 2005, while for all the other years they are abundantly present. At a first view, several species might appear more characteristic for certain vent sites, and might even appear to have a more persistent presence over the years, however these observations rarely suffice to allow a real and significant distinction.

At the EPR, the species pool present is clearly different, and appears to be equally constituted out of larvae of *Tevnia*, *Riftia* and *B. thermophilus*, due to close proximity of adult mega-faunal populations, featuring the previous species (Shank et al., 1998a). The order in which they colonise or dominate the vents, however, is different for each species. These patterns became clear as a result of one of the first opportunities to study nascent vent development (Shank et al., 1998a). However, at the MAR, such nascent vent development studies are completely lacking. In addition are the distances between hydrothermal vent fields, and thus adjacent vent populations, much larger.

Arguably, comparing the similarity of edifices or sampling year could be regarded as comparing similarity of samples taken, however we are convinced that the lack of distinct trends is not just a mere sampling artefact. Especially as the years that pooled apart showed, what looks to be, different sampling regimes (as visual observations do not comply with the sampling carried out), e.g. no mussels sampled and presence of several gastropod species, while sites that were distinctly different pooled apart as well, but for different reasons: no mussels present and presence of shrimp species. Consequently, the repeatedly visited sites that cluster in one big group do show comparable sampling and do show similarities, or rather do not show differences between year and locality. Similar findings were done at the Juan de Fuca Ridge, where vent sites investigated between 1988 and 1994 did not cluster by year, nor by geographic locality (Tsurumi & Tunnicliffe, 2001). Local habitat-scale features, such as sulfide supply, food availability, and competition are thought to be determinant in species composition (Tsurumi & Tunnicliffe, 2001). Within the Lucky Strike vent field, there are two sources of hydrothermal fluids, separating the north-western and north-eastern vents (White Castle, Helene, Bairro Alto, Elisabeth, Y3, Statue of Liberty and Sintra) from those in the south-east (i.e. Isabel, Eiffel Tower and Montsegur, Fig. 5.2) (Langmuir et al., 1997; Von Damm et al, 1998; Charlou et al., 2000; Humphris et al., 2002). There are significant differences in chlorinity-values and other chemical parameters (among others K and Ca) in the end-member fluids (Von Damm et al., 1998; Charlou et al., 2000). Despite the marked differences in the composition of the ejected vent fluid, these do not appear to impact faunal compositions as present in Biocean. There are no distinctions noticeable between the occurrence of a certain species and its location at the sites around the lava lake. If a certain species was

limited to few edifices, often these turned out to be situated on the opposite ends of the lava lake (e.g. *Lirapex costellata* on Eiffel Tower and Bairro Alto; *Paralepetopsis ferrugivora* on Sintra and Eiffel Tower, etc.), thus surpassing the regions tapping out of a different fluid source or ejecting a differently altered and composed vent fluid. This is confirmed by measuring the beta-diversity. The concentrations of physico-chemical variables, that tend to cause the distinction between the various regions at Lucky Strike, appear not to be determinant for faunal occurrences. In other words, based on the data of the Biocean database of the fauna sampled, there are no indicator species to characterise the different fluid sources at Lucky Strike.

However, temperature differences between the various sites of Lucky Strike have been recorded and tend to fluctuate over time (Langmuir et al., 1997; Von Damm et al., 1998; Sarradin et al., 1999; Charlou et al., 2000). Differences in temperature may account for small chemical differences between vents that do share a same fluid source (Von Damm et al., 1998), which may impact local species composition and emphasise the importance of local habitat-scale features as proposed by Tsurumi & Tunnicliffe (2001). Likely to be important for species presence/absence and distribution are the various and type of activity features an edifice hosts and the temperature regimes associated with it, as for example black smokers reach a much higher temperature (up to 324°C) than flanges (<200°C) and diffusion zones (~60°C) (Langmuir et al., 1997; Sarradin et al., 1999; Charlou et al., 2000). It has already been suggested that tolerance to temperature and sulfide are most important in shaping vent communities and impact occurrences and distribution of vent organisms (Tunnicliffe & Juniper, 1990; Copley et al., 1997; Desbruyères et al., 2000; Sarrazin et al., 1999; 2006; Henry et al., 2008). Furthermore is the availability and suitability of substrata and habitat a prime determinant of presence/absence of vent organisms (Copley et al. 1997; Comtet & Desbruyères, 1998; Cuvelier et al., 2009).

The edifices in the northern part of the hydrothermal field are older in age and may have been allowed more time to grow because they are set above the level of recent lava flows (Ondréas et al., 2009), explaining the existence of quite some large edifices such as Elisabeth, Bairro Alto and Sintra. The southern vent edifices are younger (Ondréas et al., 2009) and would thus have had less time to grow. Despite this finding, some of the tallest venting structures within Lucky Strike i.e. Y3 and Eiffel Tower (>10 m) are found in the south-eastern sector and attain similar or larger sizes than those in the northern sector. Edifices in the south-western venting area appear very recent, postdating the emplacement and faulting of the most recent lava (Ondréas et al., 2009) and are effectively smaller in size than the other hydrothermal edifices. However, this does not mean that hydrothermal venting itself is more recent in the southern part of the Lucky Strike field because pre-existing sulfide deposits there may have been buried by recent volcanic deposits (Ondréas et al., 2009). Concerning the

presence of assemblages delineated by Cuvelier et al. (2009) and the zonation presented therein, Elisabeth and maybe even Bairro Alto, appear visibly similar to Eiffel Tower. Conversely, Sintra, Helene, Nuno and to a lesser extent Isabel are dominated by small mytilids and new recruits. The larger-sized mussels, if present, inhabit localities immediately surrounding fluid exits. These features persist over time. The high proportion of small individuals at certain of these sites were corroborated by length-frequency measures as published by Van Dover et al. (1996b) which described that Eiffel Tower was dominated by a larger size classes of mussels (>50 mm) while samples of Statue of Liberty and Sintra were dominated by small (< 5 mm) to medium sized individuals (between 10 and 30 mm). Subsequently, Comtet & Desbruyères (1998) reported >50% of the Mytilidae sampled at Bairro Alto, Isabel and Sintra had a length of ca. 4.5 mm, while at Eiffel Tower this proportion was about~40%. These patterns thus surpass the regions with different fluid sources (Von Damm et al, 1998; Charlou et al., 2000; Humphris et al., 2002) and the proposed age differences between the sectors (Ondréas et al., 2009). On the other hand, Trask & Van Dover (1999) and Colaço et al. (2002) observed large differences in mean carbon and nitrogen isotopic compositions, and consequently in nutritional response to environmental variations, of the mussels which did correspond with the two different fluid sources as determined by Von Damm et al. (1998) and Charlou et al. (2000). Based on the differences in mussel sizes, it could be that the sites situated in the north-eastern and south-western sector are more exposed to the supply of new mytilid recruits. This supply is likely to be influenced by currents, which are located steady towards the south-east with very energetic semi-diurnal tidal oscillations in the southwest–northeast direction over time (Khripounoff et al., 2008). Due to their location and surrounding topography, Eiffel Tower and Elisabeth might be less exposed to such recruiting events, explaining the overall larger-sized mussels. In addition, the edifices should host the necessary activity to sustain their mytilid populations and sizes.

The absence of an entire suite of species on mussel-less sites, do point out the importance of mussel beds as a secondary surface for many gastropod and polychaete species. Using the data from Chapter 4, the size of the mytilids and taxonomic richness are shown to be negatively related one to another (R^2=0.67). The size that the mussels in the mussel beds attain might be important for the relative abundance of the associated species, but with the unevenly distributed sampling effort, it was impossible to thoroughly test this hypothesis.

The Y3 edifice can be considered different from the other Lucky Strike edifices as its main edifice is not inhabited by mussels, and concerning its appearance it is somewhat inclined to the aspect of the deeper hydrothermal vents along the MAR (e.g. Broken Spur) as *Rimicaris* shrimps were (are?) found at the most active part of the edifice, which is the summit, while small low-density mussel clumps can

be found at the base (Desbruyères et al., 2001). The presence of *Rimicaris* at Y3 was confirmed by Van Dover et al. (1996b), Shank et al. (1998b) and Desbruyères et al. (2001). As described by Copley et al. (1997), these species need abundantly hydrothermally bathed substrata to occupy. Such substrata could be too soft or porous (with hydrothermal fluid seeping through) for sessile organisms to colonise or settle. Contrastingly to the deeper vent fields, no dense swarms of shrimp occur at Lucky Strike. Alternatively, Desbruyères et al. (2001) hypothesised that the presence of dense mussel beds on the chimney walls at Lucky Strike vents, next to altering the microenvironment (Johnson et al., 1994), also screen the sulfide wall, and consequently preclude the development of *R. exoculata* swarms.

The shifting focus over time, going from sampling multiple vent sites to only one (=Eiffel Tower) coincides with and is likely to be enhanced in the future by the code of conduct and preliminary delineation of marine reserves at hydrothermal vents. So is Elisabeth, for example, currently part of a proposed no-take area, in which the natural state of the environment (natural condition) will be respected, as a step to creating marine reserves at hydrothermal vents (Santos et al., 2003). In the same report, both Sintra and Eiffel Tower are proposed as restricted access zones, where sampling will be regulated. At the other vent sites, the international code of conduct (Devey et al., 2007) is expected to be respected. Lucky Strike is currently being included on the OSPAR network of MPAs in 2007 and was accepted by the EC as a Site of Community Importance [SCI] under the Natura 2000 network in 2009.

5. Conclusion and future perspectives

No significant influences of locality or year are revealed for the majority of species with the data from the Biocean database. Despite the presence of two different fluid sources at the Lucky Strike vent field, no significant or recurrent differences in species composition were identified. Rather it is thought that local habitat-scale characteristics, such as e.g. type of activity features and associated temperature, suitable habitat for settlement/attachment and access to sulfide and hydrothermal fluids influence the distribution of species. However, there is a lack of quantitative studies including sample replicates to allow thorough validation of this hypothesis.

When mytilids are absent, an entire suite of species is absent as well, thus emphasising the importance of the mussels in offering secondary surfaces and altering local environment for associated organisms. Though our data did not allow testing of this hypothesis, it could be likely that the size of the mytilids inhabiting the edifices affects the abundance of the associated species. Sampling comportment of the scientists points to the concentration of effort and attention to one single edifice with time, being Eiffel Tower, resulting in an uneven distribution of sampling effort. As at this point it is impossible to

compare the different edifices concerning their diversity, therefore it would be very useful to quantitatively sample the various edifices within the Lucky Strike vent field using similar sampling protocols. Sampling protocols also should be adjusted one to another between different years, to allow comparisons over the years. Even then, we must be cautious not to underestimate the patchy nature of the hydrothermal edifices. Therefore combining both imagery, to asses local conditions and visible (dis)similarities, in addition to considered discrete sampling would be an ideal combination.

Acknowledgments

Many thanks to Marie-Claire Fabri for querying the data used, and without whose help, this chapter would have been impossible to write. Thanks to Olivier Gauthier for helping out with the triangle plots and for the idea of using them.

APPENDIX 1 - CHAPTER 5

The observed frequencies of presence and absence of the individual species as evaluated per site sampled and per year. An increasing frequency meant a higher number of samples present for the year or site in question.

MOLLUSCA

Site

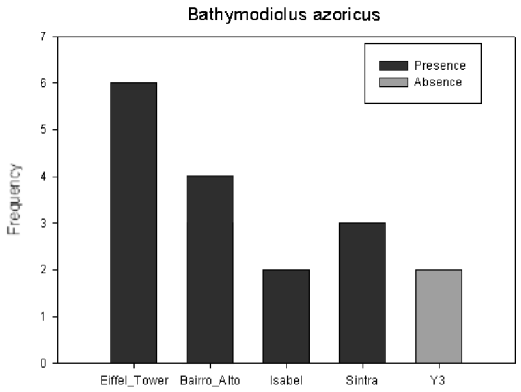

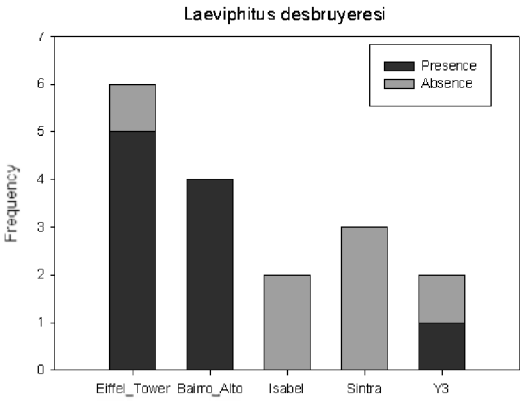

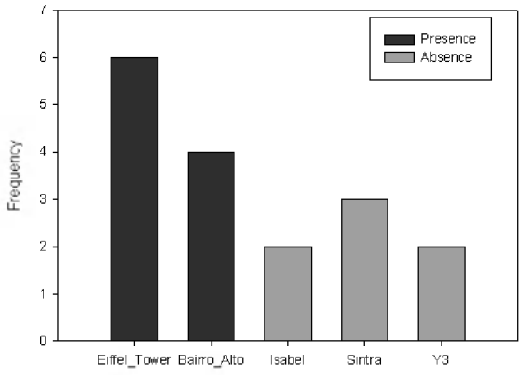

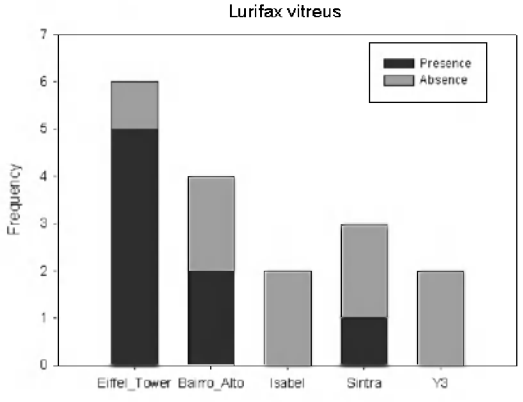

Year

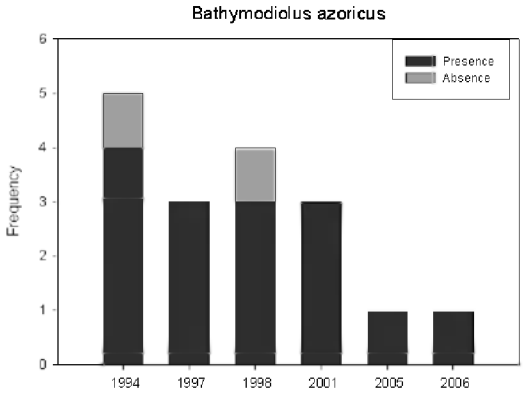

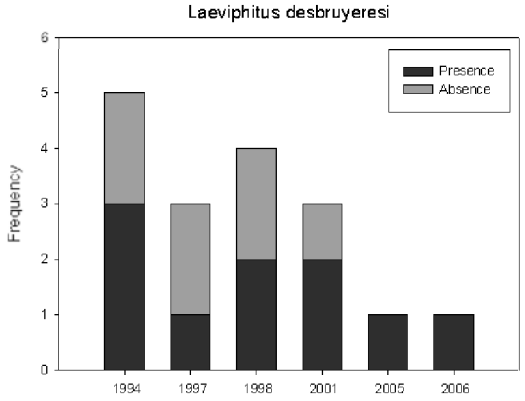

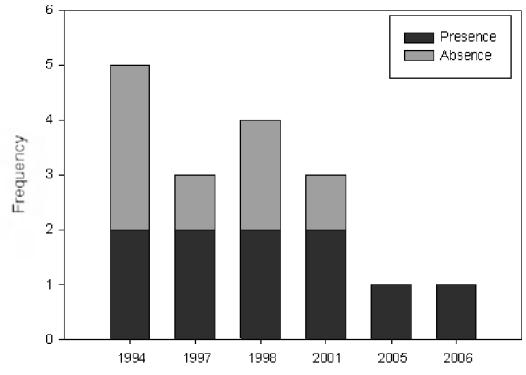

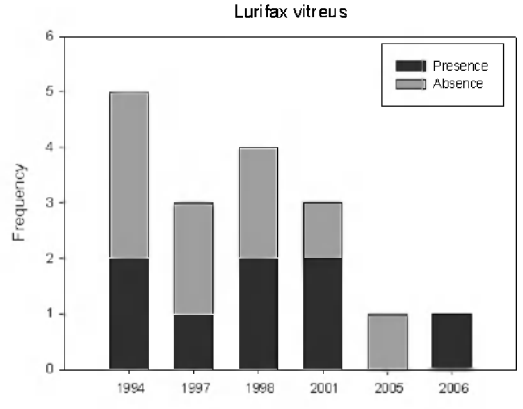

MOLLUSCA

Site

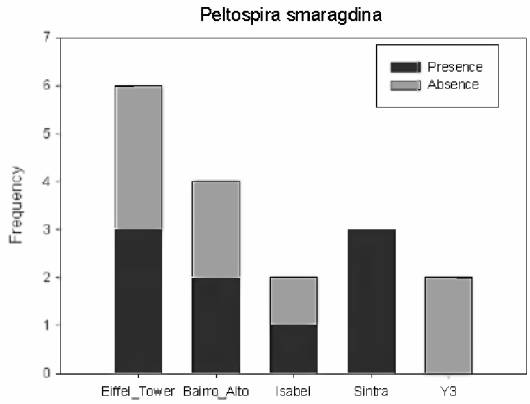

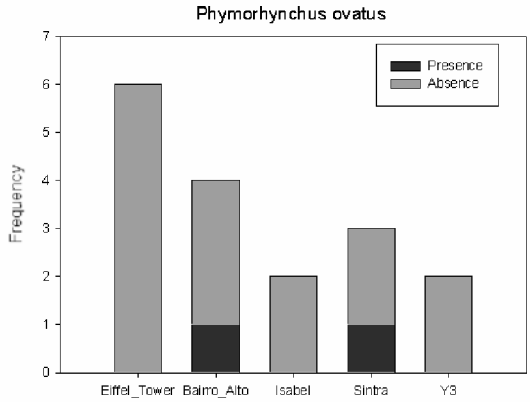

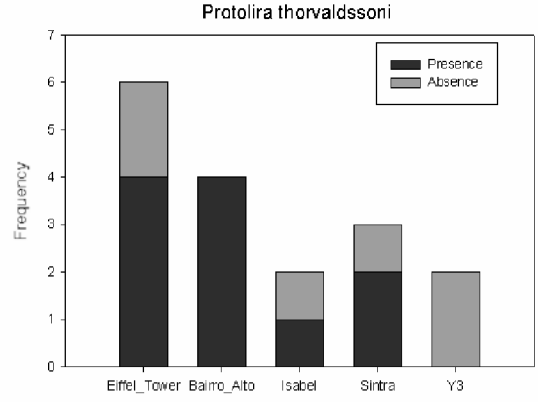

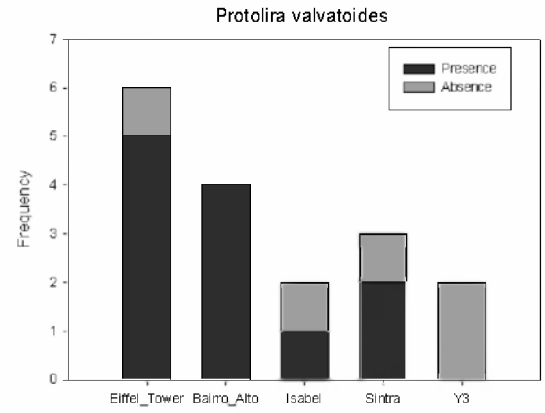

Year

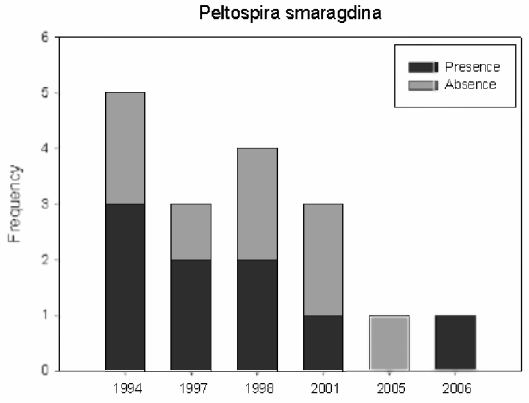

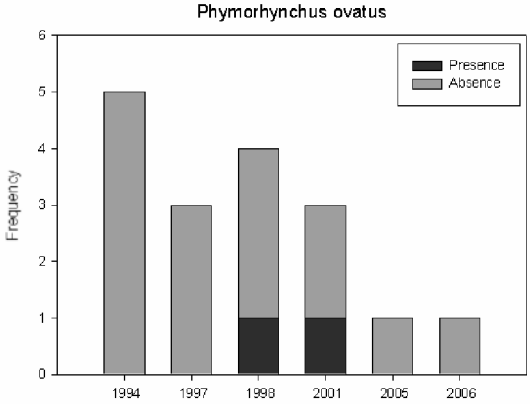

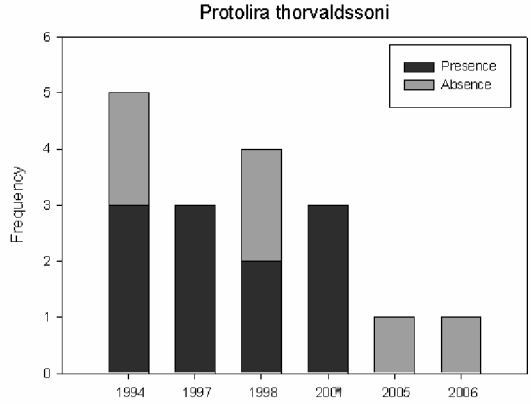

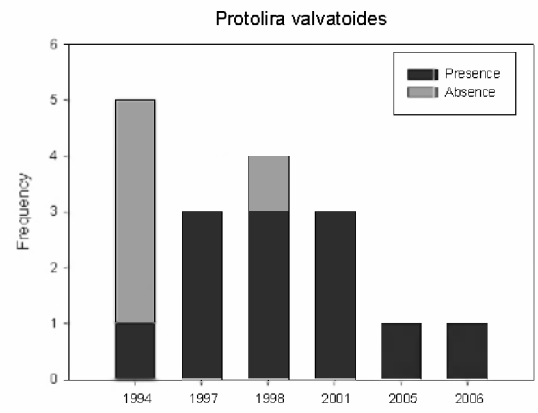

MOLLUSCA

Site

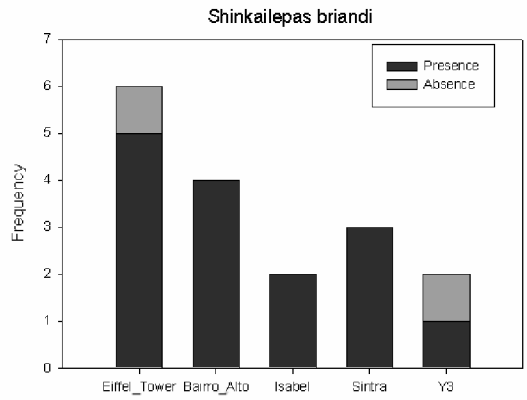

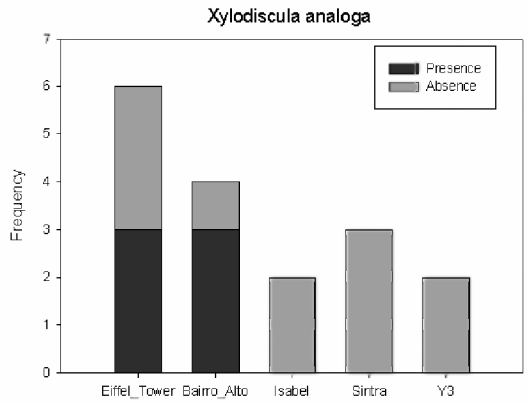

Year

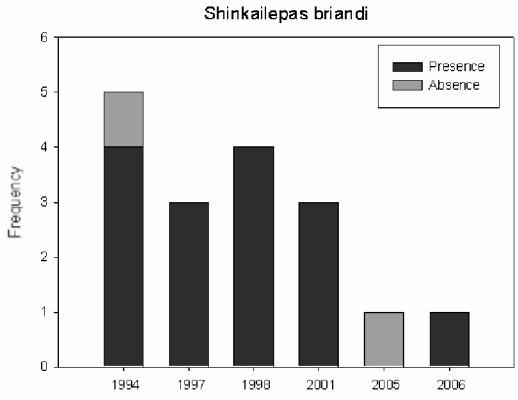

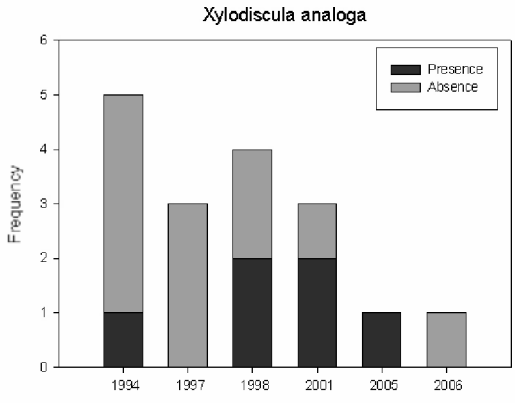

MOLLUSCA (limpets)

Site

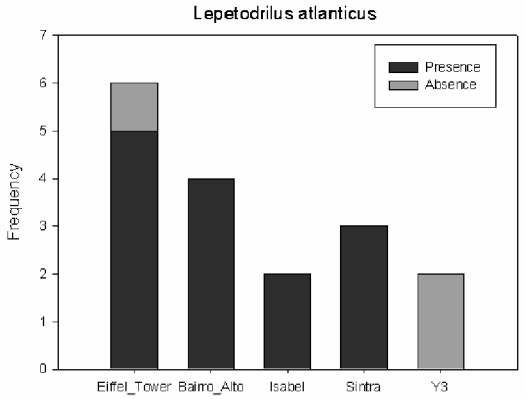

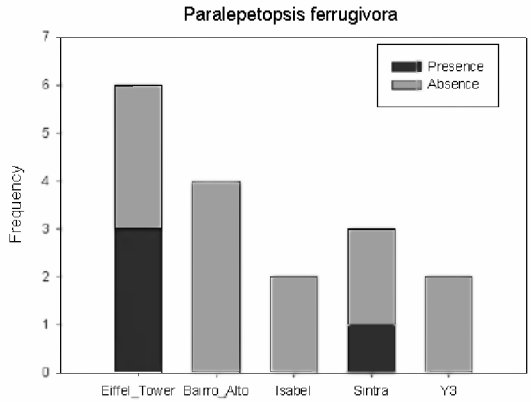

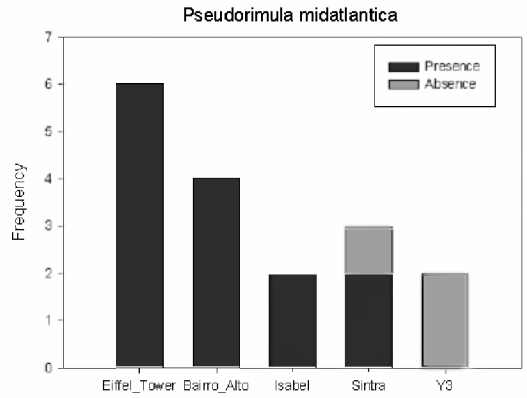

Year

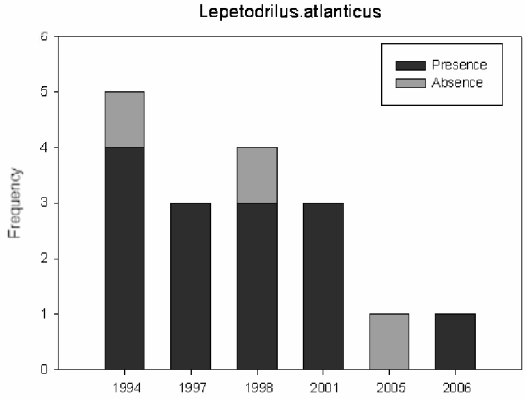

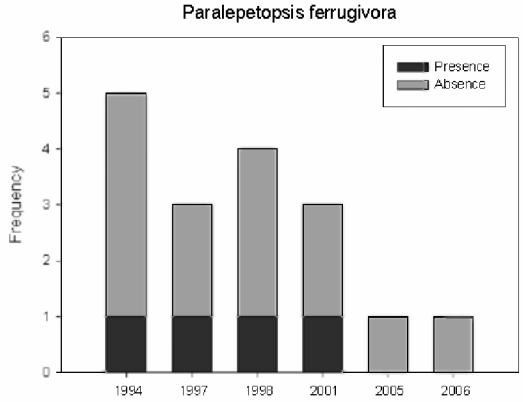

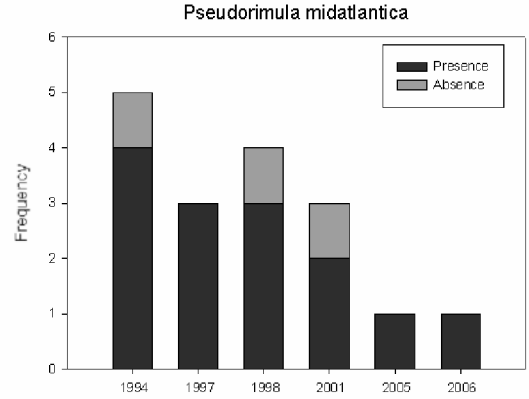

POLYCHAETA

Site

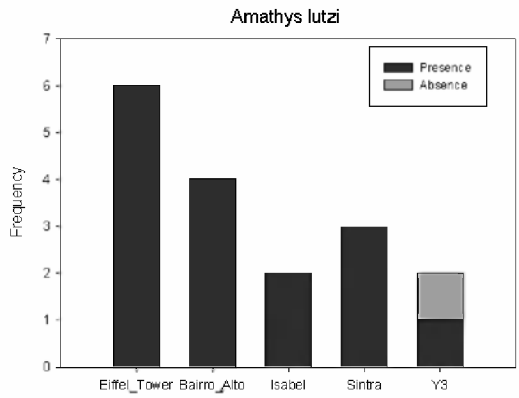

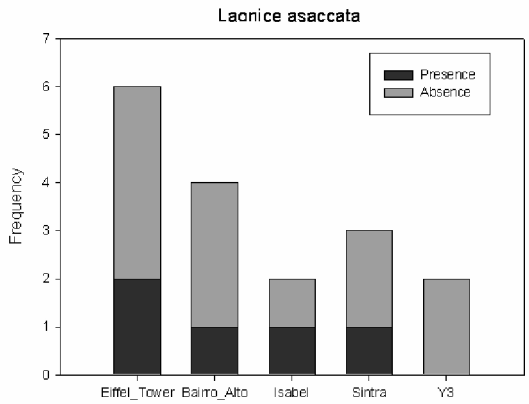

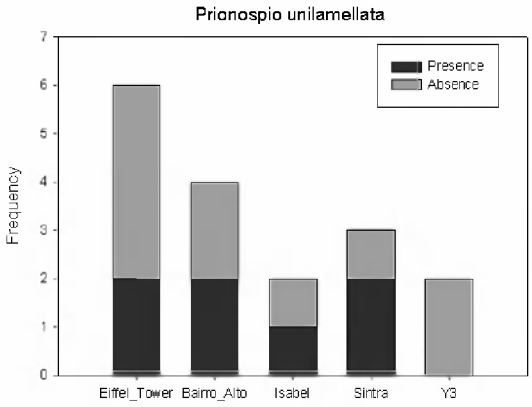

Year

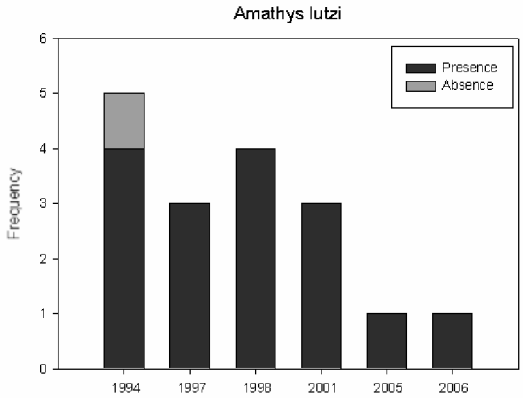

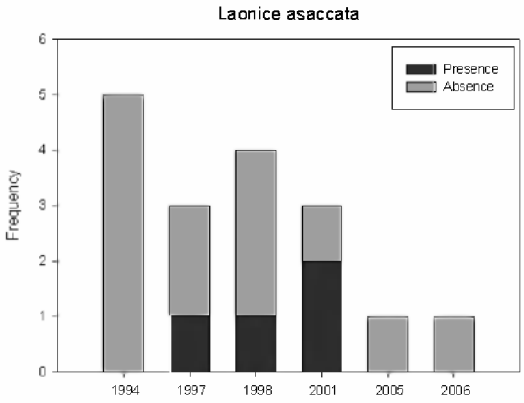

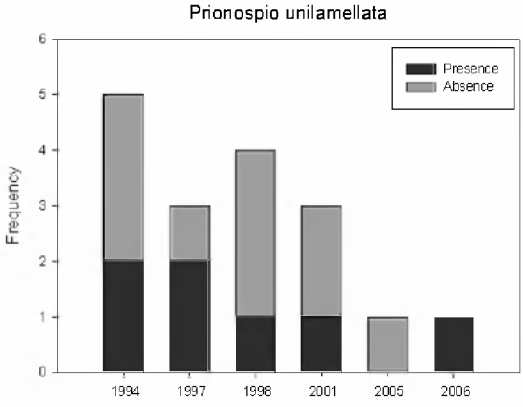

POLYCHAETA (Polynoidae)

Site

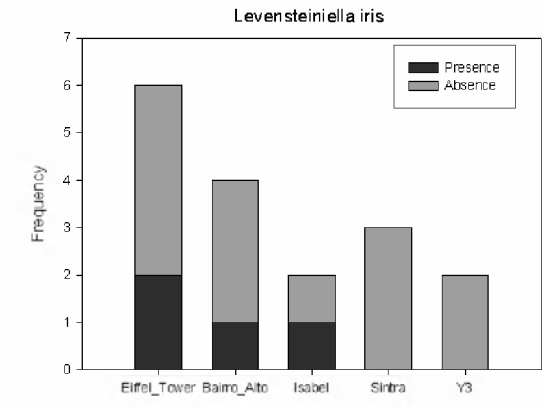

Year

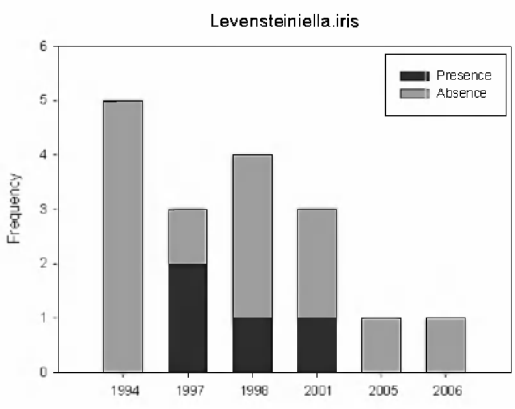

POLYCHAETA (Polynoidae)

Site

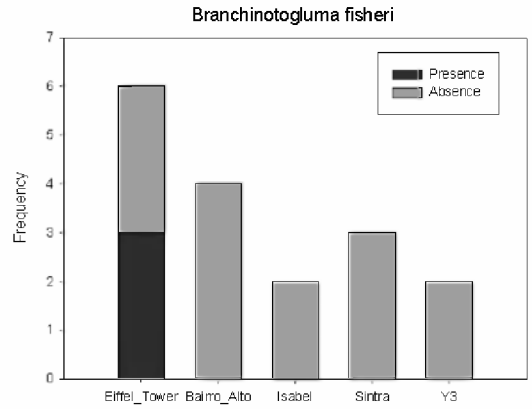

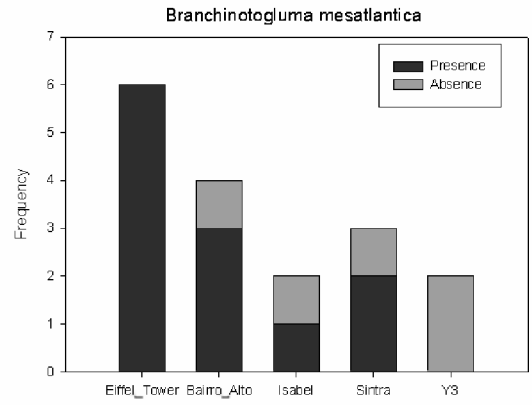

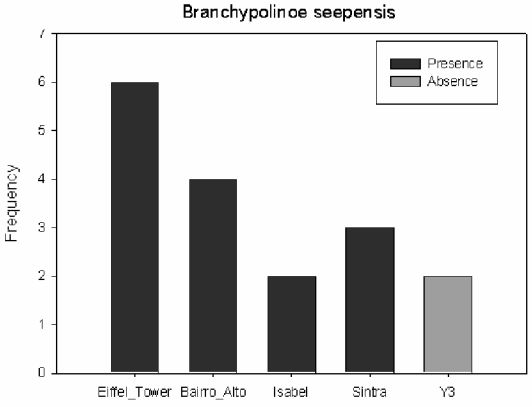

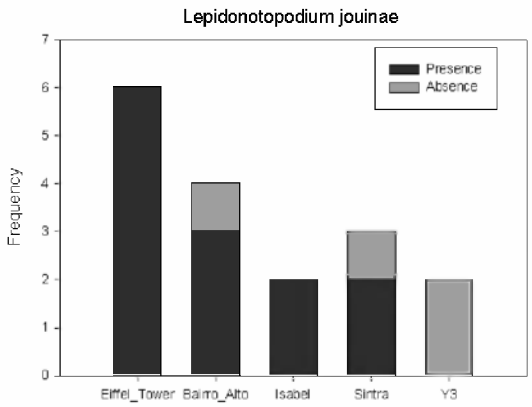

Year

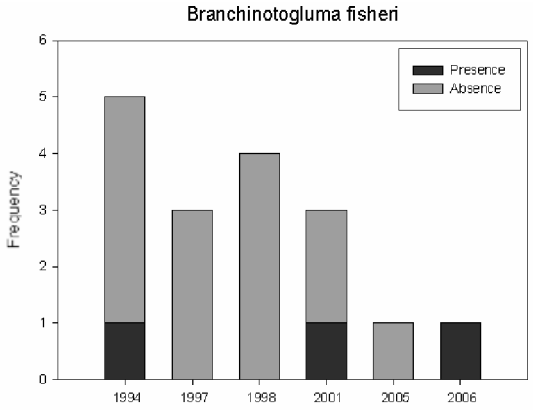

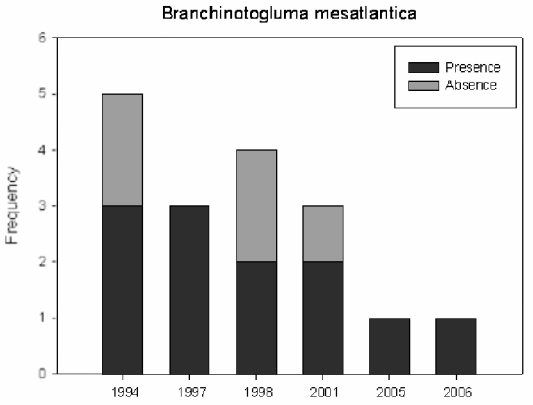

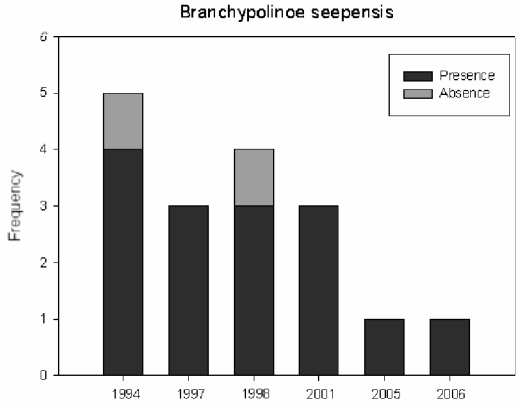

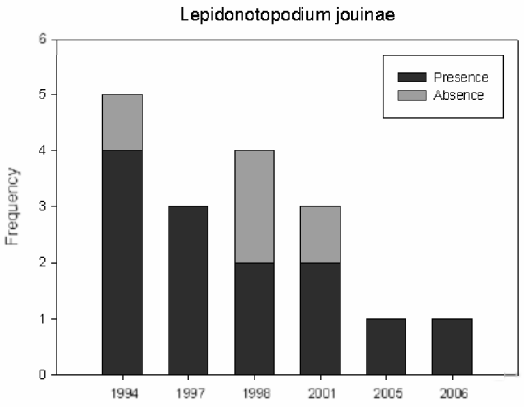

ARTHROPODA (Alvinocarididae)

Site

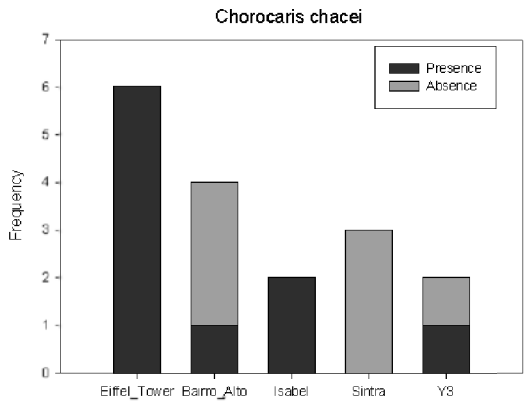

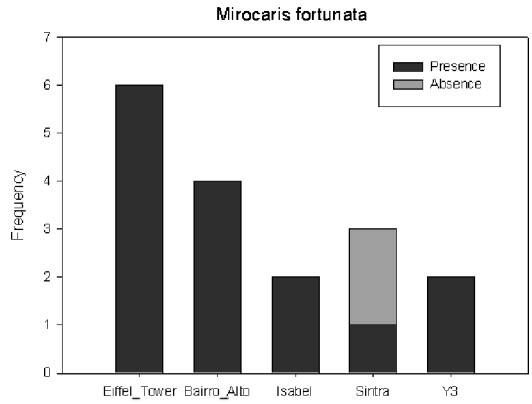

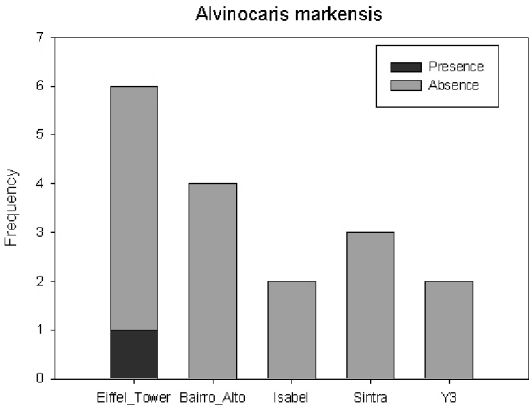

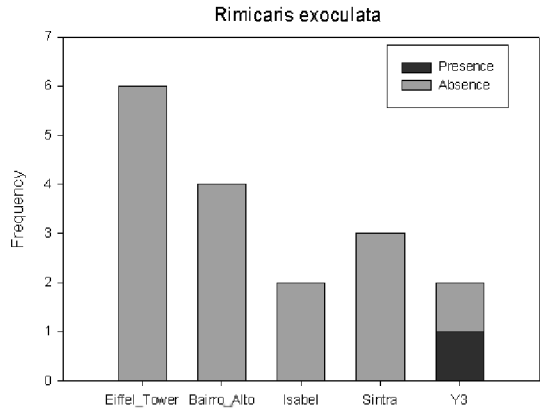

Year

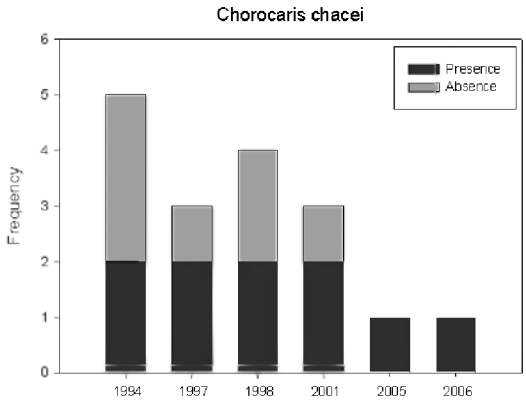

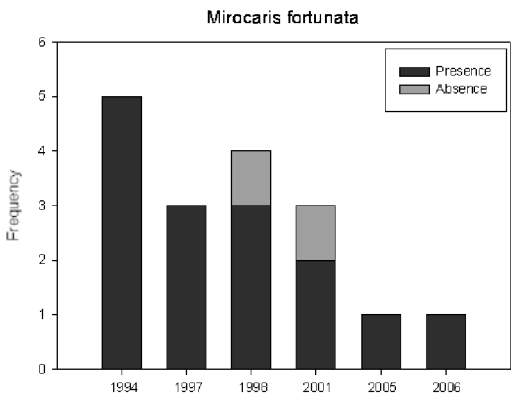

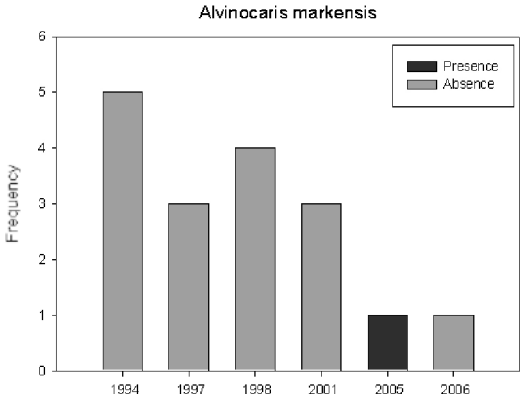

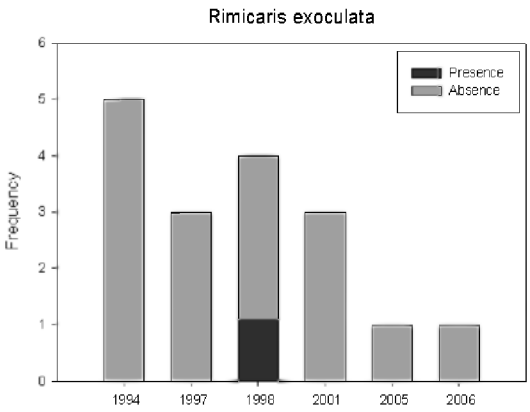

ARTHROPODA

Site

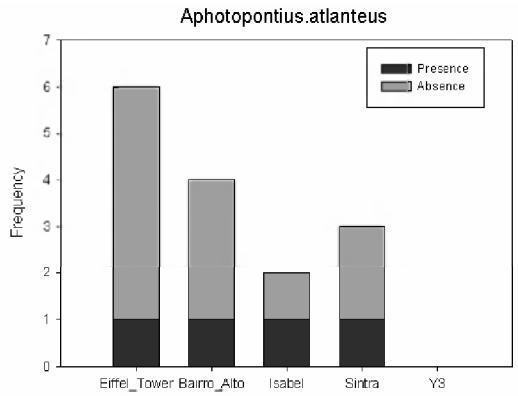

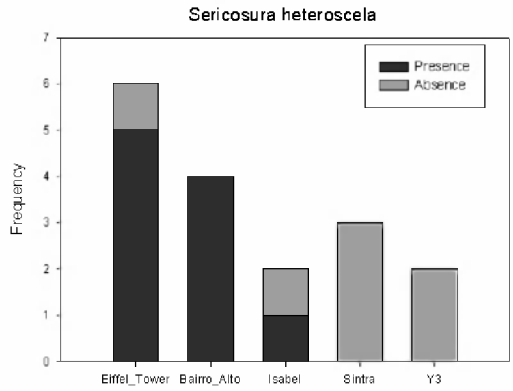

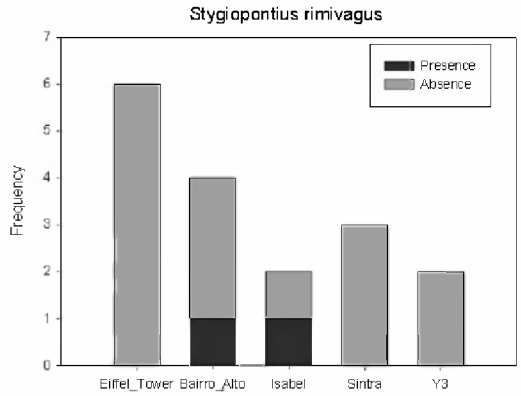

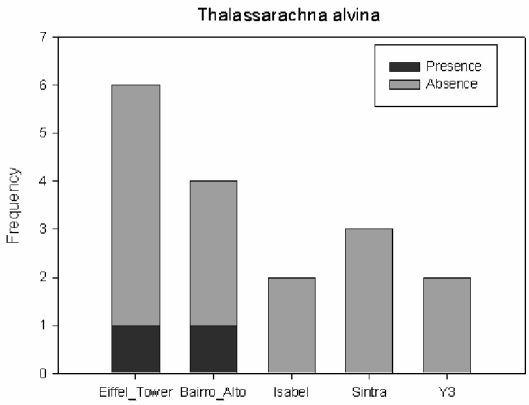

Year

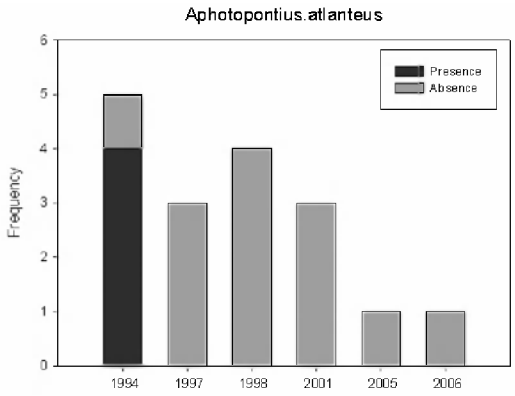

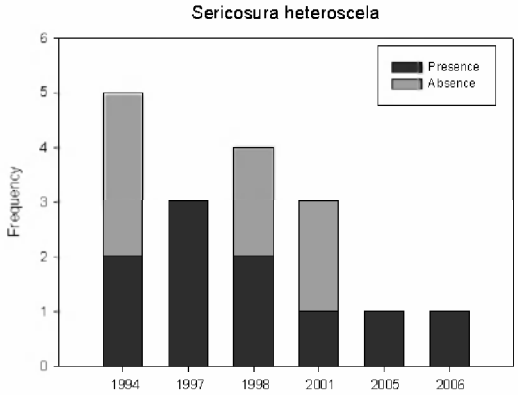

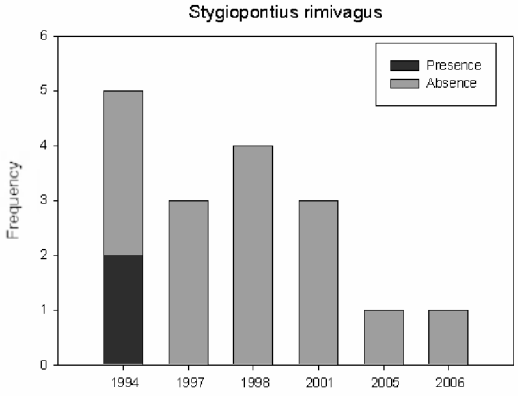

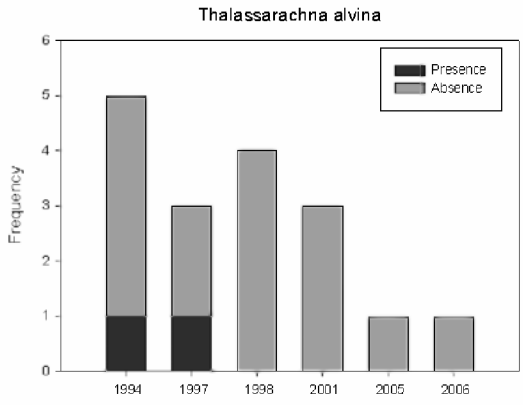

ARTHROPODA

Site

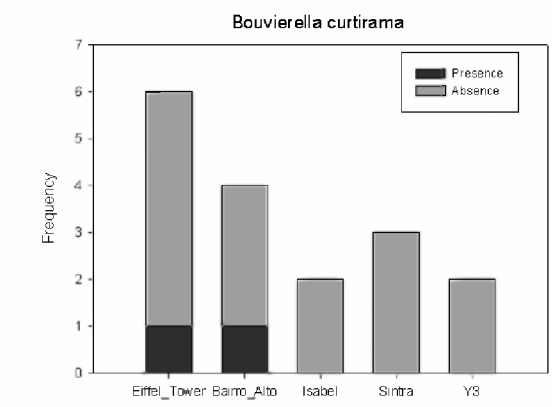

Year

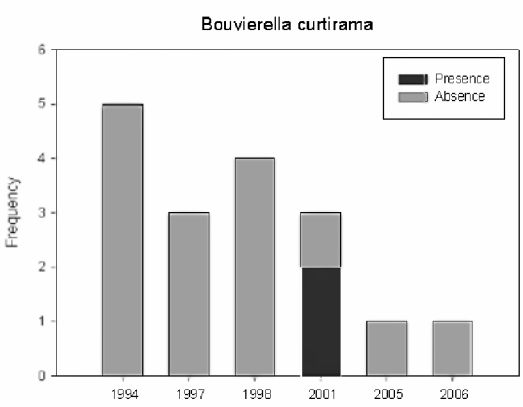

ECHINODERMATA (Ophiuroidae)

Site

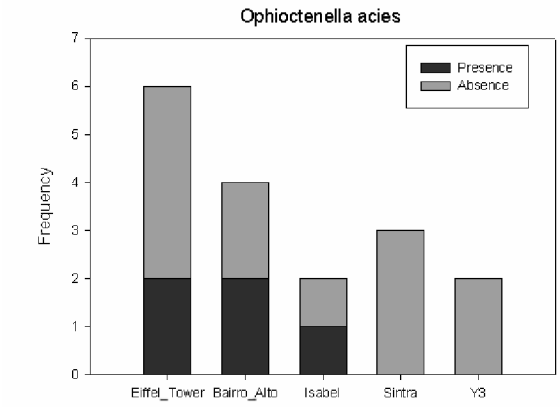

Year

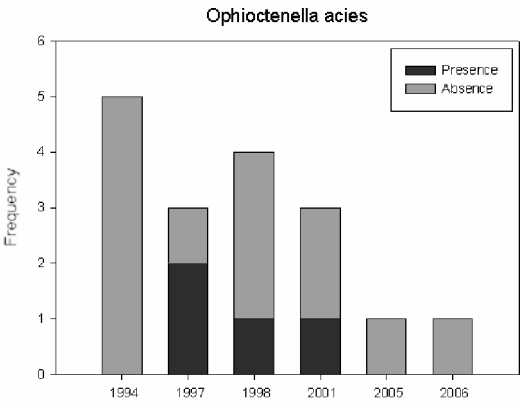

Chapter 6

Synthesis

CHAPTER 6
Synthesis

Since the discovery of hydrothermal vents in the late 1970s (Lonsdale, 1977), research on these remarkable ecosystems evolved at a quick pace. Although our knowledge of the communities inhabiting these environments has greatly improved, their long-term ecological dynamics remain unclear. Ecological time-series studies are indispensable to comprehend the functioning of an ecosystem. At hydrothermal vents, various temporal variations studies exist, mainly in the Pacific Ocean on the East Pacific Rise (EPR) and in the northern East Pacific (NEP) (Hessler et al., 1985, 1988; Fustec et al., 1987; Sarrazin et al., 1997; Tunnicliffe et al., 1997; Desbruyères, 1998; Shank et al., 1998; Tsurumi & Tunnicliffe, 2001; Shank et al., 2003; Marcus et al., 2009). Prior to this dissertation, time-series studies along the Mid-Atlantic Ridge (MAR) were limited to only a single decadal-scale study (Copley et al., 2007a). Imagery analyses play an important role in all vent temporal studies. Independent of their location, these studies can be divided in two groups: those that started after an eruption (T_0 or nascence of hydrothermal vent sites) and those under continuous venting conditions. This PhD study falls in the continuous venting category and the main objective was to describe the temporal variation of the communities living at the Lucky Strike vent field, and more specifically at the Eiffel Tower hydrothermal edifice.

The first steps in developing a methodology to assess variations in community dynamics was outlined and used to describe spatial variation, distribution and zonation of the faunal assemblages and substrata occurring at Eiffel Tower (Chapter 2). This methodology was then applied on video imagery for all the years available and an additional protocol was developed to allow comparison between the years (Chapter 3). Decadal change (14 years) and shorter time-scale (1 to 4 years) alterations were studied and described.

Visibly different faunal assemblages and substrata were identified on the Eiffel Tower edifice, based on imagery. Four of them were mussel-based assemblages that differed in size and surface coverage, completed by a shrimp assemblage. Discrete faunal sampling showed there were factual differences in species composition between these visibly different assemblages (Chapter 4). The identified assemblages and substrata showed a well-defined zonation pattern according to their adaptability and tolerance towards high temperature fluid exits (Chapter 2). In this zonation model, shrimps were found closest to the fluid exits, followed by the larger-sized mussels. A decrease in mussel-size and

surface coverage (mussel-beds to mussel-clumps to small discarded mussels on prevailing bare substrata) with increasing distance from the vent emission was observed. The spatial segregation of mussel sizes at Eiffel Tower and Lucky Strike (Comtet & Desbruyères, 1998; Sarradin et al., 1999) was thus reconfirmed, based on imagery. All faunal assemblages were able to approach lower temperature fluid exits (flanges and diffusion zones) more than the hotter black smokers. Next to these small-scale spatial variation patterns, a larger edifice-scale discrepancy was revealed. Different sides of the edifice showed different colonisation patterns and different assemblage/substratum proportions and surface coverage. Sides with a higher degree of activity (i.e. a higher number of fluid exits) were more similar, as were the sides with a lower degree of activity. This discrepancy between the different sides of the Eiffel Tower edifice continued over time (Chapter 3), as the different years analysed did not cluster together. Rather, similarity clustering occurred following the orientation of the edifice, emphasising the importance of factors inherent to this orientation. The South and East sides were always the most active, independent of the year they were sampled and the West and North sides were less active. These differences in hydrothermal activity coincide with a higher degree of colonisation (all faunal assemblages with faunal coverage >50%) for lower activity and vice versa. Despite the similarities between the sides over the years, the individual assemblages and substrata do change between the years. Overall, there is a significant difference in microbial cover among the years compared, but no significant difference was observed between the overall mussel coverage. The overall degree of colonisation remained constant between the years investigated, at about ~50%, which could imply that the Eiffel Tower edifice reached its carrying capacity.

When analysing the recurrent community dynamics, the most common transitions between the various assemblages are highlighted. For each assemblage and substrata, a large percentage of assemblage points (~43% of grid-points from a grid-overlay) remained unchanged between the time-intervals. Nonetheless, most of the grid-points (57%) did change and distinct trends were revealed. Main patterns observed are settlement and colonisation (bare substrata get colonised by fauna), migration or movement (medium and larger-sized mussels and shrimps invade bare substrata), growth (mussels grow and multiply), gain of microbial cover and mortality (animals are subsequently absent at certain locations and dead mussels can be found at the base of the edifice). There were two different cycles in community succession noticeable and discernable, with little overlap between the two. This suggests the existence of two different micro-environments, each with a proper directional and predictable succession. From this angle, the larger-sized mussels and shrimps (Assemblages 1 and 3, supplemented with Substratum 2) constituted one group, which was found close to the fluid exits (Cuvelier et al., 2009), while the other faunal assemblages with the smaller-sized mussels (2a, 2b, 4a

and 4b, supplemented with Substrata 1a and 1b) was found further away from the fluid exits which was likely to correspond to a less harsh environment. This pattern implied migration of the mussels when they attain a certain size, as there was no continuity in mussel-sizes at a large majority of locations and the larger-sized mussels were found more closely to fluid exits. The spatial segregation in mussel sizes was thus maintained over the years. Several transitions proposed in the succession model were confirmed in Chapter 4, e.g. the transition from Assemblage 4a to 2a over time, was clearly corroborated as their species compositions were very similar, only the mytilids grow.

The previously hypothesised existence of two microhabitats corresponding to the assemblages living close to the fluid exits and those living further away was tested (Chapter 4). Physico-chemical sampling confirmed some differences in the characterisation of the different assemblages. These two hypothesised microhabitats correspond to a variable and a less variable environment, as temperature fluctuations (T°C) spanned a broader range in Assemblages 1 and 3 than in the others (Assemblage 2a, 2b, 4a and 4b). Assemblage similarity (species composition and abundance) showed species that cross the borders delineated by the microhabitats. As a result of this, Assemblages 1, 2b and 3 were considered more similar as are Assemblages 2a and 4a. The presence of two distinguishable temperature-niches, separating the mussel-based assemblages from the shrimp assemblage would be the main driving factor. Mussels thrive in the "colder" regions, while shrimps prefer the "warmer" localities. However, an overlap in temperature range between the larger-sized mussels (that also occupy a broader temperature range than any of the other mussel assemblages) and the shrimps was observed. Despite the existence of one global temperature niche for the mussels, the individual mussel-based assemblages showed different amounts of overlap. In accordance with other studies at hydrothermal vents, temperature is thought to be a more limiting factor in species distribution (Sarrazin et al., 2006; Henry et al., 2008; Podowski et al., 2009).

It is important to keep in mind that what we measure in the vicinity of the fauna results from what is supplied by the fluids and what disappears through precipitation and organism consumption. Hydrothermal vent animals such as mussels modify the local environment. Larger mussels (Assemblage 1) appear to consume more $\sum S$ than smaller-sized individuals. A higher $\sum S$ consumption can also be postulated for the mussel clumps (Assemblage 2) that have a microbial cover on their shells. However, there is a seemingly opposite impact of the microbial mats on the local chemistry noticeable in the even smaller-sized mytilids of Assemblage 4, making the influence of the microbial mats difficult to assess or extrapolate.

The importance of mussels as a secondary surface, offering suitable surfaces for settlement and shelter for associated species was confirmed by the higher taxonomic richness in the mussel-based assemblages. The size of the mussels showed a negative correlation with taxonomic diversity, although the mussel size could have a positive influence on the relative abundance of the associated fauna. Also, to further support this hypothesis, an entire suite of species was shown to be absent on edifices without mussels (Chapter 5).

As all the temporal variation patterns were based on one single edifice, one could wonder if these trends apply on other mussel-dominated edifices within the Lucky Strike vent field and beyond. Analyses of species lists and samples taken on various different hydrothermal edifices within the vent field did not reveal significant differences in species composition according to locality or year sampled, based on the data present in Biocean database (Fabri et al., 2006) (Chapter 5), although additional sampling is needed to validate some of our findings and hypotheses. One of the major concerns was the existence of two types of fluids at Lucky Strike (Langmuir et al., 1997; Von Damm et al, 1998; Charlou et al., 2000) which could have an influence on local species composition. However, there are no indicator species for the different fluid sources, affirming that the local habitat characteristics such as the amount hydrothermal activity, sulfide supply and suitable habitats are prime determinants in species presence/absence and distribution (see also Chapters 2 and 3). These local habitat features result in visible differences between the sites. So is Eiffel Tower more similar to Elisabeth and Bairro Alto regarding the faunal assemblages present, and certainly regarding the presence of larger-sized mussels (Assemblage 1). The other sites (e.g. Sintra and Isabel) have a larger proportion of smaller-sized mussels and new recruits. The larger-sized mussels (if present at these sites) can only be found in the immediate surrounding of the fluid exits. Possibly, these vents do not host sufficient hydrothermal activity features to sustain populations of larger-sized mussels and are thus dominated by smaller mussels. According to the currents at Lucky Strike and the local topography (Khripounoff et al., 2008), Sintra and Isabel in the eastern region as well as the sites situated in the north-western region of the vent field could be more exposed to recruiting events or larval supply. However, no significant differences in species composition between the sites or between the years exist. Even though the proportions of faunal assemblages appear to vary, I suggest that patterns and community dynamics observed at Eiffel Tower may apply to all the other mussel-dominated sites within the Lucky Strike vent field. Large-scale sampling would be advisable to verify this hypothesis.

Decadal-scale constancy in *Rimicaris exoculata* shrimp and *Maractis rimicarivora* anemone densities were observed at the deeper Atlantic TAG sulfide mound, which coincided with a steadiness of the geochemistry of vent fluids on decadal timescales (Copley et al., 2007a). However, we cannot assume that this constancy in geochemistry applies to other vent fields, as along the axis of the MAR, a significant variability in seismic event rate was observed (Smith et al., 2003). Additional differences between the vent fields are observed as the water depth changes, the geology of source rocks and the nature of the hydrothermal deposits vary as well, causing the vent habitats to differ in their fluid chemistry (Desbruyères et al., 2000) and consequently in faunal dominance. Nonetheless, the present study showed that overall decadal-scale constancy perseveres at Lucky Strike for the dominant *Bathymodiolus* mussels, although small-scale shorter-time interval changes do occur and might not be underestimated.

Going back to the main hypothesis/question, i.e. addressing the variability of community dynamics on spatial and temporal scales on continuous venting structures in settings of different spreading rate, one of the main conclusions is that there is an effective difference between slower- and faster-spreading ridges. For instance the overall rate of change at the slower-spreading MAR was shown to be 15% lower that that of similar continuous venting edifices on the faster-spreading Juan de Fuca Ridge for similar time-scales (Sarrazin et al., 1997). While faunal composition and species pool available are visibly different, the community dynamics are different as well in settings with dissimilar spreading rate.

Vent fields dominated by mussels to a same extent as observed at Lucky Strike are not that abundant and seem to be limited to the shallower part of the MAR. Hence, the models presented would be restricted to the other currently known mussel-dominated sites, which is at present limited to the Menez Gwen vent field (at 800 m depth). However, a larger application of the models presented could be postulated, in the sense that *Bathymodiolus* spp. are present in many known vent sites or even have dominance in certain stages of succession (Hessler et al., 1985; Johnson et al., 1994; Gebruk et al., 2000b; Desbruyères et al., 2001; Henry et al., 2008; Lutz et al., 2008). Consequently the observed patterns and models could apply there. However, the spatio-temporal processes (zonation and dynamics) are likely to take place on much shorter time-scales at the vents of faster-spreading ridges, such as the EPR, because of their generally shorter lifespan. The only way to corroborate these hypotheses is through the use of time-lapse cameras, recording all the short-term changes occurring in (nascent) mussels beds at faster-spreading ridges. Alternatively, the discovery of new vent sites and associated fauna could offer opportunities for extrapolation and additional testing.

Future perspectives would consist out of further validation and testing of the proposed models. Firstly through additional and more in-detail characterisation of faunal assemblages at other edifices within the Lucky Strike vent field through a combination of sampling (biologically and chemically) and imagery analyses. The use of time-lapse cameras, in association with monitored short- and long-term experimental manipulations at Lucky Strike, could help us to better understand species dynamics and other intervening factors, including biotic interactions. Additional use of time-lapse cameras in Pacific mussel beds could account for testing the validity of the proposed models.

Bibliography

Bibliography

A

Alt J.C. (1995). Subseafloor processes in mid-ocean ridge hydrothermal systems. In: *Seafloor Hydrothermal Systems: Physical, Chemical, Biological, and Geological Interactions. S.E. Humphris, R.A. Zierenberg, L.S. Mullineaux, and R.E. Thomson, (Eds.), American Geophysical Union Monograph Series* 91, Washington, DC., pp 85-114.

B

Bachraty C., Legendre P., Desbruyères D. (2009). Biogeographic relationships among deep-sea hydrothermal vent faunas at global scale. *Deep-Sea Research part I - Oceanographic Research Papers* 56, 1371-1378.

Baker E.T., Lavelle J.W., Freely R. A., Massoth G.J., Walker S.L. (1989). Episodic venting on the Juan de Fuca Ridge. *Journal of Geophysical Research* 94, 9237-9250.

Baker E.T., Hammond S.R. (1992). Hydrothermal venting and the apparent magmatic budget of the Juan de Fuca Ridge. *Journal of Geophysical Research* 97, 3443-3456.

Baker E.T., German C.R., Elderfield H. (1995). Hydrothermal plumes over spreading-center axes: Global distributions and geological inferences. *In Seafloor Hydrothermal Systems: Physical, Chemical, Biological, and Geological Interactions. S.E. Humphris, R.A. Zierenberg, L.S. Mullineaux, and R.E. Thomson, (Eds.), American Geophysical Union Monograph Series* 91, Washington, DC., pp 47-71.

Baker E.T., German C.R. (2004). On the global distribution of hydrothermal vent fields. *In Mid-Ocean Ridges: Hydrothermal interactions between the lithosphere and oceans. C.R. German, J. Lin, and L.M. Parson (Eds.) American Geophysical Union Monograph Series* 148, Washington, DC., pp. 245–266.

Bates A.E., Tunnicliffe V., Lee R.W. (2005). Role of thermal conditions in habitat selection by hydrothermal vent gastropods. *Marine Ecology-Progress Series* 305, 1-15.

Bates A.E. (2007). Persistence, morphology, and nutritional state of a gastropod hosted bacterial symbiosis in different levels of hydrothermal vent flux. *Marine Biology* 152, 557–568.

Bergquist D.C., Fleckenstein C., Szalai E.B., Knisel J., Fisher C.R. (2004). Environment drives physiological variability in the cold seep mussel *Bathymodiolus childressi*. *Limnology and Oceanography* 49, 706-715.

Both R., Crook K., Taylor B., Brogan S., Chappell B.W., Frankel E., Liu L., Sinton J., Tiffin D. (1986). Hydrothermal chimneys and associated fauna in the Manus back-arc basin, Papua New Guinea. *EOS, Transactions of the American Geophysical Union* 67, 489-490.

Britayev T.A., Martin D., Krylova E. M., Von Cosel R., Aksiuk T. S. (2007). Life-history traits of the symbiotic scale-worm *Branchipolynoe seepensis* and its relationships with host mussels of the genus *Bathymodiolus* from hydrothermal vents. *Marine Ecology-an Evolutionary Perspective* 28, 36-48.

Butler I.B., Fallick A.E., Nesbitt R.W. (1998). Mineralogy, sulphur isotope geochemistry and the development of sulfide structures at the Broken Spur hydrothermal vent site, 29°10' N, Mid-Atlantic Ridge. *Journal of the Geological Society* 155, 773-785.

C

Cardigos F., Colaço A., Dando P.R., Avila S.P., Sarradin P.M., Tempera F., Conceição P., Pascoal A., Serrão Santos R. (2005). Shallow water hydrothermal vent field fluids and communities of the D. João de Castro Seamount (Azores). *Chemical Geology* 224, 153– 168.

Cavanaugh C.M., Gardiner S.L., Jones M.L., Jannasch H.W., Waterbury J.B. (1981). Prokaryotic cells in the hydrothermal vent tube worm *Riftia pachyptila* Jones: possible chemoautotrophic symbionts. *Science* 213, 340-342.

Charlou J.L., Dental J.P., Douville E., Jean-Baptiste P., Radford-Knoery J., Fouquet Y., Dapoigny A., Stievenard M. (2000). Compared geochemical signatures and the evolution of Menez Gwen (37° 50' N) and Lucky Strike (37°17' N) hydrothermal fluids, south of the Azores Triple Junction on the Mid-Atlantic Ridge. *Chemical Geology* 171, 49-75.

Charmasson S., Sarradin P.-M., Le Faouder A., Agarande M., Loyen J., Desbruyères D. (2009). High levels of natural radioactivity in biota from deep-sea hydrothermal vents: a preliminary communication. *Journal of Environmental Radioactivity* 100, 522–526.

Chevaldonné P., Desbruyères D., Lehaitre M. (1991). Time-series of temperature from 3 deep-sea hydrothermal vent sites. *Deep-Sea Research Part a-Oceanographic Research Papers* 38, 1417-1430.

Chevaldonné P., Desbruyères D., Childress J.J. (1992). Some like it hot... and some even hotter. *Nature* 359, 593-594.

Chevaldonné P., Jollivet D. (1993). Videoscopic study of deep-sea hydrothermal vent alvinellid polychaete populations - biomass estimation and behavior. *Marine Ecology Progress Series* 95, 251-262.

Chevaldonné P., Jollivet D., Vangriesheim A., Desbruyères D. (1997). Hydrothermal-vent alvinellid polychaete dispersal in the eastern Pacific. 1. Influence of vent site distribution, bottom currents, and biological patterns. *Limnology and Oceanography* 42, 67–80.

Chevaldonné P., Fisher C.R., Childress J.J., Desbruyères D., Jollivet D., Zal F., Toulmond A. (2000). Thermotolerance and the 'Pompeii worms'. *Marine Ecology Progress Series* 208, 293-295.

Childress J.J., Fisher C.R. (1992). The biology of hydrothermal vent animals: physiology, biochemistry, and autotrophic symbioses. *Oceanography and Marine Biology: An Annual Review* 30, 337-441.

Colaço A., Desbruyeres D., Comtet T., Alayse A.M. (1998). Ecology of the Menez Gwen hydrothermal vent field (Mid-Atlantic Ridge, Azores Triple Junction). *Cahiers de Biologie Marine* 39, 237–240.

Colaço A., Dehairs F., Desbruyeres D. (2002). Nutritional relations of deep-sea hydrothermal fields at the Mid-Atlantic Ridge: a stable isotope approach. *Deep-Sea Research Part I - Oceanographic Research Papers* 49, 395-412.

Colaço A., Bustamante P., Fouquet Y., Sarradin P.-M., Serrão Santos R. (2006). Bioaccumulation of Cu, Zn, and Hg in the Azores Triple Junction hydrothermal vent fields food chains. *Chemosphere* 65, 2260-2267.

Colaço A., Desbruyeres D., Guezennec J. (2007). Polar lipid fatty acids as indicators of trophic associations in a deep-sea vent system community. *Marine Ecology - an Evolutionary Perspective* 28, 15-24.

Company R., Serafim A., Cosson R., Fiala-Medioni A., Dixon D.R., Bebianno M.J. (2007). Adaptation of the antioxidant defence system in hydrothermal-vent mussels (*Bathymodiolus azoricus*) transplanted between two Mid-Atlantic Ridge sites. *Marine Ecology - an Evolutionary Perspective* 28, 93-99.

Comtet T., Desbruyères D., (1998). Population structure and recruitment in mytilid bivalves from the Lucky Strike and Menez Gwen hydrothermal vent fields (37° 17' N and 37° 50' N on the Mid-Atlantic Ridge). *Marine Ecology Progress Series* 163, 165-177.

Connell J.H., Slatyer R.O. (1977). Mechanisms of succession in natural communities and their role in community stability and organization. *American Naturalist* 111, 1119-1144.

Copley, J.T.P., Tyler, P.A., Murton, B.J., Van Dover, C.L. (1997). Spatial and interannual variation in the faunal distribution at Broken Spur vent field (29° N, Mid-Atlantic Ridge). *Marine Biology* 129, 723-733.

Copley, J.T.P., Tyler, P.A., Van Dover, C.L., Schultz, A., Dickson, P., Singh, S. and Sulanowska, M. (1999). Subannual temporal variation in faunal distributions at the TAG hydrothermal mound (26N, Mid-Atlantic Ridge). *Marine Ecology* 20, 291-306.

Copley, J.T.P., Jorgensen, P.B.K., Sohn, R.A. (2007a). Assessment of decadal-scale ecological change at a deep Mid-Atlantic hydrothermal vent and reproductive time-series in the shrimp *Rimicaris exoculata*. *Journal of the Marine Biological Association UK* 84, 859-867.

Copley J.T.P, Flint H.C., Ferrero T.J., Van Dover, C.L. (2007b). Diversity of meiofauna and free-living nematodes in mussel beds at hydrothermal vents on the northern and southern East Pacific Rise. *Journal of the Marine Biological Association of the UK* 84, 1141-1152.

Cordes E.E., Bergquist D.C., Fisher C.R. (2009). Macro-ecology of Gulf of Mexico cold seeps. *Annual Review of Marine Science* 1,143-168.

Corliss J.B., Dymond J., Gordon L.I., Edmond J.M., von Herzen R.P., Ballard R.D., Green K., Williams D., Bainbridge A., Crane K., van Andel T.H. (1979). Submarine thermal springs on the Galápagos Rift. *Science* 203, 1073-1083.

Cosson R.P., Vivier J.P. (1997). Interactions of metallic elements and organisms within hydrothermal vents. *Cahiers de Biologie Marine* 38, 43–50.

Cosson R.P., Thiébaut É., Company R., Castrec-Rouelle M., Colaço A., Martins I., Sarradin P.M., Bebianno M.J. (2008). Spatial variation of metal bioaccumulation in the hydrothermal vent mussel *Bathymodiolus azoricus*. *Marine Environmental Research* 65, 405–415.

Csotonyi J.T., Stackebrandt E., Yurkov V. (2006). Anaerobic respiration on tellurate and other metalloids in bacteria from hydrothermal vent fields in the Eastern Pacific Ocean. *Applied and Environmental Microbiology* 72, 4950–4956.

Cuvelier D., Sarrazin J., Colaço A., Copley J., Desbruyères D., Glover A.G., Tyler P., Serrão Santos R. (2009). Distribution and spatial variation of Atlantic hydrothermal faunal assemblages revealed by high-resolution video image analysis. *Deep Sea Research I -Oceanographic Research Papers* 56, 2026–2040.

Cuvelier D., Sarradin P.-M., Sarrazin J., Colaço A., Copley J.T., Desbruyères D., Glover A.G., Serrão Santos R., Tyler P.A. (*in press*). Hydrothermal faunal assemblages and habitat characterisation at the Eiffel Tower edifice (Lucky Strike, Mid-Atlantic Ridge). *Marine Ecology*

D

De Busserolles F., Sarrazin J., Gauthier O., Gélinas Y., Fabri M.C., Sarradin P.M., Desbruyères D. (2009). Are spatial variations in the diets of hydrothermal fauna linked to local environmental conditions? *Deep-Sea Research part II - Topical Studies in Oceanography* 56: 1649-1664.

Desbruyères D., A.-M. Alayse-Danet, S. Ohta and The Scientific Parties of Biolau and Starmer Cruises (1994). Deep-sea hydrothermal communities in the Southwestern Pacific back arc basins (the North Fiji and Lau Basins): Composition, microdistribution and food web. *Marine Geology*, 116, 227-242.

Desbruyères, D. (1998). Temporal variations in the vent communities on the East Pacific Rise and Galapagos Spreading Centre: a review of present knowledge. *Cahiers de Biologie Marine* 39, 241-244.

Desbruyères, D., Chevaldonné, P., Alayse, A.M., Jollivet, D., Lallier, F.H., Jouin-Toulmond, C., Zal, F., Sarradin, P.M., Cosson, R., Caprais, J.C., Arndt, C., O'Biren, J., Guezennec, J., Hourdez, S., Riso, R., Gaill, F., Laubier, L., Toulmond, A. (1998). Biology and ecology of the 'Pompeii worm' (*Alvinella pompejana* Desbruyères and Laubier), a normal dweller of an extreme deep-sea environment: a synthesis of current knowledge and recent developments. *Deep-Sea Research Part II Topical Studies in Oceanography* 45, 383–422.

Desbruyères D., Almeida A., Biscoito M., Comtet T., Khripounoff A., Le Bris N., Sarradin P.M. and Segonzac M. (2000). A review of the distribution of hydrothermal vent communities along the northern Mid-Atlantic Ridge: dispersal vs. environmental controls. *Hydrobiologia* 440, 201-216.

Desbruyères D., Biscoito M., Caprais J.C., Colaco A., Comtet T., Crassous P., Fouquet Y., Khripounoff A., Le Bris N., Olu K., Riso R., Sarradin P.M., Segonzac M., Vangriesheim A. (2001). Variations in deep-sea hydrothermal vent communities on the Mid-Atlantic Ridge near the Azores plateau. *Deep-Sea Research part I – Oceanographic Research Papers* 48, 1325-1346.

Desbruyères D., Hashimoto J., Fabri M.-C. (2006a). Composition and biogeography of hydrothermal vent communities in western Pacific back-arc basins. *In: Back-Arc Spreading Systems - Geological,*

Biological, Chemical, and Physical Interactions. Christie, D.M., Fisher, C.R., Lee, S.M., Givens, S. (Eds.) American Geophysical Union Monograph Series, 166, pp 215-234.

Desbruyeres D., Segonzac M., Bright M., (Eds.) (2006b). Handbook of deep-sea hydrothermal vent fauna. *Second completely revised edition. Denisia, 18. Biologiezentrum der Oberösterreichischen Landesmuseen. Linz, Austria*, pp. 544.

Devey C.W., Lackschewitz K.S., Baker E.T., (2005). Hydrothermal and volcanic activity found on the southern Mid-Atlantic Ridge. *Eos* 86, 209–212.

Devey C.W., Fisher C.R., Scott, S. (2007). Responsible science at hydrothermal vents. *Oceanography* 20 (1), 162-171.

Dreyer J. C., Knick K. E., Flickinger W. B., Van Dover C. L. (2005). Development of macrofaunal community structure in mussel beds on the northern East Pacific Rise. *Marine Ecology Progress Series* 302, 121-134.

Dupérron S., Bergin C., Zielinski F., Blazejak A., Pernthaler A., McKiness Z.P., DeChaine E., Cavanaugh C.M., Dubilier N. (2006). A dual symbiosis shared by two mussel species, *Bathymodiolus azoricus* and *Bathymodiolus puteoserpentis* (Bivalvia: Mytilidae), from hydrothermal vents along the northern Mid-Atlantic Ridge. *Environmental Microbiology* 8(8), 1441–1447.

Dziak R.P., Fox C.G., Schreiner A. (1995). The June-July 1993 seismo-acoustic event at CoAxial segment, Juan de Fuca Ridge: evidence for a lateral dike injection. *Geophysical Research Letters*, 22, 135-138.

Dziak R.P., Smith D.K., Bohnenstiehl D.R., Fox C.G., Desbruyères D., Matsumoto H., Tolstoy M., Fornari D.J. (2004). Evidence of a recent magma dike intrusion at the slow spreading Lucky Strike segment, Mid-Atlantic Ridge. *Journal of Geophysical Research (Solid Earth)*. 109.

E

Edmonds H.N., Michael P.J., Baker E.T., Connely D.P., Snow J.E., Langmuir C.H., Dick H.J.B., Muehe R., German C.R., GrahamD.W. (2003). Discovery of abundant hydrothermal venting on the ultraslow-spreading Gakkel ridge in the Arctic Ocean. *Nature* 421, 252-256.

Embley R. W., Chadwick Jr. W.W. (1994). Volcanic and hydrothermal processes associated with a recent phase of seafloor spreading at the northern Cleft segment: Juan de Fuca Ridge. *Journal of Geophysical Research*, 99(B3), 4741–4760.

Embley R.W., Chadwick Jr. W.W., Clague D., Stakes D. (1999). 1998 Eruption of Axial Volcano: Multibeam anomalies and seafloor observations. *Geophysical Research Letters* 26, 3425–3428.

F

Fabri M.C., Galéron J., Larour M., Maudire G. (2006). Combining the biocean database for deep-sea benthic data with the online Ocean Biogeographic Information System. *Marine Ecology Progress Series* 316, 215–224.

Fiala-Medioni A., McKiness Z.P., Dando P., Boulegue J., Mariotti A., Alayse-Danet A.M., Robinson J.J., Cavanaugh C.M. (2002). Ultrastructural, biochemical and immunological characterization of two populations of the mytilid mussel *Bathymodiolus azoricus* from the Mid-Atlantic Ridge: evidence for a dual symbiosis. *Marine Biology* 141, 1035–1043.

Fisher C. R., Childress J. J., Arp A. J., Brooks J. M., Distel D., Favuzzi J. A., Felbeck H., Hessler R., Johnson K. S., Kennicutt M. C., Macko S. A., Newton A., Powell M. A., Somero G. N., Soto T. (1988). Microhabitat variation in the hydrothermal vent mussel, *Bathymodiolus thermophilus*, at the Rose Garden vent on the Galapagos Rift. *Deep-Sea Research Part a-Oceanographic Research Papers* 35, 1769-1791.

Fisher C.R. (1990). Chemoautotrophic and methanotrophic symbioses in marine invertebrates. *Reviews in Aquatic Science* 2, 399-436.

Fisher, C.R. (1995). Towards an appreciation of hydrothermal vent animals: their environment, physiological ecology and tissue stable isotope values. *In Seafloor Hydrothermal Systems: Physical, Chemical, Biological, and Geological Interactions. S.E. Humphris, R.A. Zierenberg, L.S. Mullineaux, and R.E. Thomson, (Eds.), American Geophysical Union Monograph Series 91, Washington, DC.,* pp 297-316.

Fouquet Y., Ondréas H., Charlou J.-L., Donval J.P., Radford-Knoery J., Costa I., Lourenço N., Tivey M.K. (1995). Atlantic lava lakes and hot vents. *Nature* 377, 201.

Fouquet Y., Eissen J. P., Ondreas H., Barriga F., Batiza R., Danyushevsky L. (1998). Extensive volcaniclastic deposits at the Mid-Atlantic Ridge axis: results of deep-water basaltic explosive volcanic activity? *Terra Nova* 10, 280-286.

Fox M., Juniper S.K., Vali H. (2002). Chemoautotrophy as a possible nutritional source in the hydrothermal vent limpet *Lepetodrilus fucensis*. *Cahiers de Biologie Marine* 43, 371–376.

Fustec A., Desbruyères D., Juniper K. S. (1987). Deep-sea hydrothermal vent communities at 13°N on the East Pacific Rise: Microdistribution and temporal variations. *Biological Oceanography* 4(2), 121-164.

G

Gauthier O., Sarrazin J., Desbruyères D. (2010). Measure and mis-measure of species diversity in deep-sea chemosynthetic communities. *Marine Ecology Progress Series* 402, 285-302.

Gebruk A. V., Southward E. C., Kennedy H., Southward A. J. (2000a). Food sources, behaviour, and distribution of hydrothermal vent shrimps at the Mid-Atlantic Ridge. *Journal of the Marine Biological Association of the United Kingdom* 80, 485-499.

Gebruk, A.V., Chevaldonne, P., Shank, T., Lutz, R.A., Vrijenhoek R.C. (2000b). Deep-sea hydrothermal vent communities of the Logatchev area (14 degree 45 N, Mid-Atlantic Ridge): diverse biotopes and high biomass. *Journal of the Marine Biological Association of the UK*, 80, 383–393.

Genin A., Dayton P.K., Lonsdale P.F., Spiess F.N. (1986). Corals on Seamount Peaks Provide Evidence of Current Acceleration Over Deep-Sea Topography. *Nature* 322, 59-61.

German C.R., Parson L.M., Bougault F., Coller D., Critchley M., Dapoigny A., Day C., Eardley D., Fearn A., Flewellen C., Kirk R., Klinkhammer G., Landure J.Y., Ludford E., Miranda M., Needham H.D., Patching J., Pearce R., Pelle H., Radford-knoery J., Rouse I., Scott J., Stoffregen P., Taylor P., Teare D., Wynar J. (1996). Hydrothermal exploration near the Azores Triple Junction: Tectonic control of venting at slow-spreading ridges? *Earth and Planetary Science Letters* 138, 93-104.

German C.R., Yoerger D.R., Jakua M., Shank T.M., Langmuir C.H., Nakamura K. (2008a). Hydrothermal exploration with the Autonomous Benthic Explorer. *Deep-Sea Research I – Methods and Instruments* 55, 203–219.

German C.R., Bennett S.A., Connelly D.P., Evans A.J., Murton B.J., Parson L.M., Prien R.D., Ramirez-Llodra E., Jakuba M., Shank T.M., Yoerger D.R., Baker E.T., Walker S.L., Nakamura N., (2008b). Hydrothermal activity on the southern Mid-Atlantic Ridge: Tectonically- and volcanically-controlled venting at 4–5°S. *Earth and Planetary Science Letters* 273, 332–344.

Glover A.G, Gooday A.J., Bailey D.M., Billett D.S.M., Chevaldonné P., Colaço A., Copley J., Cuvelier D., Desbruyères D., Kalogeropoulou V., Klages M., Lampadariou N., Lejeusne C., Mestre N.C., Paterson G.L.J., Perez T., Ruhl H., Sarrazin J., Soltwedel T., Soto E.H., Thatje S., Tselepides A., Van Gaever S., Vanreusel A. (2010). Temporal change in deep-sea benthic ecosystems: A review of the rvidence from recent time-series studies'. *Advances in Marine Biology* 58, 1-95

Govenar B., Freeman M., Bergquist D.C., Johnson G.A., Fisher C.R. (2004). Composition of a one-year-old *Riftia pachyptila* community following a clearance experiment: insight to succession patterns at deep-sea hydrothermal vents. *Biological Bulletin* 207, 177–182.

Govenar B., Le Bris N., Gollner S., Glanville J., Aperghis A.B., Hourdez S., Fisher C.R., (2005). Epifaunal community structure associated with *Riftia pachyptila* aggregations in chemically different hydrothermal vent habitats. *Marine Ecology Progress Series* 305, 67-77.

Govenar B., Fisher C.R. (2007). Experimental evidence of habitat provision by aggregations of *Riftia pachyptila* at hydrothermal vents on the East Pacific Rise. *Marine Ecology-an Evolutionary Perspective* 28, 3-14.

Grehan A.J., Juniper S.K. (1996). Clam distribution and subsurface hydrothermal processes at Chowder Hill (Middle Valley), Juan de Fuca Ridge. *Marine Ecology Progress Series* 130, 105-115.

Guichard F., Halpin P.M., Allison G.W., Lubchenco J., Menge B.A. (2003). Mussel disturbance dynamics: signatures of oceanographic forcing from local interactions. *American Naturalist* 161, 889-904.

H

Halary S., Riou V., Gaill F., Boudier T., Duperron S. (2008). 3DFISH for the quantification of methane- and sulphur-oxidizing endosymbionts in bacteriocytes of the hydrothermal vent mussel *Bathymodiolus azoricus*. *The ISME Journal* 2(3), 284–292.

Hannington, M.D., Jonasson, I.R., Herzig, P.M., Petersen, S. (1995). Physical and chemical processes of seafloor mineralization at mid-ocean ridges. *In Seafloor Hydrothermal Systems: Physical, Chemical,*

Biological, and Geological Interactions. S.E. Humphris, R.A. Zierenberg, L.S. Mullineaux, and R.E. Thomson, (eds), American Geophysical Union Monograph Series 91, Washington, DC., pp. 115–157.

Hannington M.D., de Ronde C.E.J., Petersen S. (2005). Sea-floor tectonics and submarine hydrothermal systems. *In 100th Anniversary Volume of Economic Geology. J. Hedenquist et al., (Eds.), Society of Economic Geologists, Littleton, Colorado*, pp. 111–141.

Hashimoto J., Ohta S., Gamo T., Chiba H., Yamaguchi T., Tsuchida S., Okudaira T., Watabe H., Yamanaka T., Kitazawa M. (2001). First hydrothermal vent communities from the Indian Ocean discovered. *Zoological Science* 18, 717-721.

Haymon, R.M. (1983). Growth history of hydrothermal black smoker chimneys. *Nature* 301, 695-698.

Haymon, R.M., Fornari, D., Edwards, M., Carbotte, S., Wright, D., Macdonald, K.C. (1991). Hydrothermal vent distribution along the East Pacific Rise crest (9°09′-54′N) and its relationship to magmatic and tectonic processes on fast-spreading mid-ocean ridges. *Earth Planetary Science Letters* 104, 513-534.

Haymon, R.M., Fornari, D.J., Von Damm, K.L., Lilley, M.D., Perfit, M.R., Edmond, J.M., Shanks, W.C., Lutz, R.A., Grebmeier, J.M., Carbotte, S., Wright, D., McLaughlin, E.S.M., Beedle, N., Olson, E. (1993). Volcanic eruption of the mid-ocean ridge along the East Pacific Rise crest at 9°45-52'N: Direct submersible observations of seafloor phenomena associated with an eruption event in April, 1991. *Earth and Planetary Science Letters* 119, 85-101.

Henry M. S., Childress J. J., Figueroa D. (2008). Metabolic rates and thermal tolerances of chemoautotrophic symbioses from Lau Basin hydrothermal vents and their implications for species distributions. *Deep-Sea Research Part I-Oceanographic Research Papers* 55, 679-695.

Herring P.J., Dixon D. R. (1998). Extensive deep-sea dispersal of postlarval shrimp from a hydrothermal vent. *Deep-Sea Research Part I -Oceanographic Research Papers* 45, 2105-2118.

Herring P.J., Gaten E., Sheldon P.M.J., (1999). Are vent shrimps blinded by science? *Nature* 398, 116.

Hessler R.R., Smithey W.M., Keller C.H. (1985). Spatial and temporal variation of giant clams, tubeworms and mussels at deep-sea hydrothermal vents. *Bulletin of the Biological Society of Washington* 6, 411-428.

Hessler, R.R., Smithey, W.M., Boudrias, M.A., Keller, C.H., Lutz, R.A., Childress, J.J. (1988). Temporal change in megafauna at the Rose Garden hydrothermal vent (Galapagos Rift - eastern tropical Pacific). *Deep-Sea Research Part a-Oceanographic Research Papers* 35, 1681-1709.

Hessler, R.R., Lonsdale, P.F., (1991). Biogeography of Mariana Trough hydrothermal vent communities. *Deep-Sea Research Part a-Oceanographic Research Papers* 38, 185–199.

Hessler, R.R, Kaharl V.A., (1995). The deep-sea hydrothermal vent community: An overview. *In Seafloor Hydrothermal Systems: Physical, Chemical, Biological, and Geological Interactions. S.E. Humphris, R.A. Zierenberg, L.S. Mullineaux, and R.E. Thomson, (Eds.), American Geophysical Union Monograph Series 91, Washington, DC.*, pp 72-84.

Humphris, S.E., McCollum, T. (1998). The Cauldron beneath the seafloor: Percolating through volcanic subsurface rocks, seawater is chemically transformed into hydrothermal fluid. *Oceanus* 41(2), 18-21.

Humphris, S.E., Fornari, D.J., Scheirer, D.S., German, C.R., Parson L.M. (2002). Geotectonic setting of hydrothermal activity on the summit of Lucky Strike seamount (37 Degrees 17 ' N, Mid-Atlantic Ridge). *Geochem. Geophys. Geosyst.* 3, doi: 10.1029/2001GC000284

J

Jannasch H.W. (1985). The chemosynthetic support of life and the microbial diversity at deep-sea hydrothermal vents. *Proceedings of the Royal Society of London, Series B, Biological sciences* 225, 277-297.

Johnson K. S., Childress J. J., Beehler C. L. (1988a). Short-term temperature variability in the Rose Garden hydrothermal vent field - an unstable deep-sea environment. *Deep-Sea Research Part a-Oceanographic Research Papers* 35, 1711-1721.

Johnson K. S., Childress J. J., Hessler R. R., Sakamoto-Arnold C. M., Beehler C. L. (1988b). Chemical and biological interactions in the Rose Garden hydrothermal vent field, Galapagos Spreading Center. *Deep-Sea Research Part a-Oceanographic Research Papers* 35, 1723-1744.

Johnson K. S., Childress J. J., Beehler C. L., Sakamoto C. M. (1994). Biogeochemistry of hydrothermal vent mussel communities - the deep-sea analogue to the intertidal zone. *Deep-Sea Research Part I-Oceanographic Research Papers* 41, 993-1011.

Jollivet D. (1993). Distribution et evolution de la faune associee aux sources hydrothermales profondes a 13″N sur la dorsale du Pacifique oriental: le cas particulier des polychetes Alvinellidae. *PhD thesis, Université Bretagne Occidentale, Brest, France*

Juniper, S.K., Tunnicliffe, V., Southward, E.C. (1992). Hydrothermal vents in turbidite sediments on a Northeast Pacific spreading centre: Organisms and substratum at an ocean drilling site. *Canadian Journal of Zoology* 70, 1792-1809.

Juniper, S.K., Sarrazin, J. (1995). Interaction of vent biota and hydrothermal deposits: present evidence and future experimentation. *In Seafloor Hydrothermal Systems: Physical, Chemical, Biological, and Geological Interactions. S.E. Humphris, R.A. Zierenberg, L.S. Mullineaux, and R.E. Thomson, (Eds.), American Geophysical Union Monograph Series 91, Washington, DC.,* pp 178-193.

Juniper S. K., Martineu P., Sarrazin J., Gélinas Y. (1995). Microbial-mineral floc associated with nascent hydrothermal activity on CoAxial Segment, Juan de Fuca Ridge. *Geophysical Research Letters* 22(2), 179–182.

Juniper S.K., Tunnicliffe V. (1997). Crustal accretion and the hot vent ecosystem. *Philosophical Transactions Royal Society London A* 355, 459-474.

K

Kádár E., Costa V., Martins I., Santos R.S., Powell J.J. (2005). Enrichment in trace metals (Al, Mn, Co, Cu, Mo, Cd, Fe, Zn, Pb and Hg) of macro-invertebrate habitats at hydrothermal vents along the Mid Atlantic Ridge. *Hydrobiologia* 548, 191–205.

Kashefi K., Lovley D.R. (2003). Extending the upper temperature limit for life. *Science* 301, 934.

Kelley D. S., Karson J.A., Blackman D.K., Früh-Green G.L., Butterfield D.A., Lilley M.D., Olson E.J., Schrenk M.W., Roe K.K., Lebon G.T., Rivizzigno P. & the AT3-60 Shipboard Party (2001). An off-axis hydrothermal-vent field near the Mid-Atlantic Ridge at 30° N. *Nature* 412, 145 –149.

Kennish M.J., Lutz R.A. (1999). Calcium carbonate dissolution rates in deep-sea bivalve shells on the East Pacific Rise at 21°N: results of an 8-year in-situ experiment. *Palaeogeography, Palaeoclimatology, Palaeoecology* 154, 293-299.

Khripounoff A., Vangriesheim A., Crassous P., Segonzac M., Lafon V., Waren A. (2008). Temporal variation of currents, particulate flux and organism supply at two deep-sea hydrothermal fields of the Azores Triple Junction. *Deep-Sea Research Part I-Oceanographic Research Papers* 55, 532-551.

Kindt R., Coe R. (2005). Tree diversity analysis. A manual and software for common statistical methods for ecological and biodiversity studies. *Nairobi: World Agroforestry Centre (ICRAF)* pp. 196.

Kohler K.E., Gill S.M. (2006). Coral Point Count with Excel extensions (CPCe): A Visual Basic program for the determination of coral and substrate coverage using random point count methodology. *Computers and Geosciences* 32, 1259-1269.

Koleff P., Gaston K.J., Lennon J.L. (2003). Measuring beta diversity for presence–absence data. *Journal of Animal Ecology* 72, 367–382.

Koschinsky A., Garbe-Schönberg D., Sander S., Scmidt K., Gennerich H.-H., Strauss H. (2008). Hydrothermal venting at pressure-temperature conditions above the critical point of seawater, 5°S on the Mid-Atlantic Ridge. *Geology* 36(8), 615-618.

L

Lalou C., Labeyrie L., Brichet E., Perezleclaire H. (1984). East Pacific Rise hydrothermal deposits: radiochronology of the sulfides and isotopic geochemistry of silica deposits. *Bulletin de la Societe Geologique de France* 26, 9-14.

Lalou C. (1991). Deep-sea hydrothermal venting: A recently discovered marine system. *Journal of Marine Systems* 1, 403-440.

Lalou C., Reyss J-L, Brichet E., Arnold M., Thompson G., Fouquet Y., Rona P.A. (1993). New age data for Mid-Atlantic ridge hydrothermal sites: TAG and Snakepit chronology revisited. *Journal of Geophysical Research* 98, 9705-9713.

Langmuir C., Humphris S., Fornari D., Van Dover C., Von Damm K., Tivey M. K., Colodner D., Charlou J. L., Desonie D., Wilson C., Fouquet Y., Klinkhammer G., Bougault H. (1997).

Hydrothermal vents near a mantle hot spot: the Lucky Strike vent field at 37 degrees N on the Mid-Atlantic Ridge. *Earth and Planetary Science Letters* 148, 69-91.

Le Bris N., Govenar B., Le Gall C., Fisher C.R. (2006). Variability of physico-chemical conditions in 9°50'N EPR diffuse flow vent habitats. *Marine Chemistry* 98, 167–182.

Le Pennec M., Donval A., Herry A. (1990). Nutritional strategies of the hydrothermal ecosystem bivalves. *Progress in Oceanography* 24, 71-80.

Legendre P., Fortin M.J. (1989). Spatial pattern and ecological analysis. *Vegetatio* 80, 107-138.

Legendre P., Gallagher E.G. (2001). Ecologically meaningful transformations for ordination of species data. *Oecologia* 129, 271–280.

Legendre P. (2005). Species associations: The kendall coefficient of concordance revisited. *Journal of Agricultural, Biological, and Environmental Statistics* 10 (2), 226–245.

Lenihan H.S., Mills S.W., Mullineaux L.S., Peterson S.H., Fisher C.R., Micheli F. (2008). Biotic interactions at hydrothermal vents: Recruitment inhibition by the mussel *Bathymodiolus thermophilus*. *Deep-Sea Research part I- Oceanographic Research Papers* 55, 1707–1717.

Levesque C., Juniper S.K. (2002). Particulate matter as a food source at a nascent hydrothermal vent on the Juan de Fuca Ridge. *Cahiers de Biologie Marine* 43, 289-292.

Levesque C., Juniper S.K., Limen H. (2006). Spatial organization of food webs along habitat gradients at deep-sea hydrothermal vents on Axial Volcano, Northeast Pacific. *Deep-Sea Research part I- Oceanographic Research Papers* 53, 726-739.

Limen H., Juniper S.K. (2006). Habitat controls on vent food webs at Eifuku Volcano, Mariana Arc. *Cahiers de Biologie Marine* 47, 449-455.

Lonsdale P. (1977). Clustering of suspension-feeding macrobenthos near abyssal hydrothermal vents at oceanic spreading centers. *Deep-Sea Research* 24, 857- 863.

Luther G.W., Rozan T. F., Taillefert M., Nuzzio D.B., Di Meo C., Shank T.M., Lutz R.A., Cary S. C. (2001). Chemical speciation drives hydrothermal vent ecology. *Nature* 410, 813-816.

Lutz, R.A., Shank, T.M., Evans, R. (2001). Life after death in the deep sea. *American Scientist* 89 (5), 422-431.

Lutz R.A., Shank T.M., Luther G.W., Vetriani C., Tolstoy M., Nuzzio D.B., Moore T.S., Waldhauser F., Crespo-Medina M., Chatziefthimiou A.D., Annis E.R., Reed A.J. (2008). Interrelationships between vent fluid chemistry, temperature, seismic activity, and biological community structure at a mussel-dominated, deep-sea hydrothermal vent along the East Pacific Rise. *Journal of Shellfish Research* 27, 177-190.

M

Marchig, V., Von Stackelberg, U., Wiedicke, M., Durn, G., Milovanovic, D. (1999). Hydrothermal activity associated with off-axis volcanism in the Peru Basin. *Marine geology* 159, 179-203.

Marcus J., Tunnicliffe V. (2002). Living on the edges of diffuse vents on the Juan de Fuca Ridge. *Cahiers De Biologie Marine* 43, 263-266

Marcus J., Tunnicliffe V., Butterfield D. (2009). Post-eruption succession of macrofaunal communities at diffuse flow hydrothermal vents on Axial Volcano, Juan de Fuca Ridge, Northeast Pacific. *Deep-Sea Research part II - Topical Studies in Oceanography* 56, 1586-1598.

Marques A., Porteiro F. (2000). Hydrothermal vent mussel *Bathymodiolus* sp (Mollusca: Mytilidae): diet item of *Hydrolagus affinis* (Pisces: Chimaeridae). *Copeia* 3, 806-807.

Martins I., Colaco A., Santos R. S., Lesongeur F., Godfroy A., Sarradin P. M., Cosson R. P. (2009). Relationship between the occurrence of filamentous bacteria on *Bathymodiolus azoricus* shell and the physiological and toxicological status of the vent mussel. *Journal of Experimental Marine Biology and Ecology* 376, 1-6.

Martins I., Colaço A., Dando P.R., Martins I., Desbruyères D., Sarradin P.M., Marques J.C., Serrao-Santos R. (2008). Size-dependent variations on the nutritional pathway of *Bathymodiolus azoricus* demonstrated by a C-flux model. *Ecological Modelling* 217, 59-71.

Matabos M., Le Bris N., Pendlebury S., Thiébaut E. (2008). Role of physico-chemical environment on gastropod assemblages at hydrothermal vents on the East Pacific Rise (13°N/EPR). *Journal of the Marine Biological Association of the United Kingdom* 88, 995-1008.

McKinnes Z.P., McMullin E.R., Fisher C.R., Cavanaugh C.M. (2005). A new bathymodioline mussel symbiosis at the Juan de Fuca hydrothermal vents. *Marine Biology* 148, 109–116.

McMullin E.R., Bergquist D.C., Fisher C.R. (2003). Metazoans in extreme environments: Adaptations of hydrothermal vent and hydrocarbon seep fauna. *Gravitational and Space Biology Bulletin* 13(2), 13-24.

Menge B.A., Sutherland J.P. (1976). Species diversity gradients: synthesis of the role of predation, competition and temporal heterogeneity. *The American Naturalist* 110, 351-369.

Micheli F., Peterson C.H., Mullineaux L.S., Fisher C.R., Mills S.W., Sancho G., Johnson G.A., Lenihan H.S. (2002). Predation structures communities at deep-sea hydrothermal vents. *Ecological Monographs* 72, 365-382.

Mills S.W., Mullineaux L.S., Tyler P.A. (2007). Habitat associations in gastropod species at East Pacific Rise hydrothermal vents (9 degrees 50 ' N). *Biological Bulletin* 212, 185-194.

Mullineaux L.S., Mills S.W., Goldman E. (1998). Recruitment variation during a pilot colonization study of hydrothermal vents (9°50′N, East Pacific Rise). *Deep-Sea Research part II - Topical Studies in Oceanography* 45, 441-464.

Mullineaux L.S., Fisher C.R., Peterson C.H., Schaeffer S.W. (2000). Tubeworm succession at hydrothermal vents: Use of biogenic cues to reduce habitat selection error? *Oecologia* 123, 275-284.

Mullineaux L.S., Peterson C.H., Micheli F., Mills S.W. (2003). Successional mechanism varies along a gradient in hydrothermal fluid flux at deep-sea vents. *Ecological Monographs* 73, 523-542.

Mullineaux L.S., Mills S.W., Sweetman A.K., Beaudreau A.H., Metaxas A., Hunt H.L. (2005). Vertical, lateral and temporal structure in larval distributions at hydrothermal vents. *Marine Ecology Progress Series* 293, 1–16.

Mullineaux L.S., Micheli F., Peterson C.H., Lenihan H.S., Markus N. (2009). Imprint of past environmental regimes on structure and succession of a deep-sea hydrothermal vent community. *Oecologia* 161, 387–400.

Murton B.J., Klinkhammer G., Becker K., Briais A., Edge D., Hayward N., Millard N., Mitchell I., Rouse I., Rudnick M., Sayanagi K., Sloan H., Parson L. (1994). Direct evidence for the distribution and occurrence of hydrothermal activity between 27°-30°N on the Mid-Atlantic Ridge. *Earth Planet Science Letters* 125,119-128.

Murton B.J., Van Dover C.L., Southward E.C. (1995). Geological setting and ecology of the Broken Spur hydrothermal vent field: 29°10′N on the Mid-Atlantic Ridge. *In: Parson LM, Walker CL, Dixon DR (Eds.) Hydrothermal vents and processes. Geological Society, London,* pp 33-42.

N

Nees H.S., Moore T.S., Mullaugh K.M., Holyoke R.R., Janzen C.P., Ma S., Metzger E., Waite T.J., Yücel M., Lutz R.A., Shank T.M., Vetriani C., Nuzzio D.B., Luther III G.W. (2008). Hydrothermal vent mussel habitat chemistry, pre- and post-eruption at 9°50′North on the East Pacific Rise. *Journal of Shellfish Research* 27(1), 169-175.

O

O.D.P. Leg 106 Scientific Part (1986). Drilling the Snake Pit hydrothermal sulfide deposit on the Mid-Atlantic ridge, lat 23° 22'N. *Geology*, 14, 1004-1007.

O'Mullan G.D., Maas P.A.Y., Lutz R.A., Vrijenhoek R.C. (2001). A hybrid zone between hydrothermal vent mussels (Bivalvia: Mytilidae) from the Mid-Atlantic Ridge. Molecular *Ecology* 10, 2819–2831.

Oksanen J., Kindt R., Legendre P., O'Hara B., Simpson G.L., Solymos P., Stevens M.H.M., Wagner H. (2008). vegan: Community ecology package. R package version1.15-0. http://cran.r-project.org/S, http://vegan.r-forge.r-project.org/.

Olu K., Caprais J.C., Galéron J., Causse R., von Cosel R. , Budzinski H., Le Ménach K., Le Roux C., Levaché D., Khripounoff A., Sibuet M. (2009). Influence of seep emission on the non-symbiont-bearing fauna and vagrant species at an active giant pockmark in the Gulf of Guinea (Congo–Angola margin). *Deep-Sea Research part II - Topical Studies in Oceanography* 56, 2380–2393.

Ondréas H., Fouquet Y., Voisset M., Radford-Knoery J. (1997). Detailed study of three contiguous segments of the Mid-Atlantic Ridge, South of the Azores (37° N to 38° 30' N), using acoustic imaging coupled with submersible observations. *Marine Geophysical Research* 19, 231-255.

Ondréas H., Cannat M., Fouquet Y., Normand A., Sarradin P. M., Sarrazin J. (2009). Recent volcanic events and the distribution of hydrothermal venting at the Lucky Strike hydrothermal field, Mid-

Atlantic Ridge. *Geochemistry Geophysics Geosystems* 10.

P

Page H.M., Fialamedioni A., Fisher C.R., Childress, J.J. (1991). Experimental-evidence for filter-feeding by the hydrothermal vent mussel, *Bathymodiolus thermophilus*. *Deep-Sea Research Part a - Oceanographic Research Papers* 38, 1455–1461.

Parker C.M., Von Damm K.L., Beers K.A., Green D.R., Alker B.J., German C.R. (2005). Time series fluid compositions from the TAG hydrothermal mound, MAR: 1986-2004. *EOS, Transactions of the American Geophysical Union, 86, Fall Meeting Supplement, Abstract OS22A-07.*

Paxton H., & Morineaux M. (2009). Three species of Dorvilleidae (Annelida: Polychaeta) associated with Atlantic deep-sea reducing habitats, with the description of *Ophryotrocha fabriae*, new species. *Proceedings of the Biological Society of Washington* 122(1), 14-25.

Podowski E.L., Moore T.S., Zelnio K.A., Luther III G.W., Fisher C.R. (2009). Distribution of diffuse flow megafauna in two sites on the Eastern Lau Spreading Center, Tonga. *Deep Sea Research I-Oceanographic Research Papers* 56, 2041-2056.

R

Ramirez-Llodra E., Shank T., German C.R. (2007). Biodiversity and biogeography of hydrothermal vent species: Thirty years of discovery and investigations. *Oceanography* 20(1), 30-41.

Rona P.A., Klinkhammer G., Nelsen T.A., Trefry G.H., Elderfield H. (1986). Black smokers, massive sulfides and vent biota at the Mid-Atlantic Ridge. *Nature* 321, 33–37.

Rona P.A., Denlinger R.P, Fisk M.R., Howard K.J., Taghon G.L., Klitgord K.D., McClain J.S., McMurray G.R., Wiltshire C. (1990). Major off-axis hydrothermal activity on the northern Gorda Ridge. *Geology* 18, 493-496.

S

Saldanha L., Biscoito M. (1997). Fishes from the Lucky Strike and Menez Gwen hydrothermal vent sites (Mid-Atlantic Ridge). *Boletim do Museu Municipal do Funchal* 49(283), 189-206.

Santos R.S., Colaço A., Christiansen S. (Eds.) (2003). Planning the management of deep-sea hydrothermal vent fields MPAs in the Azores Triple Junction (Workshop proceedings). *Arquipélago – Life and Marine Sciences*, Supplement 4: xii + 70pp.

Sarradin P.M., Caprais J.C., Riso R., Kerouel R., Aminot A. (1999). Chemical environment of the hydrothermal mussel communities in the Lucky Strike and Menez Gwen vent fields, Mid Atlantic Ridge. *Cahiers De Biologie Marine* 40, 93-104.

Sarradin P.M., Waeles M., Bernagout S., Le Gall C., Sarrazin J., Riso R. (2009). Speciation of dissolved copper within an active hydrothermal edifice on the Lucky Strike vent field (MAR,

37°N). *Science of the Total Environment* 407, 869-878.

Sarrazin J., Robigou V., Juniper S. K., Delaney J. R. (1997). Biological and geological dynamics over four years on a high-temperature sulfide structure at the Juan de Fuca Ridge Hydrothermal Observatory. *Marine EcologyProgress Series* 153, 5-24.

Sarrazin J., Juniper S.K. (1999). Biological characteristics of a hydrothermal edifice mosaic community. *Marine Ecology Progress Series* 185, 1-19.

Sarrazin J., Juniper S. K., Massoth G., Legendre P. (1999). Physical and chemical factors influencing species distributions on hydrothermal sulfide edifices of the Juan de Fuca Ridge, Northeast Pacific. *Marine Ecology Progress Series* 190, 89-112.

Sarrazin J., Levesque C., Juniper S.K., Tivey M.K. (2002). Mosaic community dynamics on Juan de Fuca Ridge sulfide edifices: Substratum, temperature and implications for trophic structure. *Cahiers De Biologie Marine* 43, 275-279.

Sarrazin J., Walter C., Sarradin P.M., Brind'Amour A., Desbruyères D., Briand P., Fabri M.C., Van Gaever S., Vanreusel A., Bachraty C., Thiébaut E. (2006). Community structure and temperature dynamics within a mussel community on the southern East Pacific Rise. *Cahiers de Biologie Marine* 47, 483–490.

Schander C., Rapp H.T., Kongsrud J.A., Bakken T., Berge J., Cochrane S., Oug E., Byrkjedal I., Todt C., Cedhagen T., Fosshagen A., Gebruk A., Larsen K., Levin L., Obst M., Pleijel F., Stöhr S., Warén A., Mikkelsen M.T., Hadler-Jacobsen S., Keuning R., Petersen K.H., Thorseth I.H., Pedersen R.B. (2010). The fauna of hydrothermal vents on the Mohn Ridge (North Atlantic). *Marine Biology Research* 6, 155-171.

Segonzac M., de Saint-Laurent M., Casanova B. (1993). L'enigme du comportement trophique des crevettes Alvinocarididae des sites hydrothermaux de la dorsale medio-atlantique. *Cahiers de Biologie Marine* 34, 535-571.

Shank T.M., Fornari D.J., Von Damm K.L., Lilley M.D., Haymon R.M., Lutz R.A. (1998a). Temporal and spatial patterns of biological community development at nascent deep-sea hydrothermal vent (9°50'N, East Pacific Rise). *Deep-Sea Research part II - Topical Studies in Oceanography* 45, 465-515.

Shank T.M., Lutz, R.A., Vrijenhoek R.C. (1998b) Molecular systematics of shrimp (Decapoda: Bresiliidae) from deep-sea hydrothermal vents, I: Enigmatic ''small orange'' shrimp from the Mid-Atlantic Ridge are juvenile *Rimicaris exoculata. Molecular Marine Biology and Biotechnology* 7(2), 88–96.

Shank T., Fornari D.J., Yoerger D.R., Humphris S.E., Bradley A.L., Hammond S., Lupton J.E., Scheirer D., Collier R., Reysenbach A.L., Ding K., Seyfried W., Butterfield D.A., Olson E.J., Lilley M.D., Ward M.E., Eisen JA (2003). Deep submergence synergy: Alvin and Abe explore the Galapagos Rift at 86°W. *EOS, Transactions, American Geophysical Union* 84, 425-440.

Shillito B., Jollivet D., Sarradin P.-M., Rodier P., Lallier F., Desbruyères D., Gaill F. (2001). Temperature resistance of *Hesiolyra bergi*, a polychaetous annelid living on deep-sea vent smoker walls. *Marine Ecology Progress Series* 216, 141–149.

Shillito B., Le Bris N., Hourdez S., Ravaux J., Cottin D., Caprais J. C., Jollivet D., Gaill F. (2006).

Temperature resistance studies on the deep-sea vent shrimp *Mirocaris fortunata*. *Journal of Experimental Biology* 209, 945-955.

Smith D.K. Escartin J., Cannat M., Tolstoy M., Fox C.G., Bohnenstiehl D.R., Bazin S. (2003). Spatial and temporal distribution of seismicity along the northern Mid-Atlantic Ridge (15 degrees-35 degrees N). *Journal of Geophysical Research (Solid Earth)* 108 (B3) # 2167.

Sokal R.R., Rohlf. F.J. (1995). Biometry – The principles and practice of statistics in biological research. Third edition. W. H. Freeman, New York, USA. pp.880.

Somero G.N. (1992). Biochemical ecology of deep-sea animals. *Experientia* 48, 537-543.

T

Tarasov V.G., Gebruk A.V., Mironov A.N., Moskalev L.I. (2005). Deep-sea and shallow-water hydrothermal vent communities: Two different phenomena? *Chemical Geology* 224, 5–39.

Tivey M.K. (1995). Modeling chimney growth and associated fluid flow at seafloor hydrothermal vent sites. *In Seafloor Hydrothermal Systems: Physical, Chemical, Biological, and Geological Interactions. S.E. Humphris, R.A. Zierenberg, L.S. Mullineaux, and R.E. Thomson, (Eds.), American Geophysical Union Monograph Series 91, Washington, DC.*, pp 158-177.

Tivey M.K. (2007). Generation of seafloor hydrothermal vent fluids and associated mineral deposits. *Oceanography* 20(1), 50-65.

Trask J.L., Van Dover C.L. (1999). Site-specific and ontogenetic variations in nutrition of mussels (*Bathymodiolus* sp.) from the Lucky Strike hydrothermal vent field, Mid-Atlantic Ridge. *Limnology and Oceanography* 44, 334-343.

Tsurumi M., Tunnicliffe V. (2001). Characteristics of a hydrothermal vent assemblage on a volcanically active segment of Juan de Fuca Ridge, Northeast Pacific. *Canadian Journal of Fisheries and Aquatic Sciences* 58, 530-542.

Tsurumi M. (2003). Diversity at hydrothermal vents. *Global Ecology and Biogeography* 12, 181-190.

Tsurumi M., Tunnicliffe, V. (2003). Tubeworm-associated communities at hydrothermal vents on the Juan de Fuca Ridge, Northeast Pacific. *Deep-Sea Research Part I-Oceanographic Research Papers* 50, 611-629.

Tunnicliffe, V. (1990). Observations on the effects of sampling on hydrothermal vent habitat and fauna of Axial Seamount, Juan-de-Fuca Ridge. *Journal of Geophysical Research-Solid Earth and Planets* 95, 12961-12966.

Tunnicliffe V., Juniper S. K. (1990). Dynamic character of the hydrothermal vent habitat and the nature of sulfide chimney fauna. *Progress in Oceanography* 24, 1-13.

Tunnicliffe V., Garrett J.F., Johnson H.P. (1990). Physical and biological factors affecting the behavior and mortality of hydrothermal vent tubeworms (Vestimentiferans). *Deep-Sea Research* 37, 103-125.

Tunnicliffe V. (1991). The biology of hydrothermal vents - Ecology and evolution. *Oceanography and Marine Biology* 29, 319-407.

Tunnicliffe V., Desbruyères D., McArthur A.G. (1996). Plate tectonic history and hot vent biogeography. *In: Tectonic, Magmatic, Hydrothermal and Biological Segmentation of Mid-Oceans Ridges, vol.118 Geological Society, London, Special Publications,* pp.225–238.

Tunnicliffe V., Embley R. W., Holden J. F., Butterfield D. A., Massoth G. J., Juniper S. K. (1997). Biological colonization of new hydrothermal vents following an eruption on Juan De Fuca Ridge. *Deep-Sea Research Part I-Oceanographic Research Papers* 44, 1627-1644.

Tunnicliffe V., Juniper S.K., Sibuet M. (2003). Reducing environments of the deep-sea floor. *In Tyler, P.A. (Eds.), Ecosystems of the world: The Deep-sea. Elsevier,* pp. 81-110.

Turnipseed M., Knick K.E., Lipcius R.N., Dreyer J., Van Dover C.L. (2003). Diversity in mussel beds at deep-sea hydrothermal vents and cold seeps. *Ecology Letters* 6, 518–523.

Tyler, P.A., Young C.M. (1999). Reproduction and dispersal at vents and cold seeps. *Journal of the Marine Biological Association of the UK* 79: 193-208.

Tyler, P.A., Young, C.M.Y., (2003). Dispersal at hydrothermal vents: a summary of recent progress. *Hydrobiologia* 503 (1–3), 9–19.

Tyler P.A., German C.R., Ramirez-Llodra E., Van Dover C.L. (2003). Understanding the biogeography of chemosynthetic ecosystems. *Oceanologica Acta* 25, 227–241.

U

Urcuyo I.A., Massoth G.J., Julian, D., Fisher, C.R. (2003). Habitat, growth and physiological ecology of a basaltic community of *Ridgeia piscesae* from the Juan de Fuca Ridge. *Deep-Sea Research Part I-Oceanographic Research Papers* 50, 763-780.

V

Van Dover C.L., Fry B., Grassle J.F., Humphris S., Rona P.A. (1988). Feeding biology of the shrimp *Rimicaris exoculata* at hydrothermal vents on the Mid-Atlantic Ridge. *Marine Biology* 87, 209-216.

Van Dover C.L., Szuts E.Z., Chamberlain S.C., Cann J.R., (1989). A novel eye in "eyeless" shrimp from hydrothermal vents of the Mid-Atlantic Ridge. *Nature* 337, 458–460.

Van Dover C.L. (1995). Ecology of Mid-Atlantic Ridge hydrothermal vents. In: Parson, L.M., Walker, C.L., Dixon, D.R. (eds.). *Hydrothermal Vents and Processes,* Special Publication 87. Geological Society, London, pp. 257–294.

Van Dover C.L., Reynolds G.T., Chave A.D., Tyson J.A., (1996a). Light at deep-sea hydrothermal vents. *Geophysical Research Letters* 23, 2049–2052.

Van Dover C.L., Desbruyeres D., Segonzac M., Comtet T., Saldanha L., Fiala-Medioni A., Langmuir C. (1996b). Biology of the Lucky Strike hydrothermal field. *Deep-Sea Research Part I-Oceanographic Research Papers* 43, 1509-1529.

Van Dover C.L., Trask J.L. (2000). Diversity at deep-sea hydrothermal vent and intertidal mussel beds. *Marine Ecology Progress Series* 195, 169-178.

Van Dover C.L., German C.R., Speer K.G., Parson L.M., Vrijenhoek R.C. (2002). Evolution and biogeography of deep-sea vent and seep invertebrates. *Science* 295, 1253-1257.

Van Dover, C.L., Lutz, R.A. (2004). Experimental ecology at deep-sea hydrothermal vents: a perspective. *Journal of Experimental Marine Biology and Ecology* 300, 273–307.

Von Damm K.L., Bray A.M., Buttermore L.G., Oosting S.E. (1998). The geochemical controls on vent fluids from the Lucky Strike vent field, Mid-Atlantic Ridge. *Earth and Planetary Science Letters* 160, 521-536.

Vuillemin R., Le Roux D., Dorval P., Bucas K., Sudreau J.P., Hamon M., Le Gall C., Sarradin P. M. (2009). CHEMINI: a new *in situ* CHEmical MINIaturized analyzer. *Deep-Sea Research Part I-Oceanographic Research Papers* 56, 1319-1399.

W

Waite T.J., Moore T.S., Childress J.J., Hsu-Kim H., Mullaugh K.M., Nuzzio D.B., Paschal A.N., Tsang J., Fisher C.R., Luther G.W. (2008). Variation in sulphur speciation with shellfish presence at a Lau Basin diffuse flow vent site. *Journal of Shellfish Research* 27, 163–168.

Warèn A., Bouchet P. (1993). New records, species, genera, and a new family of gastropods from hydrothermal vents and hydrocarbon seeps. *Zoologica Scripta* 22, 1-90.

Watabe H., Hashimoto J. (2002). A new species of the genus *Rimicaris* (Alvinocarididae: Caridea: Decapoda) from the active hydrothermal vent field, "Kairei field," on the Central Indian Ridge, the Indian Ocean. *Zoological Science* 19, 1167–1174.

White S.N., Chave A.D., Reynolds G.T., Van Dover C.L., (2002). Ambient light emission from hydrothermal vents on the Mid-Atlantic Ridge. *Geophysical Reseach Letters* 29, 14977– 14980.

Wilson C., Charlou J. L., Ludford E., Klinkhammer G. , Chin C., Bougault H. , German C. , Speer K., Palmer M. (1996). Hydrothermal anomalies in the Lucky Strike segment on the Mid-Atlantic Ridge (37°17'N). *Earth and Planetary Science Letters*, 142, 467-477.

Y

Young C.M. (2003). Reproduction, development and life-history traits. *In Tyler, P.A. (Eds.), Ecosystems of the world: The Deep-sea. Elsevier,* pp. 381-426.

Young P. S. (2001). Deep-sea Cirripedia Thoracica (Crustacea) from the northeastern Atlantic collected by French expeditions. *Zoosystema* 23 (4), 705-756.

Z

Zbinden M., Le Bris N., Gaill F., Compère P. (2004). Distribution of bacteria and associated minerals in the gill chamber of the vent shrimp *Rimicaris exoculata* and related biogeochemical processes. *Marine Ecology Progress Series* 284, 237–251.

Zbinden M., Shillito B., Le Bris N., de Villardi de Montlaur C., Roussel E., Guyot F., Gaill F., Cambon-Bonavita M.-A. (2008). New insigths on the metabolic diversity among the epibiotic microbial communitiy of the hydrothermal shrimp *Rimicaris exoculata. Journal of Experimental Marine Biology and Ecology* 359, 131–140.

Zekely J., Van Dover C.L., Nemeschkal H., Bright M. (2006). Hydrothermal vent meiobenthos associated with mytilid mussel aggregations from the Mid-Atlantic Ridge and the East Pacific Rise. *Deep-Sea Research Part I-Oceanographic Research Papers* 53, 1363–1378.

Zeng X., Birrien J.L., Fouquet Y., Cherkashov G., Jebbar M., Querellou J., Oger P., Cambon-Bonavita, M.-A., Xiao X., Prieur D. (2009). *Pyrococcus* CH1, an obligate piezophilic hyperthermophile: extending the upper pressure-temperature limits for life. *The ISME Journal* 3, 873–876.